Ana Cristina da Costa Rodrigues

Bacterial Cellulose Wound Dressing

Bacterial Cellulose Wound Dressing

Ana Cristina da Costa Rodrigues

UMinho | 2020

August 2020

Universidade do Minho
Escola de Engenharia

Ana Cristina da Costa Rodrigues

Bacterial Cellulose Wound Dressing

Thesis submitted in fulfilment of the requirements for the degree of Ph.D. in Biomedical Engineering

Work developed under supervision of:
Doctor Francisco Miguel Portela da Gama
Doctor João Pedro Martins Soares de Castro Silva
Doctor Manuel Vilanova

August 2020

DIREITOS DE AUTOR E CONDIÇÕES DE UTILIZAÇÃO DO TRABALHO POR TERCEIROS

ACKNOWLEDGEMENTS

Quero aqui expressar os meus sinceros agradecimentos a todos os que, direta ou indiretamente, colaboraram para a concretização deste trabalho. O vosso apoio ajudou-me a perseverar nesta extraordinária, mas longa e muitas vezes difícil jornada.

Em primeiro lugar um agradecimento especial ao orientador deste trabalho o Professor Miguel Gama, primeiro por me ter proposto este desafio, por toda a dedicação e empenho que demonstrou ao longo do meu trabalho, através das suas orientações e do seu incentivo, e por ter acreditado nas minhas capacidades e por me ter dado liberdade de investigação. Agradeço-lhe também o facto de ter partilhado comigo todos os seus sábios conhecimentos. Quero agradecer especialmente toda a compreensão e apoio ao longo desta jornada.

Gostava também de agradecer ao meu co-orientador João Pedro Silva por ter partilhado a sua experiência laboratorial comigo e por me ter apoiado e ajudado sempre. Muito obrigada pela disponibilidade sempre demonstrada e pelo pensamento positivo mesmo nos momentos mais difíceis.

Ao Professor Doutor Manuel Vilanova por ter concordado em coorientar este trabalho, aceitando-me como sua aluna e apoiando-me mesmo antes de me conhecer.

Ao Professor Fernando Dourado, por estar sempre disponível, e por ter dado sempre inputs essenciais para o bom desenrolar dos trabalhos. Obrigado pelo seu incentivo, apoio e pelas indispensáveis sugestões na realização da dissertação.

Às professoras Salette Reis e Sofia Lima do LAQV, REQUIMTE, Departamento de Ciências Químicas, Faculdade de Fármácia, Universidade do Porto, por terem aceitado colaborar neste trabalho, com o empréstimo das câmaras de *Franz* e partilha da sua experiência em trabalhar com estes dispositivos.

À equipa do biotério da Faculdade de Medicina da Universidade do Porto, nas pessoas da Dra. Luísa Guardão, da Liliana e todas as restantes colaboradoras. À professora Raquel Soares e à Ilda Rodrigues, pelo enorme suporte que deram na execução dos ensaios *in vivo*. Ao Professor Fernando Schmitt pela sua disponibilidade e ajuda da interpretação das análises histológicas dos ensaios *in vivo*.

A toda a equipa SATISFIBRE, Ana Isabel Fontão, Aires Coelho, Ana Luísa, Tânia Miranda, Marta Leal, companheiros com quem iniciei este trabalho. Sem a vossa ajuda nem tudo teria sido fácil de ter sido executado.

À minhas meninas Beatriz Cardoso e Maria João Faria com quem iniciei os trabalhos com a Vitamina D vi-as nascer/crescer no mundo da investigação e que também com elas eu cresci e aprendi.

A todos aqueles que passaram pelo LTEB. E foram muitos os que por lá passaram nos últimos anos! Agradeço a companhia, boa-disposição, companheirismo. À Alexandra e Eugénia agradeço ainda a vossa ajuda na execução dos ensaios *in vivo,* que aventura tirar fotografias aos ratinhos. Um agradecimento especial à Vera Carvalho (aka Verinha), Catarina Gonçalves, Jorge Padrão e Isabel Pereira pela amizade, carinho, disponibilidade e apoio prestado no laboratório e não só. Obrigada por toda a vossa ajuda!

Às meninas do Laboratório de Bioprocessos por estarem sempre disponíveis para me deixarem utilizar a câmara de fluxo e emprestar os "frasquinhos de vidro" e muito mais…Às meninas do grupo "Gang das marmitas" pelo ótimo ambiente nas nossas pausas para almoço e não só, elas fazem milagres. Às meninas do grupo "Biológicas" e ainda à Joana Rodrigues. A vossa amizade foi mesmo muito importante. Aos amigos da minha inesquecível passagem pelo curso de Matemática e Ciências da Computação, Celina, Ricky, LP (o cardeal), Tiago (aka Titi), Ana Sofia (aka Aninha), Marco, Barbara, Ricardo Fortunas) e ainda à Milene, convosco aprendi o que é companheirismo, espírito de equipa e amizade verdadeira. À Sofia da Biotecnómica, a minha comercial preferida e também boa amiga! Agradeço a tua ajuda em tudo, as conversas e conselhos, os almoços de quinta-feira, os bons momentos e o teu incentivo.

Não posso esquecer o "Gang" (Patricia, António, Cláudia, Joaquim e Sofia (aka Meirinho). Obrigada pelos momentos de descontração, pelas conversas nem sempre só de café, pelo apoio e intensivo e claro pelas aventuras no mundo da dança. A minha Cláudia, a menina que um dia me disse "Arrisca e candidata-te". Patricia e Sofia, obrigada por me ouvirem, por aturarem as minhas resmunguices, pela companhia nos serões, pelas palavras amigas que têm sempre, pelas discussões científicas por estarem sempre lá quando preciso e pelos momentos de lazer que são preciosos. Obrigada por tudo amigos. Os amigos tornam tudo mais fácil…

Por fim não posso deixar de agradecer à minha família. Aos pilares da minha vida a quem dedico a minha tese, os meus pais. Obrigada mãe e pai por sempre zelarem para que tudo me corra bem e um muito obrigada por todos os meios que me proporcionaram e ainda muito obrigada por me aturarem e desculpem as ausências e o trabalho que por vezes vos dei.

A quem eu me esqueci de agradecer diretamente, um sincero obrigada a todos!

STATEMENT OF INTEGRITY

I hereby declare having conducted this academic work with integrity. I confirm that I have not used plagiarism or any form of undue use of information or falsification of results along the process leading to its elaboration.

I further declare that I have fully acknowledged the Code of Ethical Conduct of the University of Minho.

ABSTRACT
BACTERIAL CELLULOSE WOUND DRESSING

Wounds, in particular traumatic (e.g. burns) and chronic ones, are a major cause of morbidity, impaired life quality and high health care costs. They often result in long hospitalization stays, taking up substantial health resources in developed countries. Conventional treatments are often painful, expensive and may increase the infection risk, compromising the treatments' time and success. In recent years, there have been efforts to develop new advanced methodologies to heal chronic wounds, including the topic use of growth factors or cell-based therapies. However, in many cases, the therapeutic efficacy is low, the therapies are expensive and require application in a clinical facility. Therefore, development of new therapeutics is absolutely necessary and important to satisfy these unmet clinical needs. So, this work comprised the development of a safe, easy-to-use and non-expensive novel dressing, aimed at efficiently addressing these issues, by attaining faster and proper wound healing.

The use of bacterial nanocellulose (BNC) has already demonstrated positive results in the treatment of different kinds of wounds. Additionally, BNC is considered a promising drug delivery system. In this work, BNC was conceived as a protective barrier against exogenous agents (particles, microorganisms) that can impair wound healing, and as a drug carrier for the controlled release of hydrophobic drugs, namely of vitamin D_3 (Vit D_3), an inducer of the endogenous expression of antimicrobial peptide (AMP) LL37, known for accelerating the wound healing process.

In a first part of this project, the optimization of the static BNC production was performed, aiming at making it viable and economic at large scale. First, an experimental design, based on response surface methodology (RSM) - central composite design (CCD) - was used to optimize the culture medium for BNC production by *Komagataeibacter xylinus* BPR 2001, using a simple culture medium composition based on byproducts from the food industry. The optimal conditions for BNC production were (% (m/v)): molasses 5.38; CSL 1.91; ammonium sulphate 0.63; disodium phosphate 0.270; citric acid 0.115 and ethanol 1.38 % (v/v). The experimental and predicted maximum BNC production yields were 7.5 ±0.54 g/L and 6.64 ±0.079 g/L, respectively, after 9 days at 30 °C. Furthermore, the effect of the surface area and culture medium depth on the BNC production yield and productivity were evaluated. BNC dry mass production increased with the surface area and with the medium volume (depth) and fermentation time. Also, as long as nutrients were still available in the culture media, the BNC mass productivity was maintained overtime. The pre-inoculum preparation (PIP) step was also optimized with regards to the (a) identification of an inexpensive culture medium for pre-inoculum leading to a high cell density; (b) analysis of the effect of the initial cellular concentration on the static production of BNC and (c) kinetics of cell growth throughout the different steps of pre-inoculum preparation, including static and stirred - laboratorial and pilot-scale – fermentations. The best composition for PIP medium was (% (m/v)): Glucose and Fructose syrup 1.5-2.0; Corn Step Liquor (protein basis) 0.7; citric acid 0.115; Na_2HPO_4 0.27. The analysis of the cell growth kinetics in the different steps of PIP showed that a careful control on the culture time in each stage is advisable. The time required to reach the exponential phase was very different in each stage of PIP, reducing significantly from the static culture to the stirred culture and for large scale stirred culture, in a 75 L Bioreactor.

In a second part of this work, the use of BNC as a drug carrier was addressed. Since Vit D_3 is poorly water soluble, and thus not easily incorporated in the highly hydrophilic environment of the BNC membrane, Vit D_3 was encapsulated in a self-assembled hyaluronic acid (HA)-based amphiphilic nanogel and then incorporated in the BNC membrane. The carrier was obtained by grafting hexadecylamine (Hexa) into the HA backbone (HA-Hexa). Vit D_3 was successfully loaded into the nanogel (HA-Vit D_3) with an encapsulation efficiency between 60-91 %. The loaded system- HA-Vit D_3- was embedded into BNC, conceived as a transdermal delivery system. The release of Vit D_3 was monitored over time using a *Franz* cell device. Around 70 % of the initial Vit D_3 available was released from BNC membranes in the first 48 h. Most importantly, we observed that the released Vit D_3 still remained within the HA-Hexa nanogel carrier. Vit D_3 is known to stimulate the endogenous production of human cathelicidin (LL37), which is known to accelerate wound healing. Thus, formulations of HA-Vit D_3 and HA-LLKKK18 (an analogue of LL37) were tested *in vivo*, using excision and chronic wound in dexamethasone treated C57BL/6 and db+/db+ mice models, as to evaluate and compare their efficiency in wound repairing. However, the results did not confirm any wound healing improvement.

Keywords- BNC production optimization, drug delivery system, excision and chronic wound, hyaluronic acid nanogel and vitamin D_3, Kinetic´s of cell growth.

RESUMO
CELULOSE BACTERIANA COMO PENSO CURATIVO

As feridas crónicas e traumáticas (*e.g.* queimaduras) apresentam uma elevada morbilidade, afetando severamente a qualidade de vida dos pacientes. Os tratamentos convencionais implicam longos períodos de internação hospitalar, com significativo consumo de recursos dos sistemas de saúde nos países desenvolvidos. Além disso, são dolorosos, caros e podem aumentar o risco de infeção, comprometendo a duração e o sucesso dos tratamentos. Recentemente, têm sido desenvolvidos esforços para o desenvolvimento de novas metodologias avançadas para o tratamento de feridas crónicas, incluindo a aplicação tópica de fatores de crescimento ou terapias baseadas em células. Em muitos casos, estas novas abordagens são caras, devendo ser realizadas numa unidade hospitalar, e a sua eficácia terapêutica é baixa. Assim, o desenvolvimento de novas soluções para satisfazer esta necessidade clínica ainda não satisfeita é absolutamente necessário. Com este trabalho pretende-se desenvolver um penso curativo eficiente, inovador, fácil de usar e não dispendioso, através de uma abordagem segura, visando uma cicatrização mais rápida e adequada da ferida.

A nanocelulose bacteriana (BNC) demonstrou já resultados positivos no tratamento de diferentes tipos de feridas, assim como foi já demonstrado também o seu potencial como sistema de entrega de fármacos. Neste trabalho, a BNC foi utilizada como veículo para a libertação controlada de moléculas hidrofóbicas, nomeadamente a vitamina D_3 (Vit D_3), que é um indutor da expressão endógena do peptído antimicrobiano LL37, conhecido por acelerar o processo de cicatrização de feridas. Além disso, a BNC funciona como uma barreira protetora contra agentes exógenos (poeiras, microorganismos) que podem prejudicar a cicatrização de feridas.

Numa primeira parte, foram desenvolvidos trabalhos visando tornar a produção em grande escala de BNC em cultura estática económica e viável. Nesse sentido, foi usado um desenho experimental, baseado na metodologia de superfície de resposta (RSM) - planeamento composto central (CCD) - para otimizar o meio de cultura, usando subprodutos da indústria alimentar. Foi utilizada a estirpe *Komagataeibacter xylinus* BPR 2001, a 30 °C. Foram identificadas as seguintes condições ótimas para a produção de BNC (% (m/v)): melaço 5,38, xarope de milho (CSL) 1,91; sulfato de amónio 0,63; fosfato dissódico 0,270; ácido cítrico 0,115 e etanol 1,38 % (v/v). Os rendimentos máximos experimentais e previstos de produção de BNC foram 7,5 ±0,54 g/L e 6,64 ±0,079 g/L, respetivamente, após 9 dias. Adicionalmente, foram avaliados o efeito da área superficial e da profundidade/altura do meio de cultura no rendimento e produtividade em BNC. Verificou-se que a produção de BNC aumenta com a área superficial, com o volume de meio de cultura (profundidade) e com o tempo de fermentação. Além disso, observou-se que a produtividade de BNC se mantém constante até se esgotarem os nutrientes no meio de cultura. Para a etapa de preparação pré-inóculo (PIP), a otimização consistiu em diferentes estudos, especificamente: (a) otimização dum meio de cultura de custos reduzidos, que permita a obtenção de uma elevada densidade celular; (b) avaliação do efeito da concentração celular inicial na produção estática de BNC e (c) estudo da cinética de crescimento celular ao longo das diferentes etapas de PIP. A melhor composição para o PIP foi (% (m/v)): xarope de glucose e frutose 1,5- 2,0; CSL 0,7; ácido cítrico 0,115 e Na_2HPO_4 0,27. Os estudos de cinética de crescimento celular para as diferentes etapas do PIP evidenciam a necessidade dum controle cuidadoso do tempo de cultura em cada etapa do PIP. O tempo necessário para atingir a fase exponencial foi muito diferente em cada fase do PIP, reduzindo significativamente da cultura estática, para a cultura agitada, e para cultura agitada em larga escala num bioreator de 75 L.

A segunda parte do trabalho relaciona-se com o desenvolvimento da BNC como sistema de entrega de fármacos. A Vit D_3 é pouco solúvel em água e, portanto, não é facilmente incorporada no ambiente altamente hidrofílico como o da membrana de BNC. Para esse efeito foi usado um nanogel anfifílico auto-organizado obtido pela ligação de hexadecilamina (Hexa) na cadeia do ácido hialurónico (HA). A Vit D_3 foi então encapsulada no nanogel de (HA-Hexa) e em seguida impregnada na membrana de BNC, com uma eficiência de encapsulação entre 60-91 %. A libertação da Vit D_3 foi monitorizada ao longo do tempo, usando uma célula de *Franz* e realizando estudos de permeação. Observou-se a libertação de cerca de 70 % da Vit D_3, ainda dentro do nanogel de HA-Hexa, das membranas de BNC em 48h. Finalmente, foi testada a utilização de HA-Vit D_3 e de HA-LLKKK18 (um péptido análogo à LL37) em modelos de feridas de excisão e crónicas em ratinhos tratados com dexametasona e diabéticos tipo II (db + / db +) C57BL/6. No entanto, os resultados não revelaram uma maior eficiência na cicatrização de feridas na presença das referidas formulações.

Palavras chave- cinéticas de crescimento celular, feridas de excisão e crónicas, nanogeis de ácido hialurónico e vitamina D_3, otimização da produção de BNC, sistema de libertação controlada.

LIST OF CONTENTS

LIST OF FIGURES

CHAPTER 2

CHAPTER 3

CHAPTER 4

CHAPTER 5

CHAPTER 6

LIST OF TABLES

CHAPTER 2

CHAPTER 3

CHAPTER 4

CHAPTER 5

CHAPTER 6

LIST OF ABBREVIATIONS

AA, Acrylic acid;

AMPs, antimicrobial peptides;

ATP, adenosine triphosphate;

Bcs, bacterial cellulose synthesis;

BNC, bacterial nanocellulose;

CAMP, Cathelicidin Antimicrobial Peptide;

CCD, Central Composite Design;

CD44, Cluster determinant 44;

c-di-GMP, cyclic diaguanylic acid;

CFU, Colony Forming Units;

Ch, chitosan;

CSL, corn steep liquor;

Cel⁻, non cellulose producers,

DBP, vitamin-D binding protein;

DFUs, diabetic foot ulcers;

DLS, Dynamic Light Scattering;

DS, degree of substitution;

ECM, extracellular matrix;

EE, encapsulation efficiency;

EGF, epidermal growth factor;

FGF, fibroblast growth factor;

GAG, glycosaminoglycan;

Glc-1-P, glucose-1-phosphatase;

Glc-6-P, glucose-6-phosphatase;

GM-CSF, human growth hormone and granulocyte-macrophage colony-stimulating factor;

HA, Hyaluronic acid;

Hexa, hexadecylamine;

HA-Hexa nanogel, Hyaluronic acid nanogel grafted with hexadecylamine;

HA—LLKKK18, Hyaluronic acid nanogel grafted with hexadecylamine and loaded with antimicrobial peptide LLKKK18;

HA–Vit D₃, Hyaluronic acid nanogel grafted with hexadecylamine and loaded with vitamin D₃;

H&E, hematoxylin and eosin stain;

¹H-NMR, ¹H nuclear magnetic resonance;

HS medium, Hestrin-Schramm culture medium;

HMW-HA, high molecular weight HA;

IL, interleukin;

IGF-1, insulin-like growth factor;

IZD- inhibitory zone diameter;

K. xylinus, *Komagataeibacter xylinus*;

LPS, lipopolysaccharide;

Na₂HPO₄, disodium phosphate;

NHUs, non-healing ulcers;

NLRs, NOD-like receptors;

P.I., pre-inoculum.

PBS, phosphate buffered saline solution;

PDGF, platelet derived growth factor;

PdI, polydispersity index;

PEG, polyethylene glycol;

PES, Polyethersulphone;

PGM, phosphoglucomutase;

PIP, pre-inoculum culture preparation;

PLC, poly (ε-caprolactone);

PLGA, poly(lactic-co-glycolic acid);

PLA, poly(lactic acid);

PU, polyurethanes (PU);

ROS, reactive oxygen species;

rhEGF, epidermal growth factor, human recombinant;

RHAMM, hyaluronan mediated motility receptor;

RSM, Response Surface Methodology;

RT, room temperature;

SRC3, Steroid receptor coactivator 3;

STZ, streptozotocin;

TBA⁺-F, tetrabutylammonium fluoride trihydrate;

TCA cycle, citric acid cycle or Krebs cycle;

TGF-β1, transforming growth factor;

TLRs, Toll-like receptors;

UDP-glucose or UDPG, uridine diphosphate glucose;

UGPase, UDPG-pyrophosphorylase;

UVB, ultraviolet B rays;

VDR, vitamin D receptor;

VDRE, vitamin D response element;

VEGF, vascular endothelial grow factor;

PVA, poly (vinly alcohol);

Vit D₃, vitamin D₃;

WHO, world health organization

WVTR, water vapor transmission rate;

w, wet;

wBNC, wet BNC membranes compressed to 1 mm of thickness

wBNC-HA-Vit D₃, wet BNC membranes compressed to 1 mm of thickness and impregnated with hyaluronic acid nanogel grafted with hexadecylamine and loaded with vit D₃;

25(OH)D₃, 25-dihydroxycholecalciferol, calcifediol or calcidiol;

1,25(OH)₂D₃, calcitriol;

VARIABLES

L, culture medium depth;

S, surface fermentation area;

S/V, volumetric surface area;

V, culture medium volume;

Remarks:

In general, the International System of Units (SI) was used in this work. Sometimes multiples and sub-multiples of the SI units were also used, as well as other non-SI units but allowed by SI, such as the use of liter to express volume. Some units not recognized by the SI were also used to express some variables, such as the volume percent (% v/v), and mass per volume percent (% m/v) to denote the composition of some solutions, the revolutions per minute (rpm) to indicate the agitation rates and the volume of air per volume of reactor per minute (vvm) to designate the aeration rates, due to the usual use in fermentation technology area.

"All of science is nothing more than the refinement of everyday thinking."

Albert Einstein

1 MOTIVATION AND OUTLINE

This chapter introduces the background information about this work, as well as its objectives.

The outline of the thesis and its outputs are also presented.

1.1 CONTEXT AND MOTIVATION

Chronic non-healing wounds affect millions of patients each year and contribute significantly to their morbidity and mortality. These wounds have a substantial impact because of their economic burden (Jarbrink et al., 2017). A 2014 Medicare study showed that chronic non-healing wounds and associated complications affect nearly 15 % or 8.2 million Medicare beneficiaries. The study also estimated the annual cost to treat these wounds at between $28.1 billion and $31.7 billion (Nusgart, 2017). Health care reports state that the European Union spends about 4 % of the total health budget just in wound care (Nusgart, 2017). The highest costs are associated with infected or reopened surgical wounds, and outpatient care represents the highest site-of-service costs. These wounds are mostly associated with old age and often occur in obese and diabetic patients. Underlying causes often include diabetic foot ulcers, venous leg ulcers, arterial insufficiency and pressure ulcers.

Wound healing consists on several overlapping steps - hemostasis, inflammation, proliferation - efficient treatment requiring dressings appropriate for each regeneration stage. The most commonly used dressings display issues associated with skin allergies and/or inflammatory reactions due to the use of adhesive glue. Such dressings require frequent replacement, which may cause pain and wound reopening, further increasing its size and, subsequently, the treatment duration. It also may result in increased costs related with hospital admissions. Many therapeutic agents, including growth factors (e.g. EGF, TGF-beta) and hormones, have been used in wound treatment, but their high production costs deter their application (Kwon et al., 2006). Moreover, some antimicrobial agents (like providone iodine, neomycin, silver sulfadiazine, silver nitrate and others) may also be toxic when systemically absorbed (Onishi et al., 2019). A single effective product for the treatment of all types of wounds doesn´t exist. There are more than 3,000 types of wound dressings available, for different indications (https://woundeducators.com/resources/wound-dressings/). These products accelerate wound healing and alleviate the patient's condition, but their efficiency remains limited. Moreover, the substantially higher cost of the new and advanced wound dressings, along with their requirement for qualified technical assistance, represents a major challenge. The ideal dressing should achieve rapid and proper healing at reasonable cost, with minimal inconvenience to the patient.

Bacterial nanocellulose-based dressings may provide a good option for wound treatment, since they act as a protective barrier against exogenous agents and are easy to apply and remove, while maintaining a moist environment within the wound area. Most importantly, they may function as an vehicle for biologically active drugs.

1.2 RESEARCH AIMS

The main goal of this work comprises the development of a new, safe, easy-to-use and non-expensive dressing that allows a fast and proper wound healing. Bacterial nanocellulose (BNC) has been reported as an excellent wound dressing. Further elaboration on BNC dressings as a delivery system is particularly intended. This goal further subdivides into two parts:

A) A biotechnologically oriented task, aiming at establishing the grounds for the large-scale production of BNC; this work specifically focuses on:

A.1) The optimization of affordable culture medium formulations using inexpensive and readily available nitrogen and carbon sources, such as corn steep liquor and molasses that promote the efficient growth of BNC-producing species; evaluation of the effect of the surface area and culture medium depth on the BNC production yield and productivity is also envisaged;

A.2) The development of strategies to achieve better BNC static culture fermentation control at large-scale.

B) The second part concerns the development of BNC membranes as a delivery system, specifically using Vitamin D_3 (Vit D_3) as a therapeutic molecule. Vitamin D is an agent known to stimulate wound healing, due to its ability to induce the expression of LL37, an antimicrobial peptide with wound healing activity. The use of vitamin D_3, instead of peptides, represents a more affordable choice. However, this vitamin's poor water solubility hampers its exogenous administration. Specifically:

B.1) Vit D_3 was loaded into a self-assembling hyaluronic acid-based amphiphilic nanogel, established by conjugating a hydrophobic molecule – hexadecylamine - (HA-Hexa) - to create a hydrophobic core, prior to their incorporation with Vit D_3 (HA–Vit D_3) into the BNC dressings;

B.2) Testing BNC membranes impregnated with HA–Vit D_3 as a delivery system for wound healing, *in vitro* release using *Franz* cells and permeation studies.

C) *In vivo* trials to ascertain the effects of the drug formulations alone (without the BNC membranes) on wound healing.

1.3 OUTLINE OF THE THESIS

This thesis is structured in chapters that cover the research aims stated above, as indicated below:

CHAPTER 1 The current chapter presents the context, motivation and the research goals of this thesis. The structure and the scientific outputs are also outlined.

CHAPTER 2 Comprises an overview of the state of the art on the BNC production, wound care, drug delivery systems, BNC as a wound dressing and drug carrier.

The different sections of **Experimental Results** are presented from **Chapter 3** to **Chapter 6**. In each of these chapters a brief *introduction*, *material and methods*, *results and discussion*, *conclusions* and *references* are given.

CHAPTER 3 describes the optimization of BNC production by *K. xylinus* BPR 2001 under static culture conditions. In addition, the effect of the surface area and culture medium depth on the BNC production yield and productivity, were evaluated.

CHAPTER 4 relates to the development of a viable and non-expensive strategy for the pre-inoculum culture preparation (PIP) that can be implemented at large scale. The optimization consisted of different studies, namely: a) optimization of an affordable culture medium for pre-inoculum leading to a high cell density; b) evaluation of the effect of the initial cellular concentration on the static production of BNC and c) study of cell growth kinetics throughout the different steps of PIP.

CHAPTER 5 presents the production and characterization of a hyaluronic acid nanogel as a Vit D_3 carrier. The loading efficiency was analysed. Moreover, the potential of BNC membranes as a Vit D_3 - releasing system was assessed through *in vitro* diffusion and permeation studies.

CHAPTER 6 *In vivo* trials to evaluate the efficiency of topical application of Vit D_3 and LLKKK18 antimicrobial peptide to promote efficient wound healing in excision and chronic wound models using dexamethasone treated C57BL/6 *wild type* and C57BL/6 db$^+$/db$^+$ (type II diabetes induced) mice.

CHAPTER 7 Comprises the general conclusions and provides future perspectives.

1.4 SCIENTIFIC OUTPUT

According to the 2nd paragraph of the article 8 of the Portuguese Decree-Law no. 388/70, the scientific outputs of this thesis are listed below.

The results presented in this thesis have been partially published elsewhere.

BOOK CHAPTER:

Dourado, F., Fontão, A. I., Leal, M., Rodrigues, A. C., Gama, M. 2016. Chapter 12 - Process Modeling and Techno-Economic Evaluation of an Industrial Bacterial NanoCellulose Fermentation Process. In "Bacterial Nanocellulose: from biotechnology to bio-economy". Ed.: Gama, M.; Bielecky, S.; Dourado, F. Elsevier; Amsterdam, Netherlands. pp. 199–213. ISBN: 978-0-444-63458-0.

PAPERS ACCEPTED IN PEER-REVIEWED JOURNALS:

CHAPTER 3 Rodrigues, A. C., Fontão, A.I., Coelho, A., Leal, M., Soares da Silva, F.A.G., Wan, Y., Dourado, F., Gama, M., 2019. Response surface statistical optimization of bacterial nanocellulose fermentation in static culture using a low-cost medium. New Biotechnology. 49, 19-27. https://doi.org/10.1016/j.nbt.2018.12.002.

PAPERS SUBMITTED TO PEER REVIEWED JOURNALS:

CHAPTER 5 Rodrigues, A. C., Cardoso, B., Machado, A., Queirós, E., Lima, S. C., Reis, S., Dourado, F., Silva, J. P., Gama, M. Development of bacterial nanocellulose wound dressings with controlled delivery of vitamin D_3.

PAPERS IN PREPARATION FOR SUBMISSION TO PEER-REVIEWED JOURNALS:

CHAPTER 4 Rodrigues, A. C., Fontão, A. I., Coelho, A., Leal, M., Silva, J. P., Dourado, F., Gama, M. Strategies to Optimize pre-inoculum conditions for the large-scale production of bacterial nanocellulose.

CONFERENCE POSTER:

Rodrigues, A.C., Cardoso, B., Machado, A., Queirós, E., Lima, S., Reis, S., Silva, J.P., Gama, M. Development of bacterial cellulose wound dressing with controlled delivery of vitamin D_3. CEB annual meeting, 6 July 2017, Braga, Portugal.

Rodrigues, A.C., Fontão, A. I., Coelho, A., Leal, M., Dourado F., Gama, M., Response Surface Statistical Optimization of Bacterial Cellulose Production in Static Culture using a low-cost fermentation medium. 2nd Symposium on Bacterial Nanocellulose, 9-11 September 2015, Gdansk, Poland.

ORAL COMMUNICATIONS:

Rodrigues, A.C., Cardoso, B., Machado, A., Queirós, E., Lima, S., Reis, S., Silva, J.P., Gama, M. Development of bacterial nanocellulose wound dressings with controlled delivery of vitamin D$_3$. EMBRAPA Agroindústria Tropical - 21 November 2017, Fortaleza, Brasil.

Rodrigues, A.C., Cardoso, B., Machado, A., Queirós, E., Lima, S., Reis, S., Silva, J.P., Gama, M. Development of bacterial cellulose wound dressing with controlled delivery of vitamin D$_3$. GLUPOR12 – 12ª Reunião do Grupo de Glúcidos, Sociedade Portuguesa de Química, 11- 13 September 2017, Aveiro, Portugal.

1.5 REFERENCES

https://woundeducators.com/resources/wound-dressings/. Accessed 2, September, 2019.

Jarbrink, K., Ni, G., Sonnergren, H., et al. 2017. The humanistic and economic burden of chronic wounds: a protocol for a systematic review. Syst Rev. 6(15): 1–7.

Kwon, Y. B., Kim,H. W., Roh, D. H., Yoon, S. Y., Baek, R. M., Kim, J. Y., et al., 2006. Topical application of epidermal growth factor accelerates wound healing by myofibroblast proliferation and collagen synthesis in rat. Journal of veterinary Science. 7: 105-109.

Nusgart, M. 2017. Alliance of Wound Care Stakeholders update: demonstrating the impact and cost of chronic wounds. Ostomy Wound Manage. 63(10): 1943–2720.

Onishi, H., Machida, Y., Santhini, E., Vadodaria, K. 2019. Chapter 8 - Novel textiles in managing burns and other chronic wounds. in Advanced Textiles for Wound Care, Second Edition. Edited by S. Rajendran. 211-260.

2 LITERATURE REVIEW
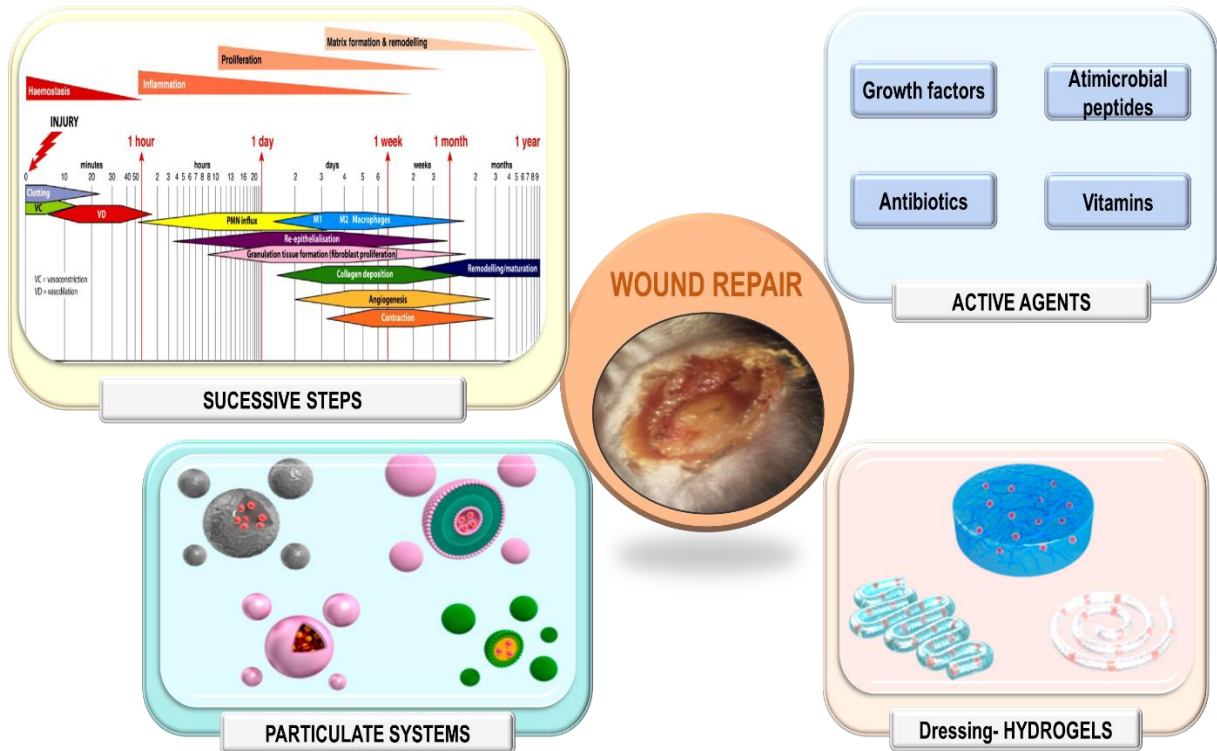
In this Chapter, an overview of the state of the art on the, wound care, drug delivery systems, BNC as a wound dressing and drug carrier and BNC production is provided.

2.1 SKIN

2.1.1 Healthy Skin

Skin is the largest organ in the human body, representing 16 % of total body weight. The integrity of healthy skin plays a crucial role in maintaining physiological homeostasis (Schauber and Gallo, 2008).

The human skin is composed of three layers: epidermis, dermis, and subcutaneous tissue (Figure 1 A). **Epidermis**, the upper layer, is very thin and forms a separation between the body´s internal and external environments. It is constantly renewed due to the proliferation of the underlying basal cells. This layer is composed by a stratified squamous epithelium and has principally two types of cells: keratinocytes and dendritic cells (melanocytes, Merkel cells, and Langerhans cells). Keratinocytes are the most abundant and their main function is to produce keratin, a protein with a protection role that also provides structural strength. Keratinocytes also produce cytokines in response to injury (Sezer and Cevher, 1992; Kolarsick et al., 2009; Venus, et al., 2011; Gilabert et al., 2016; Kaya and Pittet, 2017). The epidermis divides into five layers (from inside to outside): *stratum basale*, *stratum spinosum*, *stratum granulosum*, *stratum lucidum* and *stratum corneum* (Figure 1 B). The **first layer *stratum basale***, which is formed by a single layer of cube-shaped cells, represents the deepest layer of the epidermis and sits directly on top of the dermis. New epidermal skin cells, called keratinocytes, are formed in this layer to replace those shed continuously from the upper layers of the epidermis. Melanocytes, found in the *stratum basale*, are responsible for the production of skin pigment, melanin, helping protect the skin against ultraviolet radiation. The **second layer** of the epidermis is the ***stratum spinosum***, or the prickle-cell layer. The *stratum spinosum* is composed of 8-10 layers of polygonal keratinocytes. These cells display a mixture of cuboidal and flattened shape morphology. Langerhans cells - professional antigen-presenting cells that play a critical role in both protective immune responses in the skin and maintenance of immune homeostasis - can be identified within this layer. The **third layer** is called the ***stratum granulosum***, or the granular layer. It is composed of 3-5 layers of flattened keratin—a resistant, fibrous protein that gives skin its protective properties. Cells in this layer begin to die because they are too far from the dermis to receive nutrients through diffusion. The **fourth layer**, ***stratum lucidum***, considered to be a subdivision of *stratum corneum*, is only present in areas of thick skin, such as the palms and soles, which are subject to a high degree of shear stress. This layer is so named because its cells appear translucent with thickened cell membranes on histological examination. The **last layer**, ***stratum corneum*** is formed by corneocytes, which are dead cells linked together by corneodesmosomes. An insoluble barrier

called the cornified envelope, which replaces the plasma membrane and is composed of proteins and lipids, covers the corneocytes. This cornified cell envelope is a critical structure for the skin barrier function, minimizing water loss. This barrier also protects the skin against invading microorganisms, chemical irritants and allergens, while providing protection against mechanical abrasion and keeping the skin pH at its optimum condition (4.0-6.0). If the integrity of the moisture barrier is compromised, the skin becomes vulnerable to dryness, itching, redness, stinging, and other skin care concerns (Sezer and Cevher, 1992; Kolarsick et al., 2009; Venus, et al., 2011; Gilabert et al., 2016; Kaya and Pittet, 2017).

The **dermis** provides structural and nutritional support. It is mainly composed of extracellular matrix (ECM) produced by fibroblasts (Supp and Boyce, 2005), but it also contains blood and lymphatic vessels, nerves, excretory and secretory glands, keratinizing structures, sensory nerve receptors and immune cells. In fact, the dermis acts as a gel, where collagen fibres account for strength and toughness, elastin confers elasticity and flexibility and proteoglycans provide viscosity and hydration. The elastin and collagen network of the dermis are the main contributors to the mechanical properties of the skin (Reihsner et al., 1995).

Finally, the subcutaneous tissue links the skin to all of other body parts and is mainly formed by adipocytes (Cooper, 2002).
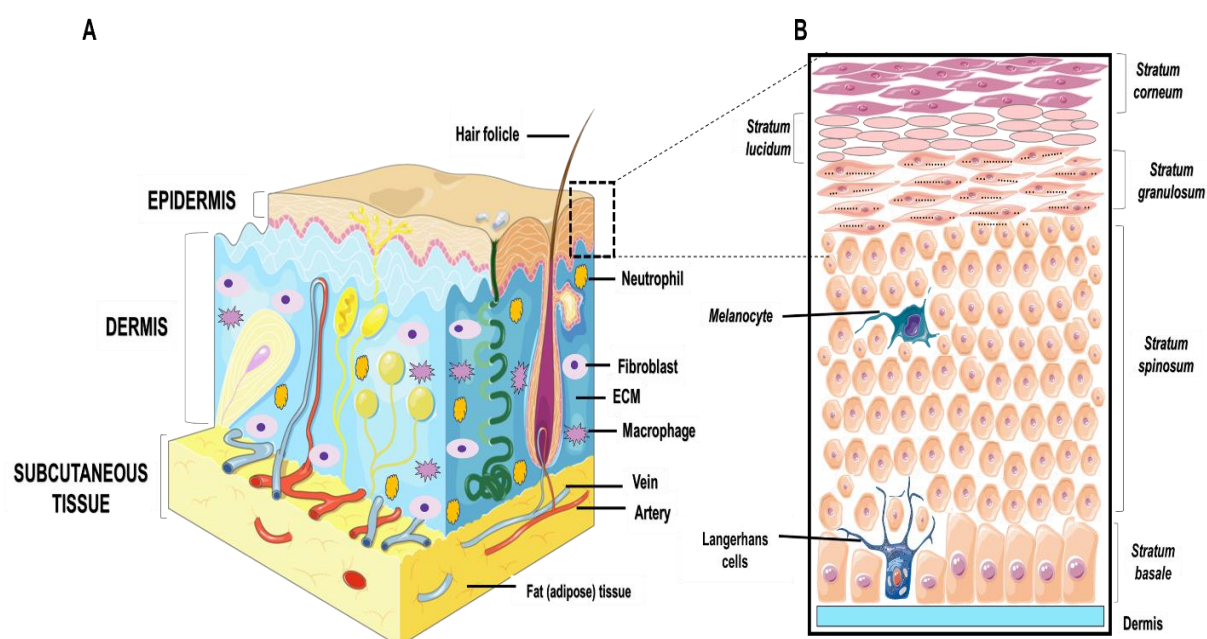
Figure 1 - A) Schematic representation of the skin, distinguishing three different layers: epidermis, dermis and subcutaneous tissue. **B)** The five epidermis sub-layers (from inside to outside): stratum basale, stratum spinosum, stratum granulosum, stratum lucidum and stratum corneum. (Adapted from: Venus et al., 2011 and Kamoun et al., 2017).

The skin functions as a first line of defense against mechanical forces and invading microorganisms, presenting chemical, physical and cellular barriers (Venus et al., 2011). The chemical barrier is provided by the low pH (between 4 and 6) and also by the host defence antimicrobial peptides (AMPs) that prevent the growth of invading microbes (Korting et al., 2006; Ali and Yosipovitch, 2013). The physical barrier is constituted by the epidermis layer *stratum corneum*. The first cellular barrier are the epidermal keratinocytes, which act against infectious agents and recognize the microbes through specific receptors (Schauber and Gallo, 2008; Reinholz et al., 2012; Wertz, 2013; Harder et al., 2013; Xu et al., 2019). It is also involved in many vital functions such as control of body temperature, keeping water and electrolytes balance and sensory perception (Venus, et al., 2011; Sorg et al., 2017), immunological response (Pasparakis et al., 2014) and vitamin D synthesis (Kaya and Pittet, 2017). Another major feature is its ability to self-repair (Schauber and Gallo, 2008).

The skin has diverse microbiota on its surface that compete with the invading microorganisms. When the microbes cross the superficial epidermis, they come into contact with *e.g.* keratinocytes, which increase the expression of antimicrobial defence molecules (such as AMPs and cytokines) (Schauber and Gallo, 2008, Harder et al., 2013). AMPs are components of cutaneous innate immunity, forming the first-line of defense used by many organisms against the invading pathogens. A range of AMPs can be found in the skin. In addition to their antimicrobial activity, they play important roles in immune modulation, apoptosis and wound healing (Diamond et al., 2009; Mahlapuu et al., 2016). The epidermal first-line antimicrobial innate defense strategies are summarized in Figure 2.
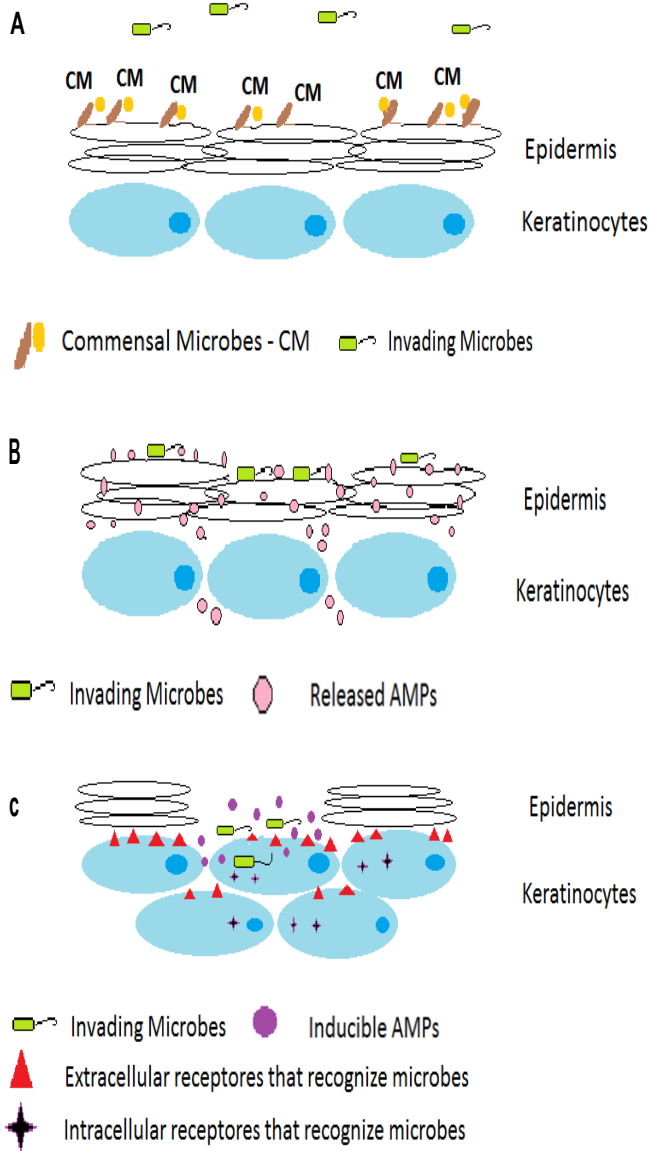
A- Invading microbes have first to compete with the commensal microbiota that provides an antimicrobial shield by the release of bacteriocins.

B- In addition, the *stratum corneum* is covered with AMPs, providing a constitutively generated antimicrobial barrier. Moreover, AMP may be actively generated by microbial proteases from antimicrobial inactive high molecular structure proteins.

C- After penetrating the *stratum corneum* (*e.g.* upon wounding), the invading microbes get into contact with living keratinocytes. The keratinocytes sense the microbes via special receptors like Toll-like receptors (TLRs) and intracellular NOD-like receptors (NLRs). This results in an increased expression of defense molecules such as inducible AMPs. In addition, other indirect defense molecules such as cytokines and chemokines further induce the expression of AMP and may additionally recruit and activate leucocytes (not depicted).

Figure 2 - First line skin antimicrobial innate defence strategies. (Adapted from: Harder et al. 2013).

2.1.2 Wound healing process

Skin injury may arise from different events such as trauma, burns, immunodeficiency or connective tissue disorders, leading to wounds, which can affect different skin layers (Toshkhani et al., 2013). A skin wound can be **superficial**, affecting the epidermis outer layer only; **partial-thickness** injuries involve damage to the epidermis and deeper dermis, including the blood vessels, sweat glands and hair follicles; in the **full-thickness** wounds, both the epidermis and dermis get separated from the underlying structures (subcutaneous fat and sometimes bone) (Boateng et al., 2008).

In normal conditions, the body is able to regenerate the damaged skin. Wound healing is a complex process, dependent on many cell types and mediators, interacting in a highly sophisticated progressive manner to maintain the integrity of skin after trauma (Sorg et al., 2017). This process generally consists of four successive but overlapping phases, including hemostasis, inflammatory, proliferative, and remodelling/regenerative phase (Singer and Clark, 1999; Gonzalez et al., 2016).

Briefly, in **hemostasis (concomitantly started with the injury)**, a phase resulting in vasoconstriction and fibrin clot, preventing excessive blood loss. Platelets trapped in the fibrin clot release vasodilators and chemoattractants and activate the cascade of complement pathways (Onishi et al., 2019; Kim et al., 2019) (Figure 3 A). The **inflammatory phase (starts instantly with the injury)** proceeds for a longer period of time, from days to weeks. In this stage, the wound is cleaned from foreign particles, bacteria and dead tissue. Neutrophils characterize the so called acute inflammatory phase. They are the first population of phagocytic cells that arrives to the wound area, removing pathogens, apoptotic bodies and particles. Then, macrophages (characteristic of the chronic inflammatory phase) migrate into the wound and continue the cleaning process. These inflammatory cells release chemical signals, allowing other cell populations such as keratinocytes, fibroblasts and endothelial cells to be attracted (Tranquillo and Lauffenburger, 1987; Kim et al., 2019) (Figure 3 A). The following **proliferative phase (occur approximately 3 days)** involves new granulation tissue formation, reepithelization and the restoration of the vascular network. Growth factors stimulate fibroblasts that proliferate and synthesize collagen, the main component of ECM and restores the mechanical properties of the healed skin (Chiquet et al., 2009). Growth factors also stimulate keratinocytes proliferation, thus allowing the reepithelization (Simpson et al., 2011). In this phase, the vascular network is also re-established through angiogenesis. This process is very important since it provides nutrients and oxygen supply to the new tissue (Li et al., 2005) (Figure 3 B). In the **maturation or remodeling phase (occur approximately 12 days after the injury)**, once the wound is closed, the remodeling phase begins. This is characterized by the re-

organization and contraction of the ECM, which decreases the dimension of the scar. Collagen fibres type-III, produced in the previous stage by fibroblasts, are gradually replaced by a much stronger type-I collagen, which increases the ultimate tensile strength of the skin. The remodeling phase may continue for months or even years, however the healed area never regains the full ultimate tensile strength of unwounded skin (Blais et al., 2013) (Figure 3 C).
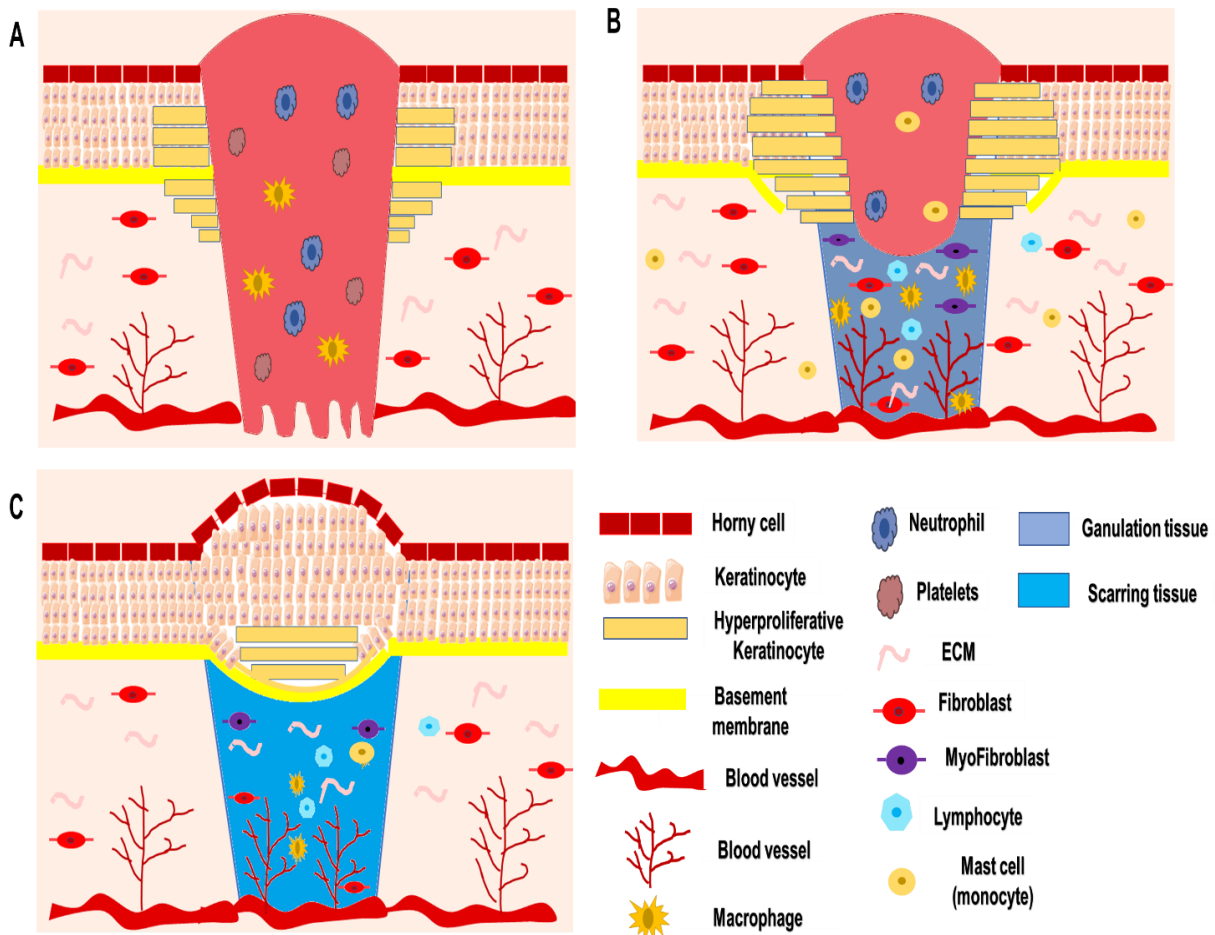
Figure 3 - Schematic representation of stages of of wound healing. **A)** hemostasis and inflammatory phase; **B)** proliferative phase and **C)** maturation or remodeling phase. (Adapted from: Saghazadeh et al., 2018 and Kim et al., 2019).

Depending on how the healing process progresses, wounds may be regarded as acute or chronic. Acute wounds usually heal completely, with minimal scarring and within the expected time frame, usually 8–12 weeks (Percival, 2002). The primary causes of acute wounds include mechanical injuries related to frictional contact between the skin and hard surfaces. Mechanical injuries also include penetrating wounds caused by knives and gunshots and surgical wounds. Burns and chemical injuries, which may arise from a variety of sources such as radiation, electricity, corrosive chemicals, and thermal sources,

are included in acute wounds. The portion of skin loss, as well as the skin layers affected, may vary, often accompanied by a decrease in the humoral and cellular immune responses (Boateng and Catanzano, 2015). The immune defence systems may also become compromised, resulting in loss of physical abilities and mobility, disfigurement or scarring (Kravitz, 1993).

Burn is a traumatic wound among the most common in modern life. According to the World Health Organization (WHO), thermal burns account for an estimated 6.6 million injuries and 300 thousand deaths each year worldwide. An estimated 95 % of these deaths occur in low-income countries due to lack of education and access to medical care as well as the more common use of open fires for heating, lighting, and cooking (Walker and Bhimji, 2018; Javia et al., 2018). Wound infection turns burns into one of the main causes of morbidity and mortality, consuming huge health resources. Hospitalizations in the case of burns represents about 1 % in USA with respect to all injuries, corresponding to treatment costs of $10.4 billion or more per year, based on the data available on the National Business Group on Health. Furthermore, surveys showed that the treatment of low to moderate intensity burns could be costly, at $206,853 or further, if any complications are found. There is an average cost of $1,617,345 to treat severe burns without any complications (Javia et al., 2018).

The normal wound healing process can be impaired by local and systemic factors. Oxygenation and infection are local factors, while age, stress, vascular supply and diseases like diabetes or cancer are systemic factors that affect wound healing (Moore et al., 2006; Guo and Dipietro, 2010; Erfurt-Berge and Renner, 2015; Mir et al., 2018). These factors may result in the alteration of the orderly sequence of events featured by the natural wound healing process, leading to a chronic wound (Trent and Kirsner, 2003; Gurtner et al., 2008; Broderick, 2009). Furthermore, impaired wound healing can lead to an excessive production of exudates and this cause maceration of healthy skin tissue around the wound (Boateng et al., 2008; Boateng and Catanzano, 2015).

Chronic wounds arise from tissue injuries that heal slowly (normally do not heal within 12 weeks) and often reoccur (Gurtner et al., 2008). This kind of wounds affects more than 1 % of the world population and represents costs in the order of several billion euros (Morgan 2015; Nussbaum et al., 2018). Usually, the healing of these wounds stops or has a delay in the inflammatory or proliferative phase (Enoch et al., 2006). In chronic wounds, protease levels exceed that of their inhibitors, leading to destruction of ECM and degradation of growth factors and their receptors. The proteolytic destruction of ECM not only prevents the wound from moving forward into the proliferative phase but also attracts more inflammatory cells, thus increasing the number of inflammation cells. Noteworthy, inflammatory cells accumulated in

the chronic wound produce high levels of reactive oxygen species (ROS) that further damage the ECM (Frykberg and Banks, 2015; Han and Ceilley, 2017; Kim et al., 2019). Chronic wounds are characterized by the presence of high quantities of necrotic tissue which decrease the healing and is the ideal pabulum for bacterial colonization and growth. Chronic wounds are often heavily contaminated and usually involve significant tissue loss that can affect important structures such as bones, joints and nerves. Chronic wounds can be classified in vascular ulcers (*e.g.* venous and arterial ulcers), diabetic ulcers and pressure ulcers (Figure 4 A-D). Arterial and venous ulcers are caused by poor blood supply. In arterial ulcers the overlying skin and tissues get deprived of oxygen, killing these tissues and causing the area to form an open wound. In addition, the lack of blood supply can result in minor scrapes or cuts failing to heal and eventually developing into ulcers (Figure 4 A). Venous ulcers occur primarily in the legs of elderly patients with blood circulation issues due to dysfunctional blood valves that prevent oxygen diffusion into the tissue, thus increasing capillary pressure and causing edema (Figure 4 B). Diabetic ulcers often start as small lesions, which diabetic patients fail to notice due to nerve damage and limited sensitivity. Compromised immune systems, damaged capillaries, poor blood sugar control, poor tissue oxygenation lead to these formerly small and benign wounds becoming dangerously infected (Figure 4 C). Pressure ulcers primarily affect patients who are bedridden or have limited mobility. Decubitus ulcers develop as a consequence of continued skin pressure over bony prominences. They lead to skin erosion, local tissue ischemia and necrosis, those in the sacral region being particularly susceptible to infection (Figure 4 D) (Fonder et al., 2008; Sehgal et al., 2019).

Burns and chronic wounds are among the most common in modern life. Currently used wound dressings are not satisfactory, since they are expensive, infection control is not sufficiently effective, and the rehabilitation time is too long. Thus, more effective wound dressings are required.

Figure 4 - Common chronic wounds. **A)** Arterial ulcer at the lateral malleolus. The surrounding skin is dry, shiny, and hairless. **B)** Venous stasis ulcer with irregular border, shallow base, and surrounding hemosiderosis and lipodermatosclerosis **C)** Diabetic foot ulcer with surrounding callus. Severe diabetic neuropathy and bony deformity contributed to wound formation. **D)** Pressure ulcer in a paraplegic patient, causing full-thickness skin loss. (From: https://www.woundsource.com).

2.2 WOUND CARE

The ideal wound care therapies should: **1)** protect the wound from external agents (*e.g.* bacterial infections, mechanical stress); **2)** accelerate closure through maintenance of wound moisture, and **3)** minimize/avoid scarring. In addition, wound therapies in patients with local/systemic disorders leading to chronic non-healing wounds should further include: **1)** removal of necrotic tissue and biofilm; **2)** modulation of inflammation (including edema) and unlocking of the inflammatory phase of healing; and **3)** boosting the reparative phase of healing (*e.g.* epithelial migration, granulation tissue formation through collagen deposition and ECM remodeling, angiogenesis, tissue blood perfusion, and lymphangiogenesis) (Fonder et al., 2008; Zielins et al., 2014; Frykberg, and Banks, 2015; Whittam et al., 2016). Furthermore, wound care research aims at achieving efficient and short wound healing times, with minimal side effects. Wound treatment strategies that are safe, non-expensive and minimize infection or wound complications are particularly required (Boateng and Catanzano, 2015; Saghazadeh et al., 2018).

The administration of topical bioactive agents to the wound sites is one of the most documented therapies for wound care in medical history (Cross, 1998; Sehgal et al., 2019). The use of topical bioactive agents in the form of solutions, creams and ointments for drug delivery is not very effective, as wounds rapidly absorb fluid and change its rheological characteristics (Katti et al., 2004). For this reason, the use of solid wound dressings is preferred in the case of exudative wounds, as they provide better exudate management and prolonged residence at the wound site.

Ideal wound dressings should be able to mimic the skin ECMs structurally and functionally. In fact, the ECM consists of proteins and polysaccharides that provide mechanical and biochemical support to surrounding cells and direct cell migration, adhesion and growth rate during tissue regeneration (Liu and Jia, 2018).

The choice of dressing is dependent on the cause, presence of infection, wound type and size, stage of wound healing, cost and patient acceptability. So, a single dressing type may not be ideal for all wounds. Specifically, the ideal wound dressings are expected to: create a moist, clean and warm environment; provide hydration if dry or desiccated; absorb excess exudates; promote hemostasis; prevent desiccation; do not cause/cause minimal trauma upon application and/or removal; provide protection to peri-wound area; allow gaseous exchange; be impermeable to microorganisms; be free of toxic or irritant particles or fibers; conform to wound shape; be easy to use; and cost-effective (Sezer and Cevher, 1992; Sood et al., 2014; Saghazadeh et al., 2018; Sehgal et al., 2019).

Unlike traditional dressings such as gauze and cotton wool, that take no active part in the wound healing process, innovative dressings (or modern dressings) are biologically active either on its own or through the release of bioactive molecules (drugs) (Figure 5) (Jones et al., 2006; Boateng et al., 2008; Mir et al., 2018). This is particularly important in the case of infected wounds (Sehgal et al., 2019, Onishi et al., 2019).

The incorporated drugs play an active role in the wound healing process either directly, as cleansing or debriding agents for the removal of necrotic tissue; or indirectly, as antimicrobial and/or anti-inflammatory drugs, which prevent or treat infection or growth factors that aid tissue regeneration, thus increasing the efficiency of the therapy. In chronic wound management, where patients usually undergo long treatments and frequent dressing changes, a system of wound dressings allowing the local release of active molecules/drugs/agents can be significantly more effective and safer than the intravenous or oral administration. The local release of pharmaceuticals allows the control of its concentration within the

therapeutic window, using lower amounts and avoiding secondary effects (Langer, 1980; Mogosanu and Grumezescu, 2014; Silva et al., 2014).
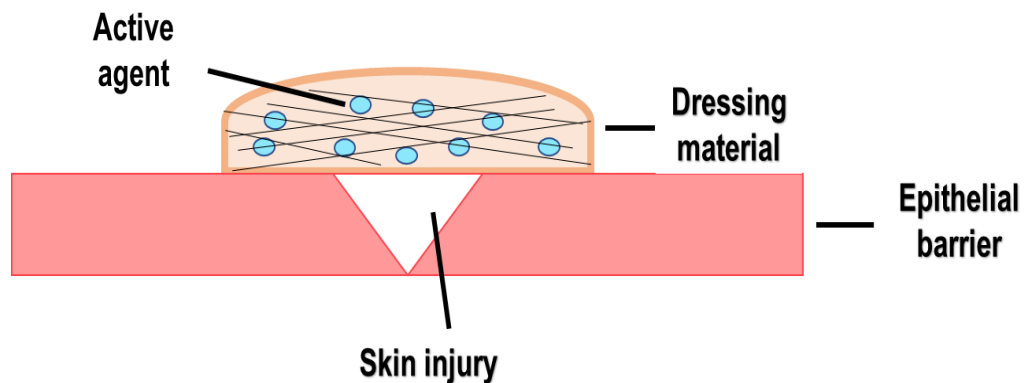
Figure 5 - Modern wound care strategy.

2.2.1 Therapeutic bioactive agents applied in wound dressings and their role in wound healing

Dressings loaded with active agents play an important role in the healing process either directly, by enhancing wound healing phases (*e.g.* antimicrobials drugs (for *e. g.* antimicrobial peptides), growth factors, enzymes, cytokines, vitamins, mineral supplements), or indirectly, by promoting the removal of necrotic tissue (*e.g.* cleaning or debriding agents like Collagenase SANTYL®Ointment, is indicated for debriding chronic dermal ulcers and severely burned areas) (Dhivya et al., 2015; Saghazadeh, et al., 2018; Schoukens, 2019).

2.2.1.1 Growth factors

Growth factors are a class of biomacromolecules locally secreted for the ECM, whose impact on wound healing has been widely demonstrated in several preclinical and clinical studies (Park et al., 2017). These control many key cellular activities involved in normal healing process, including cell migration, division, differentiation, protein expression and enzyme production, besides being essential for successful ECM formation and remodeling (Komarcevic, 2000; Boateng et al., 2008; Park et al., 2017). Moreover, they play an important role in modulating inflammatory responses, enhancement of granulation tissue formation and angiogenesis promotion. A diversity of growth factors have already been reported to participate in wound healing, including: platelet derived growth factor (PDGF), vascular endothelial grow factor (VEGF), epidermal growth factor (EGF), fibroblast growth factor (FGF), transforming growth factor

(TGF-β1), insulin-like growth factor (IGF-1), human growth hormone and granulocyte-macrophage colony-stimulating factor (GM-CSF) (Werner and Grose, 2003). In a study with full thickness wounds in transgenic mice, Mann et al. 2006, suggested that GM-CSF assumes fundamental importance in the wound healing repair, its deficiency resulting in delayed healing and poor quality of newly formed scar tissue. Lee et al. 2005, reported that, when used alone, the antibacterial agent for wound treatment silver sulphadiazine can impair wound healing. However, EGF helps reverse this impairment when both are applied together.

Recombinant human platelet-derived growth factor isoform BB homodimer (rhPDGF-BB), becaplermin (brand name Regranex®), is the only topical growth factor approved by the US Food and Drug Administration for the treatment of chronic diabetic neuropathic ulcers (lower extremity). Similarly, to the endogenous PDGF-BB, becaplermin promotes the chemotactic recruitment and proliferation of cells involved in wound repair. However, a large number of patient's don´t react positively to this treatment, probably because the growth factor is rapidly degraded in the proteolytic wound environment (Goldman, 2004; Fonder et al., 2008; Schreml et al., 2010; Park et al., 2017).

Despite the ability of growth factors to enhance wound healing, their elevated production costs and instability in wound environment hamper their use (Grazul-Bilska et al., 2003; Park et al., 2017).

2.2.1.2 Antimicrobial agents

Some of the strategies commonly used to promote wound healing fail because they do not prevent infection, one of the major causes of delayed healing. Although topical antimicrobials have a large spectrum, they are seldom able to eliminate resistant microorganisms that colonize wounds. Examples of these topical antimicrobials are: antibiotics (which should be avoided because they may lead to hypersensitivity reactions and selection of resistant microorganisms); antiseptics, like silver compounds (for which there is not enough evidence of their efficiency, besides showing some toxicity issues); medical-grade honey (used for many years with positive results but, recently, showing some toxicity issues) (Cooper, 2004; Lipsky and Hoey, 2009; Punjataewakupt et al.,2019).

- **Antimicrobial Peptides (AMPs)**

During the last years substantial progress has been made on the development and evaluation of AMPs for the treatment of skin infections as well as acute and chronic wounds.

In fact, their antimicrobial properties, along with the ability to regulate intracellular signaling and the fact that resistance acquisition to AMPs is high energy demanding, turn AMPs into very promising agents as alternatives to systemic antibiotics. Usage of AMPs is expected to increase since more and more bacteria may develop the ability to resist conventional antibiotics, due to the abuse of these drugs worldwide.

Antimicrobial peptides are important components of the innate immune system, protecting the host against infection (Diamond et al., 2009). In nature, these peptides are found in numerous organisms, including bacteria, invertebrates, vertebrates and plants (Zhao et al., 2013). Production of AMPs in the skin is a dynamic process. Although they are continuously being synthesized, their expression changes according to modifications in physiological conditions, for example, following an injury or infection (Kenshi and Richard, 2008). The main sources of AMPs vary over time, main responsible being the granules of white blood cells (neutrophils, keratinocytes, phagocytes, macrophages, natural killer cells), mouth epithelial tissue, lungs or skin, eyes, ears, airways, intestines and urinary tract (Sørensen, 2016; Kumar et al., 2018).

Despite their different amino acid sequences, most AMPs share some features: small size, usually ranging from 15 to 50 amino acid residues; cationic character (positive charge), due to the abundance of lysine and arginine residues; hydrophobic residues, which may account for up to more than 50 % of the total amino acid composition; an amphipathic structure in membrane-mimicking environments (Mangoni et al., 2016). The antimicrobial activity of these peptides depends on their specific molecular composition. The presence of hydrophilic and hydrophobic regions, and the overall positive charge, allows this amphipathic molecule to electrostatically interact with the polyanionic phospholipids of the cell membrane of most microorganisms, leading to disruption/perturbation of the lipid bilayer and resulting in cell death (William, 2010). For this reason, they have lower probability to induce resistance acquisition in microbes, as compared to conventional antibiotics, which are typically directed toward single targets, mostly enzymes. To develop resistant to AMPs, microbes need to modify the phospholipidic membrane composition (reducing its negative charge) (Nguyen et al., 2011; Mangoni et al., 2016). However, it should be noted that some AMP resistance mechanisms have been described for a few human pathogens (Biswaro et al., 2018). AMPs exhibit a large spectrum of action and ability to kill pathogenic agents such as Gram-positive and Gram-negative bacteria, viruses or fungi, through membrane disruption, inhibition of intracellular processes and/or through activation of innate and adaptive host immunity (Diamond et al., 2009; Pasupuleti et al., 2011; Li et al., 2012). Moreover, AMPs may act as regulators of the immune response and have also been reported as playing an important role in wound healing, by promoting

angiogenesis, leukocyte chemotaxis, induction of cell differentiation process, binding to lipopolysaccharide (LPS), and preventing pro-inflammatory responses (Zhang and Gallo, 2016; Mangoni et al., 2016) (Figure 6).
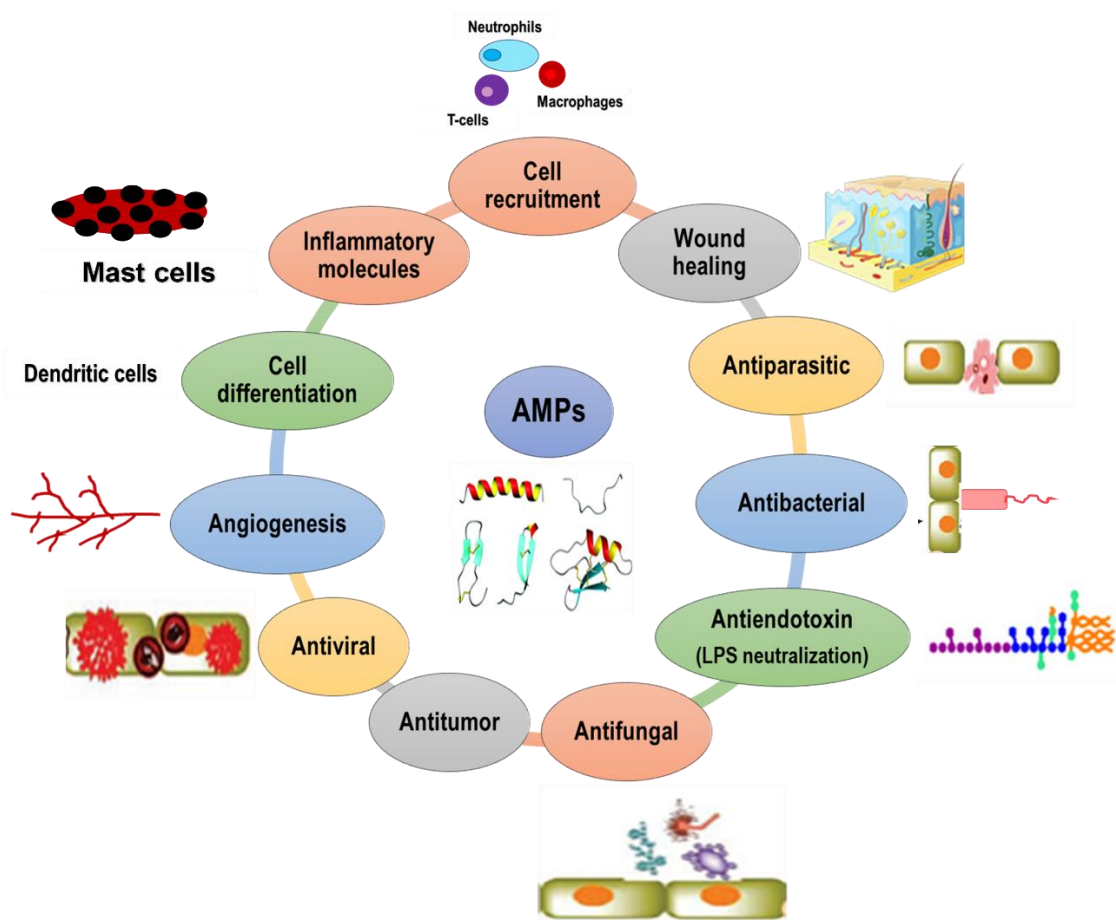
Figure 6 - Different functions of AMPs in host immune protection. (Adapted from: Pasupuleti et al., 2011 and Mangoni et al., 2016).

There are two major groups of AMP families in the skin, namely cathelicidins and defensins, although several other AMPs and proteins have been recognized within the body. Three types of defensins - α-defensins, β-defensins and Ɵ-defensins - have been identified in the skin, but only β-defensins are largely expressed (Bardan et al., 2004; Kenshi and Richard, 2008). Only one known cathelicidin gene was found in humans (*camp*), which ultimately originates the antimicrobial peptide LL37 (Vandamme et al., 2012).

- LL37 structure, expression and activities

LL-37 results from the expression of *camp* gene – Cathelicidin Antimicrobial Peptide (CAMP). The inactive precursor hCAP18 (human cationic protein, with 18 kDa) is composed of a highly hydrophobic N-terminal known as cathelin domain and a C-terminal domain with antimicrobial activity. Upon

stimulation, hCAP18 is activated and cleaved by proteases, such as proteinase 3 in neutrophils and via kallikreins in keratinocytes, originating the active form LL37 (Figure 7) (Dürr et al., 2006; Schauber and Gallo, 2008; van der Does et al, 2012; Takahashi and Gallo, 2017).
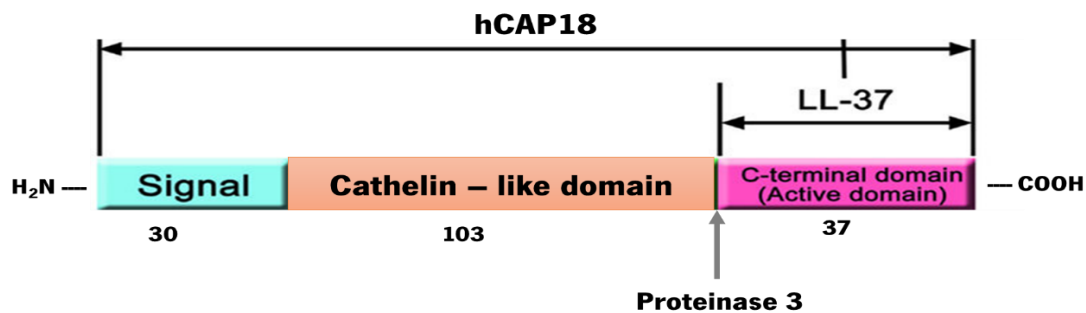
Figure 7 - hCAP18 and LL37 in cathelicidin family. The human cathelicidin hCAP18 consists of signal peptide (30 amino acids), Cathelin-like domain (103 amino acids), and C-terminal domain (37 amino acids). C-terminal domain shows various activities as active domain and is called LL37. Like most antimicrobial peptides, cathelicidins are also produced as inactive preproproteins. The signal peptide is removed, and the resulting precursor is characterized by a conserved N-terminal domain (cathelin-like domain) and a variable cationic C-terminal domain. This C-terminal domain contains the active peptide that can be released from the precursor protein by the action of serine proteinases. Neutrophil-derived proteinase 3 was the main serine proteinase responsible for extracellular cleavage of hCAP-18 released by neutrophils, resulting in the release of the AMP LL37. (Adapted from: Kahlenberg and Kaplan et al., 2013).

The peptide LL37 is composed of 37 amino acids, containing two leading leucine residues in the N-terminus, hence its name. LL37 is a positively charged molecule (+6 at pH around 7.4) with a molecular weight 4.8 kDa. This molecule displays a α-helix structure, similar to other cathelicidin-derived AMPs found in closely related species (Dürr et al., 2006). LL37 is found in some body fluids including sweat, skin wounds, breast milk, saliva and seminal plasma, among other (Dürr et al., 2006).

LL37 its constitutively expressed by several immune cell types, including monocytes, neutrophils, mast cells and B cells, natural killer cells, but also epithelial cells, macrophages, keratinocytes. In the latter, its expression can also be induced by vitamin D (Pasupuleti et al., 2011; Bernard and Gallo 2011; van der Does et al., 2012). In fact, upregulation of its expression might be caused by toll-like receptor or vitamin D receptor agonists, injury, sodium butyrate, phenyl butyrate and cytokine IL-17A (in synergy with vitamin D$_3$) (Bandurska et al., 2015).

Like most AMPs, LL37 can interact with the cell membrane of microorganisms causing its disruption, being also able to permeate the bacterial membrane, inhibiting the synthesis of cell wall components, or binding DNA and RNA by electrostatic interactions, affecting vital processes of bacterial survival and growth (Hale and Hancock, 2007; Bandurska et al., 2015).

Additionally, to antimicrobial activity, LL37 also presents significant immunomodulatory activity, playing a central role in innate immunity. LL37 is a potent chemotactic to human leucocytes, namely monocytes, mast-cells, T-lymphocytes and neutrophils, contributing to host defense against invading pathogens (Ramos et al., 2011). LL37 can have pro- or anti-inflammatory effects, depending on the cell type and on the inflammatory stimulus. Another function reported is angiogenesis. (Hancock et al. 2016

- LL37 role in wound healing

The importance of LL37 in wound healing has been demonstrated in various studies, with its expression being upregulated in some stages of wound recovery (Niyonsaba et al., 2017). Indeed, there is an upregulation of hCAP18/LL37 in the wound edge epithelium, compared with intact skin, indicating that the LL37 is involved in the healing mechanisms (Heilborn et al., 2010; Ramos et al., 2011; Reinholz et al., 2012). Low expression of LL37 is usually associated with several skin diseases, like atopic dermatitis and chronic ulcers, and can increase the risk of infection (Schröder, 2011, Korting et al., 2012). On the other hand, increased expression of LL37 was observed in skin diseases such as psoriasis and rosacea (Ramos et al., 2011; Reinholz et al., 2012; Bandurska et al., 2015).

Interestingly, several studies have demonstrated the therapeutic potential of LL37 for wound healing. Adenovirus-mediated LL37 gene transfer performed via intradermal injection to excisional wounds in obese mice improved re-epithelialization and granulation tissue formation (Carretero et al., 2008). Ramos et al. 2011 evidenced that topically applied recombinant LL37, twice a day, accelerated the healing process in mice with dexamethasone-impaired healing. After 7 days, the number of blood vessels also increased significantly in comparison to a control without the peptide, confirming its pro-angiogenic properties. The role of this peptide in angiogenesis has been particularly described. Indeed, Koczulla et al., 2003 showed that LL37 directly activates endothelial cells, resulting in increased proliferation and formation of vessel-like structures in cultured endothelial cells. Topical administration of LL37-loaded poly (lactic-co-glycolic acid) nanoparticles have also been shown to improve the wound healing and angiogenesis in full thickness wound models, as described by Chereddy et al. 2014. Fumakia and Ho, 2016 also observed that LL37 accelerated wound healing by promoting wound closure in BJ fibroblast cells and keratinocytes, as well as by synergistically enhancing antibacterial activity against *S. aureus* and *E. coli*.

2.2.1.3 Vitamins and wound healing

Although its therapeutic potential in wound healing is well substantiated, there are some concerns about the direct use of LL37 or its analogues. For example: bacterial resistance against AMPs has already been reported; inactivation of AMPs by bacterial proteases may decreases its efficiency; high production costs (Pfalzgraff et al., 2018). These concerns thus limit the direct use of AMPs as therapeutic agents. However, the induction/regulation of endogenous AMP expression could contribute to wound healing.

Vitamins are biologically active micronutrients, either water or lipid soluble. They cannot be synthetized in the organism, meaning that they need to be included in the diet in sufficient amounts (Gueli et al., 2012). Of note, some vitamins are relevant for the wound healing process. Vitamin A (or retinol), for example, is involved in epithelial cell differentiation, collagen synthesis and bone tissue development. It has also been shown to facilitate normal physiological wound healing as well as reversing the corticosteroid-induced inhibition of cutaneous wound healing and post-operative immune depression (Elson and Tennessee, 1998; Boateng et al., 2008). Vitamin C (ascorbic acid) is essential for the synthesis of collagen and other organic components of the intracellular matrix in the bones, skin and other connective tissues. It is also involved in normal responses to physiological stressors like accidental and surgical trauma. In addition, vitamin C aids in improving immune function, particularly during infection (Moores, 2013, Bikker et al., 2016; Carr and Maggini, 2017). Vitamin E (tocopherol) is able to preserve important morphological and functional features of biological membranes, besides having reported antioxidant and anti-inflammatory activity, as well as promoting angiogenesis and reduces scarring (Lin et al., 2012; Hobson, 2014). Noteworthy, the combined use of vitamins A, E and C has been reported to help accelerating wound healing (Porto da Rocha et al., 2002). In particular, vitamin D has been associated with skin disease and has evidenced direct relationship to the regulation of LL37 (Pfalzgraff et al., 2018).

- Vitamin D - Synthesis and metabolism

Vitamin D, a water insoluble molecule, is also associated to the regulation of the calcium, phosphate, and bone metabolism, to the growth and differentiation of keratinocytes and osteoblasts, as well as to the modulation of the innate immune system (Gueli et al., 2012). The most important form of vitamin D is cholecalciferol (Vit D_3), which has been suggested to enable efficient antimicrobial defense at epithelial surfaces, such as the airways or skin (Bikle, 2007; Schauber and Gallo, 2008). Several human cell types are involved in synthesizing and activating vitamin D_3. The human body is able to activating sufficient

Vit D$_3$, provided there is adequate Vit D$_3$ precursor supply and sufficient ultraviolet B (UVB) rays exposure. The 7-dehydrocholesterol or pro-vitamin D$_3$ is present in the epidermis and is converted to pre-vitamin D$_3$ in a photochemical process, in response to UVB exposure. Then, in the basal cells of the epidermis, it is isomerized to Vit D$_3$, circulating in the blood bound to vitamin-D binding protein (DBP). Vit D$_3$ needs to be hydroxylated twice to become biologically active. Firstly, it is hydroxylated in the liver to the scarcely active 25(OH)D$_3$ (also known as 25-dihydroxycholecalciferol, calcifediol or calcidiol) which is the main circulatory form and then further hydroxylated to its biologically active metabolite 1,25(OH)$_2$D$_3$ (or calcitriol), a very expensive molecule. This second hydroxylation step occurs mainly in the kidney (Figure 8, left) (Schauber and Gallo, 2008; van der Does et al., 2012; Vandamme et al., 2012; Christakos et al., 2016; Bikle, 2017). The two enzymes responsible for activating vitamin D$_3$–vitamin D 25-hydroxylase (CYP27A1) and 25-hydroxyvitamin D$_3$ 1-α-hydroxylase (CYP27B1) were initially identified in liver and kidney. Recently also, was found that these enzymes to be expressed by a variety of cells, including immune and epithelial cells. The keratinocytes express both enzymes and are capable of producing active 1,25(OH)$_2$D$_3$ independent of renal and hepatic hydroxylation steps (Figure 8, right). In skin, this is important as the presence of vitamin D$_3$ is essential for normal keratinocyte development and function. In an autocrine fashion, 1,25(OH)$_2$D$_3$ regulates keratinocyte proliferation, differentiation and the formation of an intact epidermal barrier. Alterations in local vitamin D$_3$ concentrations and/or activation will likely affect normal cutaneous immune function, barrier function and inflammation (Schauber and Gallo, 2008 and 2009; van der Does et al., 2012; Vandamme et al., 2012; Christakos et al., 2016; Bikle, 2017).

Figure 8 - Model for UVB triggered vitamin D$_3$ activation response in the skin (left) and cathelicidin response (right). Photochemical conversion of 7-dehydrocholesterol to cholecalciferol in the skin requires UVB irradiation. Extrarenal metabolism of vitamin D$_3$ by keratinocytes provides a system for rapid control of cathelicidin expression. Activation of serum 25-OH-D$_3$ to 1,25-(OH)$_2$-D$_3$ requires two hydroxylation steps that occur sequentially in the liver and kidney (left). However, keratinocytes also express enzymes to activate vitamin D$_3$. CYP27B1 is a 1-α-hydroxylase that activates 25-OH-D$_3$ by converting it to 1,25-(OH)$_2$-D$_3$ (right). Endogenous or exogenous 1,25-(OH)$_2$-D$_3$ then stimulates keratinocytes to increase the production of cathelicidin. (Adapted from: Schauber and Gallo; Antal et al., 2011; Mostafa and Hegazy 2015).

When sun exposure is not enough for endogenous production, Vit D_3 can be obtained from the diet. Animal products contain Vit D_3, while plants, fungi and yeast (when exposed to radiation) are a good source of vitamin D_2, (also called ergocalciferol) (Weber et al., 2005; Gombart, 2011) (Figure 8).

Vitamin D can act locally and regulate, for example, the epidermal keratinocytes through the modification of growth factors or cytokines. It can have either an inhibitory or a stimulatory effect. The latter occurs by increasing the production of epidermal components such as epidermal and platelet growth factors, as a result affecting wound healing (Burkiewicz et al., 2012; Mostafa and Hegazy 2015). Although Vitamin D displays a broad variety of biological actions, as reviewed by Di Rosa et al. 2011, here we will focus on the pathway involving the enhancement of LL37 expression.

- Relationship between Vitamin D and LL37 expression in wounds

Vitamin D is able to induce LL37 expression in a variety of cells, including bronchial epithelial, keratinocytes, and myeloid cells (neutrophils, monocytes), suggesting vitamin D may be a major cathelicidin regulator in humans (Wang et al., 2004; Weber et al., 2005; Gombart et al., 2007; White, 2010; Bucki et al., 2010; Gombart, 2011; Bandurska et al., 2015). The biological activity is mediated by the vitamin D receptor (VDR in target tissues) (Pike and Christakos, 2017). The target genes have vitamin D response elements (VDRE) in their promoter region. VDRs are expressed in different tissues, such as skin, bone, kidney, breast, blood, keratinocytes, neutrophils, monocytes and others, showing immunological and wound healing effects (van der Does et al., 2012). VDR is present in the cytoplasm, where it binds vitamin D (Figure 9). The CAMP gene contains three VDREs (Gombart et al, 2005 and 2007). Several studies demonstrated that vitamin D directly upregulates the hCAP18 transcription in several types of cells, namely in keratinocytes (Figure 9). In fact, it has been shown that administration of Vit D_3 in an *in vivo* acute skin inflammation model improved LL37 expression (Wang et al., 2004; Gombart et al., 2007; Heilborn et al., 2010; Lee et al., 2012; Svensson et al., 2015). Wang et al., 2004 identified a VDRE in the promoter region of cathelicidin gene and therefore demonstrated that Vit D_3 has a role in antimicrobial immunity of the skin. Subsequently, Weber et al., 2005 and Gombart et al., 2005 confirmed that treatment of human keratinocytes *in vitro* with vitamin D increases the expression of this peptide. Also, Weber et al., 2005 observed that two types of vitamin D (D_2 and D_3) and two forms (1,25(OH)$_2$D and 25(OH)D) were able to stimulate cathelicidin expression. However, Vit D_3 was more effective.

In a clinical study performed by Burkiewicz et al. 2012, patients with chronic wounds were observed to bear a deficit in hCAP18, compared to healthy individuals. Additionally, in an *in vivo* study by Heilborn

et al. in 2010, the authors demonstrated that the physiological upregulation of hCAP18⁄LL37 occurring in acute and chronic skin injuries is further enhanced by topical treatment with the Vit D_3 analog calcipotriol.

These results underline the role of vitamin D as a key regulator of hCAP18⁄LL37 in skin. Considering that patients with chronic wounds usually display reduced LL37 expression levels, administration of Vit D_3 may be quite valuable in wound treatment. Moreover, it should be noted that Vit D_3 is a widely available drug, cost-effective, easy-to-use, has a wide therapeutic window and is well tolerated by the organism. Most importantly, Vit D_3 use could reduce inappropriate antibiotic prescription and contribute to improve the therapeutic response.
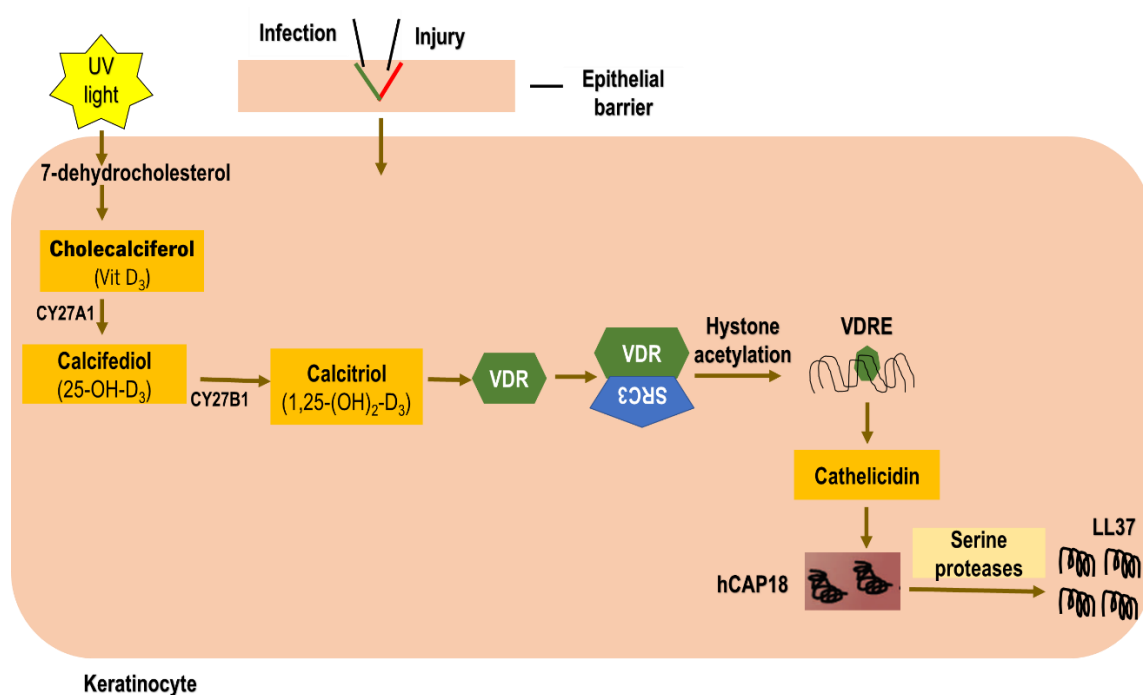
Figure 9 - Vit D_3 activation and cathelicidin response in the skin. Active calcitriol⁄1α,25-dihydroxyvitamin D_3 (1,25VitD₃) that binds to and activates the VDR in an autocrine manner. Steroid receptor coactivator 3 (SRC3) complexes with the VDR and recruit's histone acetyltransferases which open up chromatin and facilitate access to the cathelicidin gene. VDR binds to the VDRE in the cathelicidin promoter region and activates transcription. Cathelicidin is synthesized as an inactive pro-peptide (hCAP18) which is cleaved upon release to active LL37 by serine proteases. (Adapted from: Antal et al., 2011).

2.2.2 Advanced delivery systems for wound healing

Drug delivery through the conventional topical, oral or parenteral routes results in its systemic distribution. In this process, initial high blood levels are observed, followed by its exponential reduction.

The time frame of therapeutically relevant concentrations may be relatively short, depending on the pharmacokinetics of each particular drug. Furthermore, some drugs are toxic at high blood level concentrations, a balance between effective and toxic levels being difficult to achieve when blood concentration falls off rapidly. In general, topical therapy is preferred over systemic drug administration in skin diseases to avoid systemic adverse effects. However topical application requires proper tissue penetration (Stein and Wells, 2010). With regards to the transdermal delivery, the *stratum corneum* represents an effective barrier for topical treatment due to highly organized lipid layers, which severely restrict the diffusion of drugs, and particularly of peptides, through the skin (Javia et al., 2018; Pfalzgraff et al., 2018). When the skin is wounded, this biological barrier becomes compromised, facilitating local delivery. A controlled drug delivery system can play an important role for the effective healing and proper management of wounds (Javia et al., 2018). Current efforts in the area of drug release from wound dressings aim to restrict the action of drugs to the wound site only. Localized drug delivery technologies are emerging as a way to deliver an optimum dose of a bioactive substance precisely in the required timeframe, rather than distributing excessive and unnecessary drug over the wound or to systemic circulation. Targeting an optimum dose can be especially useful for drugs with a narrow therapeutic window, i.e., the difference between the dose at which the drug becomes therapeutically active and the dose at which undesired side effects can occur (Tønnesen and Karlsen 2002). In addition to improved efficacy and safety, the frequency of administration can be decreased with sustained delivery, thereby improving patient compliance. Moreover, the ideal delivery system should be biodegradable or easily excreted; be stable upon storage and with reduced production costs (Sivaram et al., 2015; Kim et al., 2019).

Controlled release systems are particularly interesting for drugs with relatively short half-lives, that require a high frequency of administration in conventional dosage forms or that have low solubility (Sehgal et al., 2019). Moreover, the controlled release systems are most suitable for healing of wounds including diabetic ulcers, decubitus ulcer, venous static ulcer, and other nonhealing wounds (Sehgal et al., 2019). As the surface of the chronic wounds usually lack sufficient blood supply, potentially high doses of antibiotics are often required to be administered by the systemic route to control the infection whereas higher localized concentration and prolonged delivery can be achieved by topical administration avoiding high-dose systemic exposure to the antibiotic (Gaspar et al., 2008). These systems comprise a bioactive agent (a drug) incorporated in a carrier.

2.2.2.1 Wound dressings materials

Delivery kinetics can be tailored, according to the desired drug release schedule, by controlling the degree of swelling, cross-linking density, and degradation rate (Boateng et al., 2015; Slaughter et al., 2009). Drug release from dressings is controlled by one or more physical processes including: **1)** hydration of the polymer. Upon contact of a polymeric dressing with a moist wound surface, the exudate penetrates into the polymer matrix, hydrating it and eventually causing swelling, which further promotes the drug's release over the wound surface; **2)** eventual degradation/erosion of the polymeric system, by the hydrolytic activity of enzymes present in the wound exudates or, in the case of infected wounds, from bacteria; and **3)** diffusion of drug through the polymer matrix (Suzuki et al., 1998; DuBose et al., 2005; Boateng et al., 2008 and 2015).

Bioadhesive, polymeric (synthetic, semisynthetic, or naturally derived polymers) dressings have already been reported for controlled drug delivery to wound sites where it may be beneficial to achieve increased local concentrations of drug, while avoiding high-systemic doses (Boateng et al., 2008 and 2015; Mogosanu and Grumezescu, 2014; Mir et al., 2018; Sehgal et al., 2019; Onishi et al., 2019). Dressing materials may be used in the form of hydrogels, sponges, membranes, hydrocolloids or films (, Mogosano and Grumezescu et al., 2014; Sehgal et al., 2019; Onishi et al., 2019; Mir et al., 2018) and different types of drug carriers have been reported for improved wound healing, including micro and nanoparticulate platforms, liposomes, solid lipid nanoparticles, and hydrogels/nanogels (Javia et al., 2018; Biswaro et al., 2018; Kim et al., 2019). Synthetic polymers are the main materials used in wound management. These can be classified as passive and interactive. Passive synthetic polymers dressings are non-occlusive used for covering wound and help in restoring function under the polymer film (for example gauze). Interactive synthetic polymer dressings are occlusive or semi-occlusive, providing a barrier against bacterial penetration in the wound (Dhivya et al., 2015; Mir et al., 2018). Synthetic polymers can be biodegradable and nonbiodegradable. Synthetic biodegradable polymers currently used in as wound dressings include: poly(lactic-co-glycolic acid) (PLGA), poly (ε-caprolactone) (PLC), polyurethanes (PU), polyethylene glycol (PEG), poly (vinly alcohol) (PVA) (Mir et al., 2018; Sehgal et al., 2019; Onishi et al., 2019). Nonbiodegrable ones include: carboxymethyl cellulose, cellulose acetate, hydroxypropyl methyl cellulose, polymethacrylates (Mir et al., 2018; Sehgal et al., 2019; Onishi et al., 2019). However, the application of synthetic polymers alone are limited by their poor adhesive and mechanical properties and by their ability to accelerate the wound healing process (Liu and Jia, 2018).

Natural materials have high biocompatibility and are environmentally friendly. In view of these appealing properties, they have recently received increased attention as promising biomaterials for biomedical applications (Naseri-Nosar and Ziora., 2018). Moreover, natural polymers are already extensively used in wound dressing preparations because of their similarity to the ECM and good acceptance by biological systems, since they may prevent the immune responses frequently detected with synthetic polymers (Mano et al., 2007; Mogosanu and Grumezescu, 2014). The natural polymers most commonly used as wound dressings include proteins (*e.g.* collagen, albumin, gelatin) and polysaccharides (*e.g.* alginate, hyaluronic acid, dextran, chitosan, cellulose) (Mogosanu and Grumezescu, 2014; Sehgal et al., 2019).

Intrinsic properties like biocompatibility or the generation of bioabsorbable degradation products generally favor natural over synthetic polymers. In addition, their use is usually not compromised by economic or environmental issues, and they are generally considered non-toxic to the human body even at high concentrations (Cai et al., 2010; Naseri-Nosar and Ziora., 2018). The brief summary of most commonly polymer dressings materials used and their wound healing efficiency is presented in (Table 1).

Due to its easiness of application, uniformity and the fact that it is not invasive, the use of bioactive transdermal patches are a promising approach for wound care.

Table 1 - Summary of most commonly polymer dressings materials used and their wound healing efficiency. (Adapted from: Hussain et al., 2017; Kamoun et al., 2017; Saghazadeh et al., 2018; Mir et al., 2018: Sehgal et al., 2019).

	Polymer	Description	Study	Delivery system	Active molecule	Highlights
Synthetic polymers	**poly(lactic-co-glycolic acid) (PLGA)**	High biocompatibility, controlled biodegradability and sustained release of bioactive molecules. PLGA supplies lactate that accelerates neovascularization and promotes wound healing.	*In vivo* studies using STZ-induced wounds using diabetic rats	PLGA microspheres	rhEGF	Efficient wound healing rate. Significant improvement in fibroblasts growth rate and granulation tissue formation. **(Dong et al., 2008).**
			In vivo studies using STZ-induced using diabetic rats	PLGA nanoparticles	rhEGF	Significantly higher rate of wound healing. Enhanced proliferation and differentiation of fibroblasts. **(Chu et al., 2010)**
			In vivo studies using RjHan:NMRI mice In full thickness excisional wounds	PLGA nanoparticles	LL37	Treatment with PLGA-LL37 significantly accelerated wound healing compared to PLGA or LL37 administration alone. PLGA-LL37 treated wounds displayed advanced granulation tissue formation by significant higher collagen deposition, re-epithelialized and neovascularized composition. PLGA-LL37 NP improved angiogenesis, significantly up-regulated IL-6 and VEGFa expression, and modulated the inflammatory wound response. (**Chereddy et al., 2014)**
	poly (ε-caprolactone) (PLC)	Biocompatible; slow rate of degradation. The slow degradation makes PLC very attractive for controlled-release applications, sutures and long-term implants.	*In vivo* studies using STZ-induced wounds using diabetic mice	PCL nanofibres	curcumin	Reduced inflammatory infiltration and faster healing. **(Chu et al., 2010; Merrel et al., 2009)**
	polyurethanes (PU)	Highly versatile, non-adherent and non-allergenic polymers, easy processable, sterilizable, non-toxic, non-carcinogenic.	Clinical studies in chronic exudative wound at lower extremity in human diabetic patient	PU- based foam	-	Accelerated wound healing rate. Cleansing of exudative and debridement tissues at the wounded area. **(Varma et al., 2008)**
	polyethylene glycol (PEG)	Hydrophilic, biocompatible, nonimmunogenic, flexible ether-based polymer, transparent and cost-effective.	*In vivo* studies in non-healing chronic wounds using diabetic rats	PEGylated fibres	rhFGF	Accelerated wound closure. Significantly higher tissue collagen formation and deposition. Enhanced TGF-b expression. **(Huang et al., 2011)**

Table 1 - (continuation)

	Polymer	Description	Study	Delivery system	Active molecule	Highlights
Natural polymers	**Collagen**	Provides tensile strength, forms part of ECM. Interact with cells and help essential cell signaling that regulate cell migration, proliferation differentiation. Collagen its biodegradable.	Clinical studies in diabetic foot ulcers (DFUs) in human diabetic patients	Collagen based dressings	without	Remarkable improvement in wound healing with 60 % of wound healed within 2 weeks of treatment. Significant reduction of infection. Increase in granulation tissue. **(Singh et al., 2011)**
			Clinical studies in DFUs at high risk of amputation in human patient	Collagen matrix		Effective treatment in 46 % of the patients. Increased bacterial clearance. Improved granulation tissue formation. **(Iorio et al., 2011)**
			In vivo studies using STZ-induced diabetic rats	Collagen matrix	Glucose oxidase	Improved cellular proliferation. Accelerated wound closure. **(Arul et al., 2012)**
	Chitosan	Antimicrobial activity, resistance against environmental conditions, adhesive, antifungal, good oxygen permeability. Chitosan enhances the granulation of wound which candidates it as accelerator agent for treating open and deep wounds. Due to its haemostatic effect it accelerates fibroblasts layer formation, increasing the healing rate.	*In vivo* studies using STZ-induced diabetic rats	Chitosan crosslinked collagen	rhFGF	Faster wound healing process. Promoted faster deposition of tissue collagen, higher expression of tissue growth factors and dermal cell proliferation. **(Takei et al., 2012)**
			Clinical study in DFUs in human diabetic patients	Chitosan	Acetyl-glucosamine oligomers	Decrease wound size. Accelerated angiogenesis and re-epithelization. Stimulated healing process. **(Ben-shalom et al., 2009)**
	Alginate or alginic acid	High biocompatibility and mucoadhesive properties. pH sensitive. The main disadvantage of alginate-based material is their inability to undergo efficient and rapid enzymatic degradation. Alginates are very hydrophilic, which hinders its interaction with skin proteins.	Clinical studies in non-healing chronic wound human diabetic patients	Alginate hydrogel	Phenytoin	Significant reduction in wound infection. Improved wound healing which led to 60 % of wound closure within 16 weeks of treatment. Reduce pain. **(Shaw et al., 2011)**

Table 1 - (continuation)

	Polymer	Description	Study	Delivery system	Active molecule	Highlights
Natural polymers	**Hyaluronic acid (HA)**	Non-allergic, non-toxic and biocompatible. Presents important physiological functions such structural and space-filling properties, lubrification, water sorption and retention abilities. HA promote mesenchymal and epithelial cell migration and differentiation, thus enhancing angiogenesis and collagen deposition.	*In vivo* studies using STZ-induced diabetic rats	HA gel	Without	Significant reduction of wound size. Remarkable increased in number of macrophages and fibroblast. Accelerated collagen deposition and re-epithelization of the wounds. **(Bayaty et al., 2010)**
			In vivo studies using STZ-induced diabetic rats	HA foam	Arginine and EGF	Accelerated wound healing. Significant reduction in wound size. Increased re-epithelization. **(Matsumoto and Kuroyanagi, 2010)**
			Clinical studies in non-healing chronic wound in human diabetic patient	Hyiodine®	HA-iodine complex	Significantly faster healing rate. Faster wound closure. **(Sobotka et al., 2007)**
			Clinical studies in chronic wound and burns in human patient	Hylomatrix®	Without	Positively impacts the natural re-epitheliazation process Proper coverage of exposed wound tissue reduces pain Matrix allows cellular invasion and capillary growth Protects wound and retains the moisture Reduces risk of infection. **(Myers et al., 2007)**
	Cellulose/ BNC	Good tensile strength for never dried film, high exudates absorption capacity, biocompatible, and unique nano-fibril morphology network structure. Non-biodegradable (in the body)	Clinical studies in non-infected chronic wound in human diabetic patients	BNC	Without	Accelerated wound healing within 32 days. Increased granulation and tissue re-epithelization. **(Solway et al., 2011)**

2.2.2.2 Hydrogels/Nanogels

Hydrogels are one the most highly used delivery vehicles, being comprehensively investigated due to its physicochemical and biological characteristics. Hydrogels comprise hydrophilic networks of polymers with the ability to swell and retain a large volume of water in its 3D matrix that is able to prevent wound dehydration while allowing oxygen permeation, drug loading and stimuli responsive release (Ahmed, 2015; Sivaram et al., 2015).

Nanogels are colloidal hydrogel nanoparticles (hydrogels in the nanoscale), with a size typically in the range of 10-100 nm suited for being administered via different routes including oral, pulmonary, nasal, parenteral, intra-ocular and topical (Yadav et al., 2017; Zarekar et al., 2017). Nanogels can be prepared from polymer precursors or via heterogeneous polymerization of monomers. Nanogels have a three-dimensional structure formed by chemically or physically crosslinked polymers with hydrophilic or amphiphilic macromolecular chains (Zhang et al. 2016; Neamtu et al., 2017). Physically cross-linked nanogels are formed through hydrogen bonds, van der Waals forces or electrostatic interactions. These interactions result in the aggregation and self-assembly of polymeric chains. Chemical nanogels may be covalently stabilized, using different chemistries, such as disulfide-, amine-, photo-induced cross-linking (Sultana et al., 2013; Wani et al., 2014).

Natural and synthetic polymers can be crosslinked to form nanogels. The first group include proteins such as collagen, gelatin, albumin, and fibrin and/or polysaccharides such as chitosan, hyaluronic acid, heparin, agarose, and alginic acid (Debele et al., 2016; García and Cuggino, 2018). The second group includes poly(lactic acid) (PLA), PCL, PLGA, polyacrylates and polymethacrylates (Neamtu et al., 2017; García and Cuggino, 2018).

Nanogels can be made of ionic or non-ionic amphiphilic polymer chains that organize in a way that the hydrophilic regions get exposed on its surface while the hydrophobic segments aggregate in its core, forming stable and well-defined aggregates that minimize thermodynamic energy (Sharma et al., 2016). Drugs can be loaded into the nanogels and, via electrostatic and/or hydrophobic interactions, become physically entrapped in the polymer matrix (Zarekar et al., 2017). Nanogels are able to encapsulate biologically active agents such as drugs, proteins, and genetic material inside the polymer networks, allowing its release in a controlled manner (Soni et al., 2016; Yadav et al., 2017). Nanogel-based formulations are used in diverse applications including biosensors, artificial muscles, biomaterials, biochemical separation, cell culture systems, biocatalysis, photonics, biomimetics, drug delivery and anticancer therapy (Sultana et al., 2013, Neamtu et al., 2017). Drugs can then be released by different

mechanisms, including diffusion, nanogel degradation, pH and temperature changes, counter ion displacement or using an external energy source (Yadav et al., 2017).

Nanogels as drug delivery systems offer a plethora of advantages compared with conventional polymeric nanoparticles (e.g., nanospheres, nanocapsules, micelles, liposomes, etc.), such as superior biocompatibility, nature mimetic, easy and super- high load of drugs, stability of entrapped bioactive molecules (hydrophobic or hydrophilic), protection from *in vivo* degradation, enhanced penetration of endothelium in pathological sites (*e.g.* solid tumors, inflammation tissue, infracted areas), controlled release, high water content and large surface area (Sivaram et al., 2015: Neamtu et al., 2017; García and Cuggino, 2018). However, nanogels have also some disadvantages like: expensive technique to completely remove potentially toxic residues of solvent and surfactants used in the production process; suboptimal regulation of drug release; Sometimes a strong interaction between drug and polymer decreases the hydrophilicity of the nanogels and causes the structure to collapse, hence irreversibly entrapping the drug molecules and enhancing the hydrophilicity of the nanogel matrix, hence irreversibly entrapping the drug molecules and enhancing the hydrophilicity of the nanogel matrix; lack of stability *in vivo*; difficult upscaling (Sultana et al. 2013; Sharma et al., 2016; Zarekar et al., 2017).

- Hyaluronic acid nanogel as a carrier for drug delivery in wound healing

Hyaluronic acid (HA), also referred to as hyaluronan, is a negatively-charged non-sulfated glycosaminoglycan (GAG) composed of repeating disaccharide units of *N*-acetyl-*D*-glucosamine and *D*-glucuronic acid linked by β(1,3) and β(1,4) glycosidic bonds (Figure 10) (Oh et al., 2010; Mero and Campisi, 2014).
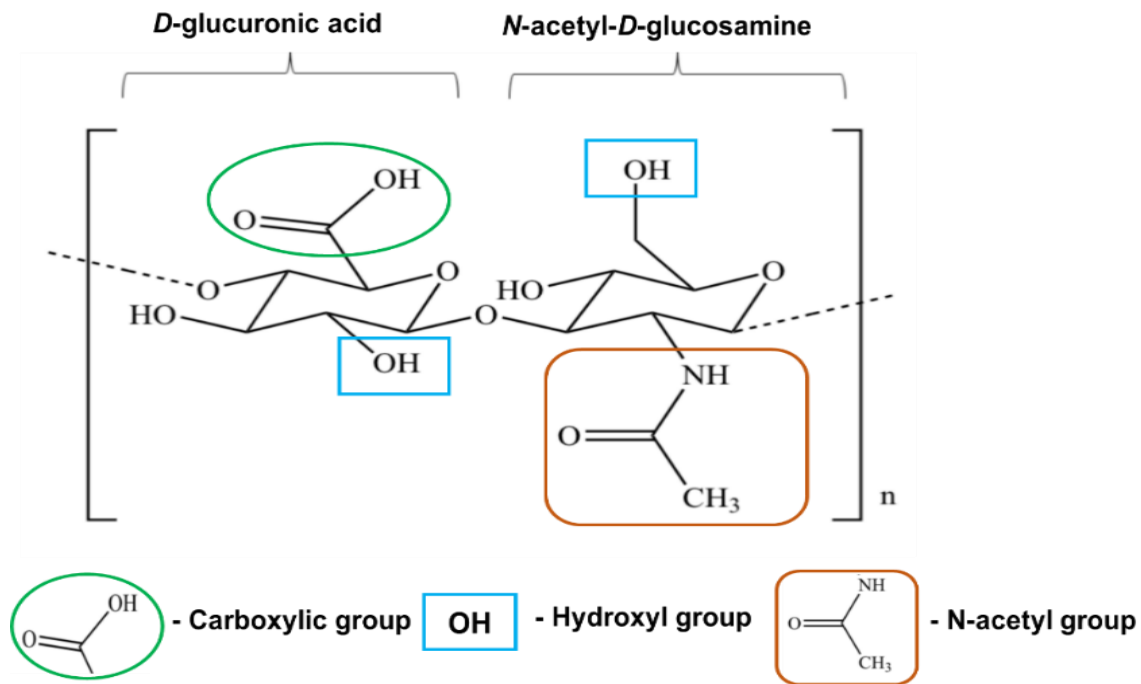
Figure 10 - Hyaluronic acid structure showing the disaccharide repeat units and sites for chemical modification. (Adapted from: Khunmanee et al., 2017).

HA is a highly hydrophilic material that constitutes an essential component of the ECM. It is present at high concentrations in various soft connective tissues such as the synovial fluid, vitreous humor, skin, eyes, skeletal muscle and the umbilical cord (Mero and Campisi, 2014). HA mainly has structural and hydration actions, but it also acts in metabolic regulation, cell migration and adhesion. This polymer is commercially available in a wide range of molecular weights – 4000 Da to 10M Da - which influences its biological properties. While low molecular weight (<100 kDa) makes the polymer pro-inflammatory and pro-angiogenic, by stimulating the production of pro-inflammatory cytokines, chemokines and growth factors and by promoting ECM remodeling, the high molecular weight turns it into anti-angiogenic and non-immunogenic, by binding fibrinogen and controlling the recruitment of inflammatory cells, levels of inflammatory cytokines and migration of stem cells (Oh et al., 2010; Schanté et al., 2011; Pedrosa and Gama, 2014; Fallacara et al., 2018). Such biological properties have turned HA into an interesting material for biomedical applications, particularly in tumor targeting, drug delivery, wound repair and tissue engineering. Specifically, HA plays an important role in cell proliferation, migration and differentiation in the epidermis, and at the dermis it acts as an extracellular filler (Oh et al., 2010; Schanté et al., 2011; Pedrosa and Gama, 2014; Fallacara et al., 2018). The HA role in wound repair has been demonstrated. Vazquez et al. 2003 used a HA matrix in diabetic, neuropathic ulcers on the weight-bearing surface of the foot. The patients were 60 years and 75 % of wounds healed by secondary intention during the 20-week

study. No epidermal grafting was used. HA matrices in mastoid wounds have also demonstrated epithelial migration and decreased time-to-healing (Martini et al., 2000). Price et al., 2005, utilized HA sheets to promote angiogenesis and to convert injured areas of chronic wound into acute wound. Damodarasamy et al., 2014, tested the effect of exogenous HA of 2; 250; or 1,000 kDa on full-thickness excisional wounds, in aged mice. Only wounds treated with 250 kDa HA were significantly improved. Treatment with 250 kDa HA was associated with increased expression of transcripts for the HA receptors CD44 and RHAMM, as well as for collagens III and I. The significantly increased expression of collagen III in aged dermal wounds treated with 250 kDa HA was confirmed, relative to control wounds. Huang et al. 2018, investigated the effects of locally injected high molecular weight HA (HMW-HA, 1650 kDa) on wound healing, in old rats. They found significantly increased proliferation, migration and tube formation in endothelial cells and protection against apoptosis. HA increases the phosphorylation of Src, ERK and AKT, leading to increased angiogenesis, suggesting that local injection of HMW-HA promotes wound healing in elderly patients.

In the ECM, hyaluronic acid interacts with cell receptors such as CD44 (Cluster determinant 44) or RHAMM (hyaluronan mediated motility receptor or CD168), which is overexpressed in injured tissues. Interaction of HA with CD44 regulates a variety of intracellular signaling pathways that control cell biological processes: receptor-mediated hyaluronan internalization/degradation, angiogenesis, cell migration, proliferation, aggregation and adhesion to ECM component. Binding of HA to RHAMM receptors is important for the regulation and promotion of macrophage and fibroblast migration during inflammation and tissue repair (Xu et al., 2012; Mero and Campisi, 2014; Vigetti et al., 2014; Fallacara et al., 2018). HA can be rapidly turned over in the body by hyaluronidase, with tissue half-lives ranging from hours to days, depending on the localization (*e.g.* in the skin about 24 h, in the eye 24-36 h, in the cartilage 1-3 weeks) (Burdick and Prestwich, 2011; Schanté et al., 2011; Aya and Stern, 2014).

This polymer is very attractive for encapsulation of hydrophilic drugs due to its multiple functional groups (hydroxyl and carboxylic acid); ability to form nanostructures after suitable chemical modifications; stability in the bloodstream (stealth properties); enhancement of drug biocompatibility; ability to deliver encapsulated drugs to target sites with high efficacy; capability to decrease drugs cytotoxicity; good biocompatibility, biodegradability and non-immunogenicity properties (Oh et al., 2010; Schanté et al., 2011; Pedrosa and Gama , 2014; Mero and Campisi, 2014).

HA can be further modified to improve its properties. One example of these alterations is the chemical modification that originates amphiphilic systems, able to self-assemble into nanostructures (Schanté et

al., 2011; Pedrosa et al., 2014). Chemical modification of HA may occur either by cross-linking or conjugation, as schematically shown on Figure 11 (Schanté et al. 2011; Khunmanee et al., 2017).
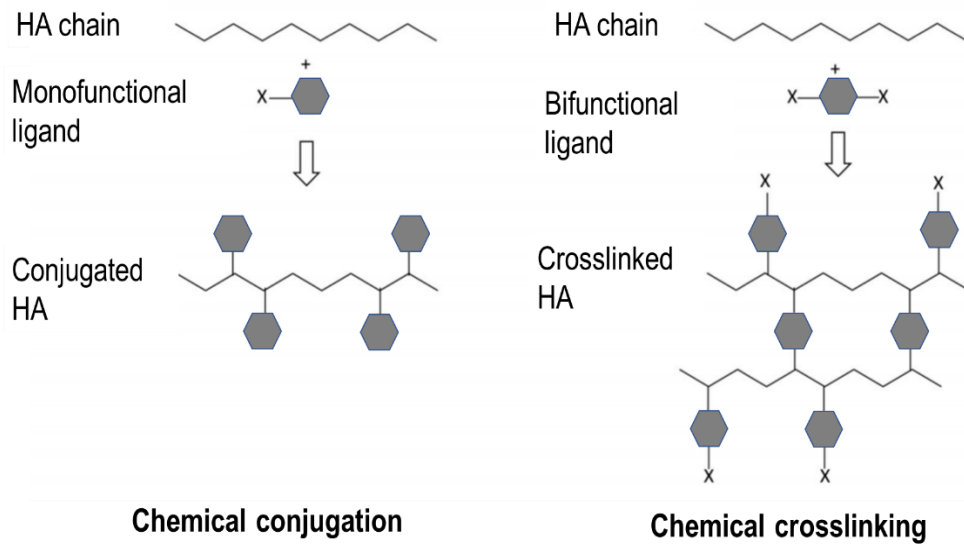
Figure 11 - Chemical cross-linking and chemical conjugation of compound to a polymer. (Adapted from: Schanté et al. 2011 and Fallacara et al., 2018).

HA chemical modifications can be mainly performed at the hydroxyl and the carboxylic acid groups. Amino group may also be made available by deacetylation of N- acetyl group ($-NHCOCH_3$) (Figure 10). Chemical conjugation of hydrophobic molecules to the HA chain forms an amphiphilic conjugate (Figure 12). In aqueous settings, these nanogels acquire an inner hydrophobic core, being able to entrap hydrophobic therapeutic drugs, and an outer hydrophilic shell, preventing protein adsorption and allowing the nanogel to evade the immune system (Pedrosa and Gama et al., 2014; Choi et al., 2010).
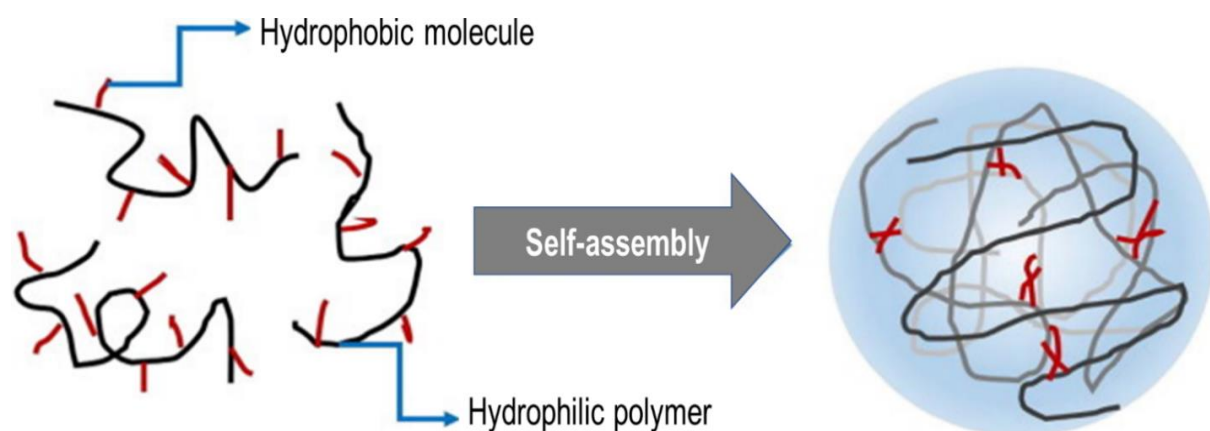
Figure 12 - Scheme of a self-assembling process with a linear polymer like hyaluronic acid and a hydrophobic molecule like hexadecylamine. (Adapted from: Khandare and Minko, 2006).

The application of HA-based nanogels as carriers of pharmaceutical agents for wound healing and principally for tumor targeting (*e.g.* to CD44 receptors, highly expressed in tumor cells) have been extensively described (Rachid et al., 2008; Matsumoto and Kuroyanagi, 2010; Kondo and Kuroyanagi, 2012; Shin et al., 2016; Lee et al., 2017).

Hong et al. 2018, applied two kinds of HA-based hydrogels to repair the full-thickness skin defects in New Zealand rabbits. The authors observed that HA reduced graft contracture during skin healing, by stimulating the expression of more CD44 receptors, and promoting wound surface vascularization. The results showed that both hydrogels were biocompatible, supporting wound repairing and the self-healing process. Others have further reported the increased expression of collagen I and III, with a decrease in the ratio between the two types, following HA administration (Zhao et al., 2013). In a study by Abbruzzese et al. 2009, an HA gel was combined with a mixture of amino acids (Vulnamin® gel; Errekappa, Milan, Italy) and used to treat non-healing ulcers (NHUs) of diabetic patients. Interestingly, the gel reduced the ulcer size, as well as microbial infection–mediated complications within 3 months, promoting elimination of necrotic tissues and protecting skin integrity.

In another study by Xie et al. 2011, HA gel enhanced the absorption and transport of vitronectin. The increased absorption of vitronectin improved the re-epithelialization in a deep dermal partial-thickness burn wound model.

Overall, the data available suggests that hyaluronic acid nanogels may be a good choice as a carrier of therapeutic molecules.

2.2.2.3 Bacterial nanocellulose as a drug delivery system and wound dressing

Cellulose is the most abundant natural polysaccharide, being produced by plants, bacteria, fungi, algae and by the unicellular plankton (Keshk, 2014). Cellulose is a neutral polysaccharide formed out of *D*-glucopyranose residues linked through β-(1, 4)-glucosidic bonds (Brown, 2004). Plant cellulose has been used in many medical applications such as cotton for hemostatic wound dressings, sutures and renal dialysis membranes (Hoenich, 2006). However, plant cellulose is not entirely pure, requiring the removal of hemicelluloses, lignin and pectin through intensive processes, such as acid treatment. In contrast with plant cellulose, bacterial nanocellulose is almost pure (Klemm et al., 2001; Shoda and Sugano, 2005). BNC is produced by *Komagataebacter xylinus* (*K. xylinus*) (formerly known as *Gluconacetobacter xylinus*), a Gram - negative bacteria. BNC is chemically identical to plant cellulose. However, BNC is preferred over the plant cellulose as it can be obtained in higher purity and exhibits a

higher degree of polymerization and crystallinity index (Jonas and Farah, 1998). BNC has been considered a suitable alternative to synthetic polymers, which, despite several undisputed advantages (*e.g.* biodegradability, controlled porosity, ease of production and modification) trigger an excessive immune response and in long-term applications often display performance issues (Liu and Jia 2018; Onishi et al., 2019). BNC presents high biocompatibility, most likely due to its high purity and absence of cytotoxic effects (Pertile et al., 2010; Andrade et al., 2010). BNC has been extensively explored over the last years as a material for wound dressings and other biomedical applications, like tissue engineering scaffolds, artificial blood vessels, (Schumann et al., 2008; Scherner et al., 2014; Leitão et al., 2016) or drug delivery systems (Müller, et al., 2013; Moritz et al., 2014; Pale et al., 2017) (Figure 13). BNC presents ultrafine network, high crystallinity; the nanothickness, great elasticity and transparency (after purification) that further allows following the wound evolution in a clinical setting; hydrophilicity (due to the presence of numerous hydroxyl group and high surface area, which is important to maintain the wound moist); high water retention (99 % of water in the tridimensional structure, most of which not bound to the polymer) and uptake (allowing exudate absorption); high chemical purity; great conformability and moldability; high degree of adherence, even to the moving parts of the body; high oxygen permeability, which is crucial to fasten skin regeneration; high tensile strength (as a result of the ultrafine network structure), displayed by high Young's modulus values; predisposition to different chemical and physical modifications during the fermentation and after purification; and fibrous structure similar to that of the ECM network (fiber diameter = 3–400 nm, length = 1–9 μm) (Bielecki et al., 2012; Sulaeva et al., 2015; Ludwicka et al., 2016; Naseri-Nosar and Ziora, 2018).
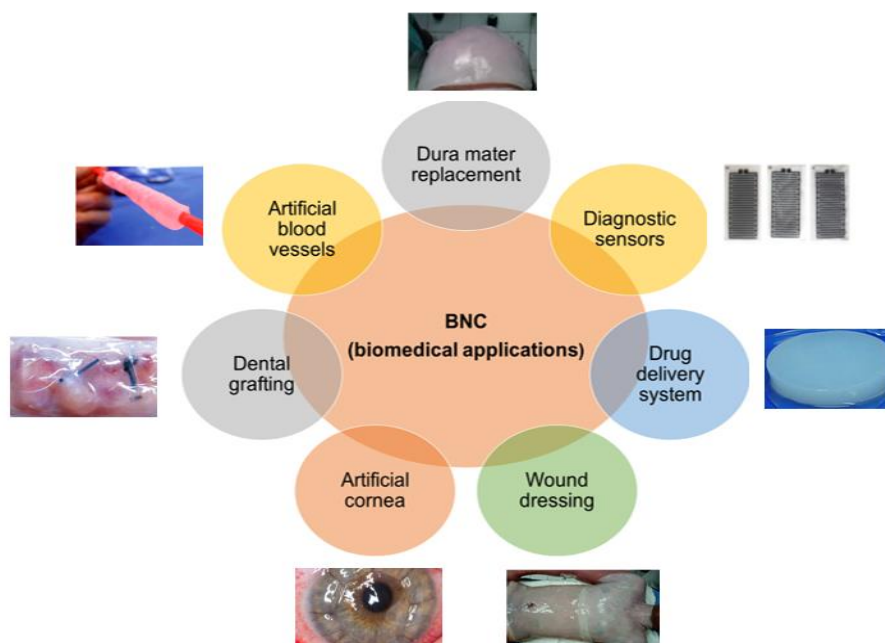
Figure 13 - Biomedical applications of bacterial nanocellulose.

Clinical trials (burns or chronic wounds) showed that, when compared with traditional treatments, wet BNC membranes can reduce pain, lead to a substantial decrease in daily wound care needs; decrease healing times; facilitate scar formation by the removal of necrotic debris; improve the formation of granulation tissue, accelerate the entire process of reepithelialization; act as a *scaffold* for regeneration and function as a drug delivery system. Furthermore, the moisture evaporation and infection are prevented, performing as a physical barrier and keeping a close contact to the open wound. So, the evidences for the advantages of BNC in wound healing are irrefutable (Kucharzewski et al., 2003; Czaja et al., 2007a and b; Abeer et al., 2014; Kwak et al., 2015) (Table 2). Nevertheless, BNC properties can be further ameliorated through the production of BNC-based composites or by loading with suitable delivery systems that confer BNC new properties such as bioactivity and or biodegradability. A summary of studies showing accelerated wound healing following application of BNC dressings is shown in Table 2.

Usually, drug loading into the BNC may be achieved by soaking cellulose in an aqueous buffered solution with the drug, until this is completely absorbed. BNC use for drug delivery has a high interest for transdermal distribution because this is an easy and very efficient method of drug loading due the nanofibrilar network and ability of BNC to adhere to irregular skin surfaces, performing as a transdermal device.

Table 2 - Studies using BNC for wound dressings. (Adapted from: Shah et al., 2013; Ludwicka et al., 2016; Moniri et al., 2017; Naseri-Nosar and Ziora, 2018).

Improvement	Modification Type	Study	Highlights
Accelerate Healing	Without modification	*In vivo* (Partial-thickness burn wounds in rats).	Accelerated wound healing with no toxicity toward liver and kidney. **(Kwak et al., 2015)**
		In vitro (MTT with NIH-3T3, RAW 264.7 and MDCK cells). *In vivo* (Full-thickness excisional wounds in rats).	Bottom side of BNC hydrogel showed better wound healing activity than the top side. **(Li et al., 2015**)
		In vitro (Light microscopic observation of HDFs and HaCaTs). *In vivo* (Full-thickness excisional wounds in mice).	Surface modified BNC had comparable vascularization and inflammation to those elicited by the autologous skin graft. Moreover, fibroblast infiltration and new collagen deposition was higher in the surface modified BNC-treated wound compared with the unmodified BNC. **(Bottan et al., 2014)**
		In vitro (MTT, LDH with L929 and Chinese hamster ovary cells).	CF4 plasma-treatment enhanced the affinity of fibroblasts to BNC. **(Kurniawan et al., 2012)**
		In vitro (WST-8 with human adipose derived stem cells). *In vivo* (Full-thickness excisional wounds in mice).	Better wound healing than sterile gauze, Vaseline gauze, mouse skin allograft and skin xenografts from rat and pig. **(Fu et al., 2012)**
		Use of a commercial mask of BNC to evaluate skin irritation in the arms of several healthy volunteers during 24 h.	Cellulose mask increased the skin moisture up to 28 % and no skin irritations were observed. **(Amnuaikit et al., 2011)**
		In vivo assays in second degree burned patients; topically applied. BNC or a traditional dressing after wound disinfection.	BNC demonstrated completely healing, while the traditional dressing only revealed the beginning of granulation tissue formation. The results obtained also showed that the BNC should be applied immediately after burn injury to achieve better results. **(Czaja et al., 2007a and b and Kucharzewski et al., 2003)**
		BNC dressing applied in patients with leg ulcers in comparison with a control group treated with a traditional dressing.	The wounds in the majority of patients treated with BNC (60 %) healed completely after some weeks while only a small number of the control patients (15 %) produced similar results in the same period of time. **(Kucharzewski et al., 2003)**
Water and exudates absorbency	BNC coating on cotton gauze	Improvement of conventional cotton gauze with BNC coating.	Results showed that cotton gauze coating with BNC increases water absorbency and wicking ability over 30 % and reduces drying time about 33 %. **(Meftahi et al., 2010)**
Antibacterial properties	Zinc oxide nanoparticles	*In vivo* (Burn wounds in mice).	The dressing achieved a wound closure of 66 % at day 15 which was higher than the bacterial cellulose-treated and untreated wounds with 50 % and 19 % wound closure, respectively at the same time point. Antimicrobial activity: *E. coli* (IZD~27 mm), *S. aureus* (IZD~28.60 mm), *P. aeruginosa* (IZD~25 mm) and *C. freundii* (IZD~26 mm). **(Khalid et al., 2017)**
	Benzalkonium chloride		Activity against Gram-positive bacteria for at least 24 h; *E. coli* (IZD~5 mm), *S. aureus* (IZD~8.50 mm) and *B. subtilis* (IZD~14.50 mm). **(Wei et al., 2011)**
	Octenidine	Investigated regarding drug loading performance, controllable drug release, mechanical characteristics, biocompatibility, and antimicrobial efficacy. *In vitro* (ATP with HaCaTs). Additionally, the preservation of the drug release characteristics and the antimicrobial activity were determined in a 6 month.	The dressing could release octenidine up to 96 h and had the shelf life of 6 months; In biological assays, drug-loaded BNC demonstrated high biocompatibility in human keratinocytes; The CFC method revealed the bactericidal activity of>50 % against *S. aureus* after 24 h. **(Moritz et al., 2014)**
	Nanosilver	*In vitro* (MTT with fetal rat epidermal cells). *In vivo* (Partial-thickness burn wounds in rats).	Higher wound healing rate than BNC; *S. aureus* (IZD~13 mm). **(Wu et al., 2014)** The release of Ag ions was pH-sensitive; *E. coli* (11.70 mm ≤IZD≤14.10 mm), *S. aureus* (11.60mm ≤IZD≤18.70 mm), *B. subtilis* (11.50mm≤IZD≤24.30 mm) and *C. albicans* (12.10mm ≤IZD≤16 mm). **(Shao et al., 2015)**

Table 2 - (continuation)

	Modification Type	Study	Highlights
	Gentamicin-RGDC grafting	BNC polymers with and without gentamicin were characterized in terms of chemical composition and morphology. Antimicrobial activity against *Streptococcus mutans* and effect on cell adhesion and proliferation using human gingival fibroblasts were investigated.	Gentamicin−RGDC-grafted BNC membranes are bactericidal against *Streptococcus mutans* but nontoxic to human dermal fibroblasts. The BNC membrane was biocompatible, allowing human fibroblast growth. This biocompatibility was further enhanced by surface modification. **(Rouabhia et al., 2014)**
Pain relief	Diclofenac (analgesics)	Potential of BNC membranes as transdermal systems for the delivery of diclofenac sodium salt. *In vitro* dissolution and permeation through human epidermis in BNC was studied and compared with two commercial formulations (gel and patch).	The membranes were very homogeneous, quite flexible and presented a considerably higher swelling behavior when compared with pure BNC. Incorporation of diclofenac in BNC membranes provided similar permeation rates to those obtained with commercial patches and substantially lower than those observed with a commercial gel. **(Silva, et al., 2014)**
	Lidocaine hydrochloride; ibuprofen (analgesics)	Potential of BNC membranes as systems for topical or transdermal drug delivery. *In vitro* diffusion study using *Franz* cells was conducted, using human epidermal membranes.	Incorporation of lidocaine hydrochloride in BNC membranes provided lower permeation rates than those obtained with the conventional formulations. Permeation of ibuprofen in BNC was almost three times higher than that of the drug in the gel or in a PEG400 solution. These results indicate that this technology can be successfully applied to modulate the bioavailability of drugs for percutaneous administration. Composites showed ability to absorb exudates and to adhere to irregular skin surfaces. **(Trovatti et al., 2012)**
Acceleration of healing	Acrylic acid (AA)	The BNC/AA hydrogels were characterized by SEM, tensile strength, water absorptivity, and water vapor transmission rate (WVTR). The cytotoxicity was investigated in L929 cells. Skin irritation and wound healing properties were evaluated in *Sprague-Dawley* rats	BNC/AA hydrogels had a macroporous network structure, high swelling ratio (4000-6000 % at 24 h), and high WVTR (2175-2280 g/m/day). The hydrogels were non-toxic. *In vivo* experiments indicated that hydrogels promoted faster wound-healing, enhanced epithelialization, and accelerated fibroblast proliferation compared to that in the control group. **(Mohamad et al., 2014)**
	Epidermal growth factor (EGF)	A novel wound-dressing biodevice, sensitive to lysozyme, an enzyme commonly found in infected skin wounds, was assembled by the layer-by-layer deposition of nano-polymeric chitosan and alginate films onto oxidized BNC membranes incorporated with EGF.	Nano-polymeric layers were capable of slowly releasing EGF and this can enhance the process of re-epithelialization. Distinct EGF release profiles were obtained according to specific stimuli caused by infection. *In vitro* conditions simulating noninfected wounds, the EGF rate and burst release effect were reduced by three deposited layers. **(Picheth et al., 2014)**
	Hyaluronates	Incorporation of different amounts of HA into BNC (BNC-HA) and evaluate its effects in *in vivo* wound repair.	The samples with BNC-HA increased the healing times and the wound diameter decreased after 7 days, showing better results than BNC dressings alone. **(Li et al., 2015)**
Acceleration of healing	Chitosan (Ch)	The swelling characteristics, water retention properties, water vapor transmission, and tensile strength of BNC and BNC−Ch membranes were evaluated. Cytocompatibility and antibacterial activities were assessed *in vitro*. The effects of BNC and BNC−Ch on wound healing were examined in rat skin models.	Both membranes maintained proper moisture contents for an extensive period without dehydration. The tensile strength and elongation at break for BNC−Ch were slightly lower while the Young's modulus was higher. BNC and BNC−Ch had no cytotoxicity. In the antibacterial test, the addition of chitosan in BNC showed significant growth inhibition against *E. coli* and *S.aureus*. *In vivo* trials by rat models revealed that wounds treated with BNC−Ch epithelialized and regenerated faster than those treated with BNC or Tegaderm. **(Lin et al., 2013)**

Table 2 - (continuation)

Improvement	Modification Type	Study	Highlights
Water holding capacity	Alginate	The novel composite sponge of BNC/alginate (BNCA) has been developed for the use as mucosal flaps in oral tissue regeneration.	*In vitro* studies with human keratinocytes (HaCat) and gingival fibroblasts demonstrated that the pure BC and the BNCA sponges supported proliferations of the cells. In the wet state, only the BNCA sponge with 30 % alginate had a good tear resistance for sewing. **(Chiaoprakobkij et al., 2011)**
	Aloe vera	The surface morphology, pore structure, tensile strength, water absorption capacity, crystallinity and water vapor permeability of the modified films were examined and compared with those of the typical BNC film.	With the 30 % (v/v) aloe gel supplement in the culture medium, a fibre-reinforced bio-polymer film displayed significantly improved properties in mechanical strength, crystallinity, water absorption capacity and water vapor permeability in comparison to those of the unmodified BC film. **(Saibuatong and Phisalaphong, 2010)**
Mechanical properties	P(3HB-co-4HB)	Preliminary biodegradation test was performed for P(3HB-co-4HB) and P(3HB-co-4HB)/BNC composite scaffold in buffer solution and enzyme solution. The biocompatibility of the composite scaffold was preliminarily evaluated by cell adhesion studies using Chinese Hamster Lung (CHL) fibroblast cells.	An great increase in hydrophilicity and mechanical properties is observed for P(3HB-co-4HB)/BNC composite scaffold compared with pure P(3HB-co-4HB) scaffold. The cells incubated with composite scaffold for 48 h were capable of forming cell adhesion and proliferation, which showed better biocompatibility than pure P(3HB-co-4HB) scaffold. **(Zhijiang et al., 2012)**
	Collagen	Composite of BC and collagen by post-modification in an attempt to use the synergic beneficial aspects of both materials.	With the incorporation of collagen in the BNC, no changes happened in the crystal structure, but the thermal stability was improved. Tensile test results indicate that the Young's Modulus and tensile strength have a big increase while the elongation at break has a slight decrease. **(Zhijiang and Guang, 2011)**

- Commercially available BNC based medical and cosmetic products

BNC was approved by the FDA as a component of other products used in various clinical applications. FDA also indicated that BNC is the primary and sole component of some approved products for wound dressings. So, the high potential of BNC in wound care and in other medical areas lead to the development of clinical trials and some products are now available in the market. BOWIL Biotech Ltd. started the production of BNC wound dressings and BNC-based cosmetic products (face and eye masks) under the name of CELMAT®, using the BNC production method developed by Lodz University of Technology. In addition to this company there are several BNC-producing companies already known to the medical market. BioFill Industrias (currently, Fibrocel Produtos Biotecnologicos Ltd.) from Brazil and American Xylos Corporation have been already producing BNC on industrial scale for the application as dressings and internal implants for more than 10 years and today are well recognized as BNC medical products manufacturers.

Table 3 summarizes the use of BNC medical products already commercially available in different countries. Burns healing has been the leading area of BNC membranes application and still, wound dressings are the most recognizable medical products made of BNC.

Table 3 - Commercially available BNC based medical and cosmetic products. (Adapted from: Abeer et al., 2013; Ludwicka et al., 2016; Gama and Dourado et al., 2018).

Company (country)	Product Name /Type	Clinical Application
Fibrocel *Produtos Biotecnológicos*[a] (Brazil)	BioFill® Wound care system	Temporary substitute for human skin.
	BioProcess® Artificial skin	Skin transplant, treatment of third-degree burns, ulcers, and decubitus.
	NexFill® Wound care system	Dry bandage for burns and wounds.
	Gengiflex® Non-resorbable cellulose membrane	Bandage for dental wounds (Periodontitis).
Lohmann & Rauscher (Germany)	Suprasorb® X[b] Wound care system	HydroBalance wound dressing for lightly to moderately exuding, noninfected wounds.
	Suprasorb® X[b] + PHMB Wound care system	Antimicrobial HydroBalance wound dressing containing 0.3% polyhexamethylene biguanide, for lightly to moderately exuding wounds at risk of infection or infected.
Bowil Biotech (Poland)	CELMAT® Wound/Eye/Face	Hydrated wound dressing.
	CELMAT®Wound/Eye/Face H Protective dressings/jackets	Hydrated wound dressing containing sodium hyaluronate utilized in chronic wounds (pressure ulcers, diabetic ulcers, venous ulcers); atopic skin changes; partial-thickness dermal burns; face cosmetic treatments (i.e.: needleless or micro-needle mesotherapy, microdermabrasion, peeling, laser ablatio.
	CELMAT® Wound/Eye/Face P Protective dressings/jackets	Hydrated, antiseptic wound dressing containing polyhexanide- utilized after professional face treatments; after cosmetic procedures.
Cellulose Solutions (USA)	DermaFill[TM] Wound care dressing	Translucent wound dressing.
Xylos (USA)	Securian® Tissue reinforcement matrix	Macro-porous surgical mesh (tendo repair).
Synthes (USA)	SyntheCel®	Dura replacement devices (dura matter).
BC Genesis (USA)	BioCelltrix Surgical mesh	Surgical mesh.
POLYMET Jena (Germany)	BASYC Vessel implant (tubes)	Artificial blood vessels (CABG (Coronary artery bypass surgery).
[a]Earlier Biofill Industrias, Brazil; [b]Earlier XCell® delivered by Xylos, USA.		

2.3 BNC PRODUCTION STRATEGIES

2.3.1 BNC biosynthesis and its different commercial interest

BNC is produced by strictly aerobic bacteria without flagellum belonging to the genera *Gluconacetobacter (Acetobacter)*, *Rhizobium*, *Agrobacterium, Sarcina, Aerobacter* and others (Shoda and Sugano, 2005) in the air/culture medium interface, when grown in static culture. Bacteria produce an extracellular cellulose in the form of swollen membranes, depicted in Figure 14 and 15 A and B. *K. xylinus* is not able to metabolize glucose anaerobically due to the fact it lacks phosphofructose kinase, which is required for glycolysis (Lee et al., 2014; Reiniati et al., 2017).

BNC biosynthesis consists of a complex process which involves first the polymerization of glucose residues inside the bacteria, followed by the secretion and crystallization of β-1-4-glucan chains through hydrogen bounds and Van der Waals forces. The cellulose molecules are hierarchically arranged in strips, resulting in formation of a tough three-dimensional structure called microfibrils (Ross et al., 1991; Saxena et al., 1994; Lee et al., 2014; Jozala et al., 2016; Moniri et al., 2017). BNC generated by these bacterial species has special characteristics of unidirectional polarity and variable thickness. The crystallization mechanism of the microfibrils in *K. xylinus* can give rise to two cellulose forms, the cellulose I (parallel arrangement) and cellulose II (antiparallel). In *K. xylinus*, BNC synthesis is associated to the cycle of pentoses and of the Krebs cycle (Figure 14) (Ross et al., 1991; Lee et al., 2014; Lustri et al., 2015; Reiniati et al., 2017). Cellulose biosynthesis is a multi-step reaction involving individual enzymes, catalytic complexes and regulatory proteins. The four enzymatic steps for glucose conversion to BNC are: **1)** phosphorylation of glucose by glucokinase to glucose-6-phosphatase (Glc-6-P); **2)** isomerization of Glc-6-P to glucose-1-phosphate (Glc-1-P) by phosphoglucomutase (PGM); **3)** synthesis of uridine diphosphate glucose (UDP-glucose or UDPG) by UDPG-pyrophosphorylase (UGPase) and **4)** the synthesis of cellulose from UDP-glucose by cellulose synthase reaction which polymerizes the glucose units into the β-1,4-glucan chains. (Lee et al., 2014; Reiniati et al., 2017). UGPGase is a key enzyme in this process it is the direct cellulose precursor. UGPase is thought to play an important role in cellulose synthesis, as it is approximately one hundred times more active in cellulose producers (Lee et al., 2014; Reiniati et al., 2017, Jacek et al., 2019). The biosynthesis process is complex and not totally understood. Bacterial cellulose is synthesized by cellulose synthesis operon, which is a functional unit of genomic DNA containing multiple genes - *Acetobacter* cellulose synthesis operon (*acs*ABCD) and BNC synthesis operon (*bcs*ABCD). Bacteria produce cellulose from uridine diphosphate glucose (UDP-glucose) via a

protein complex Bcs operon (bacterial cellulose synthase), encodes three (*acs*AB, *acs*C, and *acs*D) or four (*bcs*A, *bcs*B, *bcs*C, and *bcs*D) subunits (Lee et al., 2014; Reiniati et al., 2017, Jacek et al., 2019).
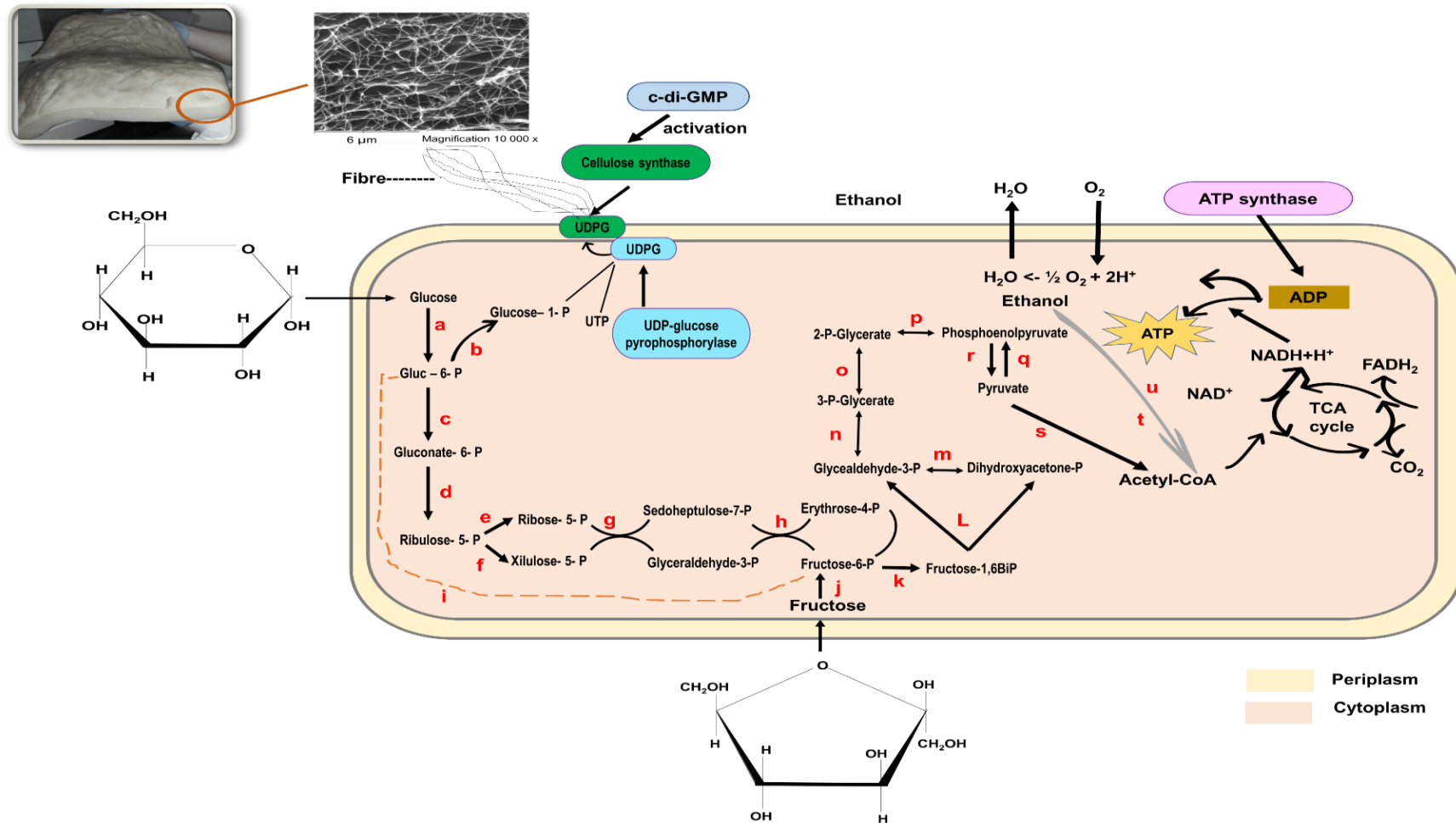
Figure 14 - Pathways for the biosynthesis of BNC by *K. xylinus* and assembly of cellulose molecules into nanofibrils: **(a)** Glucokinase-ATP, **(b)** Phosphoglucomutase, **(c)** Glucose-6-phosphate dehydrogenase, **(d)** 6-phosphogluconate dehydrogenase, **(e)** Phosphorribulose isomerase, **(f)** Phosphorribulose epimerase, **(g)** Transaketolase, **(h)** Transaldolase, **(i)** Phosphoglucoisomerase, **(j)** Fructokinase, **(k)** Fructokinase ATP, **(L)** Aldolase, **(m)** Triosephosphate isomerase, **(n)** Glyceraldehyde 3-phosphate dehydrogenase, **(o)** Phosphoglycerate mutase, **(p)** Enolase, **(q)** Pyruvate kinase **(r)** Pyruvate biphosphate kinase, **(s)** Pyruvate dehydrogenase, **(t)** Alcohol dehydrogenase and **(u)** Aldehyde dehydrogenase. (Adaptated from: Lee et al., 2014; Reiniati et al., 2017; Jacek et al., 2019).

The unique properties of BNC supports a wide range of applications in human and veterinary medicine, filter and acoustic membranes, biotechnological devices, textile, paper and food industry (Bielecki et al., 2012; Gama et al., 2016). BNC application in the medical and food markets has received particular attention over the past years. In the food segment, BNC could effectively be used as a low-calorie additive, thickener, stabilizer, texture modifier and as a vegetarian additive. BNC can be used in a variety of food formulations at low concentrations, as an additive to stabilize solid-liquid, liquid-liquid and gas-liquid colloidal systems. It has been shown to present excellent properties, namely lack of flavor, stability under broad pH and freeze-thaw conditions, in addition to excellent stabilizing properties (Dourado et al., 2016 and 2018; Gama and Dourado et al., 2018). Companies producing and commercializing BNC or BNC-based food products are mainly settled in Asian countries (Philippines, Vietnam, Thailand and Indonesia), where BNC is marketed under the name 'Nata de coco', where it is obtained from the fermentation of coconut water by cellulose-producing acetic acid bacteria, using traditional fermentation methods. Nata de coco is mostly incorporated into low-calorie sweetened desserts, fruit salads and high-fibre foods (Piadozo, 2016; Phisalaphong et al., 2016; Dourado et al., 2018).

In the US, Cetus Co. (Berkeley, CA) and Weyerhaeuser Co. (Seattle, WA) have used a patented, genetically modified *Acetobacter* strain for the fermentation of BNC under agitated culture (using a deep-tank fermentation technique). The obtained BNC, Cellulon®, is used as a food stabilizer and thickener. Kelco, Inc. (Lexington, KY) launched the product under the brand PrimaCels®, which is also used in the food industry (Vandamme et al., 1998; Czaja et al., 2006; Abeer et al., 2013; Dourado et al., 2018). Currently, with the exception of nata de coco, there are no other commercially available BNC products for food applications.

A fermentative process affording high BNC yields with low investment and operating costs will allow the release onto the market of a product with a range of potential applications for biomedical and non-biomedical applications. The economic feasibility of BNC production is directly dependent on its production (BNC yield).

2.3.2 Fermentative production of BNC

Much effort has been devoted to designing an economical process for BNC production (Table 4), by optimizing both upstream and downstream processes, including the evaluation of several culture media compositions, culture conditions (pH, temperature and oxygen transfer rate), fermentation systems (using agitated, airlift, membrane and horizontal bioreactors), overproducing mutant strains (genetic

engineering), and postproduction modification processes. The most commonly used medium is the Hestrin–Schramm (HS); however other adequate media include Yamanaka's and corn steep liquor (CSL)-fructose media (Hestrin & Schramm, 1954; Yamanaka et al., 1989; Chao et al., 2001). Date syrup (Moosavi-Nasab and Yousefi, 2011) and molasses (Çakar et al., 2014) have also been used to decrease the production cost, showing competitive results when comparing to the traditional HS and Yamanaka media (Table 4). The optimal growth conditions for *Gluconacetobacter* strains are between 20 and 30 °C and in a pH range between 4.0 and 7.0 (Thakur, 2015).

Two fermentation methods have been traditionally explored to produce BNC: the static and the agitated culture. The selection of the production method depends on the final application of BNC as the physical, mechanical and morphological characteristics vary based on the culture process. Under static conditions, BNC production occurs at the air–water interface, where the assembly of reticulated crystalline ribbons results in a gel or pellicle (Figure 15 A and B). The pellicle grows downward until the entrapped cells become inactive and eventually die, due to oxygen and nutrient deprivation. Alternatively, BNC may be produced by submerged fermentation in aerated (*e.g.* airlift) or agitated culture (*e.g.* stirring tank) (Figure 15 C). An advantage of the stirring tank reactor consists in its ability to prevent the heterogeneity of the culture broth by strong mechanical agitation, whereas the high energy requirements to generate mechanical power represents its major drawback. Contrarily, the energy requirements of an airlift reactor is typically one-sixth of that of a stirred tank reactor. However, the agitation power of an airlift reactor is limited, resulting in low fluidity of the culture broth, especially at high cellulose concentrations. Both agitation and aeration systems can result in cellulose-negative mutants (non-cellulose producers, Cel[-]), highly branched, three-dimensional, reticulated BNC structure (thus limiting BNC applications). With membrane bioreactors, the major drawbacks include the high operating costs and the difficulty in collecting the cellulose from the reactors (Chawla et al., 2009; Andrade et al., 2010; Shah et al., 2013; Keshk et al., 2014; Lee et al., 2014; Dourado et al., 2018).
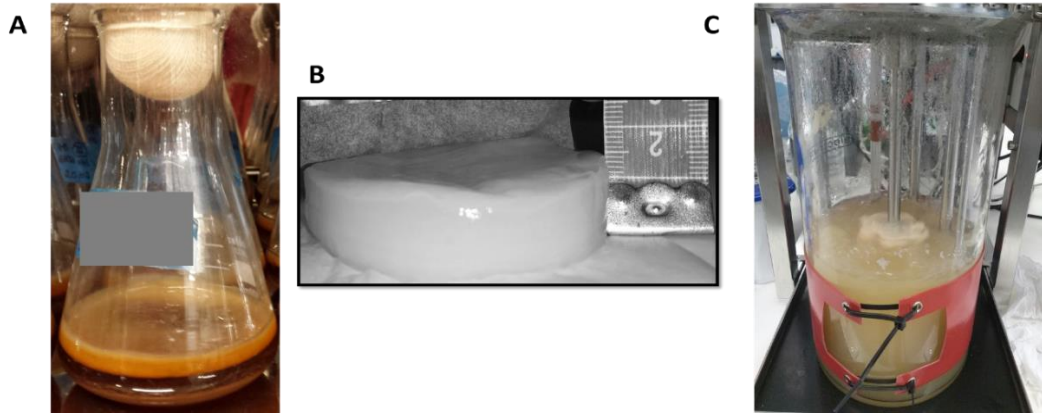
Figure 15 - BNC membranes**. A)** BNC production by *K. xylinum* BPR 2001 (ATCC 700178) using optimized fermentation media under static culture. **B)** BNC membrane produced in static culture after purification. **C)** BNC production under agitated conditions.

Table 4 - Summary of a literature survey on BNC production with different strains and different culture conditions.

Strain	Medium composition			Culture conditions				Best results (BNC yield)	Obs
	Carbon Source	Nitrogen Source	Additives	pH	Temperature	Culture time	Type of culture		
IFO 13693 (Masaoka et al., 1993)	D-Glucose (0.5 % w/v)	Peptone (2 % w/v) Yeast extract (0.5 % w/v)	Hestrin-Schramm medium; Ethanol (0.2 % v/v)	6	30 °C	3 d	Static	10.8 g/L	Cellulose production rate 36 g/d.m²
AJ 12712 (Watanabe et al., 1995)	Sucrose (5 % w/v)	Yeast extract (0.5 % w/v)	Complex medium	5	30 °C	7 d	Static	22.1 % (g BNC/g sucrose)	Best result with 10 % oxygen
KU-1 (Oikawa et al., 1995)	D-Mannitol (2 % w/v)	Yeast Extract (0.5 % w/v) Polypeptone (0.5 % w/v)		6	30 °C	168 h	Static	4.6 g/L	Best result with D-Mannitol 1.5 % (w/v)
ITDI 2.1 (De Wulf et al., 1996)	Coconut water (sucrose 10 % w/v)		Dipotassium phosphate (0.3 % w/v)	4,5	30 °C	7-8 d	Static	12.53 g/L	
LMG 1518 (Bernardo et al., 1998)	Sucrose (7 % w/v); Glucose (3.5 % w/v)	not reported	Acetic acid (0.75 % v/v)	5,5	no description	100 h	Static	28.4 g/L	
E25 (Krystynowicz et al., 2002)	Glucose (2 % w/v)	Yeast Extract (0.5 % w/v) Bacto Peptone (0.5 % w/v)	Ethanol (1 % v/v), Magnesium sulfate heptahydrate (0.005 % w/v)	5.7	30 °C	7 d	Static	3.5 g/L	
IFO 13693 (Keshk and Sameshima, 2006)	D – Glucose (2.0 % w/v)	Peptone (0.5 % w/v) Yeast extract (0.5 % w/v)	Lignosulfonate (1 % w/v)	6	28 °C	7 d	Static	16.32 g/L	Lignosulfonate reduces the concentration of gluconic acid
IFO 13772 Keshk and Sameshima, 2006	Sugar cane molasses (4 % w/v)	Peptone (0.5 % w/v) Yeast extract (0.5 % w/v)	Lignosulfonate (1 % w/v)	6	28 °C	7 d	Static (90-mm petri dishes)	5.99 g/L	Best results without lignosulfonates: 5.79 g/L
ATCC 10245 (Keshk et al., 2006)	Molasses (2 % w/v)	Yeast Extract (0.5 % w/v) Bacto Peptone (2.9 % w/v)	Hestrin- Schramm medium	6	28 °C	5 d	Static	7 g/L	Molasses hydrolyzate

Table 4 - (continuation)

Strain	Medium composition			Culture conditions				Best results (BNC yield)	Obs
	Carbon Source	Nitrogen Source	Additives	pH	Temperature	Culture time	Type of culture		
ATCC 10245 (Premjet et al., 2007)	Sugar cane molasses (7 % w/v)	Peptone (0.5 % w/v) Yeast extract (0.5 % w/v)	Study of different component addition (amino acids, vitamins, carbohydrates, minerals, non-nitrogenous acids and nucleic acids bases	6	29 °C	7 d	Static	2.4 g/L	Best results with non-supplemented medium
K3 (Nguyen et al., 2008)	Mannitol (2 % w/v)	Corn Steep Liquor (4 % w/v)	HS medium Green tea (0.3 % w/v)	5	30 °C	7 d	Static	3.34 g/L	Isolated from Kombucha
ATCC 53524 (Mikkelsen et al., 2009)	Sucrose (2 % w/v)	Peptone (0.5 % w/v) Yeast extract (0.5 % w/v)		5	30 °C	96 h	Static	3.83 g/L	
NBRC 13693 (Kurosumi et al., 2009)	Fruit Juice	Peptone (2 % w/v) Yeast extract (0.5 % w/v)	Orange; Pineaple; Apple; Japanese pear; Grape	6	30 °C		Static	5.8 g/L	Best results with orange juice
AGR 60 (Kanjanamosit et al., 2010)	Coconut water (sucrose 5 % w/v)	Ammonium sulfate (0.5 % w/v)	Acetic acid (1.0 % v/v) Alginate		30 °C	7 d	Static	-	Morphological analyses of the membranes
BCRC 12335 (Chen et al., 2011)	Mannitol (2.5 % w/v)	Peptone (0.3 % w/v) Yeast extract (0.5 % w/v)	Carboxymethyl cellulose (0-1 % w/v)		30 °C	14 d	Static	-	Water Holding Capacity and crystallinity improved with Carboxymethyl cellulose
CGMCC 2955 (Liu, et al., 2017)	Glucose (2.5 % w/v)	Peptone (1 % w/v) Yeast extract (0.7 5 % w/v),	disodium phosphate (1 % w/v)	6	30 °C	15 d	Static	4.3 g/L	conversion rate 184.7 mg/g
Acetobacter xylinum 0416 (Lotfiman et al., 2016)	extracted date syrup (2 and 3 % w/v)	Peptone (0.5 % w/v) yeast extract (0.5 % w/v	Na_2HPO_4 (0.27 % w/v) citric acid (0.115 % w/v)	5	30 °C	10 d	Static	5.8 g/L	3 % extracted syrup

Table 4 - (continuation)

Strain	Medium composition			Culture conditions				Best results (BNC yield)	Obs
	Carbon Source	Nitrogen Source	Additives	pH	Temperature	Culture time	Type of culture		
K. medellinensis (Molina-Ramirez et al., 2017)	glucose, fructose, and sucrose (1, 2, and 3 % w/v)	yeast extract (0.5 % w/v) peptone (0.5 % w/v)	Na₂HPO₄ (0.267 % w/v) citric acid (0.115 % w/v)	3.6	30 °C	8 d	Static	3.5 g/L	2 % (w/v) glucose
CH001 (Yang et al., 2016)	Litchi extract	sago liquid waste medium contained sucrose (20 % w/v) ammonium sulfate (1.5 % w/v)		5	28 °C	14 d	Static	2.53 g/L.	
BC-11 (Zhao et al., 2018)	Reducing sugar: from fermentation wastewater (15 % w/v)			7	30 °C	10 d	Static	1.117 g/L fermentation wastewater 1.757 g/L HS medium	
ATCC 23770 (Chen et al., 2013)	Total sugars: From Wheat straw hydrolysate (1.2 % w/v)	Peptone (0.3 % w/v) yeast extract (0.5 % w/v)		5	30 °C	7 d	Static	8.3 g/L	
K .europaeus SGP37 (Dubey et al., 2017)	Glucose (2 % w/v)	Yeast extract and peptone (0.5 % w/v)	HS medium and alternative medium (fructose, sucrose) sodium pyruvate, ethanol, n-propanol, isoamyl alcohol, gallic acid, tartaric acid, oxalic acid	6	30 °C	15 d	Static	9.98 ± 0.24 g/L BNC at the expense of 12.08 ± 1.94 g/L	conversion yield of 0.82 g BNC/g
***Acetobacter sp.* A9** (Son et al., 2001)	Glucose (2 % w/v)	Yeast Extract (0.5 % w/v) Polypeptone (0.5 % w/v)	Ethanol (0-2 % v/v)	6.5	30 °C	8 d	Agitated (200 rpm)	15.2 g/L	Isolated from apple
ATCC 23767 (Cheng et al., 2017)	agricultural corn stalk pre-hydrolysate	Baco-Peptone (0.5 % w/v)	Ethanol (0.5 % v/v)	5	30 °C	7 d	Static	2.86 g/L	

Table 4 - (continuation)

Strain	Medium composition			Culture conditions				Best results (BNC yield)	Obs
	Carbon Source	Nitrogen Source	Additives	pH	Temperature	Culture time	Type of culture		
G. xylinus **CH001** (Luo et al., 2017)	durian shell dilute acid hydrolysate (8 % v/v)	Peptone (0.5 % w/v) Yeast extract (0.5 % w/v)		6	28 °C	10 d	Static	2.67 g/L at the 8 day	Durian - is one tropical fruit with high nutritional value, but its shell is usually useless and considered as waste.
G. hansenii **UCP1619** (Costa et al., 2017)	Sugarcane molasses (2 % w/v) Glucose (2 % w/v) Acetylated glucose (2 % w/v)	CSL (0.5 % w/v) Peptone (0.5 % w/v) Yeast extract (0.5 % w/v)	Jeans laundry effluent	5-6	30 °C	10 d	Static	9.63 g/L	Using 1.5 % (w/v) of glucose, 2.5 % (w/v) of CSL, 0.27 % (w/v) disodium phosphate and 0.15 % (w/v) citric acid monohydrate
AJ 12368 (Okiyama et al., 1992)	Sucrose (5 % w/v)	Yeast extract (0.5 % w/v)	Ammonium hydrogen sulphate (0.5 % w/v), Monopotassium phosphate (0.3 % w/v) Magnesium sulfate heptahydrate (0.000 5 % w/v)	5	30 °C	3 d+3 d	Agitated (air-lift fermenter) + Static (petri dishes)	1.07 g/L	
BPR 3001A (Naritomi et al., 2002)	Fructose (7 % w/v)	CSL (4 % w/v)	Complex medium	5	30 °C	48 h	Fed-batch Agitated (1L jar fermenter)	27.9 % of fructose convertion	Best result in batch culture (60mL of medium)
Acetobacter sp. **A9** (Heo and Son, 2002)	Glucose (4 % w/v)	Yeast Extract (0.1 % w/v) Polypeptone (0.7 % w/v)	Complex medium		30 °C	7 d	Agitated	7.21 g/L	Best result with 1.4 % (w/v) Ethanol
K. Xylinus sp. **St60-12** (Seto et al., 2006)	Sucrose (4 % w/v)	CSL (4 % w/v)		-	28 °C	72 h	Agitated (150 rpm)	4.5 g/L	
Acetobacter sp. **V6** (Son et al., 2003)	Glucose (1 % w/v)		Ethanol, lactic acid, acetic acid, fumaric acid, pyruvic acid, succinic acid, inorganic salts	6.5	30 °C	8 d	Agitated (200 rpm)	4.16 g/L	Best results with synthetic medium

Table 4 - (continuation)

Strain	Medium composition			Culture conditions				Best results (BC yield)	Obs
	Carbon Source	Nitrogen Source	Additives	pH	Temperature	Culture time	Type of culture		
Gluconacetobacter hansenii PJK (KCTC 10505BP) (Park et al., 2002)	Glucose (1 % w/v)	Peptone (1 % w/v) Yeast extract (0.7 % w/v)	Ethanol (0-2 % v/v)	5	30 °C	5 d	Agitated (200 rpm)	2.31 g/L	Best result with 1 % (v/v) Ethanol
Gluconacetobacter hansenii PJK (KCTC 10505BP) (Jung et al., 2005)	Glucose (1 % w/v)	Peptone (1 % w/v) Yeast extract (0.7 % w/v)	Ethanol (1 % v/v)	5	30 °C	48 h	Agitated (Jar-fermenter 200 rpm)	1.72 g/L	Best result with 1 % (v/v) Ethanol
NUST4.1 (Zhou et al., 2007)	Glucose (2 % w/v)	Corn Steep Liquor (2 % w/v)	Sodium alginate (0-0.1 % w/v)	6	29 °C	5 d	Agitated (150 rpm)	6.0 g/L	Best result with 0.4 % (w/v) sodium alginate
PJK (KCTC 10505BP) (Jung et al., 2007)	Glucose (1 % w/v)	Peptone (1 % w/v) Yeast extract (0.7 % w/v)	Ethanol (1 % v/v)	5	30 °C	140 h	Agitated (Jar-fermenter with spin filter)	4.57 g/L	Best result with aeration 1 vvm
RKY5 (KCTC 10683BP) (Kim et al., 2007)	Glucose (2 % w/v)	Peptone (0.5 % w/v) Yeast extract (0.5 % w/v)		-	30 °C	96 h	Agitated (rotatory biofilm contactor)	6.15 g/L	
DSM 46604 (Adnan et al., 2017)	D-glucose (4 – 10 % w/v)	Peptone (0.5 % w/v) (NH₄)₂SO₄ (0.3 % w/v)	magnesium heptahydrate (0.005 % w/v)	6.8	30 °C	5 d	Agitated (150 rpm shake-flasks)	1,113 g/L (5 % w/v glucose)	
0416 (Esa et al., 2017)	Glucose Matured coconut water (8 % w/v)		Ammonium sulphate (0.5 % w/v)	5.5	30 °C	7 d	Agitated (200 rpm incubator shaker)	0.137 g	
BRC5 (Yang et al., 1998)	Glucose (2 % w/v)	CSL (8 % w/v)	Oxygen enriched air; Ethanol	5.5	30 °C	50 h	Agitated (5L Jar fermenter)	15.3 g/L	Best result with 10 % oxygen
BRC5 (Vandamme et al., 1998)	Fructose (3.5 % w/v); Glucose (0.5 % w/v)	CSL (8 % w/v)	carbon substrate supply (0.5 % w/v)	6	30 °C	48 h	Fed-batch Agitated (5L Jar fermentor)	6.8 g/L	

The need to upgrade the traditional BNC fermentation method has for long been recognized. The scientific literature conveys the idea that the technological production of BNC is extremely expensive. For a successful development of a plant design, location and layout, the availability of raw materials, structural design, utilities, storage facilities, material handling, safety, waste disposal, taxations, patents, transportation and markets need to be considered. Biotechnological processes can only be performed by controlling several operating parameters (such as fermentation time, temperature, pH, substrate pre-treatment, inoculum–substrate ratio) and using optimized fermentation medium. Extensive studies have been dedicated to determining the scientific and technological factors mediating BNC production. As observed by Dourado et al., (2016 and 2018) through process simulation using software SuperProDesigner software (Inteligen, Inc.), biotechnological processes require high capital investments as compared with traditional methods. Coupled to the low BNC yields, and despite the use of low-cost substrate in these simulations, the high capital investment and high operating costs associated, present a strong economic constraint to the commercialization of BNC at a "low" cost (compared to nata de coco). Moreover, results in those studies showed that, although it is possible to devise an economically feasible biotechnological process for BNC production, the high selling costs would indeed restrain BNC to high-value niche markets.

2.4 REFERENCES

Abbruzzese, L., Rizzo, L., Fanelli, G., Tedeschi, A., Scatena, A., Goretti, C., et al. 2009. Effectiveness and safety of a novel gel dressing in the management of neuropathic leg ulcers in diabetic patients: a prospective double-blind randomized trial. The International Journal of Lower Extremity Wounds. 8: 134–140.

Abeer, M. M., Amin, M. C. I. M., Martin, Claire. 2014. A review of bacterial cellulose-based drug delivery systems: their biochemistry, current approaches and future prospects. Journal of Pharmacy and Pharmacology. 66: 1047–1061.

Adnan, A., Nair, G. R., Lay, M. C., Swan, J. E., Umar, R., Yursa, F.I. 2017. Influences of saccharides types and initial glucose concentration of microbial cellulose production by *G. xylinus*. Journal of Fundamental and Applied Sciences. 9(2S): 174-181.

Ahmed, E., 2015. Hydrogel: Preparation, characterization, and applications: A review. Journal of Advanced Research. 6: 105–121.

Ali, S .M. and Yosipovitch, G. 2013. Skin pH : From Basic Science to Basic Skin Care. Acta Dermato- venereologica. 93(3): 261–267.

Amnuaikit, T., Chusuit, T., Raknam, P., Boonme, P. 2011. Effects of a cellulose mask synthesized by a bacterium on facial skin characteristics and user satisfaction. Medical Devices Evidence Research. 4: 77–81.

Andrade, F. K, Pertile, R. A. N., Dourado, F., Gama, F. M. 2010. Bacterial cellulose: Properties, production and applications. In: Lejeune A, Deprez T (Eds.). *"Cellulose: Structure and Properties, Derivatives and Industrial Uses ".* New York: Nova Science Publishers. 427–458.

Andrade, F.K., et al., 2010. Improving the affinity of fibroblasts for bacterial cellulose using carbohydrate-binding modules fused to RGD. Journal of Biomedical Materials Research Part A. 92A(1): 9-17.

Antal, A. S., Dombrowski, Y., Koglin, S., Ruzicka, T., Schauber, J. 2011. Impact of vitamin D_3 on cutaneous immunity and antimicrobial peptide expression. Dermato-Endocrinology. 3(1): 18-22.

Arul, V., Masilamoni, J. G., Jesudason, E. P., Jaji, P. J., Inayathullah, M., Dicky John, D. G., Vignesh, S., Jayakumar, R. 2012. Glucose oxidase incorporated collagen matrices for dermal wound repair in diabetic rat models: a biochemical study. Journal of Biomaterials Applications. 26: 917- 38.

Aya, K. L. and Stern R. 2014. Hyaluronan in wound healing: Rediscovering a major player. Wound Repair and Regeneration. 22: 579–593.

Bandurska, K., Berdowska, A., Barczynska-Felusiak, R., Krupa, P. 2015. Unique features of human cathelicidin LL-37. International Union of Biochemistry and Molecular Biology. 41(5):289–300.

Bardan, A., Nizet, V., Gallo, R. L. 2004. Antimicrobial peptides and the skin. Expert Opinion on Biological Therapy. 4(4):543-549.

Bayaty, F., Abdulla, M., Hassan, M. I. A., Masud, M. 2010. Wound healing potential by hyaluronate gel in streptozotocin-induced diabetic rats. Scientific Research and Essays. 5: 2756-60.

Ben-shalom, N., Zvi, N., Abraham, P., Dror, R. 2009. Novel injectable chitosan mixtures forming hydrogels. EP2121026 2009.

Bernard, J. J., and Gallo, R. L. 2011. Protecting the boundary: the sentinel role of host defense peptides in the skin. Cellular and Molecular Life Science. 68: 2189–2199.

Bernardo, E. B., Neilan, B. A., Couperwhite, I. 1998. Characterization, Differentiation and Identification of Wild-type Cellulose-synthesizing Acetobacter strains Involved in Nata de Coco Production. Sytematic and Applied Microbiology. 21: 599–608.

Bielecki, S., Kalinowska, H., Krystynowicz,A., Katarzyna. K., Kolodziejczyk, M., De Groeve, M. 2012. Bacterial Nanocellulose: A Sophisticated Multifunctional Material, CRC Press, Taylor & Francis Group, Boca Raton, FL.157–174.

Bikker, A., Wielders, J., van Loo, R., Loubert, M. 2016. Ascorbic acid deficiency impairs wound healing in surgical patients: Four case reports. International Journal of Surgery Open 2. 2:15-18.

Bikle, D. 2017. Vitamin D: Production, Metabolism, and Mechanisms of Action. Endotext. Available at: https://www.ncbi.nlm.nih.gov/books/NBK278935/.

Bikle, D. D. 2007. What is new in vitamin D: 2006–2007. Current Opinion in Rheumatology. 19: 383–8.

Biswaro, L. S., Sousa, M. G. da C., Rezende, T. M. B., Dias, S. C., Franco, O. L. 2018. Antimicrobial Peptides and Nanotechnology, Recent Advances and Challenges. Frontiers in Microbiology.

Blais, M., Parenteau-Bareil, R., Cadau, S., Berthod, F. 2013. Concise review: tissue- engineered skin and nerve regeneration in burn treatment. Stem Cells Translational Medicine. 2: 545–551.

Boateng, J. and Catanzano, O. 2015. Advanced Therapeutic Dressings for Effective Wound Healing—A Review. Journal of Pharmaceutical Sciences. 104: 3653–3680.

Boateng, J. S., Matthews, K. H., Stevens, H. N.E., Eccleston, G. M. 2008. Wound Healing Dressings and Drug Delivery Systems: A Review. Journal of Pharmaceutical Sciences. 97(8):2892-2923.

Bottan, S., Robotti, F., Jayathissa, P., Hegglin, A., Bahamonde, N., Heredia-Guerrero, J. A., et al. 2014. Surface-structured bacterial cellulose with guided assembly-based biolithography (GAB). ACS Nano. 9: 206–219.

Broderick, N. 2009. Understanding chronic wound healing. Nurse Practitioner 34(10): 16–22.

Brown, R.M., 2004. Cellulose structure and biosynthesis: what is in store for the 21st century? Journal of Polymer Science Part A: Polymer Chemistry. 42(3): 487-495.

Bucki, R., Leszczynska, K., Namiot, A., Sokołowski, W. 2010. Cathelicidin LL-37: A Multitask Antimicrobial Peptide. Archivum Immunologiae et Therapiae Experimentalis. 58:15–25.

Burdick, J. A. and Prestwich, G. D. 2011. Hyaluronic Acid Hydrogels for Biomedical Applications. Advanced Materials. 23(12): H41–H56.

Burkiewicz, C. J. C. C., Guadagnin, F. A., Skare, T. L., do Nascimento, M. M., Servin, S. C. N., de Souza, G. D. 2012. Vitamin D and skin repair: a prospective, double-blind and placebo controlled study in the healing of leg ulcers. Revista do Colegio Brasileiro de Cirurgioes. 39: 401–7.

Cai, Z.-X., Mo, X.-M., Zhang, K.-H., Fan, L.-P., Yin, A.-l., He, C.-l., et al. 2010. Fabrication of chitosan/silk fibroin composite nanofibers for wound-dressing applications. International Journal of Molecular Sciences. 11: 3529–39.

Çakar, F., Özer, I., Aytekin, A. Ö., Şahin, F. 2014. Improvement production of bacterial cellulose by semi-continuous process in molasses medium. Carbohydrate Polymers. 106: 7–13.

Carr, A. C. and Maggini, S. 2017. Vitamin C and Immune Function. Nutrients. 9(11): 1211.

Carretero, M., Escámez, M. J., García, M., Duarte, B., Holguín, A., Retamosa, L., et al. 2008. *In vitro* and *in vivo* wound healing-promoting activities of human cathelicidin LL-37. Journal of Investigative Dermatology. 128: 223–236.

Chao, Y. P., Sugano, Y., Shoda, M. 2001. Bacterial cellulose production under oxygen-enriched air at different fructose concentrations in a 50-L, internal-loop airlift reactor. Applied Microbiology and Biotechnology. 55: 673–9.

Chawla, P. R., Bajaj, I. B., Survase, S. A., Singhal RS. 2009. Microbial cellulose: Fermentative production and applications. Food Technology and Biotechnology. 47(2): 107–124.

Chen, H.-H., Chen, L.-C., Huang, H.-C., Lin, S.-B. 2011. In situ modification of bacterial cellulose nanostructure by adding CMC during the growth of *Gluconacetobacter xylinus.* Cellulose. 18: 1573–1583.

Chen, L., Hong, F., Yang, X.-X., Han, S.-F. 2013. Biotransformation of wheat straw to bacterial cellulose and its mechanism. Bioresource Technology. 135: 464–468.

Cheng, Z., Yang, R., Liu, Xu, Liu, X., Chen, H. 2017. Green synthesis of bacterial cellulose via acetic acid pre-hydrolysis liquor of agricultural corn stalk used as carbon source. Bioresource Technology 234: 8–14.

Chereddy, K.K., Her, C.-H., Comune, M. et al. 2014. PLGA nanoparticles loaded with host defense peptide LL37 promote wound healing. Journal Controlled Release. 194: 138–147.

Chiaoprakobkij, N., Sanchavanakit, N., Subbalekha, K., Pavasant, P., Phisalaphong, M. 2011. Characterization and biocompatibility of bacterial cellulose/alginate composite sponges with human keratinocytes and gingival fibroblastos. Carbohydrate Polymers. 85: 548–553.

Chiquet, M., Gelman, L., Lutz, R., Maier, S. 2009. From mechano transduction to extracellular matrix gene expression in fibroblasts. Biochimica et Biophysica Acta 1793: 911–920.

Choi, K. Y., Chung, H., Min, K. H., Yoon, H. Y., Kim, K., Park, J. H., *et al*. 2010. Self-assembled hyaluronic acid nanoparticles for active tumor targeting. Biomaterials. 31(1): 106-114.

Christakos, S, Dhawan, P., Verstuyf, A., Verlinden, L., Carmeliet, G. 2016. Vitamin D: Metabolism, Molecular Mechanism of Action, and Pleiotropic Effects. Physiological Reviews. 96(1): 365–408.

Chu, Y., Yu, D., Wang, P., Xu, J., Li, D., Ding, M. 2010. Nanotechnology promotes the full thickness diabetic wound healing effect of recombinant human epidermal growth factor in diabetic rats. Wound Repair and Regeneration: Official Publication of the Wound Healing Society and the European Tissue Repair Society. 18: 499-505.

Cooper, R. 2004. A review of te evidence for the use of topical antimicrobial agents in wound care.

Cooper, S. 2002. The biology of the skin. Journal of the Royal Society of Medicine. 95: 109 -109.

Costa, A. F. S., Almeida, F. C. G., Vinhas, G. M., Sarubbo, L. A. 2017. Production of Bacterial Cellulose by *Gluconacetobacter hansenii* using Corn Steep Liquor as Nutrient Sources. Frontiers in Microbiology. 8 (2027): 1-12.

Cross, S. E. 1998. Topical Therapeutic Agents Used in Wound Care. Dermal Absorption and Toxicity Assessment, Marcel Dekker, New York.

Czaja, W. K., Young, D. J., Kawecki, M., Brown, R. M. 2007a. The future prospects of microbial cellulose in biomedical applications. Biomacromolecules. 8: 1–12.

Czaja, W., Krystynowicz, A. Kawecki, M. Wysota, K. Sakiel, S. Wroblewski, P. Glik, J. Nowak, P. Bielecki S. 2007b. Biomedical Applications of Microbial Cellulose in Burn Wound Recovery. In: "Cellulose: Molecular and Structural Biology". Springer. 307–321.

Czaja, W., Krystynowicz, A., Bielecki, S., Brown, J. R. R. 2006. Microbial cellulose-The natural power to heal wounds. Biomaterials. 27(2): 145–151.

Damodarasamy, M., Johnson, R. S., Bentov, I., MacCoss, M. J., Vernon, R. B., Reed, M. J. 2014. Hyaluronan enhances wound repair and increases collagen III in aged dermal wounds. Wound Repair and Regeneration. 22(4):521–526.

De Wulf, P., Joris, K., Vandamme, E. J. 1996. Improved Cellulose Formation by an *Acetobacter xylinum* Mutant Limited in (keto)GLuconate Synthesis. Journal of Chemical Technology and Biotechnology 67: 376-380.

Debele, T.A., Mekuria, S.L., Tsai, H.-C., 2016. Polysaccharide based nanogels in the drug delivery system: application as the carrier of pharmaceutical agents. Materials Science and Engineering C. 68:964–981.

Dhivya, S., Padma, V. V., Santhini, E. 2015. Wound dressings – a review. Biomedicine. 5: 22.

Di Rosa, M., Malaguarnera, M., Nicoletti, F., Malaguarnera, L. 2011. Vitamin D$_3$: a helpful immuno-modulator. Immunology. 134: 123–139.

Diamond, G., Beckloff, N., Weinberg, A., Kisic, K. O. 2009. The Roles of Antimicrobial Peptides in Innate Host Defense. Current Pharmaceutical Design. 15(21): 2377-92.

Dong, X., Xu, J., Wang, W., Hao Luo, Liang, X., Zhang, L., Wang, H., Wang, P., Chan, J. 2008. Repair effect of diabetic ulcers with recombinant human epidermal growth factor loaded by sustained release microspheres. Science in China Series C: Life Sciences. 51: 1039-44.

Dourado, F., Fontão, A. I., Leal, M., Rodrigues, A. C., Gama, M. 2018. Chapter 1 - Process Modeling and Techno-Economic Evaluation of an Industrial Air-Lift Bacterial Cellulose Fermentation Process. In "Nanocellulose and Sustainability: Production, Properties, Applications, and Case Studies". Ed.: Koon-Yang Lee, CRC Press; Taylor & Francis Group. Boca Raton. 1-16. ISBN: 978-1-498-76103-1.

Dourado, F., Leal, M., Martins, D., Fontão, A., Rodrigues, A., C., Gama, M. 2016. Chapter 7- Cellulose as Food Ingredients/Additives: Is there a Room for BNC?, In "Bacterial Nanocellulose: from biotechnology to bio-economy". Ed.: Gama, M., Bielecky, S., Dourado, F. Elsevier; Amsterdam, Netherlands. 123–133. ISBN: 978-0-444-63458-0.

Dubey, W., Sharma, R. K., Agarwal, P., Singh, J., Sinha, N., Singh, R. P. 2017. From rotten grapes to industrial exploitation: *Komagataeibacter europaeus* SGP37, a micro-factory for macroscale production of bacterial nanocellulose. International Journal of Biological Macromolecules. 96: 52–60.

DuBose, J. W., Cutshall, C., Metters, A. T. 2005. Controlled release of tethered molecules via engineered hydrogel degradation: Model development and validation. Journal of Biomedical Materials Research A. 74(1): 104–116.

Dürr, U. H. N., Sudheendra, U. S., Ramamoorthy, A. 2006. LL-37, the only human member of the cathelicidin family of antimicrobial peptides. Biochimica et Biophysica Acta (BBA) – Biomembranes. 1758(9): 1408-1425.

Elson, M. L. and Tennessee, M. D. N. 1998. The role of retinoids in wound healing. 39(2): Supplement 2, S79–S81.

Enoch, S., Grey, J. E., Harding, K. G. 2006. Recent advances and emerging treatments. Bmj 332, 962–965.

Erfurt-Berge, C. and Renner, R. 2015. Chronic wounds – Recommendations for diagnostics and therapy. Reviews in Vascular Medicine. 3(1): 5-9.

Esa, F., Rahman, N. Abd., Kalil, M. S., Tasirin, S. M. 2017. Effects of agitation conditions on bacterial cellulose production by *Acetobacter xylinum 0416* in fermentation of matured coconut water medium. Malaysian Journal of Analytical Sciences. 21(1): 261-266.

Fallacara, A., Baldini, E., Manfredini, S., Vertuani, S. 2018. Hyaluronic Acid in the Third Millennium. Polymers. 10: 701.

Fonder, M. A., Lazarus, G. S., Cowan, D. A., Aronson-Cook, B., Kohli, A. R., Mamelak, A. J. 2008. Treating the chronic wound: A practical approach to the care of nonhealing wounds and wound care dressings. Journal of the American Academy of Dermatology. 58: 185–206.

Frykberg, R.G. and Banks, J. 2015. Challenges in the treatment of chronic wounds. Advances in Wound Care. 4: 560–582.

Fu, L., Zhang, Y., Li, C., Wu, Z., Zhuo, Q., Huang, X., et al. 2012. Skin tissue repair materials from bacterial cellulose by a multilayer fermentation method. Journal of Materials Chemistry. 22: 12349–12357.

Fumakia, M. and Ho E. A. 2016. Nanoparticles Encapsulated with LL37 and Serpin A1 Promotes Wound Healing and Synergistically Enhances Antibacterial Activity. Molecular Pharmaceutics. 13: 2318–2331.

Gama, F. M. and Dourado, F. 2018. Bacterial NanoCellulose: what future? BioImpacts, 8(1): 1-3.

Gama, M., Dourado, F., Bielecki, S. 2016. Bacterial nanocellulose a sophisticated multifunctional material. ELSEVIER.

García, M. C., and Cuggino, J. C. 2018. Stimulus-responsive nanogels for drug delivery. In: Stimuli Responsive Polymeric Nanocarriers for Drug Delivery Applications, 1(12): 321–341.

Gaspar, M. M., Cruz, A., Fraga, A. G., Castro, A. G., Cruz, M. E., and Pedrosa, J. 2008. Developments on drug delivery systems for the treatment of mycobacterial infections. Current Topics in Medicinal Chemistry, 8(7): 579-591.

Gilaberte, Y., Prieto-Torres, L., Pastushenko, I., Juarranz, A. 2016. Anatomy and Function of the Ski. Nanoscience in Dermatology. 1-14.

Goldman, R. 2004. Growth factors and chronic wound healing: Past, present, and future. Advances in Skin Wound Care. 17: 24–35.

Gombart, A. F. 2011. The vitamin D-antimicrobial peptide pathway and its role in protection against infection. Future Microbiology. 4: 1151–1165.

Gombart, A. F., Borregaard, N., Koeffler, H. P. 2005. Human cathelicidin antimicrobial peptide (CAMP) gene is a direct target of the vitamin D receptor and is strongly up-regulated in myeloid cells by 1,25-dihydroxyvitamin D3. FASEB Journal. 19: 1067–1077.

Gombart, A. F., O'Kelly, J., Saito, T., Koeffler, H. P. 2007. Regulation of the CAMP gene by 1,25(OH)2D3 in various tissues. The Journal of Steroid Biochemestry and Molecular Biology. 103: 552–557.

Gonzalez, A. C. de O., Costa, T. F., Andrade, Z. de A., Medrado, A. R. A. P. 2016. Wound healing - A literature review. Anais Brasileiros de Dermatologia. 91(5): 614-20.

Grazul-Bilska, A., T., Johnson, M. L., Bilski, J. J., Redmer, D. A., Reynolds, L. P., Abdullah, A., Abdullah, K. M. 2003. Wound healing: the role of growth factors. Drugs of Today. 39(10): 787-800.

Gueli, N., Verrusio, W., Linguanti, A., et al. 2012. Vitamin D: Drug of the future. A new therapeutic approach. Archives of Gerontology and Geriatrics. 54: 222–227.

Guo, S. and DiPietro, L. A. 2010. Factors Affecting Wound Healing. Journal of Dental Research. 89(3): 219-229.

Gurtner, G. C., Werner, S., Barrandon, Y., Longaker, M. T. 2008. Wound repair and regeneration. Nature. 453(7193): 314–321.

Hale, J. D., and Hancock, R. E. 2007. Alternative mechanisms of action of cationic antimicrobial peptides on bacteria. Expert Review of Anti Infective Therapy. 5(6):951-959.

Han, G. and Ceilley, R. 2017. Chronic Wound Healing: A Review of Current Management and Treatments. Advances in therapy. 34: 599–610.

Hancock, R. E., Haney, E. F., and Gill, E. E. 2016. The immunology of host defence peptides: beyond antimicrobial activity. Nature Reviews: Immunology. 16(5): 321-334.

Harder, J., Schroder, J. M., Glaser, R. 2013. The skin surface as antimicrobial barrier: Present concepts and future outlooks. Experimental Dermatology. 22: 1–5.

Heilborn, J. D., Weber, G., Grönberg, A., Dieterich, C., Ståhle, M. 2010. Topical treatment with the vitamin D analogue calcipotriol enhances the upregulation of the antimicrobial protein hCAP18/LL-37 during wounding in human skin *in vivo*. Experimental Dermatology. 19: 332–338.

Heo, M.-S. and Son, H.-J. 2002. Development of an optimized, simple chemically defined medium for bacterial cellulose production by *Acetobacter* sp. A9 in shaking cultures. Biotechnology and Applied Biochemistry. 36: 41–45.

Hestrin, S., Schramm, M. 1954. Synthesis of cellulose by Acetobacter xylinum: 2. Preparation of freeze-dried cells capable of polymerizing glucose to cellulose. Biochemical Journal. 58: 345–52.

Hobson, R., 2014. Vitamin E and wound healing: an evidence-based review. International Wound Journal. 13(3): 331-335.

Hoenich, N. 2006. Cellulose for medical applications: past, present, and future. BioResources. 1: 270–80.

Hong, L., Shen, M., Fang, J. Wang, Y., Bao, Z., Bu, S., Zhu, Y. 1. 2018. Hyaluronic acid (HA)-based hydrogels for full-thickness wound repairing and skin regeneration. Journal of Materials Science: Materials in Medicine. 29: 150.

Huang, L., Wang, Y., Liu, H., Huang, J. 2018. Local injection of high-molecular hyaluronan promotes wound healing in old rats by increasing angiogenesis. Oncotarget. 9(9): 8241-8252.

Huang, Z., Lu, M., Zhu, G., Gao, H., Xie, L., Zhang, X., Ye, C., Wang, Y., Sun, C., Li, X. 2011. Acceleration of diabetic wound healing with PEGylated rhaFGF in healing-impaired streptozocin diabetic rats. Wound Repair and Regeneration: Official Publication of the Wound Healing Society [and] the European Tissue Repair Society. 19: 633-44.

Hussain, Z., Thu, H. E., Shuid, A. N., Katas, H., Hussain, F. 2017. Recent Advances in Polymer-based Wound Dressings for the Treatment of Diabetic Foot Ulcer: An Overview of State-of-the-art. Current Drug Targets. 18(11): 1-24.

Iorio, M. L., Goldstein, J., Adams, M., Steinberg, J., Attinger, C. 2011. Functional limb salvage in the diabetic patient: the use of a collagen bilayer matrix and risk factors for amputation. Plastic and Reconstructive Surgery. 127: 260-7.

Jacek, P., Dourado, F., Gama, M., Bielecki, S. 2019. Molecular aspects of bacterial nanocellulose biosynthesis. Microbial Biotechnology. 1-17.

Javia, A., Amrutiya, J., Lalani, R., Patel, V., Bhatt, P., Misra, A. 2018. Antimicrobial peptide delivery: an emerging therapeutic for the treatment of burn and wounds. Therapeutic delivery. 9(5): 375–386.

Jonas, R. and Farah, L. F. 1998. Production and application of microbial cellulose. Polymer Degradation and Stability. 59: 101–106.

Jones, V., Grey, J. E., Harding, K. G. 2006. Wound dressings. BMJ. 332(7544): 777–780.

Jozala, A. F., de Lencastre-Navaes, L. C., lopes, A. M., Santos-Ebinuma, V. de C., Mazzola, P. G., Pessoa-Jr, A., Grotto, D., Gerenutti, M., Chaud, M. V. 2016. Bacterial nanocellulose production and application: a 10-year overview. Applied Microbiology Biotechnology. 100: 2063-2072.

Jung, J. Y., Khan, T., Park, J. K., Chang, H. N., 2007. Production of bacterial cellulose by *Gluconacetobacter hansenii* using a novel bioreactor equipped with a spin filter. Korean Journal of Chemical Engineering. 24(2): 265–271.

Jung, J.Y., Park, J.K., Chang H.N., 2005. Bacterial cellulose production by *Gluconacetobacter hansenii* in an agitated culture without living non-cellulose producing cells. Enzyme Microbial Technology. 37: 347–354.

Kahlenberg, J. M. and Kaplan, M. J. 2013. Little Peptide, Big Effects: The Role of LL-37 in Inflammation and Autoimmune Disease. The Journal of Immunology, 91:4895-4901.

Kamoun, E. A., Kenawy, E. -R. S., Chen. X., 2017. A review on polymeric hydrogel membranes for wound dressings applications: PVA-based hydrogel dressings. Journal of Advanced Research. 8:217-233.

Kanjanamosit, N., Muangnapoh, C., Phisalaphong, M. 2010. Biosynthesis and characterization of bacteria cellulose–alginate film. Journal Applied Polymer Science. 115: 1581–1588.

Katti, D. S., Robinson, K.W., Ko, F.K., Laurencin, C.T. 2004. Bioresorbable nanofiber-based systems for wound healing and drug delivery: optimization of fabrication parameters, Journal of Biomedical Materials Research. Part B, Applied Biomaterials. 70B: 286–296.

Kaya, G. and Pittet, D. 2017. Chapter 3- Flora and Physiology of Normal Skin. In "*Hand Hygiene: A Handbook for Medical Professionals*", First Edition. Edited by Didier Pittet, John M. Boyce and Benedetta Allegranzi. John Wiley & Sons, Inc. Published. pp. 12-17.

Kenshi, Y. and Richard, L. G. 2008. Antimicrobial peptides in human skin disease. European Journal of Dermatology. 18(1): 11–21.

Keshk S. 2014. Bacterial cellulose production and its industrial applications. Journal Bioprocessing & Biotechniques. 4:10.

Keshk, S and Sameshima, K. 2006. The utilization of sugar cane molasses with/without the presence of lignosulfonate for the production of bacterial cellulose. Applied Microbiology and Biotechnology. 72: 291–296.

Keshk, S. and Sameshima, K. 2006. Influence of lignosulfonate on crystal structure and productivity of bacterial cellulose in a static culture. Enzyme Microbial Technology. 40(1): 4–8.

Keshk, S.M.A.S., Razek, T.M.A., Sameshima, K. 2006. Bacterial cellulose production from beet molasses. African Journal of Biotechnology. 5(17): 1519–1523.

Khalid, A., Khan, R., Ul-Islam, M., Khan, T., Wahid, F. 2017. Bacterial cellulose-zinc oxide nanocomposites as a novel dressing system for burn wounds. Carbohydrate Polymers, 164: 214–221.

Khandare, J., and Minko, T. 2006. Polymer-drug conjugates: Progress in polymeric prodrugs. Progress and Polymer Science. 31:359–397.

Khunmanee, S., Jeong, Y, Park, Hansoo. 2017. Crosslinking method of hyaluronic-based hydrogel for biomedical applications. Journal of Tissue Engineering. 8: 1–16.

Kim, H. S., Sun, X., Lee, J.-H., Kim, H.-W., Fu, X., Leong, K. W. 2019. Advanced drug delivery systems and artificial skin grafts for skin wound healing. Advanced Drug Delivery. In Press, Corrected Proof.

Kim, Y.-J., Kim, J.-N., Wee, Y.-J., Park, D.-H., Ryu H.-W. 2007. Bacterial Cellulose Production by *Gluconacetobacter* sp. RKY5. In "Rotary Biofilm Contactor" in: J. Mielenz, K.T. Klasson, W. Adney, J. McMillan (Eds.). Applied Biochemistry and Biotechnology. Humana Press. USA. 529–537.

Klemm, D., Schumann, D., Udhardt, U., Marsch, S. 2001. Bacterial synthesized cellulose—Artificial blood vessels for microsurgery. Progress in Polymer Science, 26: 1561–1603.

Koczulla, R., von Degenfeld, G., Kupatt, C., Krötz, F., Zahler, S., Gloe, T., Issbrücker K., Unterberger, P., Zaiou, M., Lebherz, C,. Karl, A., Raake, P., Pfosser, A., Boekstegers, P., Welsch, U., Hiemstra, P. S., Vogelmeier, C., Gallo, R. L., Clauss, M., Bals, R. 2003. An angiogenic role for the human peptide antibiotic LL-37/hCAP-18. The Journal Clinical Investigation. 111(11): 1665-72.

Kolarsick, P. A. J., Kolarsick, M. A., Goodwin, C. 2009. Anatomy and physiology of the skin. In: Skin Cancer. Oncology Nursing Society, 1–11.

Komarcevic, A. 2000. The modern approach to wound treatment. Medicinski Pregled. 53: 363–368.

Kondo, S. and Kuroyanagi, Y. 2012. Development of a wound dressing composed of hyaluronic acid and collagen sponge with epidermal growth factor. Journal of Biomaterials Science. Polymer Edition. 23(5): 629–643.

Korting, H.C., Schöllmann, C. Stauss-Grabo, M. Schäfer-Korting M. 2012. Antimicrobial Peptides and Skin: A Paradigm of Translational Medicine. Skin Pharmacology and Physiology. 25:323–334.

Korting, M. S. H. C. 2006.The pH of the Skin Surface and Its Impact on the Barrier Function. Skin Pharmacology and Physiology. 19: 296 -302.

Kravitz, M. 1993. Immune consequences of burn injury. AACN Clinical Issues in Critical Care Nursing. 4: 399–413.

Krystynowicz, A., Czaja, W., Wiktorowska-Jezierska, A., Gon alves-Mi kiewicz, M., Turkiewicz, M., Bielecki, S. 2002. Factors affecting the yield and properties of bacterial cellulose. Journal of Industrial Microbiology and Biotechnology. 29(4): 189–195.

Kucharzewski, M., Ślęzak, A., Franek, A. 2003. Topical treatment of non-healing veneous leg ulcers by cellulose membrane. Phlebologie. 32: 147–151.

Kumar, P., Kizhakkedathu, J. N., Straus, S. K. 2018. Antimicrobial Peptides: Diversity, Mechanism of Action and Strategies to Improve the Activity and Biocompatibility *In Vivo*. Biomolecules. 8(1): 4.

Kurniawan, H., Lai, J.-T., Wang, M.-J. 2012. Biofunctionalized bacterial cellulose membranes by cold plasmas. Cellulose. 19: 1975–1988.

Kurosumi, A., Sasaki, C., Yamashita, Y., Nakamura, Y., 2009.Utilization of various fruit juices as carbon source for production of bacterial cellulose by *Acetobacter xylinum* NBRC 13693. Carbohydrate Polymers. 76: 333–335.

Kwak, M. H., Kim, J. E., Go, J., et al. 2015. Bacterial cellulose membrane produced by Acetobacter sp. A10 for burn wound dressing applications. Carbohydrate Polymers. 122: 387–398.

Langer, R. 1980. Polymeric delivery systems for controlled drug release. Chemical Engeneering Communications 6: (1-3):1–48.

Lee, A. R. C., Leem, H., Jaegwan, L., Park, K.C. 2005. Reversal of silver sulfadiazine-impaired wound healing by epidermal growth factor. Biomaterials. 26: 4670–4676.

Lee, J., Yoo, K.C., Ko, J., Yoo, B., Shin, J., Lee, S.J., et al. 2017. Hollow hyaluronic acid particles by competition between adhesive and cohesive properties of catechol for anticancer drug carrier. Carbohydrate Polymer. 164: 309-316.

Lee, K. Y., Buldum, G., Mantalaris, A., Bismarck, A. 2014. More than meets the eye in bacterial cellulose: Biosynthesis, bioprocessing, and applications in advanced fiber composites. Macromolecules Bioscience. 14(1): 10–32.

Lee, W. J., Cha, H. W., Sohn, M. Y., Lee, S. J., Kim, D. W. 2012. Vitamin D increases expression of cathelicidin in cultured sebocytes. Archives of Dermatological Research. 304: 627–632.

Leitão, A. F., Faustino, A. M. R.; Faria, M. A.; Moreira, R., Mela, P., Silva, I., Loureiro, L., Gama, M. 2016. A Novel Small-Caliber Bacterial Cellulose Vascular Prosthesis: Production, Characterization and Preliminary *In vivo* Testing. Macromolecular Bioscience. 102(2): 579-92.

Li ,Y., Jiang, H., Zheng, W., et al. 2015. Bacterial cellulose–hyaluronan nanocomposite biomaterials as wound dressings. for severe skin injury repair. Journal of Materials Chemistry B. 3: 3498–3507.

Li, W. W., Talcott, K. E., Zhai, A. W., Kruger, E. A., Li, V.W. 2005. The role of therapeutic angiogenesis in tissue repair and regeneration. Advanced Skin Wound Care. 18: 491–500.

Li, Y., Wang, S., Huang, R., Huang, Z., Hu, B., Zheng, W., et al. 2015. Evaluation of the effect of the structure of bacterial cellulose on full thickness skin wound repair on a microfluidic chip. Biomacromolecules. 16: 780–789.

Li, Y., Xiang, Q., Zhang, Q., Huang, Y., Su, Z. 2012. Overview on the recent study of antimicrobial peptides: Origins, functions, relative mechanisms and application. Peptides. 37(2): 207-215.

Lin, T. S., Latiff, A. A., Hamid, A. A., Wan Zurinah bt, Ngah, W., Musalmah, Mazlan. 2012. Evaluation of Topical Tocopherol Cream on Cutaneous Wound Healing in Streptozotocin-Induced Diabetic Rats. Evidence-Based Complementary and Alternative Medicine. 1-6.

Lin, W.-C., Lien, C.-C., Yeh, H.-J., Yu, C.-M., Hsu, S.-H. 2013. Bacterial cellulose and bacterial cellulose–chitosan membranes for wound dressing applications. Carbohydrate Polymers. 94: 603–611.

Lipsky, B. and Hoey, C. 2009. Topical antimicrobial therapy for treating chronic wounds. Clinical Infection Diseases. 49: 1541–1549.

Liu, M., Li, S., Xie, Y., Jia, S., Hou, Y., Zou, Y., Zhong, C. 2017. Enhanced bacterial cellulose production by *Gluconacetobacter xylinus* via expression of Vitreoscilla hemoglobin and oxygen tension regulation. Applied Microbiology and Biotechnology. 102(3): 1155-1165.

Liu, X. and Jia, G. 2018. Modern Wound Dressing Using Polymers/Biopolymers. Journal of material Sciences & Engineering. 7: 454.

Lotfiman, S., Biak, D. R. A., Ti, T. B., Kamarudin, S., Nikbin, S. 2016. Influence of Date Syrup as a Carbon Source on Bacterial Cellulose Production by *Acetobacter xylinum* 0416. Advances in Polymer Technology. 37(4): 1085-1091.

Ludwicka, K., Jedrzejczak-Krzepkowska, M., Kubiak, K., Kolodziejczyk, M., Pankiewicz, T, Bielecki, Stanislaw. 2016, Chapter 9 - Medical and Cosmetic Applications of Bacterial NanoCellulose. In "Bacterial Nanocellulose:

from biotechnology to bio-economy". Ed.: Gama, M.; Bielecky, S.; Dourado, F. Elsevier; Amsterdam, Netherlands. 145–165. ISBN: 978-0-444-63458-0.

Luo, M. -T., Zhao, C., Huang, C., Chen, X. -F., Huang, Q. -L., Qi, G. -X., Tian, L. -L., Xi, L., Li, H. -L., Chen, X. -D. 2017. Efficient Using Durian Shell Hydrolysate as Low-Cost Substrate for Bacterial Cellulose Production by *Gluconacetobacter xylinus.* Indian Journal Microbiology. 57(4): 393–399.

Lustri, W. R., Barud, H. Gomes de Oliveira., Barud, Hernane da Silva., Peres, M. F. S., Gutierrez, J., Tercjak, A., Junior, O. Batista de Oliveira., Ribeiro, S. J. L. 2015. Chapter 6- Microbial Cellulose — Biosynthesis Mechanisms and Medical Applications. In "Cellulose Fundamental Aspects and Current Trends". 133-157.

Mahlapuu, M., Håkansson, J., Ringsta, L., Björn, C. 2016. Antimicrobial Peptides: An Emerging Category of Therapeutic Agents. Frontiers in cellular and Infection Microbiology. 6: 194.

Mangoni, M. L., McDermott, A. M., Zasloff, M. 2016. Antimicrobial peptides and wound healing: biological and therapeutic considerations. Experimental Dermatology. 25: 167–173.

Mann, A., Niekisch, K., Schirmacher, P., Blessing, M. 2006. Granulocyte-macrophage colony-stimulating factor is essential for normal wound healing. Journal of Investigative Dermatolology Symposium Proceedings. 11: 87–92.

Mano, J., Silva, G., Azevedo, H. S., Malafaya, P., Sousa, R., Silva, S., et al. 2007. Natural origin biodegradable systems in tissue engineering and regenerative medicine: Present status and some moving trends. Journal of the Royal Society Interface. 4: 999–1030.

Martini, A., Morra, B., Aimoni, C., Radice, M. 2000. Use of a hyaluronan-based biomembrane in the treatment of chronic cholesteatomatous otitis media. The American Journal of otology. 21(4): 468-73.

Masaoka M., Ohe, S., Sakota, N. 1993. Production of Cellulose from Glucose by *Acetobacter xylinum.* Journal of Fermentation and Bioengineering. 75(1): 18-22.

Matsumoto, Y. and Kuroyanagi, Y. 2010. Development of a wound dressing composed of hyaluronic acid sponge containing arginine and epidermal growth factor. Journal of Biomaterials Science. Polymer Edition. 21(6): 715–726.

Meftahi, A., Khajavi, R., Rashidi, A. Sattari, M., Yazdanshenas, M.E., Torabi, M. 2010. The effects of cotton gauze coating with microbial cellulose. Cellulose. 17: 199–204.

Mero, A. and Campisi, M. 2014. Hyaluronic acid bioconjugates for the delivery of bioactive molecules. Polymers. 6: 346–369.

Merrel, J. G., McLaughlin, S. W., Tie, L., Laurencin, C. T., Chen, A. F., Nair, L. S. 2009. Curcumin-loaded poly(epsilon-caprolactone) nanofibres: diabetic wound dressing with anti-oxidant and anti-inflammatory properties. Clinical and Experimental Pharmacology & Physiology. 36: 1149-56.

Mikkelsen, D., Flanagan, B.M., Dykes, G.A., Gidley, M. J. 2009. Influence of different carbon sources on bacterial cellulose production by *Gluconacetobacter xylinus* strain ATCC 53524. Journal of Applied Microbiology. 107: 576–583.

Mir, M., Ali, M. N., Barakullah, A., Gulzar, A., Arshad, M., Fatima, S., Asad, M. 2018. Synthetic polymeric biomaterials for wound healing: a review. Progress in Biomaterials. 7: 1-21.

Mogosanu, G. D., and Grumezescu, A. M. 2014. Natural and synthetic polymers for wounds and burns dressing. International Jounal of Pharmaceutics. 463:127–136.

Mohamad, N., Amin, M.C.I. M., Pandey, M., Ahmad, N., Rajab, N.F. 2014. Bacterial cellulose/acrylic acid hydrogel synthesized via electron beam irradiation: Accelerated burn wound healing in an animal model. Carbohydrate Polymers. 114: 312–320.

Molina-Ramírez, C., Castro, M., Osorio, M., Torres-Taborda, M., Gómez, B., Zuluaga, R., Gómez, C., Gañán, P., Rojas, O. J., Cristina, C. 2017. Effect of Different Carbon Sources on Bacterial Nanocellulose Production and Structure Using the Low pH Resistant Strain *Komagataeibacter Medellinensis*. Materials. 10(639): 2-13.

Moniri, M., Moghaddam, A. B., Azizi, S., Rahim, R. A., Ariff, A. B., et al., 2017. Production and status of Bacterial Cellulose in Biomedical Engineering Nanomaterials. 7(257): 1-26.

Moore, K., McCallion, R., Searle, R. J., Stacey, M. C., Harding, K. G. 2006. Prediction and monitoring the therapeutic response of chronic dermal wounds. International Wound Journal. 3(2) :89–96.

Moores, J. 2013. Vitamin C: a wound healing perspective. British journal of community nursing.18(Suppl 12): S6-S11.

Moosavi-Nasab, M. and Yousefi, A. 2011. Biotechnological production of cellulose by *Gluconacetobacter xylinus* from agricultural waste. Iran Journal of Biotechnology. 9: 94–101.

Morgan, T. 2015. Are your wound management choices costing your money? JCN. 29:17–20.

Moritz, S., Wiegand, C., Wesarg, F., Hessler, N., Müller, F. A., Kralisch, D., Hipler, U. C., Fischer, D. 2014. Active wound dressings based on bacterial nanocellulose as drug delivery system for octenidine. International Journal of Pharmaceuticals. 471(1-2): 45-55.

Mostafa, W. Z. and Hegazy, R. A. 2015. Vitamin D and the skin: Focus on a complex relationship: A review. Journal of Advanced Research. 6: 793–804.

Müller, A. Ni., Z., Hessler, N., Wesarg, F., Müller, F. A., Kralisch, D., Fischer, D. 2013. The biopolymer bacterial nanocellulose as drug delivery system: investigation of drug loading and release using the model protein albumin. Journal of Pharmaceutical Sciences. 102(2): 579-92.

Myers, S. R., Partha, V. N., Soranzo, C., Price, R. D., Navsaria, H. A. 2007. Hyalomatrix: a temporary epidermal barrier, hyaluronan delivery, and neodermis induction system for keratinocyte stem cell therapy. Tissue Engineering. 13(11):2733-41.

Naritomi, T., Kouda, T., Yano, H., Yoshinaga, F., Morimura, T. S, S., Kida, K. 2002. Influence of broth exchange ratio on bacterial cellulose production by repeated-batch culture. Process Biochemistry. 38(1): 41–47.

Naseri-Nosar, M. and Ziora, Z. M. 2018. Wound dressings from naturally-occurring polymers: A review on homopolysaccharide-based composites. Carbohydrate polymers. 189: 379-398.

Neamtu, I., Rusu, A.G., Diaconu, A., Nita, L.E., Chiriac, A. P. 2017. Basic concepts and recent advances in nanogels as carriers for medical applications, Drug Delivery. 24(1): 539–557.

Nguyen, L. T., Haney, E. F., Vogel, H. J. 2011.The expanding scope of antimicrobial peptide structures and their modes of action. Trends in biotechnology. 29(9): 464-72.

Nguyen, V. T., Flanagan, B., Gidley, M.J., Dykes, G.A. 2008. Characterization of Cellulose Production by a *Gluconacetobacter xylinus* Strain from Kombucha. Current Microbiology. 57: 449–453.

Niyonsaba, F., Kiatsurayanon, C., Chieosilapatham, P., and Ogawa, H. 2017. Friends or Foes? Host defense (antimicrobial) peptides and proteins in human skin diseases. Experimental Dermatology. 26: 989–998.

Nussbaum, S. R., Carter, M. J., Fife, C. E., DaVanzo, J., Haught, R., Nusgart, M., Cartwright, D. 2018. An Economic Evaluation of the Impact, Cost, and Medicare Policy Implications of Chronic Nonhealing Wounds. Value in Health. 21(1): 27-32.

Oh, E. J., Park, K., Kim, K. S., et al. 2010. Target specific and long-acting delivery of protein, peptide, and nucleotide therapeutics using hyaluronic acid derivatives. Journal of Controlled Release; 141: 2–12.

Oikawa, T., Ohtori, T., Ameyama, M., 1995. Production of cellulose from D-mannitol by *Acetobacter xylinum* KU-1. Bioscience Biotechnology and Biochemistry. 59: 331–332.

Okiyama, A., Shirae, H., Kano, H., Yamanaka, S. 1992. Bacterial cellulose I. Two-stage fermentation process for cellulose production by *Acetobacter aceti.* Food Hydrocolloids. 6(5): 471–477.

Onishi, H., Machida, Y., Santhini, E., Vadodaria, K. 2019. Chapter 8 - Novel textiles in managing burns and other chronic wounds. in Advanced Textiles for Wound Care, Second Edition. Edited by S. Rajendran. 211-260.

Pale, S., Nisi, R., Stoppa, M., Licciulli, A. 2017. Silver-Functionalized Bacterial Cellulose as Antibacterial Membrane for Wound-Healing Applications. ACS Omega, 2(7): 3632-39.

Park, J. W., Hwang, S. R., Yoon, I.-S. 2017. Advanced Growth Factor Delivery Systems in Wound Management and Skin Regeneration. Molecules. 22: 1259.

Park, J.K., Jung, J.Y., Park, Y.H. 2002. Cellulose production by *Gluconacetobacter hansenii* in a medium containing ethanol. Biotechnology Letters. 25: 2055–2059.

Pasparakis, M., Haase, I., Nestle, F.O. 2014. Mechanisms regulating skin immunity and inflammation. Nature Reviews Immunology. 14, 289–301.

Pasupuleti, M., Schmidtchen, A., Malmsten, M. 2011. Antimicrobial peptides: key components of the innate immune system. Critical Reviews in Biotechnology. 1-29.

Pedrosa, S. and Gama, M. 2014. Hyaluronic acid and its application in nanomedicine. Carbohyfrates Applications in Medicine. 55-89.

Pedrosa, S. S., Gonçalves, C., David, L., Gama, M. 2014. A Novel Crosslinked Hyaluronic Acid Nanogel for Drug Delivery. Macromolecular Bioscience. 14(11): 1556-68.

Percival J. 2002. Classification of wounds and their management. Surgery. 20: 114–117.

Pertile, R.A.N., et al. 2010. Surface modification of bacterial cellulose by nitrogen-containing plasma for improved interaction with cells. Carbohydrate Polymers. 82(3): 692-698.

Pfalzgraff, A., Brandenburg, K., Weindl, G. 2018. Antimicrobial Peptides and Their Therapeutic Potential for Bacterial Skin Infections and Wounds. Frontiers in Pharmacology. 9:281.

Phisalaphong, M., Tran, T. -K., Taokaew, S., Budiraharjo, R., Febriana, G. G., Nguyen, D. -N., Chu-Ky, S., Dourado, F. 2016. Chapter 14- Nata de coco Industry in Vietnam, Thailand, and Indonesia. In "Bacterial Nanocellulose: from biotechnology to bio-economy". Ed.: Gama, M.; Bielecky, S.; Dourado, F. Elsevier; Amsterdam, Netherlands. 215–229. ISBN: 978-0-444-63458-0.

Piadozo, Ma. E. S. 2016, Chapter 13- Nata de Coco Industry in the Philippines. In "Bacterial Nanocellulose: from biotechnology to bio-economy". Ed.: Gama, M.; Bielecky, S.; Dourado, F. Elsevier; Amsterdam, Netherlands. 215–229. ISBN: 978-0-444-63458-0.

Picheth, G.F., Sierakowski, M.R., Woeh, M.A. I, Ono, L., Cofre, A.R., Vanin, L.P., Pontarolo, R., De Freitas, R. A. 2014. Journal of Pharmaceutical Sciences. 103: 3958–3965.

Pike, J. W. and Christakos S. 2017. Biology and mechanisms of action of the vitamin D hormone. Endocrinolology and Metabolism Clinics of North America. 46: 815–843.

Porto da Rocha, R., Lucio, D. P., Souza, Tde L., Pereira, S. T., Fernandes, G. J. 2002. Effects of a vitamin pool (vitamins A, E, and C) on the tissue necrosis process: Experimental study on rats. Aesthetic Plastic Surgery. 26: 197–202.

Premjet, S., Premjet, D., Ohtani, Y. 2007. The Effect of Ingredients of Sugar Cane Molasses on Bacterial Cellulose Production by *Acetobacter xylinum* ATCC 10245. Sen'i Gakkaishi. 63:193–199.

Price, R. D., Myers, S., Leigh, I. M., Navsaria, H. A. 2005. The role of hyaluronic acid in wound healing: assessment of clinical evidence. American Journal of Clinical Dermatology. 6(6): 393-402.

Punjataewakupt, A., Napavichayanun, S., Aramwit, P. 2019. The downside of antimicrobial agents for wound healing. European Journal of Clinical Microbiology & Infectious Diseases. 38: 39–54.

Rachid, M., Pamela, K., Tobias, N., Irina, N., Markus, W.B., Margot, Z. 2008. CD44 and EpCAM: cancer-initiating cell markers. Current Molecular Medicine. 8:784–804.

Ramos, R., Domingues, L., and Gama, M. 2011. LL-37, a human antimicrobial peptide with immunomodulatory properties. In A. Mendez-Vilas (Ed.), Science against microbial pathogens: communicating current research and technological advances (Vol. 1). Badajoz: Formatex Research Center.

Ramos, R., Silva, J. P., Rodrigues, A. C., et al. 2011. Wound healing activity of the human antimicrobial peptide LL37. Peptides. 32: 1469–1476.

Reihsner, R., Balogh, B., Menzel, E. J. 1995. Two-dimensional elastic properties of human skin in terms of an incremental model at the *in vivo* configuration. Medical Engineering & Physics. 17: 304–313.

Reinholz, M., Ruzicka, T., Schauber, J. 2012. Cathelicidin LL-37: An Antimicrobial Peptide with a Role in Inflammatory Skin Disease. Annals of Dermatology. 24:126–135.

Reiniati, i., Hrymak, A. N., Margaritis, A. 2017. Recent developments in the production and applications of bacterial cellulose fibers and nanocrystals. Critical Reviews in biotechnology. 37(4): 510-524.

Ross, P., Mayer, R., Benziman, M. 1991. Cellulose biosynthesis and function in bacteria. Microbiological Reviews. 55: 35-58.

Rouabhia, M., Asselin, J., Tazi, N., Messaddeq, Y., Levinson D., Zhang, Z. 2014. Production of Biocompatible and Antimicrobial Bacterial Cellulose. Polymers Functionalized by RGDC Grafting Groups and Gentamicin. ACS Applied Materials & Interfaces. 6: 1439–1446.

Saghazadeh, S., Rinoldi, C., Schot, M., Kashaf, S. S., Sharifi, F., Jalilian, E., Nuutila, K., Giatsidis, G., Mostafalu, P., Derakhshandeh, H., Yue, K., Swieszkowski, W., Memic, A., Tamayol, A., Khademhossein, A. 2018. Drug delivery systems and materials for wound healing applications. Advanced Drug Delivery Reviews. 127: 138-166.

Saibuatong, O. and Phisalaphong, M. 2010. Novo aloe vera–bacterial cellulose composite film from biosynthesis. Carbohydrate Polymers. 79: 455–460.

Saxena, I. M., Kudlicka, K., Okuda, K., Brown, R. M. Jr. 1994. Characterization of genes in the cellulose-synthesizing operon (acs operon) of *Acetobacter xylinum*: implications for cellulose crystallization. Journal of Bacteriology. 176: 5735-5752.

Schanté, C. E., Zuber, G., Herlin, C., Vandamme, T. F. 2011. Chemical modifications of hyaluronic acid for the synthesis of derivatives for a broad range of biomedical applications. Carbohydrate Polymers. 85: 469–489.

Schauber, J. and Gallo, R. L. 2008. Antimicrobial peptides and the skin immune defense system. Journal of Allergy and Clinical Immunology. 122(2): 261–266.

Schauber, J. and Gallo, R. L. 2009. The vitamin d pathway: a new target for control of the skin´s immune response?. Experimental Dermatology. 17(8): 633–639.

Scherner, M., Reutter, S., Klemm, D., Sterner-Kock, A., Guschlbauer, M., Richter, T., Langebartels, G., Madershahian, N., Wahlers, T., Wippermann, J. 2014. *In Vivo* application of tissue-engineered blood vessels of bacterial cellulose as small arterial substitutes: Proof Of Concept? The Journal of Surgical Research. 189: 340-7.

Schoukens, G. 2019. Chapter 5 – Bioactive dressings to promote wound dressing. In "Advanced Textile for Wound Care", Second Edition. Edited by S. Rajendran. 211-260.

Schreml, S., Szeimies, R. M., Prantl, L., Landthaler, M., Babilas, P. 2010. Wound healing in the 21st century. Journal of the American Academy of Dermatology. 63: 866–881.

Schröder, J.-M. 2011. Antimicrobial Peptides in Healthy Skin and Atopic Dermatitis. Allergology International. 60: 17-24

Schumann, D. A., Wippermann, J., Klemm, D. O., Kramer, F., Koth, D., Kosmehl, H., Wahlers, T., Salehi-Gelani, S. 2008. Artificial vascular implants from bacterial cellulose: preliminary results of small arterial substitutes. Cellulose. 16: 877–85.

Sehgal, P.K., Sripriya, R., Senthilkumar, M., Rajendran, S. 2019. Chapter 9 - Drug delivery dressings. In Advanced Textiles for Wound Care, Second Edition. Edited by S. Rajendran. 261-288.

Seto, A., Saito, Y., Matsushige, Kobayashi, M., Sasaki, H., Tonouchi, Y., N., Tsuchida, T., Yoshinaga, F., Ueda, K., Beppu, T. 2006. Effective cellulose production by a coculture of *Gluconacetobacter xylinus* and *Lactobacillus mali*. Applied Microbiology Biotechnology. 73: 915–921.

Sezer, A. D. and Cevher, E. 1992. Biopolymers as Wound Healing Materials: Challenges and New Strategies. Biomaterials Applications for Nanomedicine. 383–414.

Shah, N. Ul-Islam, M., Khattak, W. a., Park, J. K. 2013. Overview of bacterial cellulose composites: A multipurpose advanced material. Carbohydrate Polymers. 98: 1585- 1598.

Shao, W., Liu, H., Liu, X., Sun, H., Wang, S., & Zhang, R. 2015. pH-responsive release behavior and anti-bacterial activity of bacterial cellulose-silver nanocomposites. International Journal of Biological Macromolecules, 76: 209–217.

Sharma, A., Garg, T., Aman, A., Panchal, K., Sharma, R., Kumar, S., et al. 2016. Nanogel–an advanced drug delivery tool: Current and future. Artificial Cells, Nanomedicine, and Biotechnology. 44(1): 165-177.

Shaw, J., Hughes, C. M., Lagan, K. M., Stevenson, M. R., Irwin, C. R., Bell, P. M. 2011. The effect of topical phenytoin on healing in diabetic foot ulcers: a randomized controlled trial. Diabetic Medicine. 28: 1154-7.

Shin, Y. C., Shin, D. M., Lee, E. J., Lee, J. H., Kim, J. E., Song, S. H., Hwang, D. Y., Lee, J. J., Kim, B., Lim, D., Hyon, S. H., Lim, Y. J., Han, D. W. 2016. Hyaluronic Acid/PLGA Core/Shell Fiber Matrices Loaded with EGCG Beneficial to Diabetic Wound Healing. Advanced Healthcare Materials. 5(23): 3035-3045.

Shoda, M. and Sugano, Y. 2005. Recent advances in bacterial cellulose production. Biotechnology and Bioprocess Engineering, 10: 1–8.

Silva, N. H. C. S., Rodrigues, A. F., Almeida, I. F., et al. 2014. Bacterial cellulose membranes as transdermal delivery systems for diclofenac: *In vitro* dissolution and permeation studies. Carbohydrate. Polymers. 106: 264–269.

Simpson, C. L., Patel, D. M., Green, K. J. 2011. Deconstructing the skin: cytoarchitectural determinants of epidermal morphogenesis. Nature Reviews. Molecular Cell Biology. 12: 565–580.

Singer, A. J. and Clark, R. A. 1999. Cutaneous wound healing. The New England journal of medicine. 341: 738–746.

Singh, O., Gupta, S. S., Soni, M., Moses, S., Shukla, S., Mathur, R. K. 2011. Collagen dressing versus conventional dressings in burn and chronic wounds: a retrospective study. Journal of Cutaneous and Aesthetic Surgery. 4: 12-6.

Sivaram, A. J., Rajitha, P., Maya, S., Jayakumar, R., Sabitha, M. 2015. Nanogels for delivery, imaging and therapy. Wiley Interdisciplinary Reviews Nanomedicine Nanobiotechnology. 7(4): 509-533.

Slaughter, B. V., Khurshid, S. S., Fisher, O. Z, Khademhosseini, A., Peppas, N. A. 2009. Hydrogels in regenerative medicine. Advanced Materials. 21(32– 33): 3307–3329.

Sobotka L, Smahelova A, Pastorova J, Kusalova M. 2007. A case report of the treatment of diabetic foot ulcers using a sodium hyaluronate and iodine complex. The International Journal Low Extremity Wounds. 6: 143-7.

Solway, D. R., Clark, W. A., Levinson, D. J. 2011. A parallel open-label trial to evaluate microbial cellulose wound dressing in the treatment of diabetic foot ulcers. International Wound Journal. 8: 69-73.

Son, H., Kim, H., Kim, K., Kim, H., Kim, Y., Lee, S. 2003. Increased production of bacterial cellulose by *Acetobacter* sp. V6 in synthetic media under shaking culture conditions Bioresource Technology. 86: 215–219.

Son, H.J., Heo, M.S., Kim, Y.G., Lee, S. J. 2001. Optimization of fermentation conditions for the production of bacterial cellulose by a newly isolated *Acetobacter.* Biotechnology and Applied Biochemistry. 33(1): 1–5.

Soni, K.S., Desale, S.S., Bronich T.K. 2016. Nanogels: an overview of properties, biomedical applications and obstacles to clinical translation, Journal Controlled Release. 240: 109–126.

Sood, A., Granick, M. S., and Tomaselli, N. L. 2014. Wound Dressings and Comparative Effectiveness Data. Advances in Wound Care. 3(8): 511-529.

Sørensen, O.E. 2016. Antimicrobial Peptides in Cutaneous Wound Healing. In: "Antimicrobial Peptides". Part of: Birkhäuser Advances in Infectious Diseases. Harder J., Schröder JM. (eds) Springer.

Sorg, H., Tilkorn, D. J., Hager, S., Hauser, J. Mirastschijski, U. 2017. Skin Wound Healing: An Update on the Current Knowledge and Concepts. European Surgical Research. 58: 81–94.

Stein, G. E., and Wells, E. M. 2010. The importance of tissue penetration in achieving successful antimicrobial treatment of nosocomial pneumonia and complicated skin and soft-tissue infections caused by methicillin-resistant *Staphylococcus aureus*: vancomycin and linezolid. Currrent Medicine Research Opinion. 26: 571–588.

Sulaeva, I., Henniges, U., Rosenau, T., Potthast, A., 2015. Bacterial cellulose as a material for wound treatment: Properties and modifications. A review. Biotechnology Advances. 33: 1547-1571.

Sultana, F., Manirujjaman, Imran-Ul-Haque, Md., Arafat, M., Sharmin, S. 2013. An Overview of Nanogel Drug Delivery System. Journal of Applied Pharmaceutical Science. 3(8) Suppl 1: S95-S105.

Supp, D. M. and Boyce, S.T. 2005. Engineered skin substitutes: practices and potentials. Clinics in Dermatology. 23: 403–412.

Suzuki, Y., Tanihara, M., Nishimura, Y., Suzuki, K., Kakimaru, Y., Shimizu, Y. 1998. A new drug delivery system with controlled release of antibiotic only in the presence of infection. Journal of Biomedical Materials Research. 42(1): 112–116.

Svensson, D., Nebel, D., Nilsson, B-O. 2015. Vitamin D$_3$ modulates the innate immune response through regulation of the hCAP-18/LL-37 gene expression and cytokine production. Inflammation Research. 65(1): 25-32.

Takahashi, T., and Gallo, R. L. 2017. The critical and multifunctional roles of antimicrobial peptides in dermatology. Dermatology Clinics. 35: 39–50.

Takei, T., Nakahara, H., Ijima, H., Kawakami, K. 2012. Synthesis of a chitosan derivative soluble at neutral pH and gellable by freeze-thawing, and its application in wound care. Acta Biomaterialia. 8: 686-9.

Thakur, V. K., 2015. editor. Nanocellulose Polymer Nanocomposites. Scrivener Publishing LLC.

Tønnesen, H.H. and Karlsen, J. 2002. Alginate in drug delivery systems, Drug Development and Industrial Pharmacy. 28(6): 621–630.

Toshkhani, S., Shilakari, G., Asthana, A. 2013. Advancements in Wound Healing Biodegradable Dermal Patch Formulation Designing. Inventi Rapid: Pharm Tech. (3): 1-11.

Tranquillo, R.T. and Lauffenburger, D. A. 1987. Stochastic model of leukocyte chemosensory movement. Journal Mathematical Biology. 25: 229–262.

Trent, J. T. and Kirsner, R. S. 2003. Wounds and malignancy. Advanced Skin Wound Care 16(1): 31–34.

Trovatti, E., Freire, C.S.R., Pinto, P. C., Almeida, I.F., Costa, P., Silvestre A.J.D., Neto, C.P., Rosado, C. 2012. Bacterial cellulose membranes applied in topical and transdermal delivery of lidocaine hydrochloride and ibuprofen: *In vitro* diffusion studies. International Journal Pharmaceuticals. 435: 83–87.

van der Does, A. M., Bergman, P., Agerberth, B., Lindbom, L., 2012. Induction of the human cathelicidin LL-37 as a novel treatment against bacterial infections. Journal of Leukocyte Biology. 92: 735- 742.

Vandamme, D., Landuyt, B., Luyten, W., Schoofs, L. 2012. A comprehensive summary of LL-37, the factotum human cathelicidin peptide. Cell Immunology, 280(1):22-35.

Vandamme, E. J., De Baets, S., Vanbaelen, A., Joris, K., De Wulf, P. 1998. Improved Production of Bacterial Cellulose and its Application Potencial. Polymer Degradation and Stability. 59: 93-99.

Varma, A. K., Bal, A., Kumar, H., Kesav, R., Nair, S. 2008. Efficacy of polyurethane foam dressing in debrided diabetic lower limb wounds. Wounds. 12: 5-8.

Vazquez, J. R., Short, B., Findlow, A.H., Nixon, B. P., Boulton, A. J., Armstrong, D. G. 2003. Outcomes of hyaluronan therapy in diabetic foot wounds. Diabetes Research and Clinical Practice. 59(2): 123-7.

Venus, M., Waterman, J., McNab, I. 2011. Basic physiology of the skin. Surgery. 29: 10.

Vigetti, D., Karousou, E., Viola, M., Deleonibus, S., De Luca, G., Passi, A. 2014. Hyaluronan: Biosynthesis and signaling. Biochimica et Biophysica Acta. 1840(8): 2452–2459.

Walker, N. J. and Bhimji, S. S. 2018. Thermal Burns. https://www.ncbi.nlm.nih.gov/books/NBK430730/.

Wang, T. T., Nestel, F. P., Bourdeau, V., Nagai, Y., Wang, Q., Liao, J., Tavera-Mendoza, L., Lin, R., Hanrahan, J. W., Mader, S., White, J. H. 2004. Cutting edge: 1,25-dihydroxyvitamin D_3 is a direct inducer of antimicrobial peptide gene expression. Journal of Immunology. 173: 2909–2912.

Wani, T. U., Rashid, M., Kumar, M., Chaudhary, S., Kumar, P., Mishra, N. 2014. Targeting Aspects of Nanogels: An Overview. International Journal of Pharmaceutical Sciences and Nanotechnology. 7(4): 2612-30.

Watanabe, K., Yamanaka, S., 1995. Effects of Oxygen Tension in the Gaseous Phase on Production and Physical Properties of Bacterial Cellulose Formed under Static Culture Conditions. Bioscience Biotechnology and Biochemistry. 59: 65–68.

Weber, G., Heilborn, J., Jimenez, C., Hammarsjo, A., Torma, H., Stahel, M. 2005. Vitamin D induces the Antimicrobial Protein hCAP18 in human skin. The Journal of Investigative Dermatology. 124: 1080–1082.

Wei, B., Yang, G., Hong, F. 2011. Preparation and evaluation of a kind of bacterial cellulose dry films with antibacterial properties. Carbohydrate Polymers. 84: 533–538.

Werner, S. and Grose, R. 2003. Regulation of Wound Healing by Growth Factors and Cytokines. Physiological Reviews. 83(3): 835-870.

Wertz, P. W. 2013. Current Understanding of Skin Biology Pertinent to Skin Penetration: Skin Biochemistry. Skin Pharmacology Physiology. 26: 217-226.

White, J. H. 2010. Vitamin D as an inducer of cathelicidin antimicrobial peptide expression: past, present and future. The Journal of Steroid Biochemestry and Molecular Biology. 121: 234–238.

Whittam, A.J., Maan, Z.N., Duscher, D., Wong, V.W., Barrera, J.A., Januszyk, M., Gurtner, G.C., 2016. Challenges and opportunities in drug delivery for wound healing, Advances in wound care. 5:79–88.

William, C. W. 2010. Describing the Mechanism of Antimicrobial Peptide Action with the Interfacial Activity Model. ACS chemical biology. 5(10): 905-17.

Wu, J., Zheng, Y., Wen, X., Lin, Q., Chen, X., & Wu, Z. 2014. Silver nanoparticle/bacterial cellulose gel membranes for antibacterial wound dressing: investigation *in vitro* and *in vivo*. Biomedical Materials. 9: 035005.

Xie, Y., Upton, Z., Richards, S., Rizzi, S.C., Leavesley, D.I. 2011. Hyaluronic acid: evaluation as a potential delivery vehicle for vitronectin: growth factor complexes in wound healing applications. Journal Control Release. 153: 225–232.

Xu, H., Timares, L., Elmets, C.A. 2019. Chapter 19 - Host Defenses in Skin. Clinical Immunology (Fifth Edition) Principles and Practice. 273-283.e1.

Xu, X., Jha, A. K., Harrington, D. A., Farach-Carson, M. C., Jia, X. 2012. Hyaluronic acid-based hydrogels: from a natural polysaccharide to complex networks. Soft Matter. 8: 3280.

Yadav, H. K.S., Halabi, N. A. A., Alsalloum, G. A. 2017. Nanogels as Novel Drug Delivery Systems - A Review. Journal of Pharmacy and Pharmaceutical Research. 1: 1-5.

Yamanaka, S., Watanabe, K., Kitamura, N., Iguchi, M., Mitsuhashi, S., Nishi, Y., Uryu, M. 1989. The structure and mechanical properties of sheets prepared from bacterial cellulose. Journal of Material Science. 24: 3141–5.

Yang, X. -Y., Huang, C., Guo, H. -J., Xiong, L., Luo, J., Wang, B., Lin, X. -Q., Chen, X. -F, Chen, X. -D. 2016. Bacterial cellulose production from the litchi extract by *Gluconacetobacter xylinus*. Preparative Biochemistry and Biotechnology. 46: 139-43.

Yang, Y. K., Park, S. H., Hwang, J. W., Pyun, Y. R., Kim, Y. S. 1998. Cellulose Production by *Acetobacter xylinum* BRC5 under Agitated Condition. Journal of Fermentation and Bioengineering. 85(3): 312-317.

Zarekar, N. S., Lingayat, V. J., Pande, V. V. 2017. Nanogel as a Novel Platform for Smart Drug Delivery System. Nanoscience and Nanotechnology Research. 4(1): 25-31.

Zhang L.-J. and Gallo, R. L. 2016. Antimicrobial peptides. Current Biology. 26(1): R1-R21.

Zhang, H., Zhai, Y., Wang, J., Zhai, G. 2016. New progress and prospects: The application of nanogel in drug delivery. Materials Science and Engineering C. 60: 560–568.

Zhao, H., Xia, J., Wang, J., Yan, X., Wang, C., Lei, T., Xian, M., Zhang, H. 2018. Production of bacterial cellulose using polysaccharide fermentation wastewater as inexpensive nutrient sources, Biotechnology & Biotechnological Equipment. 32(2): 350-356.

Zhao, J.-Y., Chai, J.-K., Song, H.-F., Zhang, J., Xu, M.-H., Liang, Y.-D. 2013. Influence of hyaluronic acid on wound healing using composite porcine acellular dermal matrix grafts and autologous skin in rabbits. International Wound Journal. 10: 562–572.

Zhijiang, C. and Guang, Y. 2011. Bacterial Cellulose/Collagen Composite: Characterization and First Evaluation of Cytocompatibility Journal of Applied Polymer Science. 120: 2938–2944.

Zhijiang, C., Chengwei, H., Guang. Y. 2012. Poly(3-hydroxubutyrate-co-4-hydroxubutyrate)/bacterial cellulose composite porous scaffold: Preparation, characterization and biocompatibility evaluation. Carbohydrate Polymers. 87: 1073–1080.

Zhou, L. L., Sun, D. P., Hu, L. Y., Li, Y.W., Yang, J. Z., 2007. Effect of addition of sodium alginate on bacterial cellulose production by *Acetobacter xylinum.* J Journal of Industrial Microbiology & Biotechnology. 34: 483–489.

Zielins, E. R., Atashroo, D. A., Maan, Z. N., Duscher, D., Walmsley, G. G., Marecic, O., Hu, M., Senarath-Yapa, K., McArdle, A., Tevlin R. 2014. Wound healing: an update. Regenerative Medicine 9: 817–830.

3 RESPONSE SURFACE STATISTICAL OPTIMIZATION OF BACTERIAL NANOCELLULOSE FERMENTATION IN STATIC CULTURE USING A LOW-COST MEDIUM
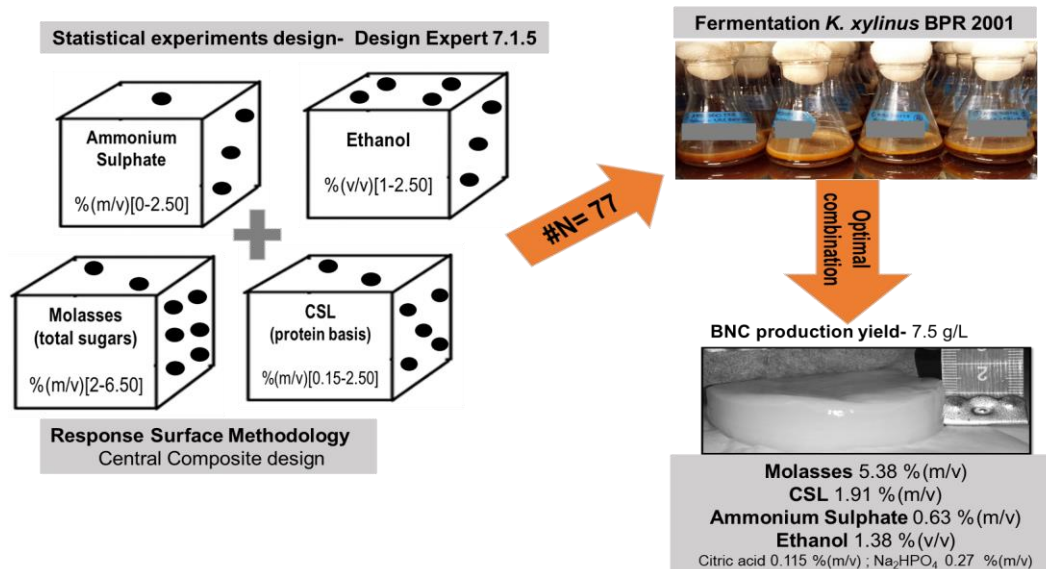
This work aimed at the optimization of bacterial nanocellulose (BNC) production by static culture, using *Komagataeibacter xylinus* BPR 2001 *(K. xylinus)*. Response surface methodology - central composite design was used to evaluate the effect of inexpensive and widely available nutrient sources, namely molasses, ethanol, corn steep liquor (CSL) and ammonium sulphate, on BNC production yield. The optimized parameters for maximum BNC production were: % (m/v): molasses 5.38, CSL 1.91, ammonium sulphate 0.63, disodium phosphate 0.270, citric acid 0.115 and ethanol 1.38 % (v/v). The experimental and predicted maximum BNC production yields were 7.5 ±0.54 g/L and 6.64 ±0.079 g/L, respectively and the experimental and predicted maximum BNC productivity were 0.829 ±0.046 g/L/day and 0.734 ±0.079 g/L/day, after 9 days of static culture fermentation, at 30 °C. The effect of surface area and culture medium depth on production yield and productivity were also studied. BNC dry mass production increased linearly with surface area, medium depth and fermentation time. So long as nutrients were still available in the culture media, BNC mass productivity was constant. The results show that a high BNC production yield can be obtained by static culture of *K. xylinus* BPR 2001 using a low-cost medium. These are promising conditions for the static industrial scale BNC production, since as compared to agitated bioreactors, higher productivities may be reached, while avoiding high capital and operating costs.

3.1 INTRODUCTION

Bacterial nanocellulose (BNC) is an exopolysaccharide produced by *Komagataeibacter xylinus* (formerly *Gluconacetobacter xylinus*), a Gram negative and strictly aerobic bacterium of the *Acetobacteraceae* family (Yamada et al., 1997; Yamada et al., 1999; Matsushita et al., 2005; Sievers and Swings, 2005; Kersters et al., 2006; Cleenwerck et al., 2009). BNC shows several unique physicochemical and mechanical properties, including high purity, high crystallinity, high degree of polymerization (Ashori et al., 2012), an ultrafine fiber network, high water holding and absorbing abilities (Saibuatong et al., 2010), high tensile strength in the wet state (Andrade et al., 2010), and the possibility to be shaped into 3D structures during synthesis. It is biocompatible and biofunctional (Klemm et al., 2011). Due to these properties, the biopolymer has been studied in several applications, including tissue regeneration, drug delivery systems, vascular grafts, *in vitro* and *in vivo* scaffolds for tissue engineering, electronic paper displays and in food applications (Czaja et al., 2007; de Azeredo, 2013; Zhou et al., 2013; Almeida et al., 2014; Esa et al., 2014; Oliveira et al., 2015; Martínez-Sanz et al., 2016). These properties and applications have generated a growing interest in the development of new strategies aimed at large-scale BNC production. Several fermentation technologies have been attempted, such as agitated, air-lift, membrane and horizontal bioreactors, using different fermentation media and overproducing mutant strains. Stirred tank reactors can prevent the heterogeneity of the culture broth, at the expense of a high energy cost for generation of mechanical power. Airlift reactors typically require only one sixth of the energy power used in stirred tank reactors. Nonetheless, the agitation power of an airlift reactor is limited, resulting in low fluidity of the culture broth, especially at high cellulose concentrations. In addition, both agitation and aeration systems have been reported to result in the development of cellulose-negative mutants (non-cellulose producers, Cel⁻) (Krystynowicz et al., 2002; Chawla et al., 2009; Lee et al., 2014;). In the case of membrane bioreactors, the major drawbacks include high operating costs and difficulty in collecting the cellulose from the reactors following fermentation (Krystynowicz et al., 2002; Chawla et al., 2009; Andrade et al., 2010; Shah et al., 2013; Lee et al., 2014; Keshk, 2014; Dourado et al., 2016a).

"Traditional" static cultivation methods for BNC production, mostly used in Asian countries, are difficult to implement on a large scale. Although the yield is relatively high, the long fermentation times required, the need for large areas and intensive manpower and high labour costs have deterred such processes from implementation in large scale, modern facilities. Alongside the fermentation method (static versus agitated/aerated), which impacts on the capital investment and operating costs), the economic feasibility of BNC production is directly dependent on product yield. The production parameters

in static culture include the composition of the culture media, fermentation temperature, pH and time, inoculum ratio (Jonas and Farah 1998; Chawla et al., 2009) and surface area to volume ratio (air-liquid interface) of the culture medium (S/V) (Krystynowicz et al., 2002; Ruka et al., 2012). The greater the medium surface area, the higher the production of BNC, given the aerobic character of the bacterium. Several reports have analysed the optimal surface area/volume ratio for BNC production in static culture (Joris et al., 1990; Krystynowicz et al., 2002; Ruka et al., 2012), but the results obtained cannot be easily compared, due to differences in fermentation times, culture media composition and strains used. As with many fermentation processes, the cost and availability of the substrates play a determining role in the economic feasibility of the process. Thus, it is important to explore the use of widely available low-cost substrates, especially agro-industrial by-products, to improve BNC yield. While several reports have addressed the use of different culture media to optimize BNC production using *K. xylinus* BPR 2001 under agitated condition, less attention has been paid to the use of static culture specifically for *K. xylinus* BPR 2001. Those studies relied on the use of fructose and corn steep liquor (CSL) as the carbon and nitrogen sources, combined with a large number (sometimes more than 20) of other nutrients, such as different vitamins, amino acids and salts. Such complex culture media are impractical for the large-scale implementation of a BNC production process (Table 1). The cost of the nutrients, media composition, available surface area, fermentation depth and time, should all be considered for economic BNC production in static culture.

Table 1- Summary of the data available on the BNC production with *K. xylinus* BPR2001.

Carbon Source	Nitrogen Source	Type of culture	Additives/ [a]BNC production yield
Fructose	CSL	Agitated Jar fermenter (with oxygen supplementation, batch and fed-batch conditions)	• **BNC production yield** 7.7 g/L (Toyosaki et al., 1995); • [b]Complex medium • endo-p-l,4-glucanase from *Bacillus suhtilis* • **BNC production yield** 4.5 g/L (Tonouchi et al., 1995); • Agar • **BNC production yield** 12.8 g/L (Bae et al., 2004); • Complex medium • **BNC production yield** 7.5 g/L (Bae and Shoda 2005a); • Complex medium • Agar • **BNC production yield** 14.3 g/L (Bae and Shoda 2005b); • KH_2PO_4 • $(NH_4)_2SO_4$ • $MgSO_4 \cdot 7H_2O$ • **BNC production yield** 1.13 g/L (Reinalti et al., 2017).
		Agitated Shaken flasks	• Complex medium and Polyacrylamide-co-acrylic acid • **BNC production yield** 6.5 g/L (Joseph et al., 2003); • Complex medium • Carboxymethyl celulose • Microcrystalline celulose • Agar and Sodium alginate • **BNC production yield** 8.2 g/L (Cheng et al., 2009).
		Agitated air-lift reactor	• Complex medium • Agar • Xanthan • **BNC production yield** 8.7 g/L (Chao et al., 2001a); • Complex medium • **BNC production yield** 3.8 g/L and 10.4 g/L (Chao et al., 2000 and 2001b).
		Agitated Plastic composite support rotating disk bioreactor (PCS-RDB),	• Complex medium • Carboxymethyl celulose • **BNC production yield** 13 g/L (Cheng et al., 2011); • Complex medium • Microcrystalline cellulose (Avicel) • Carboxymethylcellulose (CMC) • Agar • Sodium alginate • **BNC production yield** 0.64 g/slice (Lin et al., 2016).
Treated Molasses		Agitated jar fermenter	• Complex medium • **BNC production yield** 14.3 g/L and 12.8 g/L (Bae et al., 2004 and 2005a).
Wheat straw hydrolysate		Agitated Flask shaken	• Complex medium • **BNC production yield** 10.6 g/L (Al-Abdallah et al., 2013).
Wheat straw hydrolysate Corn fibers Distilller´s dried grains with Solubles		Agitated Flask shaken	• Complex medium • **BNC production yield** 5.2 g/L (Dahman et al., 2010).
Glucose or dextrose		Flask shaken	• 1-Methylcyclopropene • magnesium sulphate • ammonium sulphate • **BNC production yield** 1.2 g/L (Hu et al., 2010).
Maple syrup	Yeast extract	Flask shaken	• Ethanol • Acetic acid • $MgSO_4 \cdot 7H_2O$ • Agar • **BNC production yield** 3.2 g/L (Zeng et al., 2011).
Carob	Haricot bean	Static	• **BNC production yield** 6.5 g/L (Bilgi et al., 2016).

[a]BNC production yield is represented as g dry BNC mass/Litre of culture media.

[b]By complex medium is meant a combination of culture medium to which different vitamins, amino acids and salts were added. Sometimes the culture medium contains about 20 or more components.

Here, we report optimization of BNC production by *K. xylinus* BPR 2001 under static culture conditions, using a simple culture medium composition. Optimization was performed using response surface methodology (RSM) - central composite design (CCD). The effect of four nutrients - molasses and ethanol as the carbon sources, CSL as the nitrogen and protein source and ammonium sulphate - on the BNC production yield (g/L) (as the response variable) was assessed. In addition, the effect of the surface area and culture medium depth on the BNC production yield and productivity, were evaluated.

3.2 MATERIAL AND METHODS

3.2.1 Bacterial Strain

K. xylinus subsp *sucrofermentants* BPR 2001 (ATCC 700178), from the American Type Culture Collection, was used for the production of BNC under static conditions. The strain was maintained in Hestrin-Schramm culture medium (HS medium) (Hestrin and Schramm, 1954), in solid state with 2 % (m/v) agar (Acros Organics).

3.2.2 Inoculum preparation and static culture fermentation

BPR 2001 cells were grown in 1 L conical flasks, containing 100 mL HS medium, comprising (in % m/v) glucose 2.0 (Fisher Chemical), peptone 0.5 (OXOID), yeast extract 0.5 (OXOID), disodium phosphate (Na_2HPO_4) 0.27 (Panreac) and citric acid 0.115 (Panreac). The initial pH was set to 5.5 using 18 % (v/v) HCL (Fisher-Chemical). The medium was autoclaved at 121 °C, 1 bar for 20 min before use. The culture was incubated for 2 d at 30 °C under static conditions. Thereafter, the cellulose pellicle formed was vigorously shaken in order to remove active cells entrapped within the cellulose matrix; 4 mL (10 % (v/v) of the final volume) of this inoculum was transferred to 100 mL conical flasks, containing a final volume of 40 mL of different combinations of culture media, prepared using molasses (a gift from RAR Refinarias de Açúcar Reunidas, S.A.; Portugal), CSL (a gift from COPAM Companhia Portuguesa de Amidos, S.A.; Portugal), ammonium sulphate (Panreac) and ethanol (Fisher-Chemical), as described below. The inoculated media were incubated for 9 d, at 30 °C under static conditions. After cultivation, the BNC membranes were collected, purified and the production yield (in g/L) was determined as described below.

3.2.3 Optimization of BNC production using response surface methodology (RSM) - central composite design

In this study, the optimization process of BNC production firstly entailed identifying the preferred nutrients (carbon and nitrogen sources) for BNC production based on the literature (Table 1) and varying one factor at a time while keeping the others constant (data not shown). Based on the collected information, preliminary fermentation assays were performed to evaluate the effect of the selected nutrients (and their concentrations), on BNC yield. Data collected from these experiments allowed better determination of the boundaries for each variable to be tested (levels of factors). Molasses and CSL are the most economical carbon and nitrogen sources commonly used in industrial fermentations (Bae and Shoda, 2004; Premjet et al., 2007) (Table 1). CSL is a nutrient-rich by-product supply of amino acids, vitamins and minerals, and has been reported to have buffering capacity (Noro et al., 2004). According to the literature review, ethanol and ammonium sulphate have been observed to increase BNC production yield (Naromiti et al., 1998; Son et al., 2001; Park et al., 2003; Krystynowicz et al., 2005; Hu and Catchmark 2010;). Also, certain *Acetobacteraceae* strains are known to be capable of using ethanol as an additional carbon source (Naromiti et al., 1998; Son et al., 2001; Park et al., 2003; Chawla et al., 2009; Keshk, 2014). Supplementing a culture medium with ethanol also allowed repression of the spontaneous mutations of BNC producing cells (Cel$^+$) to non-producing cells (Cel$^-$) and increased cells ATP production (Naromiti et al., 1998; Son et al., 2001; Krystynowicz et al., 2002; Park et al., 2003; Dourado et al., 2016b). As such, these compounds were included in our media formulations.

The optimization process then focused on evaluating the effect of four independent variables: molasses (A) and ethanol (D) as carbon sources, nitrogen from CSL (B) and ammonium sulphate (C), on the yield of BNC, using response surface methodology based on central composite design (Tables 2, 3). The software Design Expert 7.1.5 (Stat-Ease, Inc., USA, Windows operating system) was used to determine the experimental design matrix and its statistical experimental design analysis. All the assays/formulations were performed in triplicate, except the central point of the factorial design, were 5 replicates were performed, resulting in a total of 77 experiments and 25 different culture media formulations (Table 3). All combinations of the fermentation medium included 0.27 % (m/v) Na$_2$HPO$_4$ and 0.115 % (m/v) citric acid. The initial pH used was set to 5.5 in all media. HS medium was used as control.

Table 2- Levels of factors chosen for the experimental central composite design.

Sources	Variable	Symbol	Lower Limit (-2)	Low Coded (-1)	Center Coded (0)	High Coded (+1)	Higher Limit (+2)	Units
Carbon	Molasses (total sugars)	(A)	2.00	3.13	4.25	5.38	6.50	% (m/v)
	Ethanol	(D)	1.00	1.38	1.75	2.13	2.50	% (v/v)
Nitrogen	CSL (protein basis)	(B)	0.15	0.74	1.33	1.91	2.50	% (m/v)
	Ammonium Sulphate total	(C)	0.00	0.63	1.25	1.88	2.50	% (m/v)

Table 3- Central Composite design matrix for the four variables. Coded values and real values, where coded values given in parentheses.

# Run	A:Molasses % m (total of sugar/v)	B:CSL % m (total of protein/v)	C:Ammonium Sulphate % (m/v)	D:Ethanol % (v/v)
1 |2 |15	(-2) 2.00	(0) 1.33	(0) 1.25	(0) 1.75
4 |55 |72	(-1) 3.13	(+1) 1.91	(+1) 1.88	(-1) 1.38
5 |20 |49	(-1) 3.13	(-1) 0.74	(+1) 1.88	(-1) 1.38
8 |59 |74	(-1) 3.13	(-1) 0.74	(+1) 1.88	(+1) 2.13
14 |32 |68	(-1) 3.13	(+1) 1.91	(-1) 0.63	(-1) 1.38
39 |56 |58	(-1) 3.13	(+1) 1.91	(+1) 1.88	(+1) 2.13
9 |29 |52	(-1) 3.13	(-1) 0.74	(-1) 0.63	(-1) 1.38
33 |60 |66	(-1) 3.13	(-1) 0.74	(-1) 0.63	(+1) 2.13
23 |43 |71	(-1) 3.13	(+1) 1.91	(-1) 0.63	(+1) 2.13
7 |24 |64	(0) 4.25	(+2) 2.50	(0) 1.25	(0) 1.75
12 |16 |40	(0) 4.25	(0) 1.33	(-2) 0.00	(0) 1.75
21 |26 |28 |48 |65	(0) 4.25	(0) 1.33	(0) 1.25	(0) 1.75
27 |34 |62	(0) 4.25	(0) 1.33	(0) 1.25	(+2) 2.50
31 |50 |73	(0) 4.25	(-2) 0.15	(0) 1.25	(0) 1.75
35 |45 |61	(0) 4.25	(0) 1.33	(+2) 2.50	(0) 1.75
51 |54 |70	(0) 4.25	(0) 1.33	(0) 1.25	(-2) 1.00
25 |75 |76	(+1) 5.38	(+1) 1.91	(+1) 1.88	(-1) 1.38
22 |44 |77	(+1) 5.38	(-1) 0.74	(-1) 0.63	(-1) 1.38
10 |63 |69	(+1) 5.38	(+1) 1.91	(-1) 0.63	(+1) 2.13
6 |30 |42	(+1) 5.38	(-1) 0.74	(-1) 0.63	(+1) 2.13
41 |46 |57	(+1) 5.38	(+1) 1.91	(-1) 0.63	(-1) 1.38
11 |36 |67	(+1) 5.38	(+1) 1.91	(+1) 1.88	(+1) 2.13
19 |37 |53	(+1) 5.38	(-1) 0.74	(+1) 1.88	(-1) 1.38
3 |13 |47	(+1) 5.38	(-1) 0.74	(+1) 1.88	(+1) 2.13
17 |18 |38	(+2) 6.50	(0) 1.33	(0) 1.25	(0) 1.75

Three-dimensional curves of the response surfaces were generated using Design Expert 7.1.5 (Stat-Ease, Inc., USA, Windows operating system) to visualize individual effects and interaction between significant parameters. All experiments were performed independently, following the sequential order shown in Table 3. Each run was performed in triplicate and an average value of the responses was used for the presentation of the results. The model was evaluated using the Fisher´s statistical test for analysis or variance (ANOVA).

3.2.4 Effect of surface area at a constant S/V ratio on BNC production yield

The effect of surface fermentation area (S) on BNC yield was evaluated. Containers having variable fermentation areas and a fixed fermentation broth depth (of 2.5 cm) were used, resulting in a fixed S/V ratio of 0.4 cm^{-1}. Fermentation broth containing molasses 4 % (m/v), CSL 0.7 % (m/v) (protein basis), ethanol 1.5 % (v/v), ammonium sulphate 0.5 % (m/v), Na_2HPO_4 0.27 % (m/v) and citric acid 0.115 % (m/v), initial pH 5.5, was sterilized. The medium was then inoculated and transferred to the containers with the different surface areas. These were incubated for 15 d under static conditions at 30 °C. BNC was then collected, purified and the production yield (in g/L) determined as described below.

3.2.5 Effect of surface area/culture medium depth ratio (S/L) on BNC production yield

The effect of the culture medium depth (L) on the BNC yield was evaluated. Containers having the same fermentation area (S, 336 cm^2), were filled with inoculated fermentation broth (as described above) at a depth (L) of 1 cm (320 mL), 2.5 cm (620 mL) and 4 cm (1000 mL), yielding S/L ratios of 336, 134.4 and 84 cm and S/V ratios of 1.05, 0.54 and 0.34 cm^{-1}, respectively. All were incubated for 9, 15 and 21 d under static conditions at 30 °C. BNC was purified and the production yield (g/L) was determined as described below.

3.2.6 BNC purification and BNC yield determination

After cultivation, the BNC membranes obtained were washed with distilled water at room temperature (RT) to remove culture medium residues, then washed with 0.1 M NaOH (Fisher-Chemical) at RT; this solution was changed twice daily until the membranes turned completely white by visual inspection. The bleached membranes were then washed with distilled water at RT until the pH became that of the distilled water. The purified BNC was oven dried to constant mass at 50 °C and weighed to determine production yield (expressed in g of dry BNC/L of culture media).

3.2.7 Analytical methods- Total sugars and protein quantification

Analysis of total molasses sugars was by HPLC, using a Metacarb 87 H column (300, 7.8 mm, Varian, USA), PU-2080 Plus pump (JASCO), DG-2080-53 degasser (JASCO), AS2057-Plus automatic sample injector (JASCO) and a 2031 Plus RI detector (JASCO) under the following conditions: mobile phase

0.005 M H$_2$SO$_4$, flow rate 0.5 mL/min, and column temperature 35 °C (Oven Elder CH-150). The injected volume was 20 µL. The concentrations of sucrose, glucose and fructose were determined based on calibration curves obtained using pure compounds. The composition of molasses (g/L) determined was sucrose 687.7 ±1.23, glucose 20.6 ±6.22 and fructose 12.8 ±2.05.

Total protein analysis of CSL was performed by BCA Protein assays kit (Pierce® BCA 23227 Protein Assay Kit, Thermo Scientific). The total protein CSL composition was 167.5 ±8.6 g/L.

3.2.8 Statistical Analysis

The statistical analyses One-way and Two-way ANOVA were performed using GraphPad Prism version 5 for Windows, GraphPad Software, San Diego, California, USA.

3.3 RESULTS AND DISCUSSION
3.3.1 Response surface methodology – central composite design

A statistically designed study was conducted to investigate the individual and interactive effect of four medium components on BNC yield. The experimental results from the 77 experiments (Table 3) are presented in Figure 1.

The first set of optimal statistical conditions, maximizing BNC production yield by *K. xylinus* BPR 2001 under static culture were obtained with experiments 41, 46 and 57, which corresponded to the same medium composition, i.e. molasses 5.38 % (m/v), CSL 1.91 % (m/v) (protein basis), ammonium sulphate 0.63 % (m/v), ethanol 1.38 % (v/v) (Table 3). Under these conditions, 87 % of the initial sugars were consumed by the bacteria after 9 d static culture fermentation, as determined by total sugars assay (results not shown). The average BNC production yield and productivity were 7.5 ±0.54 g/L and 0.829 ±0.046 g/L/day, respectively (Figure 1). Independent assays were performed (triplicates) under the optimal conditions and the results for BNC production yield were confirmed (p>0.05). This average yield value, as obtained with a low-cost formulation represents a 6.3 fold increase in BNC production yield compared with the HS medium (Figure1, HS control). Interestingly, the experiment trials 51, 54 and 70, corresponding to a medium composition of molasses 4.25 % (m/v), CSL 1.33 % (m/v) (protein basis), ammonium sulphate 1.25 % (m/v) and ethanol 1.0 % (v/v), resulted in a similar BNC production yield (p>0.05). These trials generated an average BNC production yield of 7.0 ±0.25 g/L. While achieving a (statistically) similar yield, in this second set of experiments, with the exception of ammonium sulphate, all other nutrients were used in smaller amounts. This had a positive impact on the cost of the culture

media. It should be noted that much higher BNC productivities have been reported in the literature (Table 1), under agitated conditions and using complex medium. However, for industrial production, it is necessary to consider capital investment and operating costs. Scaling up of BNC fermentation implies first the use of increasingly larger seed vessels for inoculum propagation. Under agitated conditions, multiple agitated fermenters (stirred tank or airlift fermenters) also have to be used. Together, this equipment represents a significant capital investment. In addition, high operating costs are involved, associated mainly with the fermenters' operation and cleaning processes. In contrast, the capital investment and operating cost of a cleanroom, for static culture, should be lower (Dourado et al., 2016 a and 2018).
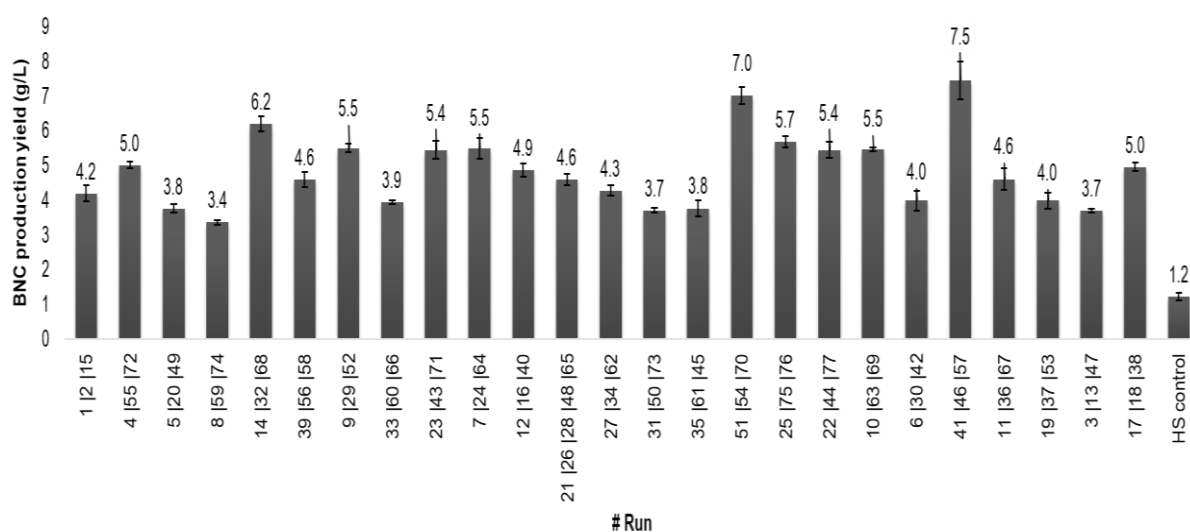
Figure 1 - Experimental BNC production yield using different medium formulations after 9 d, 30 °C in static conditions. Bars with standard deviations represent the means of triplicate experiments.

RSM technique will allow us to find the combination of input variables that will optimize a response variable of interest (Table 2) where 3D contour plots or surface curves (Supplementary material, Figure S1 and Figure 2) can be generated by linear effects, quadratic effects and two-way interactions between the factors. From these profiles, a semi-empiric model (Eq. 1) can be derived that best fits the experimental data. This allows calculation of the optimal responses of the system, in this case the maximum BNC yield. The parameters and results from the CCD experiments are presented in Tables 2, 3 and 4, Figure 1 and supplementary material Figure S1. The statistical significance of the quadratic model was tested through F- and p- values (Table 4).

Results from ANOVA indicated that the quadratic regression used to produce a second order model was significant, as revealed from the p- and F-values: the calculated Model F-value of 29.56 and the p-value of < 0.0001 indicate that the model is significant (i.e. there is only 0.01 % probability that the value

of "Model F- Value" is due to noise). The "Lack of Fit-F-Value" of 2.81 indicates that the Lack of Fit is significant. There is only a 0.74 % chance that a "Lack of Fit F-value" this large could occur due to noise. Also, a significant lack of fit (0.0074, Table 4) suggests that there may be some systematic variation, unaccounted for in the hypothesized model. This may be due to the exact replicate values of the independent variable in the model that provide an estimate of pure error.

Table 4 - ANOVA analysis of the Response Surface Reduced Quadratic Model, before eliminating the non-significant terms.

Source	Before eliminating non-significant terms					
	Sum of Squares	Df	Mean Square	F-Value	p-value Prob > F	
Model	64.50	14	4.61	29.56	< 0.0001	**Significant**
A-molasses	1.63	1	1.63	10.43	0.0020	Significant
B-CSL	22.90	1	22.90	146.93	< 0.0001	Significant
C-ammonium sulphate	12.89	1	12.89	82.71	< 0.0001	Significant
D-ethanol	19.27	1	19.27	123.64	< 0.0001	Significant
AB	0.18	1	0.18	1.16	0.2851	
AC	0.032	1	0.032	0.20	0.6525	
AD	0.30	1	0.30	1.92	0.1705	
BC	7.191E-003	1	7.191E-003	0.046	0.8306	
BD	9.847E-003	1	9.847E-003	0.063	0.8024	
CD	1.44	1	1.44	9.24	0.0035	Significant
A^2	3.340E-003	1	3.340E-003	0.021	0.8841	
B^2	9.256E-003	1	9.256E-003	0.059	0.8083	
C^2	0.15	1	0.15	0.99	0.3226	
D^2	3.19	1	3.19	20.45	< 0.0001	Significant
Residual	9.66	62	0.16			
Lack of Fit	3.39	10	0.34	2.81	0.0074	Significant
Pure Error	6.27	52	0.12			
Cor Total	74.16	76	4.61	29.56	< 0.0001	Significant
R^2				0.8697		
Adj R^2				0.8403		
Pred R^2				0.7992		
Adeq Precision				18.993		

The second–order polynomial equation of the model fitted for BNC production before eliminating the non-significant terms is:

BNC$_{production\ yield}$ (g/L) = + 12.77 + 0.24 * molasses + 0.30 * CSL – 1.80 * ammonium sulphate – 8.06 * ethanol + 0.093 * molasses * CSL + 0.037 * molasses * ammonium sulphate – 0.19 * molasses * ethanol + 0.033 * CSL * ammonium sulphate + 0.065 * CSL * ethanol + 0.74 + ammonium sulphate * ethanol + 6.65E-03 * molasses^2 + 0.041 * CSL^2 – 0.15 * ammonium sulphate^2 + 1.85 * ethanol^2

(Eq. 1)

{Degree of freedom = 14; F-value = 29.56; p-value < 0.0001; R^2 = 0.8697}

Model terms with values of p-value Prob > F (Table 4) lower than 0.05 indicated that the model terms are significant; for p-value Prob > F higher than 0.1, the model terms are non-significant. In this case, the model terms A (molasses), B (CSL), C (ammonium sulphate), D (ethanol), CD and D^2 were considered significant. The R^2 value provides a measure of how much variability in the observed response values can be explained by the experimental factors and their interactions. The closer R^2 value to 1.00, the stronger the model is and the better it predicted the observed response. It was suggested that the R^2 value should be at least 0.80, for a good model fitness (Joglekar et al., 1987). Here, the calculated R^2 value of 0.8697 (Table 4), indicated that 13.03 % of the total variation could not be explained by the empirical model; this expresses a good enough quadratic fit to navigate the design space. Thus, the response surface model developed in this study for predicting the BNC production may be considered satisfactory. The signal to noise ratio was measured by Adeq Precision value (of 18.993); a ratio greater than 4 also indicates that this model can be used to navigate the design space.

From the above, the second order polynomial equation of the model fitted for BNC production, after eliminating the non-significant terms (Table 4), is:

BNC$_{production\ yield}$ (g/L) = 13.43 + 0.13 * molasses + 0.96 * CSL - 1.97 * ammonium sulphate - 8.99 * ethanol + 0.74 * ammonium sulphate * ethanol + 1.91 * ethanol^2

(Eq. 2)

{Degree of freedom = 6; F-value = 70.70; p-value < 0.0001; R^2 = 0.8584}

whereby the F-value increased, meaning that the mean squares of the model are larger than the square residual average. Thus, with a higher the F-value, the more significant p-value for ANOVA and the more significant the model is.

The optimal concentrations of the four factors that maximized BNC production yield were predicted using the optimization function of the statistical experimental designs Design Expert 7.1.5. Molasses 5.38

% (m/v), CSL 1.91 % (m/v) (protein basis), ammonium sulphate 0.63 % (m/v), ethanol 1.38 % (v/v) were chosen as the optimal concentrations (optimized medium), allowing the highest BNC yield. The predicted medium composition coincided with experiment trials 41, 46 and 57 (Table 3). No statistical differences were observed between the predicted maximum production yield and productivity (6.64 ±0.4 g/L and 0.737 ±0.079 g/L/d) and the experimental results (7.5 ±0.54 g/L and 0.829 ±0.046 g/L/d) (p>0.05). The optimized results were also confirmed (p>0.05) by conducting a further fermentation experiment in triplicate at the above-optimized values, resulting in a production yield and productivity of 7.6 ±0.56 g/L and 0.849 ±0.062 g/L/d, respectively. A Parity plot illustrating the distribution of experimental (actual) and predicted (model) values is shown in Supplementary material, Figure S1. Data points are scattered along the diagonal line, also suggesting that the model is adequate to explain BNC production within the experimental range studied.

3.3.2 Effect of terms on bacterial nanocellulose production

3D response surface graphs (Figure 2) were plotted to illustrate the interaction of the different paired factors and to determine the optimum of each paired factor for maximum response. Each graph represents the combinations of two test factors in relation to BNC production yield (g/L).
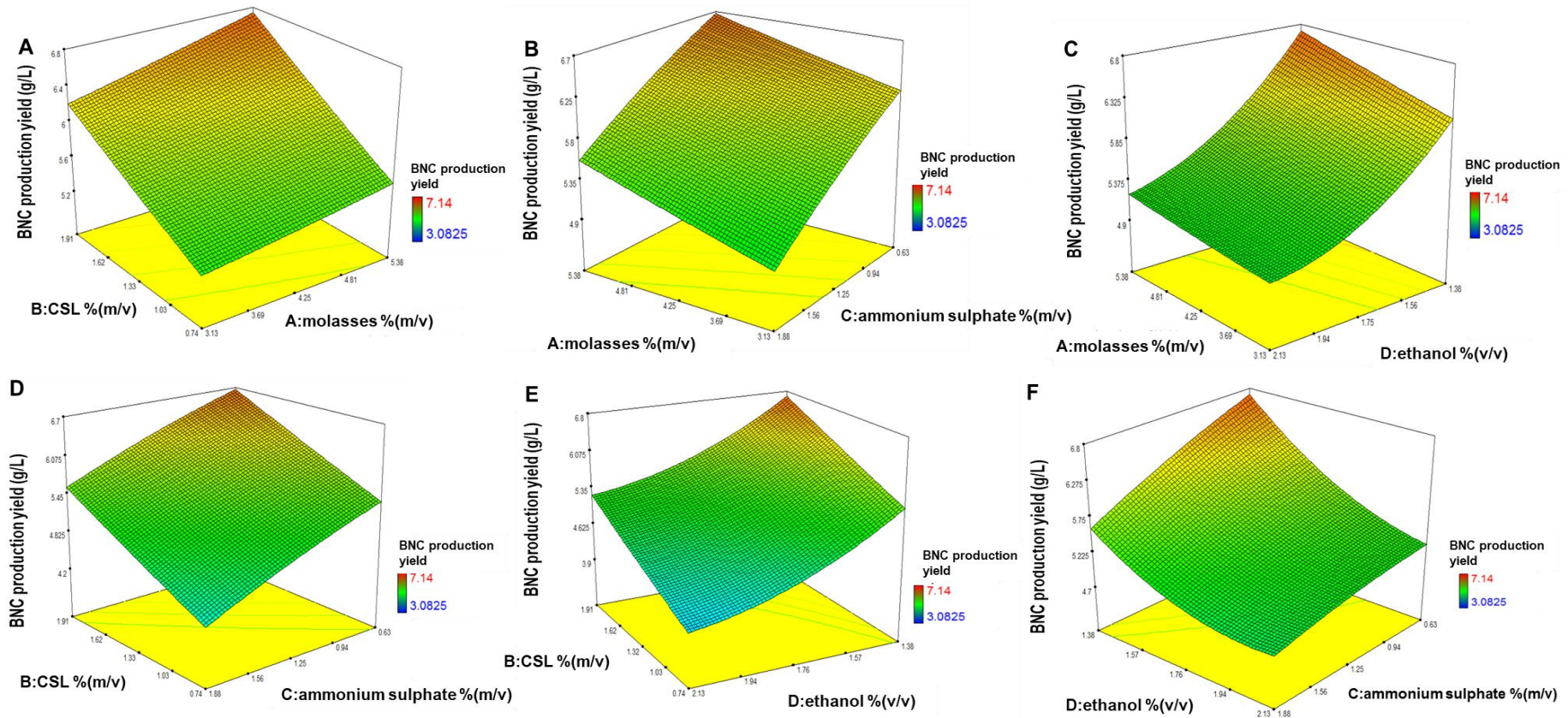
Figure 2 - Response surface curves for BNC production yield. Effect of: **A)** CSL and molasses; **B)** molasses and ammonium sulphate; **C)** molasses and ethanol; **D)** CSL and ammonium sulphate; **E)** CSL and ethanol; **F)** ethanol and ammonium sulphate, on the BNC production yield.

The data in Figure 2 A indicate that the increase in both the carbon (molasses) and protein/nitrogen sources (CSL) resulted in increased BNC production. From the combined effect of molasses and ammonium sulphate concentration (Figure 2 B), the highest production was obtained with the lowest ammonium sulphate concentration and the highest molasses concentration. Similar results were obtained with the combined effect of molasses and ethanol (Figure 2 C). The effects of CSL and ethanol concentrations, and of CSL and ammonium sulphate, on BNC production yield are illustrated in Figure 2 D and 2 E. Yield increased as the concentrations of CSL and ethanol/ammonium sulphate increased and decreased, respectively. The main medium combination of ethanol and ammonium sulphate (CD, Table 4) showed the highest p-value for Prob > F (0.0035) and therefore represents a more significant model term combination. Finally, BNC production yield increased with the decrease in ethanol and ammonium sulphate (Figure 2 F). Ethanol is a well-known carbon source during BNC fermentation and ammonium sulphate is a source of nitrogen (Naromiti et al., 1998; Son et., 2001; Krystynowicz et al., 2002; Park et al., 2003; Dourado et al., 2016b). It is possible that higher concentrations of these nutrients could have led to a substrate growth inhibition and/or affected BNC production. Indeed, Figures 2 B, C, D and E, where ethanol or ammonium sulphate are present, all show an increase in BNC yield, along with the decrease in these nutrients.

3.3.3 Effect of variable surface area, at constant S/V ratio

Under static culture conditions, due to the aerobic nature of *K. xylinus*, BNC is produced at the air/liquid interface. As synthesis progresses, the extracellular 3D nanofibrillar pellicle accumulates downward into the culture medium, while the metabolically active layer remains at the uppermost interface. In the lower pellicle layer, entrapped cells become inactive or die due to lack of oxygen. BNC yield is known to be dependent on the interplay between surface area and volume of the culture medium and the fermentation time (Borzani and Desouza, 1995). Previous studies have examined the ratio of surface area to medium volume, attempting to optimize the BNC yield. In one case (Joris et al., 1990), an optimal surface area/volume ratio of 2.2 cm^{-1} was reported whereas another (Krystynowicz et al., 2002) found that a ratio (S/V) of 0.71 cm^{-1} gave the highest yield using the strain *Acetobacter xylinum* E_{25} and 7 days of fermentation. In addition, it was reported (Ruka et al., 2012) that a ratio of 0.39 cm^{-1} gave the best yield using *Gluconacetobacter xylinus* ATCC 53524 and 14 d of fermentation.

Here, containers with different areas but with a fixed culture medium depth (2.5 cm) and consequently constant S/V ratio (0.4 cm^{-1}) were used to produce BNC under static culture for 15 d. The amount of

BNC dry mass (g) was observed to be directly proportional to the surface area (Figure 3 A). On the other hand, at a constant S/V ratio of 0.4 cm^{-1}, no statistically significant differences ($p>0.05$) in production yield (g/L) nor in productivity (g/L/day) were observed between the different surface areas (Figure 3 B). Accordingly, total sugar consumption (around 72 %) and the remaining medium after fermentation (around 17 %) were also similar in all assays. These results show that the selected culture medium depth and fermentation time were sufficient to allow the bacteria to produce a BNC pellicle at maximum productivity (Figure 3 B).
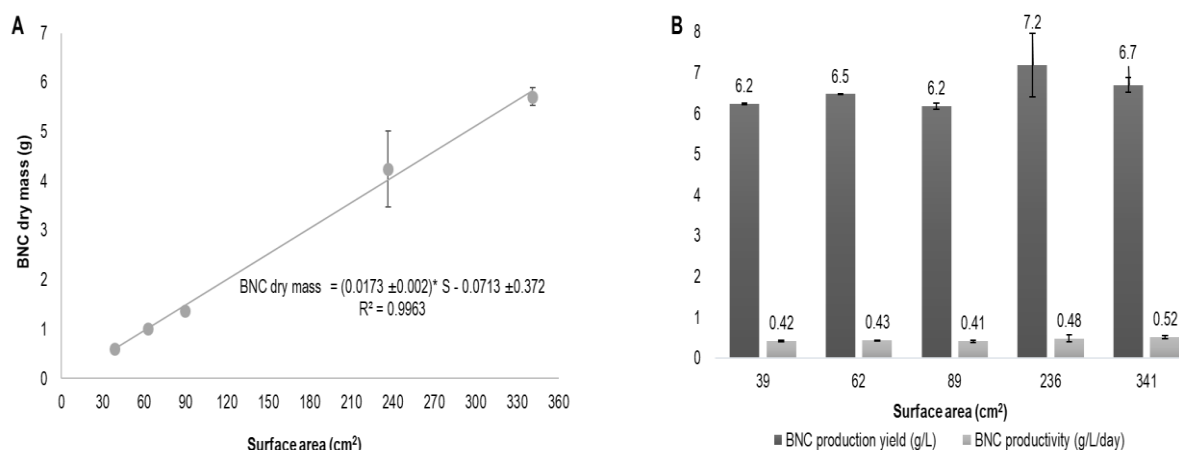
Figure 3 - A) Relationship between BNC dry mass (g) and surface area (cm^2), after 15 d of static fermentation. **B)** BNC production yields (g/L) and BNC productivity (g/L/day) obtained using containers with different surface area. after 15 d of static culture. For A and B a fixed culture medium depth of 2.5 cm was used. Bars with standard deviations represent the means of triplicate experiments.

3.3.4 Effect of variable medium depth at constant surface area

When grown under static conditions, a BNC pellicle forms at the air–surface interface. The thickness of this pellicle increases with time, up to a point of stagnation. This is proposed to occur due to oxygen or nutrient limitations: the bacteria across the top layer have poor access to nutrients due diffusional limitations, while those on the bottom layer are deprived of oxygen.

Containers with the same surface area (336 cm^2) were used to evaluate the interplay of these parameters on BNC production yield and productivity, while varying the culture medium depth and fermentation time (Figure 4). After 9 d fermentation (Figure 4 A), no statistical differences were observed in the obtained dry mass of BNC using different culture medium depths (1, 2.5 and 4 cm). The same was observed after 15 d for the cultures carried out with a medium depth of 2.5 and 4 cm. BNC production increased linearly with time, until a plateau was reached (Figure 4 B). Decline in production rate occurred earlier for the cultures with less fermentation medium. For a higher volume (4 cm depth), production progressed linearly

until day 21 (Figure 4 B). The highest BNC production yield (g/L) and productivity (g/L/day) were achieved using a culture depth of 1 cm, as calculated for day 9 (Figure 4 B and C). In this case, the remaining liquid volume (6 % of the initial) and sugars (15 % of the initial) were already very low (Figure 4 D). This suggested that the most efficient production may achieved by maximizing the S/V ratio. Indeed, even higher production yields and volumetric productivities would be reached by further reduction of the culture depth and cultivation time. However, this would not be a feasible alternative for a large-scale static culture of BNC production process, since it would demand a high number of shallow containers and require the frequent replacement of the cultivation vessels (i.e. short cycle times). On the other hand, the BNC mass productivity expressed as g/day, actually increased slightly over time and culture medium depth, as can be concluded by comparing the slopes obtained in Figure 4 A. Mass productivity for the 4 cm culture depth was higher (0.351 g/day) than those using 1 cm (0.287 g/day) and 2.5 cm (0.296 g/day), possibly due to a slower production rate at the early stage of the fermentation (a lag phase). This could be explained by a lower cell density at early stages, while as the fermentation progressed, for 1 cm culture depth (lower volume), nutrients will have been consumed, limiting productivity. It is important to recall that, for a fixed surface area, cell density is roughly the same, regardless of culture media depth, because bacteria grow at the interface air/liquid. Thus, mass productivity may represent a more relevant parameter of the performance of the static culture fermentation system than the volumetric productivity.

These results demonstrate that, for a culture medium depth of 4 cm, there were no oxygen or nutrient limitations affecting BNC production for up to 21 d, since mass productivity was constant within that time range. In this case, although significant fraction of sugars were still available (34 % of the initial), the residual liquid volume was already very low (7 % of the initial), hence the BNC production was likely to decline thereafter (Figure 4 D). Furthermore, these results allow one to plan a cost-effective large scale production of BNC, by equating the volume of fermentation trays and fermentation periods; lower volumes will have shorter cycling times and higher volumetric productivity, but possibly higher operating costs (related to trays discharging, refilling with new fermentation batch and downstream BNC processing), whereas larger volumes may require wider fermentation areas, as the trays will be stored for longer fermentation times, but larger equipment will be required for the downstream processing.
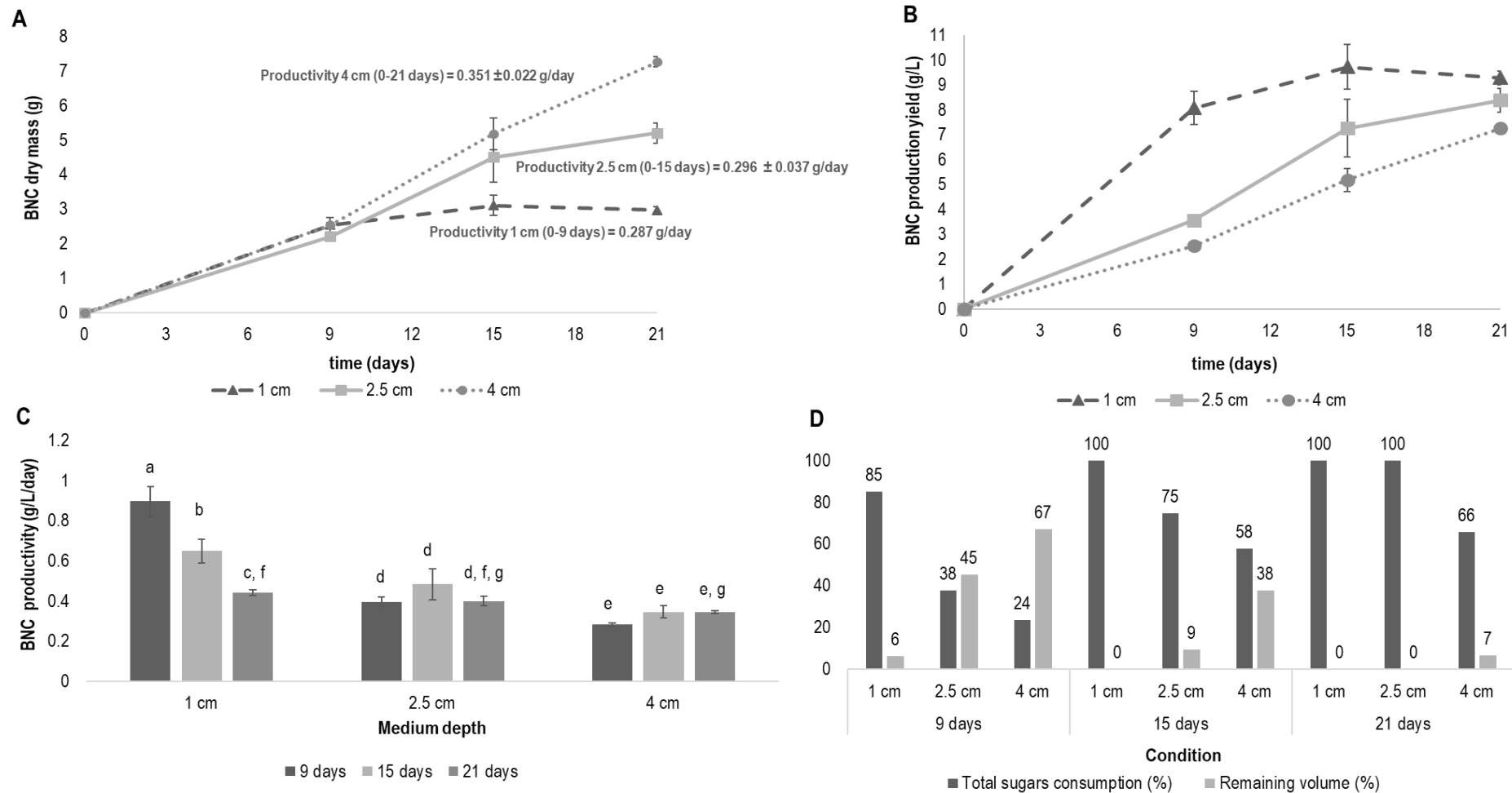
Figure 4 - A) Relationship between the BNC dry weight (g) and the medium depth (cm) at different fermentation periods. The BNC productivity (g/day) was obtained from the slope of the linear regressions: **(1 cm)**- [0-9 days]; **(2.5 cm)**- [0-15 days] and **(4 cm)**- [0-21 days]. **B)** BNC production yield (g/L) at different depths, using the same surface area. **C)** BNC productivity (g/L/day) at different depths, using the same surface area. Different letters between distinct columns denote significant differences using two-way ANOVA ($p < 0.05$). **D)** Total sugars consumed and remaining volume of culture medium after 9, 15 and 21 d for each tested culture medium depth. Data are presented as average ± standard deviations of experiments run in triplicate.

3.4 CONCLUSIONS

In this study, response surface methodology with central composite design was used to optimize the culture medium formulation for *K. xylinus* BPR 2001, using inexpensive and widely available nutrient sources. Through RSM, the optimum medium composition was % (m/v) molasses 5.38, CSL 1.91 (protein basis), ammonium sulphate 0.63 and ethanol 1.38 % (v/v). With this composition, after 9 d static culture fermentation, BNC production yield and productivity were of 6.4 ±0.54 g/L and 0.74 ±0.079 g/L/day, respectively. For 15 d fermentation, at a fixed culture media depth, a direct correlation between the fermentation area and BNC dry mass was observed. Also, at a fixed fermentation area, an almost linear BNC productivity of 0.32 ±0.037 g/L/day, could be maintained for up to 21 d, using a 4 cm culture medium depth. Moreover, for this experimental set up, no nutrient diffusional limitations were observed, the mass productivity being fairly constant overtime.

To date, most studies on BNC production by *K. xylinus* BPR 2001 have used agitated bioreactors and complex culture medium. This work demonstrates that is possible to obtain high yields in static culture, using low cost substrates and a minimal medium composition. This strain and substrates combination should expectably decrease the costs of BNC production.

3.5 APPENDIX A. SUPPLEMENTARY DATA
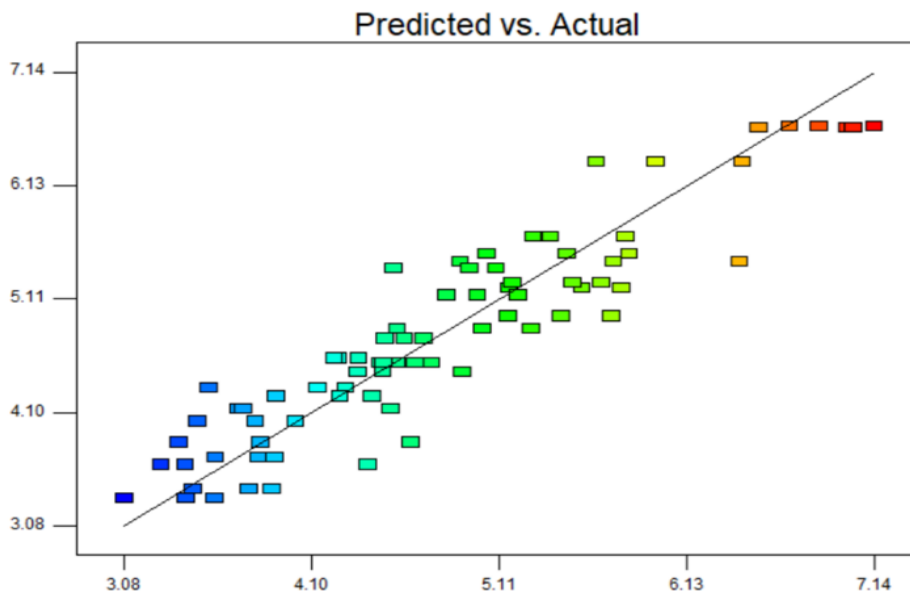
Supplementary material, Figure S1 - Parity plot showing the distribution of experimental (actual) and predicted values of BNC production yield (g/L).

3.6 REFERENCES

Al-Abdallah, W., Dahman, Y. 2013. Production of green biocellulose nanofibers by *Gluconacetobacter xylinus* through utilizing the renewable resources of agriculture residues. Bioprocess Biosystems Engineering. 36: 1735–1743.

Almeida, I.F., Pereira, T., Silva, N. H. C. S., Gomes, F.P., Silvestre, A. J. D, Freire, C. S. R., Sousa Lobo, J.M., Costa, P. C. 2014. Bacterial cellulose membranes as drug delivery systems: an *in vivo* skin compatibility study. European Journal of Pharmaceutics and Biopharmaceutics. 86: 332–336.

Andrade, F. K., Pertile, R. A. N., Dourado, F., Gama, F. M. 2010. Bacterial cellulose: Properties, production and applications. In A. Lejeune & T. Deprez (Eds.), Cellulose: Structure and Properties, Derivatives and Industrial Uses (pp. 427-458). New York: Nova Science Publishers Inc.

Ashori, A., Sheykhnazari, S., Tabarsa, T., Shakeri, A., Golalipour, M. 2012.   Bacterial cellulose/silica nanocomposites: Preparation and characterization. Carbohydrate Polymers. 90(1): 413–418.

Bae S. and Shoda, M. 2005b. Statistical Optimization of Culture Conditions for Bacterial Cellulose Production Using Box-Behnken Design. Biotechnology and Bioengineering. 90: 20-28.

Bae, S. and Shoda, M. 2004. Bacterial cellulose production by fed-batch fermentation in molasses medium. Biotecnology Progress. 20: 1366-1371.

Bae, S., Sugano, Y., Shoda, M. 2004. Improvement of bacterial celulose production by addition of agar in a jar fermentor. Journal of Bioscience and Bioengineering. 97: 33-38.

Bae, S.O. and Shoda, M. 2005a. Production of bacterial cellulose by *Acetobacter xylinum* BPR2001 using molasses medium in jar fermentor. Applied Microbiology and Biotechnology. 67: 45-51.

Bilgi, E., Bayir, E., Sendemir-Urkmez, A., Hames, E. E. 2016. Optimization Bacterial cellulose production *Gluconacetobacter xylinus* using carob and haricot bean. International Journal of Biological Macromolecules. 90: 2-10.

Borzani, W. and Desouza, S. J. 1995. Mechanism of the film thickness increasing during the bacterial production of cellulose on non-agitated liquid-media. Biotechnology Letters. 17: 1271–1272.

Chao, Y., Ishida, T., Sugano, Y., Shoda, M. 2000. Bacterial cellulose production by *Acetobacter xylinum* in a 50-L internal-loop airlift reactor. Biotechnology and Bioengineering. 68: 345-352.

Chao, Y., Mitarai, M., Sugano, Y., Shoda, M. 2001a. Effect of addition of water soluble polysaccharides on bacterial cellulose production in a 50 L airlift reactor. Biotechnology Progress. 17: 781-785.

Chao, Y., Sugano, Y., Shoda, M. 2001b. Bacterial cellulose production under oxygen-enriched air at different fructose concentration in a 50-liter, internal-loop airlift reactor. Applied Microbiology and Biotechnology. 55: 673-679.

Chawla, P. R., Bajaj, I. B., Survase, S. A., & Singhal, R. S. 2009. Microbial Cellulose: Fermentative Production and Applications. Food Technology and Biotechnology. 47(2): 107-124.

Cheng, K.-C., Catchmark, J. M., Demirci, A. 2009. Effect of different additives on bacterial cellulose production by acetobacter xylinum and analysis of material property. Cellulose. 16: 1033-1045.

Cheng, K.-C., Catchmark, J. M., Demirci, A. 2011. Effects of CMC addition on bacterial cellulose production in a biofilm reactor and its paper sheets analysis. Biomacromolecules. 12: 730-736.

Cleenwerck, I., De Wachter, M., Gonzalez, A., De Vuyst, L., De Vos, P. 2009. Differentiation of species of the family *Acetobacteraceae* by AFLP DNA fingerprinting: *Gluconacetobacter* kombuchae is a later heterotypic synonym of *Gluconacetobacter* hansenii. International Journal of Systematic and Evolutionary Microbiology. 59 (7):1771-1786.

Czaja, W.K., Young, D.J., Kawecki, M., Brown, R.M. 2007. The future prospects of microbial cellulose in biomedical applications. Biomacromolecules. 8(1): 1–12.

Dahman, Y., Jayasuriya, K. E., Kalis, M. 2010. Potential of Biocellulose Nanofibers Production from Agricultural Renewable Resources: Preliminary Study. Applied Biochemistry Biotechnolology. 162: 647–1659.

de Azeredo H.M.C. 2013. Antimicrobial nanostructures in food packaging. Trends Food Science Technology. 30: 56–69.

Dourado, F., Fontão, A. I., Leal, M., Rodrigues, A. C., Gama, M. 2016a. Chapter 12 - Process Modeling and Techno-Economic Evaluation of an Industrial Bacterial NanoCellulose Fermentation Process. In "Bacterial Nanocellulose: from biotechnology to bio-economy". Ed.: Gama, M.; Bielecky, S.; Dourado, F. Elsevier; Amsterdam, Netherlands.

Dourado, F., Fontão, A. I., Leal, M., Rodrigues, A. C., Gama, M. 2018. Chapter 1- Process modelling and techno-economic evaluation of an industrial air-lift bacterial cellulose fermentation process. in "Nanocellulose and Sustainability: Production, Properties, Applications, and Case Studies". Ed.: Koon-Yang Lee. CRC Press, USA. 1-13.

Dourado, F., Ryngaillo, M., Jedrzejczak-Krzeptowska, M., Bielecki, S., Gama, M. 2016b. Chapter 1 - Taxonomic Review and Microbial Ecology. in Bacterial Nanocellulose Fermentation. In "Bacterial Nanocellulose: from biotechnology to bio-economy". Ed.: Gama, M.; Bielecky, S.; Dourado, F. Elsevier; Amsterdam, Netherlands. 1-17.

Esa, F., Tasirin, S. M., Rahman, N.A. 2014. Overview of Bacterial Cellulose Production and Application. Agriculture and Agricultural Science Procedia. 2: 113-119.

Hestrin, S., and Schramm, M. 1954. Preparation of freeze-dried cells capable of polymerizing glucose to cellulose. Biochemical Journal. 58: 345-352.

Hu, Y. and Catchmark, J. M. 2010. Influence of 1-methylcyclopropene (1-MCP) on the production of bacterial cellulose biosynthesized by *Acetobacter xylinum* under the agitated culture. Letters in Applied Microbiology. 51: 109–113.

Joglekar, A. M., and May, A. T. 1987. Product excellence through design of experiments. Cereal Food World. 32: 857-868.

Jonas, R. and Farah, L.F. 1998. Production and application of microbial cellulose. Polymer Degradation Stability. 59: 101–106.

Joris, K., Biliet, F., Drieghe, S., Brack, D., Vandamme, E. 1990. Microbial production of β-1,4-glucans. Meded Fac Landbouwwet-Rijksuniv Gent. 55: 1563-1566.

Joseph, G., Rowe, G. E., Margaritis, A., Wan, W. 2003. Effects of polyacrylamide co-acrylic acid on cellulose production by *Acetobacter xylinum*. Journal of Chemical Technology & Biotechnology. 78: 964-970.

Kersters, K., Lisdiyanti, P., Komagata, K., Swings, J. 2006. The family *Acetobacteraceae*: the genera *Acetobacter, Acidomonas, Asaia, Gluconacetobacter, Gluconobacter, and Kozakia*. In M. Dworkin, S. Falkow, E. Rosenberg, K.-H. Schleifer, & E. Stackebrandt (Eds.), *Prokaryotes* (3 ed., Vol. 5, pp. 163-200). New York: Springer.

Keshk, S. M. A. S. 2014. Bacterial Cellulose Production and its Industrial Applications. Journal of Bioprocessing & Biotechniques. 04(02): 1-10.

Klemm, D., Kramer, F., Moritz, S., Lindström, T., Ankerfors, M., Gray, D., Dorris, A. 2011. Nanocelluloses: a new family of nature-based materials. Angewandte Chemie International Edition. 50: 5438–5466.

Krystynowicz, A., Czaja, W., Wiktorowska-Jezierska, A., Gonçalves-Mi´skiewicz, M., Bielecki, S. 2002. Factors affecting the yield and properties of bacterial cellulose. Journal of Industrial Microbiology & Biotechnology. 29: 189-195.

Lee, K. Y., Buldum, G., Mantalaris, A., Bismarck, A. 2014. More than meets the eye in bacterial cellulose: biosynthesis, bioprocessing, and applications in advanced fiber composites. Macromolecule Bioscience. 14(1): 10-32.

Lin, S.-P., Liu, C.-T., Hsu, K.-D., Hung, Y.-T., Shih, T., Y., Cheng, K.-C. 2016. Production of bacterial cellulose with various additives in a PCS rotating disk bioreactor and its material property analysis. Cellulose. 23: 367-377.

Martínez-Sanz, M., Lopez-Rubio, A., Villano, M., Oliveira, C. S. S., Majone, M. Reis, M., Lagarón, J. M. 2016. Production of bacterial nanobiocomposites of polyhydroxyalkanoates derived from waste and bacterial nanocellulose by the electrospinning enabling melt compounding method. Journal of Applied Polymer Science. 133.

Matsushita, K., Inque, T., Theeragool, G., Trcek, J., Toyama, H., & Adachi, O. 2005. Acetic acid production in acetic acid bacteria leading to their "death" and survival. In M. Yamada (Ed.), Survival and death in bacteri. Research Signpost. Kerala/India. 169-18.

Naromiti, T., Kouda, T., Yano, H., Yoshinaga, F. 1998. Effect of ethanol on bacterial cellulose production in continuous culture from fructose. Journal Fermentation Bioengineering. 85: 598-603.

Noro, N., Sugano, Y, Shoda, M. 2004. Utilization of the buffering capacity of corn steep liquor in bacterial cellulose production by *Acetobacter xylinum*. Applied Microbiology Biotechnology. 64: 199–205.

Oliveira Barud, H. G., Barud Hda S., Cavicchioli, M., do Amaral, T.S., de Oliveira Junior, O.B., Santos, D. M., Petersen, A. L., de O A, Celes F., Borges, V. M., de Oliveira, C. I., de Oliveira, P. F., Furtado, R. A., Tavares, D. C, Ribeiro, S.J.L. 2015. Preparation and characterization of a bacterial cellulose/silk fibroin sponge scaffold for tissue regeneration. Carbohydrate Polymer. 128: 41–51.

Park, J.K., Jung, J.Y., Park, Y.H. 2003. Cellulose production by *Gluconacetobacter hansenii* in a medium containing ethanol. Biotechnology Letters. 25: 2055–2059.

Premjet, S., Premjet, D., Ohtani, Y. 2007. The effect of ingredients of sugar cane molasses on bacterial cellulose production by *Acetobacter xylinum* ATCC 10245. Sen-I Gakkaishi. 63: 193–199.

Reinalti, I., Hrymak, A. N., Margaritis, A. 2017. Kinetics of cell growth and crystalline nanocellulose production by *Komagataeibacter xylinus*. Biochemical Engineering Journal. 127: 21-31.

Ruka, D., Simon, G., Dean, K. 2012. Altering the growth conditions of *Gluconacetobacter xylinus* to maximize the yield of bacterial cellulose. Carbohydrate Polymers. 89: 613-622.

Saibuatong, O. A., Phisalaphong, M. 2010. Novo aloe vera-bacterial cellulose composite film from biosynthesis. Carbohydrate Polymers. 79(2): 455–460.

Shah, N., Ul-Islam, M., Khattak, W. A., & Park, J. K. 2013. Overview of bacterial cellulose composites: A multipurpose advanced material. Carbohydrate Polymers. 98(2): 1585-1598.

Sievers, M. and Swings, J. 2005. Family II. *Acetobacteraceae*. In J. T. Staley, D. R. Boone, D. J. Brenner, P. De Vos Editor, M. Goodfellow, N. R. Krieg, F. A. Rainey, G. M. Garrity, K.-H. Schleifer, & G. G. Editor (Eds.), *Bergey's Manual® of Systematic Bacteriology* (2nd ed., Vol. 2C, pp. 41-94). New York: Springer-Verlag New York, LLC.

Son, H. J., Heo, M. S., Kim, Y. G., Lee, S. J. 2001. Optimization of fermentation conditions for the production of bacterial cellulose by a newly isolated Acetobacter sp. A9 in shaking cultures. Biotechnology and Applied Biochemistry. 33: 1-5.

Tonouchi, N., Tahara, N., Tsuchida, T., Yoshinaga, F., Beppu, T., Horinouchi, S. 1995. Addition of a Small Amount of an Endoglucanase Enhances Cellulose Production by *Acetobacter Xylinum*. Bioscience Biotechnology and Biochemistry. 59: 805-808.

Toyosaki, H., Naritomi, T., Akira, S., Matsuoka, M., Tschuida, T., Yoshinaga, F. 1995. Screening of bacterial cellulose-producing acetobacter strains suitable for agitated culture. Bioscience Biotechnology and Biochemistry. 59: 1498–1502.

Yamada, Y., Hoshino, K.-I., Ishikawa, T. 1997. Taxonomic Studies of Acetic Acid Bacteria and Allied Organisms. Part XI. The Phylogeny of Acetic Acid Bacteria Based on the Partial Sequences of 16S Ribosomal RNA: The Elevation of the Subgenus *Gluconoacetobacter* to the Generic Level. Bioscience Biotechnology and Biochemistry. *61*(8): 1244-1251.

Yamada, Y., Hosono, R., Lisdyanti, P., Widyastuti, Y., Saono, S., Uchimura, T., & Komagata, K. 1999. Identification of acetic acid bacteria isolated from Indonesian sources, especially of isolates classified in the genus *Gluconobacter*. The Journal of General and Applied Microbiology. *45*(1): 23-28.

Zeng, X., Small, D. P., Wan, W. 2011. Statistical optimization of culture conditions for bacterial cellulose production by *Acetobacter xylinum* BPR 2001 from maple syrup. Carbohydrate Polymers. 85: 506-513.

Zhou, T., Chen, D., Jiu, J., Nge, T. T., Sugahara, T., Nagao, S., Koga, H., Nogi, M. 2013. Electrically Conductive Bacterial Cellulose Composite Membranes Produced by the Incorporation of Graphite Nanoplatelets in Pristine Bacterial Cellulose Membranes. Polymer Letters. 7(9): 756– 766.

4 STRATEGIES TO OPTIMIZE PRE-INOCULUM CONDITIONS FOR THE LARGE-SCALE PRODUCTION OF BACTERIAL NANOCELLULOSE
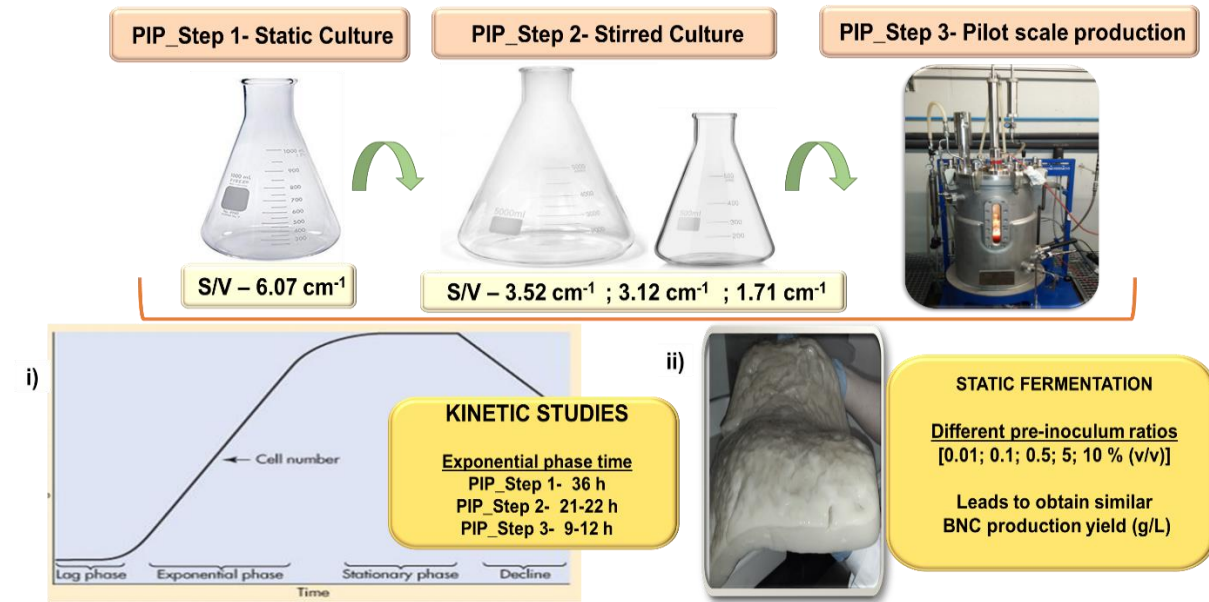
The methodology of *Komagataeibacter xylinus* subsp *sucrofermentants* BPR 2001 pre-inoculum culture preparation (PIP) and its impact on the bacterial nanocellulose (BNC) production yield was assessed. The following aspects were considered relevant, in particular envisaging the large scale production of BNC by static culture: **i)** development of a low cost fermentation medium providing high cell density; **ii)** optimization of the cellulase concentration added during pre-inoculum and evaluate the effect in static fermentation; **iii)** evaluation of the effect of initial cell density on BNC production yield; **iv)** kinetic studies of cell growth at laboratorial and pilot scale, taking in account different processing sequences for the PIP. Specifically, the pilot scale process includes three successive steps: PIP_Step 1- static culture; PIP_Step 2 – small volume stirred culture and PIP_Step 3 – large scale stirred culture in a 75 L Bioreactor. The best results were obtained using a pre-culture fermentation medium with the following composition (in % (m/v)): Glucose and Fructose syrup 1.5- 2.0, Corn Step Liquor (protein basis) 0.7, citric acid 0.115, Na_2HPO_4 0.27. Importantly, it was found that the initial cell density in the static BNC culture did not impacted on the BNC production yield. Indeed, the reduction of the initial percentage to very low inoculum rates, such as 0.1 - 0.5 % (v/v), allowed to obtain the same production yield as with the traditional 6-10 % (v/v), an observation of paramount economic impact for the large-scale production of BNC. The analysis of the cell growth kinetics in the different steps of PIP showed that the time required to reach the exponential phase was very different in each stage, reducing significantly from the static culture 36 h to the 21-22 h for stirred culture and to 9-12 h for large scale stirred culture in a 75 L Bioreactor. Thus, a careful control on the culture time in each stage of the PIP is advisable. Altogether, this study showed that pre-inoculum optimization is very relevant as to achieve satisfactory productivities and in particular for the implementation of low-cost large-scale BNC production at large scale.

4.1 INTRODUCTION

BNC is recognized as a unique material due to its physiochemical characteristics like high purity, biocompatibility, high crystallinity, high porosity, high water holding and high mechanical strength (Dahman et al., 2009; Keshk, 2014; Saibuatong and Phisalaphong, 2010; Khan et al., 2015; Mohite and Patil, 2014). Potential applications have been identified, namely for nanocomposites production, biomedical devices, drug delivery systems, cosmetics, diagnostic biosensors, environmental remediation, food industries, and materials science (Czaja et al., 2007; de Azeredo 2013; Almeida et al., 2014; Oliveira Barud et al., 2015; Martínez-Sanz et al., 2016; Wu and Liu 2012; Ashjaran et al., 2013; Lin and Dufresne, 2014; Chawla et al., 2009; Shi et al., 2014). However, it is still difficult to achieve the high BNC production in a large-scale fermentation at low costs. Static culture is traditionally used however, it requires a period of cultivation of at least 2 weeks (Hornung et al., 2006). Several types of bioreactors have been used to enhance the BNC production rate, including stirred tank (Kouda et al., 1997; Bae and Shoda, 2005; Cheng et al., 2009), rotating disk (Krystynowicz et al., 2002; Kim et al., 2007), air-lift bubble (Chao et al., 2005; Wu and Li, 2015) and variations of surface culture reactors (Hornung et al., 2007; Kralisch et al., 2010). However, some problems associated with the industrial implementation of these different configurations have been identified, namely associated with the increase of the medium's viscosity and decrease of oxygen diffusion with BNC production and the spontaneously forming non-cellulose producing (Cel⁻) mutants accumulate which contributes to the decline in the BNC production yield (Krystynowicz et al., 2002; Park et al., 2003,).

The literature commonly identifies the use of expensive culture medium as one of the main reasons for high cost of BNC production and therefore a great effort has been dedicated to the identification of low-cost substrates. The production of BNC using agricultural and industrial food wastes, including saccharified food wastes (Song et al., 2009), grape medium (Rani et al., 2011), pineapple juice (Castro et al., 2011), grape bagasse (Vasquez et al., 2013), glycerol from biodiesel (Vasquez et al., 2013), low quality date syrup (Moosavi-Nasab and Yousef, 2011), molasses (Bae and Shoda, 2005) and many others (Cacicedo et al., 2016) have been previously demonstrated. These media have different types of carbon and nitrogen sources which affect differently the kinetics of cell growth and BNC production. Although these authors do not share this general opinion that the culture media is the main cost determinant of BNC production, it must be acknowledged that finding a low-priced culture medium available in large amounts throughout the year may enhance an economically feasible solution (Padmanaban et al., 2015). However, much less effort has been dedicated to other relevant aspects of the BNC production, like PIP,

affordable large-scale fermentation and downstream processing (washing/purification/drying). Indeed, optimization of the PIP, could have a major impact on the capital investment, when considering the large-scale BNC production (Dourado et al., 2016 and 2018), as will be further explained bellow.

Information regarding the kinetics of cell growth is essential for the pre-inoculum bioreactor design and process scale-up. Unfortunately, very little work has been dedicated to this topic using BNC producing strains (Chao et al., 2000; Bae and Shoda, 2004 and 2005; Reiniati et al., 2017). In this work, kinetic studies were conducted to provide kinetic information of bacterial growth of *Komagataeibacter xylinus* subsp *sucrofermentants* BPR 2001 (*K. xylinus* BPR2001), BNC production yield. Commercial fermentations involve growing cells from a stock culture (Gershater et al., 2010). It is important to limit the lag period or fermentations will take a long time, tying up expensive equipment and facilities. The normal method is to use an inoculum 'train', which involves transferring actively growing cells (e.g. from the exponential growth phase) to successively larger reactors (Meyrath and Suchanek, 1972).

Thus, our main goal in this work relates to the development of a viable and economic strategy for the PIP that can be implemented at industrial scale. The optimization consisted of different studies, namely: **(i)** optimization of an affordable culture medium for pre-inoculum leading to a high cell density; **(ii)** evaluation of the effect of the amount of cellulase used, namely on BNC production yield and membrane quality; **(iii)** evaluation the effect of the initial cellular concentration on the static production of BNC and **(iv)** study the kinetics of cell growth throughout the different steps of pre-inoculum preparation, including static and stirred - laboratorial and pilot-scale - fermentations.

4.2 MATERIALS AND METHODS

4.2.1 Bacterial strain

In this work, *Komagataeibacter xylinus subsp sucrofermentants* BPR 2001 (ATCC 700178), was purchased from American Type Culture Collection, was used for the production of BNC under static conditions. The strain was maintained in Hestrin-Schramm culture medium (HS medium) (Hestrin & Schramm, 1954) in solid state with 2 % (m/v) agar (Acros Organics) until used.

4.2.2 Optimization of pre-inoculum culture preparation (PIP) and effect of inoculum ratio on the BNC production by static fermentation

PIP was performed in two steps of propagation using different culture medium combinations (A – L, Table 1).

PIP_Step 1- Static culture: One colony was transferred from solid media to 1 L conical flasks containing 100 mL of each different medium, at pH 5.5. These cultures were incubated during 3 days at 30 °C under static conditions. Afterwards, the cellulose pellicle formed on the surface of culture medium was vigorously shaken to remove active cells entrapped in the cellulose membrane and 10 % (v/v) of inoculum was transferred for:

PIP_Step 2- Stirred culture: 500 mL conical flasks containing 112.5 mL of different culture medium (A – L, Table 1) and 0.1 % (v/v) of cellulase (Cellucast 1.5 L, Novozymes); Hestrin–Schramm (HS) medium (Hestrin & Schramm, 1954) was used as a control. The enzyme was used to hydrolyse the BNC fibres as they are produced, allowing the cells to multiply rapidly in the fermentation broth, thereby yielding, expectedly, higher cell density. The culture was carried out in a rotatory shaker (MaxQ 481R HP Thermo Scientific) at 30 °C and 160 rpm during 30 h. Then, the cellulase was removed by centrifuging the fermentation broth at $3667 \times g$ (ScanSpeed 1580 R) for 30 min at 4 °C and discharging the supernatant. The collected cells were resuspended with fresh culture medium and using the same volume of supernatant discharging. After that different concentrations of cells (0.01, 0.1, 0.5, 5 and 10 % (v/v)) was transferred to 40 mL of fresh culture medium; the composition of fresh culture medium obtained was (% (m/v)): 4 molasses (a gift from RAR Refinarias de Açúcar Reunidas, S.A.; Portugal); 0.5 yeast extract (OXOID); 0.5 peptone (OXOID); 0.115 citric acid (Panreac); 0.27 Na_2HPO_4 (Panreac) and 1.5 % (v/v) ethanol (Fisher-Chemical), the initial pH was set to 5.5 using 18 % (v/v) HCL (Fisher-Chemical). The medium was autoclaved at 121 °C, 1 bar for 20 minutes before use. The culture was incubated in 100 mL conical flask during 7 days at 30 °C under static conditions. The BNC was purified and the production yield (g/L) determined as described in section 4.2.4. At the end of PIP Steps 1 and 2 the viable cell number/concentration present in fermentation broth was measured using the colony forming units (CFU´s) method (section 4.2.5). The total sugars were analysed by HPLC to estimate the consumption during fermentation (section 4.2.6).

Table 1 - Medium composition tested in different steps of pre-inoculum preparation.

	A	B	C	D	E	F	G	H	I	J	K	L	Control HS medium
4 % (m/v) [a]Fructose	X	X											
1.5 % (m/v) [b] Glucose and Fructose syrup			X	X									
1.5 % (m/v) [a]Glucose					X	X	X	X					X
1.5 % (m/v) [b]Molasses									X	X			
1.5 % (m/v) [a]Sucrose											X	X	
0.7 % (m/v) [c]CSL (protein basis)	X	X	X	X			X	X	X	X	X	X	
0.5 % (m/v) Peptone					X	X							X
0.5 % (m/v) Yeast extract					X	X							X
1.5 % (v/v) Ethanol		X		X		X		X		X		X	
0.115 % (m/v) Citric acid						X							X
0.27 % (m/v) Na$_2$HPO$_4$						X							X

[a] purchased from Sigma-Aldrich; [b] a gift from RAR Refinarias de Açúcar Reunidas, S.A., (Portugal); [c] a gift from COPAM Companhia Portuguesa de Amidos, S.A. (Portugal).

4.2.3 Cell growth kinetic´s in the different stages of the PIP using alternative medium to BNC production

4.2.3.1 PIP_Step 1- Static Culture

Conical Flasks (1 L) containing 100 mL of culture medium (composition C, but with 2 % (m/v) of sugars - Table 1) were inoculated and placed in static culture without (A) and with (B) addition of 0.1 % (v/v) of cellulase, to hydrolyse the BNC pellicle. The static culture was incubated for 3 days at 30 °C and every 6 h a sample was collected; for this a slow agitation of culture medium A and vigorously shaking the culture medium B was done. The cell concentration was determined as described in section 4.2.5. Sugars consumption was analysed by HPLC (section 4.2.6).

4.2.3.2 PIP_Step 2- Stirred Culture

The Step 1 pre-inoculum, (10 % (v/v)), collected at the exponential phase, identified as described on section 4.2.3.1, was transferred to flasks with fresh culture medium as in section 4.2.3.1, with 0.025 % (v/v) of cellulase. The cellulase concentration was optimized (data not shown) taking in account: **1)** the minimum amount leading to the reduction of the formation of BNC flocks which entrap the microbial cells and make it more difficult to pump the inoculum and cleaning the equipment's (relevant at large scale); **2)** the maximum amount that does not compromise the quality of the BNC membranes produced in the

following static culture, not requiring a separation of the cellulases between the two stages. Thus, the optimal concentration of 0.025 % (v/v) was found, when using an inoculum ratio of 0.5 % (v/v). It must be remarked that the use of higher amounts of inoculum (5 % (v/v)) prepared with cellulase (even with only 0.0125 % (v/v)) compromises the quality of the membranes obtained (gelatinous and with poor mechanic properties). Thus, the optimization of the cellulase concentration is advisable, taking in account the activity of the cellulase cocktail used and the inoculum ratio.

Flasks with different dimensions and culture medium volumes were used: **A)** 500 mL conical Flask with 112.5 mL of medium **B)** 5 L conical Flask with 550 mL of medium and **C)** 5 L conical Flask with 1 L of medium, corresponding to a volumetric surface area (S/V) of 3.52 cm^{-1}; 3.12 cm^{-1} and 1.71 cm^{-1}, respectively. The cultures were incubated in a rotatory shaker operated at 160 rpm for 30 h, at 30 °C. Every 3 h a sample was collected, and the cell concentration was determined (section 4.2.5). The sugars consumption was analysed by HPLC (section 4.2.6).

4.2.3.3 PIP_Step 3 - Pilot scale production

After optimizing the PIP Steps 1 and 2, the large-scale production was attempted using a 75 L bioreactor. Thus, the pilot scale PIP includes 3 steps. PIP_Steps 1 and 2 were performed as described on section 4.2.3.1 and 4.2.3.2, with slight differences: In PIP_Step 1 fermentation was carried out for 48 h and Step 2 for 21 h, on a 5 L conical flask with 1 L of culture medium. The PIP_Step 2 pre-inoculum (10 % (v/v)) was transferred to a 75 L reactor (LP351 75L from Bioengineerig®) with 45 L of culture medium as in Step 2, with antifoaming agent (Antifoam 204, Sigma-Aldrich) and 0.025 % (v/v) of fresh cellulase (PIP_Step 3). The aeration rate was set at 1 vvm and providing high agitation of the culture medium. Samples were collected every 3 h during 33 h and analysed for cell counting (section 4.2.5) and total sugars (section 4.2.7). At 9, 12 and 30 h, the fermentation broth was collected and used to inoculate static cultures which performed in vessels with a dimensions (length=24 x width =9.5x height= 14 cm), filled up to 2.5 cm height of medium with composition (% (m/v)): 4 molasses; 0.7 CSL (protein basis); 0.115 citric acid; 0.27 Na$_2$HPO$_4$; 0.5 ammonium sulphate 1.5 % (v/v) ethanol, and with initial pH of 5.5; these vessels were incubated for 15 days at 30 °C under static conditions. The total volume of the static culture was 620 mL, and the ratio of inoculum used was 0.5 % (v/v). Finally, the BNC was purified and the production yield (g/L) determined (section 4.2.4).

4.2.4 Purification and BNC production yield determination

The BNC membranes obtained were washed with distilled water, at room temperature, to remove culture medium residues. Afterwards, the membranes were washed with 0.1 M NaOH solution (Fisher-Chemical), also at room temperature; this solution was changed twice daily, until the membranes turned completely white, as observed by visual inspection. The bleached membranes were then washed with distilled water, at room temperature, until the pH remained stable. The purified BNC was oven-dried to constant mass, at 50 °C and then weighed for calculation of the production yield (expressed in g of dry BNC/L of culture medium).

4.2.5 Cell counting (Colony Forming Units – CFU method)

Eight millilitres of HS medium and 1 mL of 20 % (v/v) cellulase, dissolved in medium HS, were added to 1 mL of culture broth from each step of pre-inoculum preparation and incubated at 30 °C for 1 h to hydrolyse BNC. Then, the cell concentrations were measured by the plate dilution method. The HS agar plates were incubated at 30 °C until colonies formed on the agar plate. Thereafter, the CFU were counted.

4.2.6 Analytical methods - Total sugars and protein quantification

The analysis of total sugars of molasses was made by HPLC, using a Metacarb 87 H column (300, 7.8 mm, Varian, USA), PU-2080 Plus pump (JASCO), DG-2080-53 degasser (JASCO), AS2057-Plus automatic sample injector (JASCO) and a 2031 Plus RI detector (JASCO) under the following conditions: mobile phase 0.005 M H_2SO_4, flow rate 0.5 mL/min, and column temperature 35 °C (Oven Elder CH-150). The injected volume was 20 µL. The concentration of sucrose, glucose and fructose were determined based on calibration curves obtained using pure compounds.

The following composition of molasses (g/L) was obtained: sucrose 687.7 ±1.23, glucose 20.6 ±6.22 and fructose 12.8 ±2.05; the composition of glucose and fructose syrups (g/L) was: glucose 668.2 ±101.9 and fructose 535.73 ±93.2.

Total protein analysis of CSL was performed by BCA Protein assays kit (Pierce® BCA 23227 Protein Assay Kit, Thermo Scientific). The total protein concentration of 167.5 ±8.6 g/L was obtained.

4.2.7 Statistical analysis

The statistical analyses One-way and Two-way ANOVA were performed using GraphPad Prism version 5 for Windows, GraphPad Software, San Diego, California, USA.

4.3 RESULTS AND DISCUSSION

4.3.1 Optimization of pre-inoculum culture preparation (PIP) and effect of inoculum ratio on the BNC production by static fermentation

Some studies reported that high BNC productivity is favoured by higher cell density. Indeed, for a given strain and under specific operational conditions, productivity is expected to be proportional to the concentration of cells (Jung et al., 2007). In this paper we address the optimization of the preparation of pre-inoculum methodology, by attempting the production of highly active cells, while reducing the number of cells required to start the culture under static conditions, not compromising the final productivity of BNC. This is highly relevant for the large-scale fermentation since the use of around 10 % (v/v) of inoculum in stirred tanks, as it is common practice in industrial fermentation, represents a significant cost (high capital investment and operating costs) (Dourado et al., 2016 and 2018).

The effects of different culture media on cell growth were examined by determination of viable cell number (CFU/mL). Figure 1 A shows that in Step 1 the culture media G, I and L lead to the highest number of viable cells, in average 3.4×10^8 CFU/mL ($p > 0.05$). However, in Step 2, culture media A and C provide higher cellular density, 1.2 - 1.5×10^9 CFU/mL ($p < 0.05$). As a matter of fact, the cell concentration reached in the stirred culture with medium A and C supported a much higher cell growth on Step 2 as compared to Step 1. On the other hand, medium G and L supported a much lower cell growth on Step 2 as compared to Step 1. So, in these cases (A and C), culture medium agitation didn´t affect negatively the cellular viability of the *K. xylinus* BPR 2001, the same was also observed by other authors (Chao et al., 2000; Bae and Shoda, 2004 and 2005). Thus, it appears that, on the perspective of culture growth, the optimal medium in static culture isn´t the optimal also in stirred culture. It may be speculated that the balance of medium culture composition, oxygen concentration and hydrodynamic stress, all play a role in determining the metabolic pathways, significantly impacting the cell proliferation.
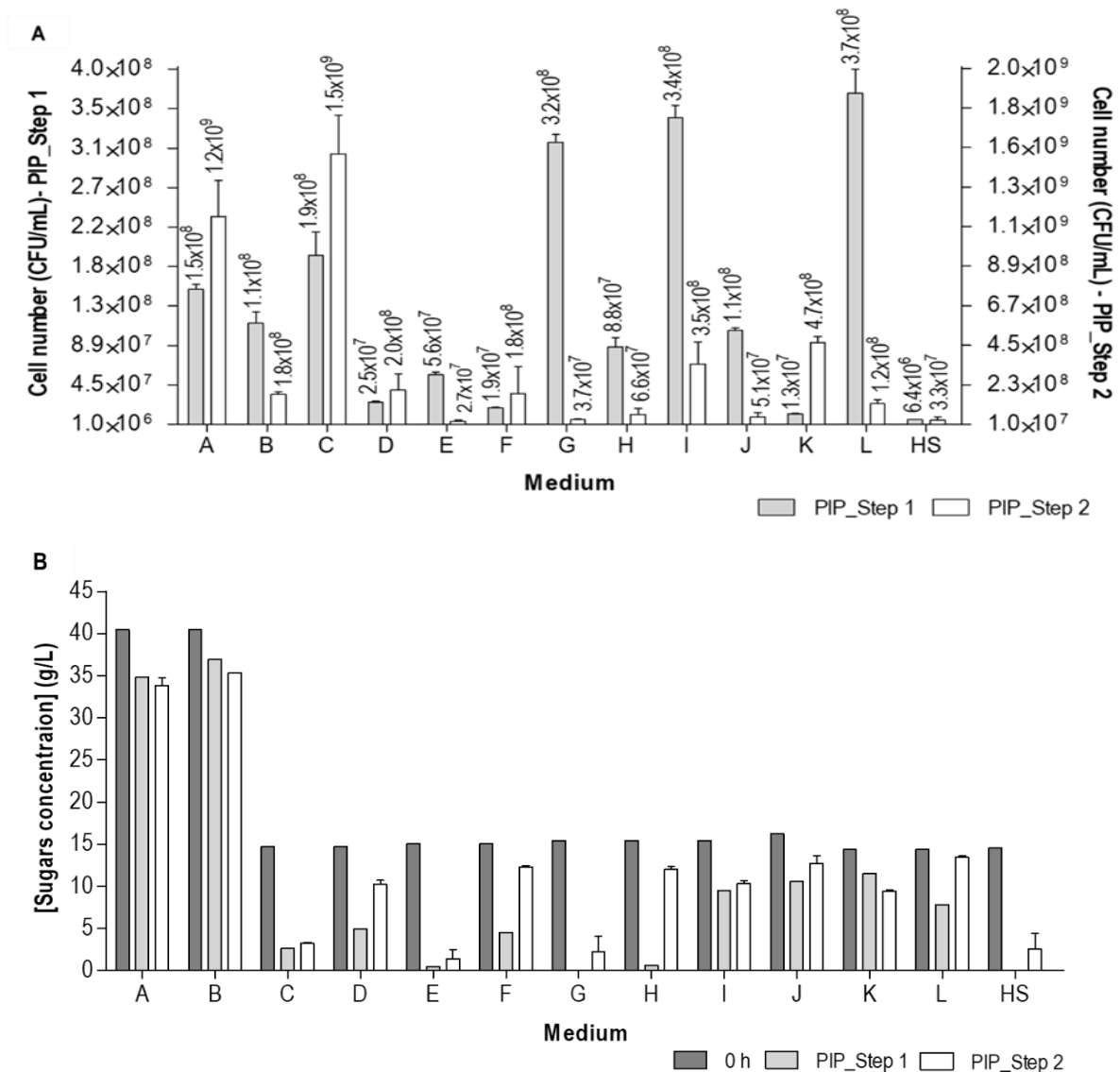
Figure 1 - A) Viable cell number (CFU/mL); **B)** Total sugars concentration obtained after different steps of PIP with different medium composition. **PIP_Step 1**: Static culture, 3 days at 30 °C and **PIP_Step 2**: Stirred culture, 30 h at 160 rpm and 30 °C. Bars with standard deviations represent the average of experiments done in triplicate.

The analysis of total sugars concentration (Figure 1 B) didn´t reveal any correlation with cell growth, as can be seen for example: comparing the results obtained using the culture media I and HS (PIP_Step 1) or E (PIP_Step 1 and 2).

In order to understand whether high viable cell number obtained in PIP_Step 2 has a relevant impact on the BNC production yield, different cell ratios were used in a 7 days long static culture. Interestingly, Figure 2 shows that, for each culture medium composition studied (A – L) and for 7 days of static culture, the BNC yield was independent of the inoculum density, with a ratio as low as 0.1 % (v/v) yielding a final BNC yield similar to that of 10 % (v/v). This result is unexpected since it demonstrates that the generally recognized rule of "10 fold dilution" of the inoculum doesn´t apply in this system. On the other hand,

slight differences in the BNC production yield were observed between different culture media. On average, a BNC yield of 6 g/L was obtained. Reinforcing this observation, it may be remarked that the culture media A and C, with higher cell densities obtained in PIP_Step 2, do not lead to higher BNC yield in static culture. It may be speculated that, once inoculated in the static culture, the cells migrate to the interface culture medium-air, seeking for the higher concentration of oxygen. Thus, the cells concentrate in the available interfacial surface. It may be concluded that a surface concentration of 2.5×10^2 cells/cm^2 (to 0.1 % (v/v) of inoculum G, E, HS medium average) is sufficient to start the culture, leading to the maximum productivity reached with higher initial cell densities (1.2×10^4 cells/cm^2 to 0.1 % (v/v) of inoculum A and C medium average). The effect of cell surface concentration tentatively explains the requirement of a lower inoculum ratio than commonly practiced.

Although the inoculum with 0.01 % (v/v) ratio, the lowest tested, doesn´t lead to significantly lower productivities ($p>0.05$), we believe it would be advisable to use an inoculum of around 0.1-0.5 % (v/v), to ensure the starting of the culture, especially in an industrial environment. Nevertheless, such conditions represent a significant reduction in costs associated to the preparation of pre-inoculum. Moreover, although with H and J culture media a higher BNC production yield was achieved, we selected medium C as the optimum pre-inoculum medium because it has a simpler composition and is made of low-cost components (Figure 2 and Table 1), which will have a strong impact if considering the large-scale BNC production.
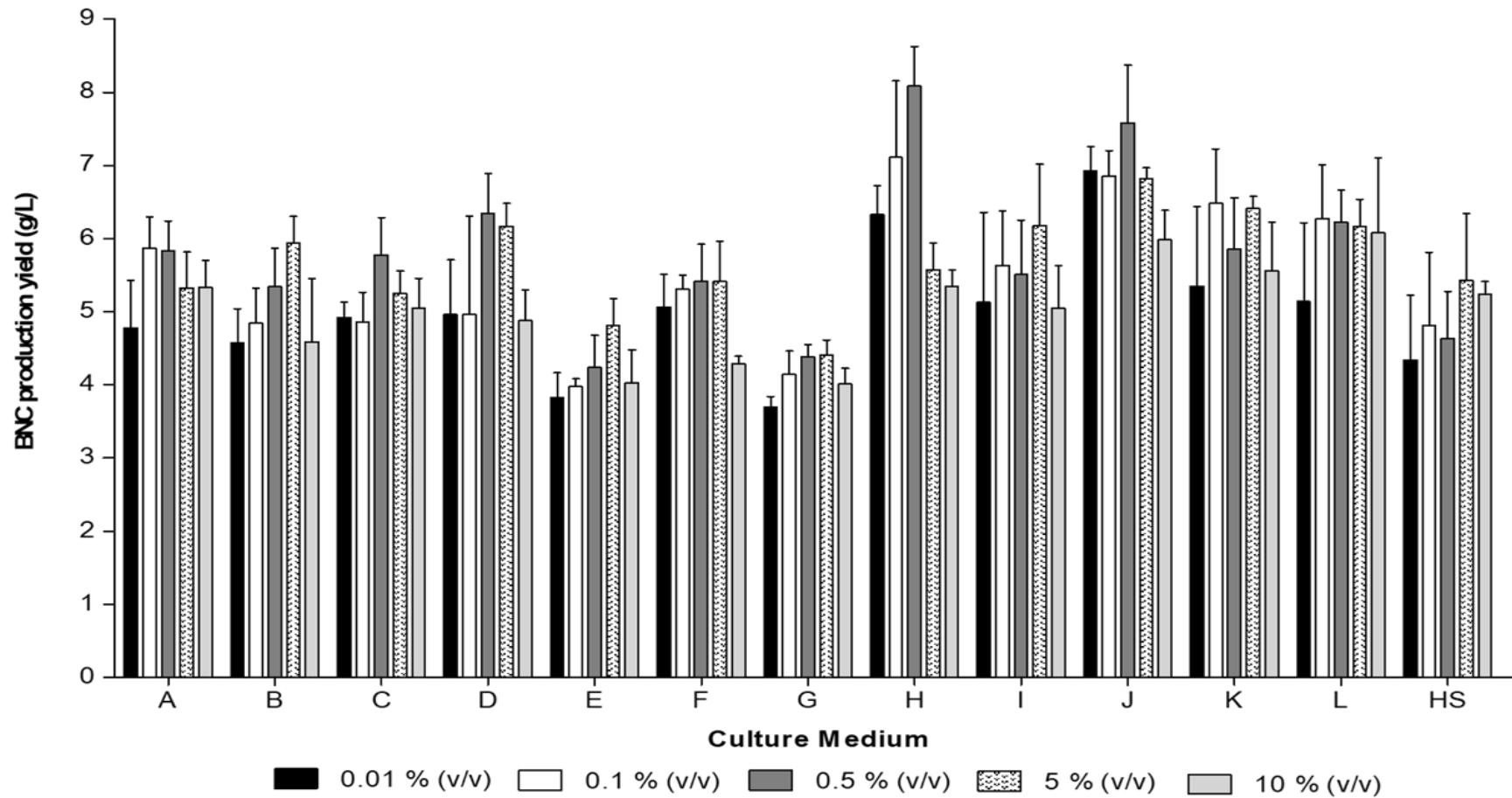
Figure 2 - BNC production yield (g/L) obtained after inoculation with different pre-inoculum ratios, after 7 days of static fermentation. Cells were obtained from different culture medium studied without cellulase from PIP_Step 2. Bars with standard deviations represent the average of experiments done in triplicate.

4.3.2 Cell growth kinetic´s in the different stages of the pre-inoculum preparation using alternative medium to BNC production

The kinetics of the pre-inoculum culture was studied, in order to optimize this stage of the process.

4.3.2.1 PIP_Step 1- Static Culture

Figure 3 A and B show the growth kinetics of *K. xylinus* 700178 during step 1 of pre-inoculum preparation, with and without cellulase addition, respectively. Overall, the growth profile was similar, however, the presence of cellulase allowed for a cell density of more than 5 fold to be achieved (Figure 3 A and B). This may be due to the release of bacteria that without the presence of enzyme remain trapped within the BNC pellicle. In the case of the fermentation in the absence of cellulase (Figure 3 A), a lag phase of around 18 h was observed, followed by the exponential phase for another 18 h, corresponding to the sugars consumption of only around 20 % (Figure 3 A and C). In the presence of cellulase (Figure 3 B), the lag phase wasn´t observed, the cells growed continuously from the early stage of the culture up to around 36 h (exponential growth). Again, surprisingly, the sugars consumption associated to the exponential stage is fairly low, around 20 % (Figure 3 B and D). Although, in both cases, the overall sugar consumption reached 80 % (the remaining sugars corresponding to fructose only), most of the sugars consumption seems not to be associated to an increase in the number of viable cells.
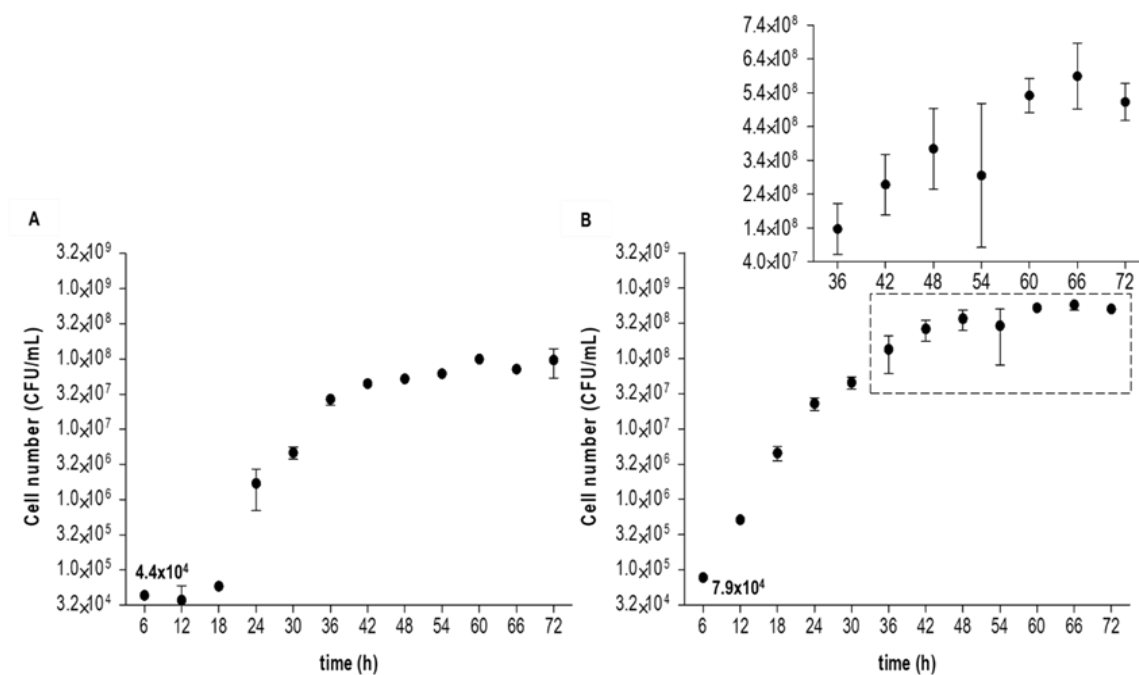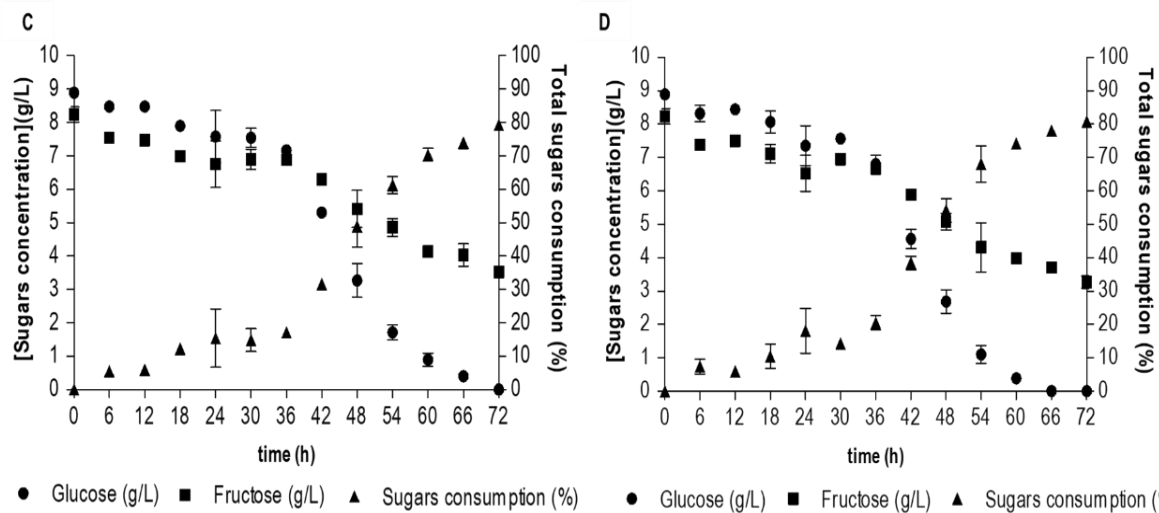
Figure 3 - A) and **B)** Growth kinetics of *K. xylinus* during the PIP_Step 1, for A (without cellulase) and B (with cellulase), respectively. **C)** and **D)** Remaining and consumption of sugars throughout the cell growth of PIP_Step 1, for conditions A and B, respectively. Data are presented as the average ± standard deviations of experiments run in triplicate.

Considering these results, a period of 36 h of static fermentation was set for the collection of cells to PIP_Step 2. Although this is not the time at which cell density was maximized, it corresponds to the period when cells are metabolically more active, proliferating faster. The addition of cellulase was also considered unnecessary, since the increase in cell density is not very significant to increase the BNC production yield.

4.3.2.2 PIP_Step 2- Stirred Culture

The results presented in Figure 4 A, B and C represent the growth kinetics along the PIP_Step 2 in containers with different volumetric surface area and culture medium volume.
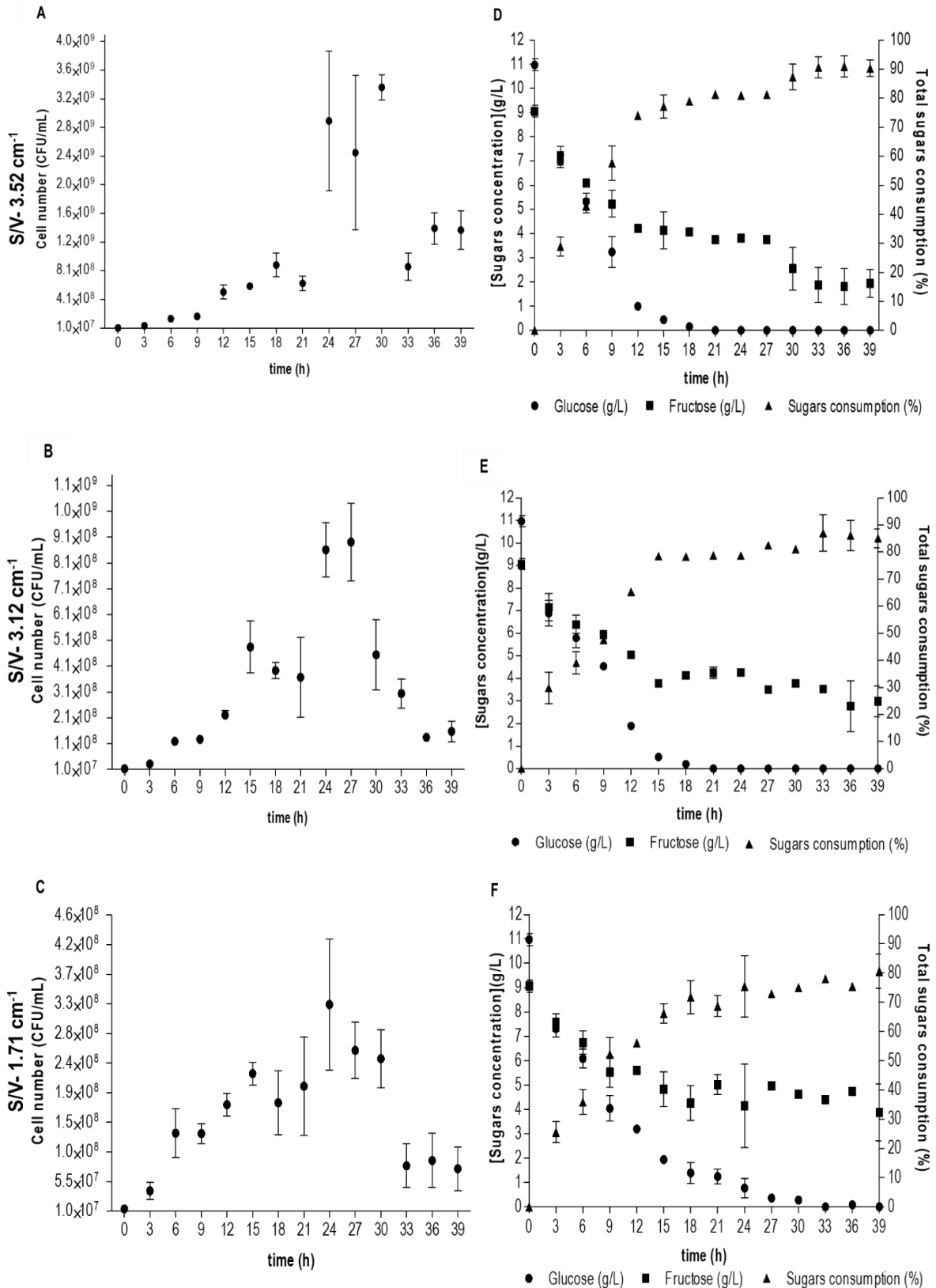
Figure 4 - A, B and **C)** Growth kinetics of *K. xylinus* during the PIP_Step 2, for A (S/V-3.52 cm⁻¹), B (S/V-3.12 cm⁻¹) and C (S/V-1.71 cm⁻¹) condition, respectively. **D, E** and **F)** Remaining and consumption of sugars throughout the cell growth of PIP_Step 2, for conditions A, B and C, respectively. Data are presented as the average ± standard deviations of experiments run in triplicate.

From the analysis of the growth profiles presented in Figure 4, A, B and C, it was observed that, for different volumetric surface areas studied, the growth kinetics profiles were similar. No lag phase was observed, as could be expected, since the cells were transferred to the stirred vessels at the exponential phase in PIP_Step 1 into the culture media with the same composition, thus adaptation was very quick. In the case of Figure 4 A, B and C, a slightly lower proliferation was observed at the beginning of the culture, but according to the sugar consumption rate the cells were very active (Figure 4 D, E and F).

The maximum number of viable cells depended on the volumetric surface area, with higher values (A – 3.52 cm^{-1} > B – 3.12 cm^{-1} > C – 1.71 cm^{-1}) leading to higher number of cells. These differences are likely related to the higher oxygen transfer rates for the containers with higher volumetric surface area. Interestingly, the culture growth seems to proceed for a few hours beyond the point of depletion of glucose; however, soon after, the culture declines and the number of viable cells reduces significantly. Thus, there is a relatively small-time frame for the harvest of active and quickly proliferating cells to be done, the concentration of glucose playing a key role in the "good shape" of the culture (Figure 4 A-F).

According to the results obtained, the time points for collection of the inoculum: i) for the static culture and BNC production or ii) the pilot bioreactor-PIP_Step 3 and further cell propagation was set at around 21 - 22 h, irrespective of the conditions used, although a larger volumetric surface seems advisable for a larger number of viable cells to be obtained.

4.3.2.3 PIP_Step 3- Pilot scale production

In order to develop a large-scale process for the production of BNC, even though the ratio of inoculum to be used can be substantially reduced (0.1-0.5 %(v/v)), the amount required for a 10-100 m^3 operation scale is in the range of the tenths of liters. Thus, the inoculum was further propagated in a stirred tank reactor with 45 L of culture medium. The growth kinetics was monitored, and the results are shown on Figure 5.
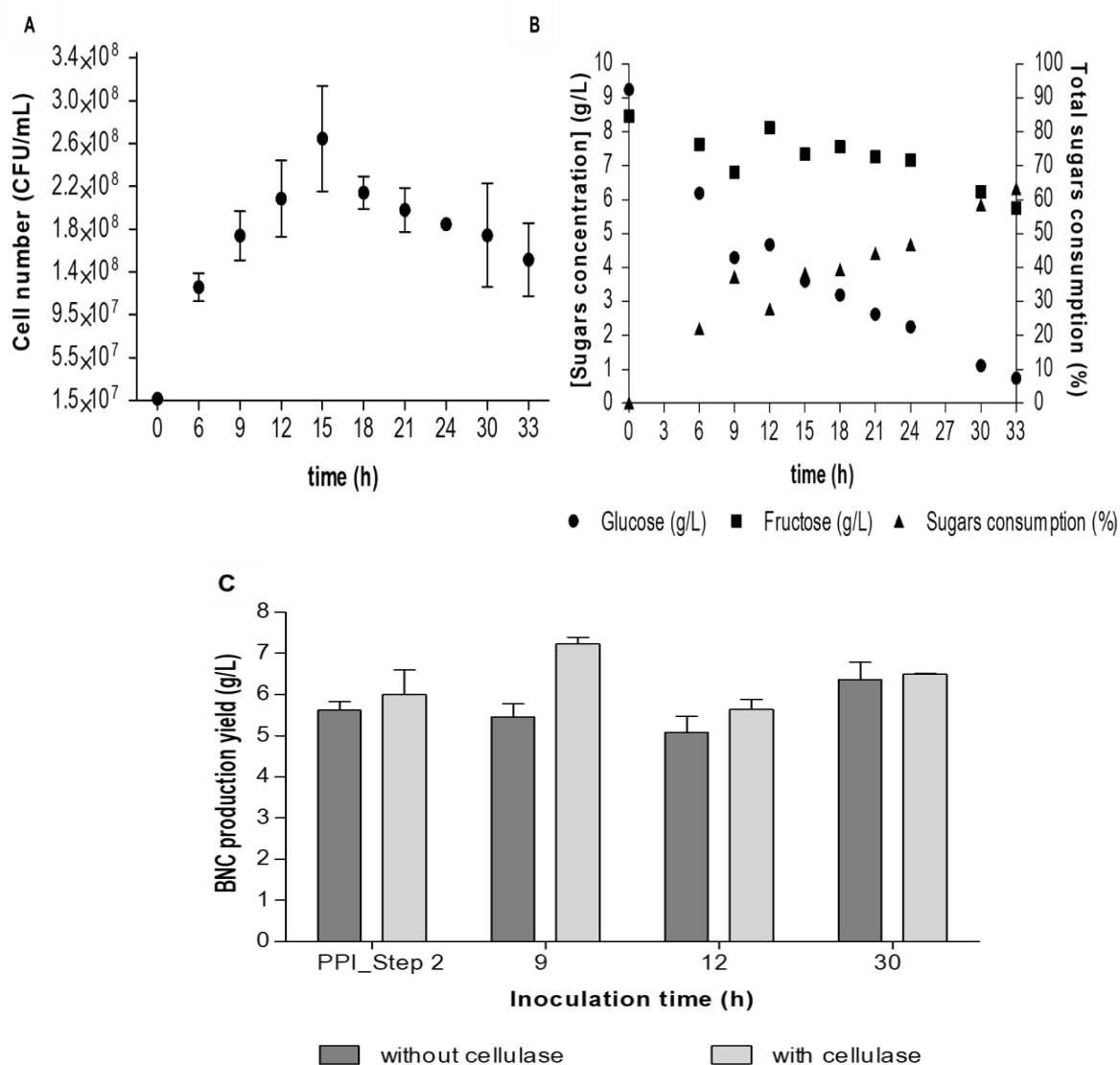
Figure 5 - A) Growth kinetics of *K. xylinus* during the PIP_Step 3 in bioreactor at pilot scale. **B)** Remaining and consumption of sugars throughout the cell growth in bioreactor at pilot scale. **C)** BNC production in static culture (g/L) after inoculation with 0.5 % (v/v) of cells obtained after PIP_Step 2 and after 9, 12 and 30 h of fermentation in a 75 L biological reactor. Data are presented as the average ± standard deviations of experiments run in triplicate.

From the analysis of the results presented in Figure 5 A, a very short or even non-existent lag phase existed, since a rapid growth occurred between 0 and 6 h. Cell growth occurred gradually up to 15 h of fermentation, where maximum number of viable cells was achieved, with a value of 2.6×10^8 CFU/mL (Figure 5 A). Henceforward, the culture starts declining, an effect that may be explained as arising from the reduced glucose concentration, which was reduced to 3.6 g/L (Figure 4 B).

The ability of cells cultured in a 75 L biological reactor (stirred conditions) to BNC in static culture was evaluated by collecting cell samples at 9, 12 and 30 h of fermentation. A vessel of dimensions (length=24 x width =9.5 x height= 14 cm) with 2.5 cm height of culture medium (corresponding to 620 mL) was

inoculated with 0.5 % (v/v) of pre-inoculum (P.I.) prepared as described above and BNC was produced under static conditions. Inoculum harvested directly from PIP_Step 2 (at 21 h) was also used for the BNC production assessment under static conditions. The influence of cellulase concentration (0.025 %(v/v)) during fermentation was also analyzed, as can be seen in Figure 5 C. It was observed that the presence of cellulase at the chosen concentration didn´t affect the productivity in BNC ($p > 0.05$). The quality of membranes, obtained in the presence of cellulase, as assessed by visual inspection and handling, were the same as those obtained without cellulase. The BNC membrane obtained present a good integrity, cohesive and mechanically resistant. Moreover, we only transferred 0.5 % of inoculum that indicates a high dilution of cellulase in static culture and this didn´t negatively affect the BNC membrane integrity. Again, regardless of the number of initial viable cells from the inoculum, the static production of BNC was similar at all times. Interestingly, the inoculum collected from the bioreactor after 30 h (corresponding to the death phase) yielded a similar BNC production yield to that of the more active, exponentially growing cells (9 and 12 h).

4.4 CONCLUSIONS

The goal of the current investigation was to optimize the pre-inoculum preparation to minimize the costs of this step and consequently the global BNC production process of. Salient conclusions are listed below:

The simple pre-inoculum culture medium composition that provided high cellular density using alternative and economic substrates was % (m/v): 1.5- 2.0 Glucose and Fructose syrup, 0.7 CSL (protein basis), 0.115 citric acid and 0.27 Na_2HPO_4.

The addition of high cellulase yield of this cocktail enzymatic in PIP_Step 2 lead to an inferior quality of membranes produce (soft, gelatinous/viscous and easily crumble to the touch).

The studies on the effect of the initial cells number on the static production of BNC allowed to conclude that BNC production is independent of the initial cell number. Higher concentration of cells did not lead to higher BNC production yield on static culture for the same time and conditions. Thus, only 0.1-0.5 % (v/v) of P.I. can be used to inoculate the static production of BNC and with this decrease the costs of BNC production.

Comparing the kinetic studies of the 3 steps of PIP it was observed that successive cell propagations promote rapid growth from step to step. Thus, the time required to reach the exponential phase of growth in the bioreactor decreases, which leads to a decrease in the operating costs of the bioreactor;

The ability of BNC production by the cells of *K. xylinus* 700178 was maintained after were submitted to successive agitation conditions;

This work represents a good implementation strategy for the large scale-up of PIP and scale-out of BNC production and decrease the costs of pre-inoculum preparation and consequently all BNC production process of.

4.5 REFERENCES

Almeida, I. F., Pereira, T., Silva, N. H. C. S., Gomes, F. P., Silvestre, A. J. D., Freire, C. S. R., Sousa Lobo, J. M., Costa, P. C. 2014. Bacterial cellulose membranes as drug delivery systems: an *in vivo* skin compatibility study. European Journal Pharmaceutics and Biopharmaceutics. 86:332–336.

Ashjaran, A., Yazdanshenas, M. E., Rashidi, A., Khajavi, R., Rezaee, A. 2013. Overview of bio nanofabric from bacterial cellulose. The Journal of the Textile Institute. 104: 121–131.

Bae, S. and Shoda, M. 2004. Bacterial cellulose production by fed-batch fermentation in molasses medium. Biotecnology Progress. 20: 1366-1371.

Bae, S.O. and Shoda, M. 2005. Production of bacterial cellulose by *Acetobacter xylinum* BPR2001 using molasses medium in a jar fermentor. Applied Microbiology Biotechnololy. 67: 45–51.

Cacicedo, M. L., Castro, M. C., Servetas, I., Bosnea, L., Boura, K., Tsafrakidou, P., Dima, A., Terpou, A., Koutinas, A., Castro, G.R., 2016. Progress in bacterial cellulose matrices for biotechnological applications. Bioresource Technology. 213:172–180.

Castro, C., Zuluaga, R., Putaux, J.-L., Caro, G., Mondragon, I., Gañán, P. 2011. Structural characterization of bacterial cellulose produced by *Gluconacetobacter swingsii sp.* from Colombian agroindustrial wastes. Carbohydrate Polymers. 84: 96–102.

Chao. Y., Ishida. T., Sugano, Y., Shoda, M. 2000. Bacterial cellulose production by *Acetobacter xylinum* in a 50-L internal-loop airlift reactor. Biotechnololy Bioengineering. 68: 345–352.

Chawla, P. R., Bajaj, I. B., Survase, S. A., Singhal, R. S. 2009. Microbial Cellulose: Fermentative Production and Applications. Food Technology & Biotechnology. 47:107–124.

Cheng, K.C., Catchmark, J.M., Demirci, A. 2009. Enhanced production of bacterial cellulose by using a biofilm reactor and its material property analysis. Journal of Biological Engineering. 3:12.

Czaja, W. K., Young, D. J., Kawecki, M., Brown, R. M. 2007. The future prospects of microbial cellulose in biomedical applications. Biomacromulecules. 8:1–12.

Dahman, Y. 2009. Nanostructured biomaterials and biocomposites from bacterial cellulose nanofibers. Journal of Nanoscience and Nanotechnology. 9: 5105–5122.

de Azeredo, H. M. C. 2013. Antimicrobial nanostructures in food packaging. Trends in Food Science Technology. 30:56–69.

Dourado, F., Fontão, A. I., Leal, M., Rodrigues, A. C., Gama, M. 2016. Chapter 12 - Process Modeling and Techno-Economic Evaluation of an Industrial Bacterial NanoCellulose Fermentation Process. In "Bacterial Nanocellulose: from biotechnology to bio-economy". Ed.: Gama, M.; Bielecky, S.; Dourado, F. Elsevier; Amsterdam, Netherlands; 199-214.

Dourado, F., Fontão, A. I., Leal, M., Rodrigues, A. C., Gama, M. 2018. Chapter 1 - Process modelling and techno-economic evaluation of an industrial air-lift bacterial cellulose fermentation process. In "Nanocellulose and Sustainability: Production, Properties, Applications, and Case Studies". Ed.: Koon-Yang Lee. CRC Press, USA; 1-13.

Gershater, C.J.L. and Flickinger, M.C. 2010. Inoculum Preparation. In: "Encyclopedia of Industrial Biotechnology. England": John Wiley & Sons. 1-16.

Hestrin, S. and Schramm, M. 1954. Preparation of freeze-dried cells capable of polymerizing glucose to cellulose. Biochemical Journal. 58: 345-352.

Hornung, M., Ludwig, M., Gerrard, A.M., Schmauder, H.P. 2006. Optimizing the production of bacterial cellulose in surface culture: evaluation of substrate mass transfer influences on the bioreaction (Part 1). Engineering in Life Sciences. 6:537–545.

Hornung, M., Ludwig, M., Schmauder, H. P. 2007. Optimizing the production of bacterial cellulose in surface culture: a novel aerosol bioreactor working on a fed batch principle (Part 3). Engineering in Life Sciences. 7: 35–41.

Jung, J. Y., khan, T., Park, J. K., Chang, H. N. 2007. Production of bacterial cellulose by *Gluconacetobacter hansenii* using a novel bioreactor equipped with a spin filter. Korean Journal of Chemical Engineering. 24: 265-271.

Keshk, S.M. 2014. Bacterial cellulose production and its industrial applications. Journal of Bioprocessing & Biotechniques. 4: 150.

Khan, S., Ul-Islam, M., Khattak, W.A., Ullah, M. W., Park, J. K. 2015. Bacterial cellulose-titanium dioxide nanocomposites: Nanostructural characteristics, antibacterial mechanism, and biocompatibility. Cellulose. 22: 565–579.

Kim, Y.-J., Kim, J.-N., Wee, Y.-J., Park D.-H., Ryu, H.-W. 2007. Bacterial cellulose production by *Gluconacetobacter sp. PKY5* in a rotary biofilm contactor. Applied Biochemistry and Biotechnology.137–140 529–537.

Kouda, T., Yano, H., Yoshinaga, F. 1997. Effect of agitator configuration on bacterial cellulose productivity in aerated and agitated culture. Journal of Fermentation Bioengineering. 83371–376.

Kralisch, D., Hessler, N., Klemm, D., Erdmann, R., Schmidt, W. 2010. White biotechnology for cellulose manufacturing—The HoLiR concept, Biotechnology and Bioengineering. 105: 740–747.

Krystynowicz, A., Czaja, W., Wiktorowska-Jezierska, A., M. Gonc̦alves-Mi´skiewicz, Turkiewicz, M., Bielecki, S. (2002). Factors affecting the yield and properties of bacterial cellulose. Journal of Industrial Microbiology & Biotechnology. 29: 189–195.

Lin, N., Dufresne, A. 2014. Nanocellulose in biomedicine: current status and future prospect. European Polymer Journal. 59:302–325.

Martínez-Sanz, M., Lopez-Rubio, A., Villano, M., Oliveira, C. S. S., Majone, M., Reis, M., Lagarón, J. M. 2016. Production of bacterial nanobiocomposites of polyhydroxyalkanoates derived from waste and bacterial

nanocellulose by the electrospinning enabling melt compounding method. Journal of Applied Polymer Science 133.

Meyrath, J. and Suchanek, G. 1972. Chapter III - Inoculation Techniques—Effects Due to Quality and Quantity of Inoculum. In: "Methods in Microbiology". Volume 7, Part B, 159-209.

Mohite, B.V. and Patil, S.V. 2014. A novel biomaterial: Bacterial cellulose and its new era applications. Biotechnology and Applied Biochemistry. 61: 101–110.

Moosavi-Nasab, M. and Yousefi, A., 2011. Biotechnological production of cellulose by *Gluconacetobacter xylinus* from agricultural waste. Iranian Journal Biotechnolology. 9: 94–101.

Oliveira Barud, H. G., Barud, H. da S., Cavicchioli, M., Amaral, T. S., de Oliveira Junior, O. B., Santos D. M., Petersen, A. L. de O. A., Celes, F., Borges, V. M., de Oliveira C. I., de Oliveira, P. F., Furtado, R. A., Tavares, D. C, Ribeiro, S. J. L. 2015. Preparation and characterization of a bacterial cellulose/silk fibroin sponge scaffold for tissue regeneration. Carbohydrate Polymers. 128:41–51.

Padmanaban, S., Balaji, N., Muthukumaran, C., Tamilarasan, K. 2015. Statistical optimization of process parameters for exopolysaccharide production by *Aureobasidium* pullulans using sweet potato based medium. 3 Biotech. 5: 1067–1073.

Park, J. K., Yung. J. Y, Park, Y. H. 2003. Cellulose production hansenii in a medium containing ethanol. Biotechnology Letters. 25: 2055-2059.

Rani, M.U., Udayasankar, K., Appaiah, K. A. A. 2011. Properties of bacterial cellulose produced in grape medium by native isolate *Gluconacetobacter sp*. Journal of Applied Polymer Science. 120: 2835–2841.

Reiniati, I., Hrymak, A. N., Margaritis, A. 2017. Kinetics of cell growth and crystalline nanocellulose production by *Komagataeibacter xylinus.* Biochemical Engineering Journal. 127: 21-31.

Saibuatong, O., Phisalaphong, M. 2010. Novo aloe vera–bacterial cellulose composite film from biosynthesis. Carbohydrate Polymers. 79: 455–460.

Shi, Z., Zhang, Y., Phillips, G. O., Yang, G. 2014. Utilization of bacterial cellulose in food. Food Hydrocolloids. 35:539–545.

Song, H.-J., Li, H., Seo, J.-H., Kim, M.-J., Kim, S.-J. 2009. Pilot-scale production of bacterial cellulose by a spherical type bubble column bioreactor using saccharified food wastes. Korean Journal of Chemical Engineering. 26 141–146.

Vasquez, A., Foresti, M., Cerrutti, P., Galvagno, M. 2013. Bacterial cellulose from simple and low cost production media by *Gluconacetobacter xylinus*. Journal of Polymers and the Environment. 21: 545–554.

Wu, J.-M. and Liu, R.-H. 2012. Thin stillage supplementation greatly enhances bacterial cellulose production by *Gluconacetobacter xylinus*. Carbohydrate Polymers. 90:116–121.

Wu, S.-C., Li, M.-H. 2015. Production of bacterial cellulose membranes in a modified airlift bioreactor by *Gluconacetobacter xylinus*. Journal of Bioscience Bioengineering. 120444–449.

5 DEVELOPMENT OF BACTERIAL NANOCELLULOSE WOUND DRESSINGS WITH CONTROLLED DELIVERY OF VITAMIN D₃
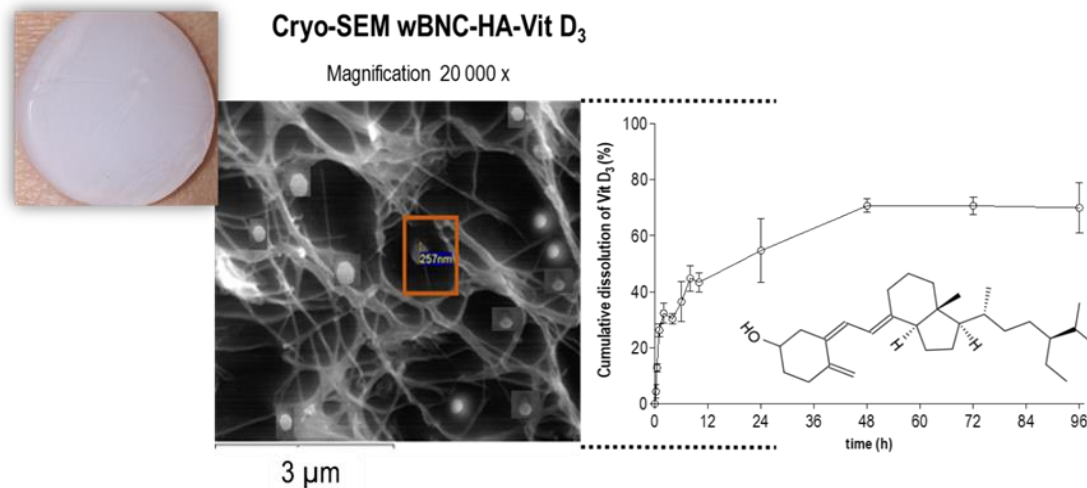
Cryo-SEM observations were performed in the Laboratory for Scanning Electron Microscopy, at Materials Centre of the University of Porto (CEMUP), using a High resolution Scanning Electron Microscope (JEOL JSM 6301F) with X-Ray Microanalysis (Oxford INCA Energy 350) and CryoSEM experimental facilities (Gatan Alto 2500).

Burns and chronic wounds are a worldwide concern due to the loss of patient's life quality, mortality and high health care costs. Conventional treatments are often painful, expensive and may increase the risk of infection, compromising the treatments' length and success. In this work, we propose a safe, inexpensive and easy-to-use dressing, combining natural materials with high potential for wound dressing and healing, namely bacterial nanocellulose (BNC) and vitamin D_3 (Vit D_3). Vit D_3 is known to stimulate wound healing, due to its ability to induce the expression of LL37, an antimicrobial peptide with angiogenic activity. However, its poor water solubility hampers exogenous administration. In this work, BNC membranes were loaded with Vit D_3 using a self-assembling hyaluronic acid (HA) nanogel as a carrier.

The carrier was obtained by grafting hexadecylamine (Hexa) into the HA backbone (HA-Hexa). HA-Hexa conjugate with a degree of substitution of 10.3 ±1.1 %, showed no toxicity to L929 fibroblast cells. Vit D_3 was loaded into the nanogel (HA-Vit D_3) with an encapsulation efficiency between 60-91 %. The nanogel's colloidal suspension showed stable drug load, size and polydispersity index along time, both at 4 and 36 ±1 °C. Furthermore, the Vit D_3-loaded nanogel was impregnated into BNC membranes, conceived as dressing delivery system. Around 70 % of the initial Vit D_3 available was released from BNC membranes in the first 48 h. Most importantly, that the released Vit D_3 still remained within the HA-Hexa nanogel carrier. Overall, the data obtained showed promising perspectives regarding the use of BNC-based dressings for the incorporation and release of HA-Vit D_3.

5.1 INTRODUCTION

Wound dressings are no longer considered a passive supplement, but an active component of the healing process, designed to control infection and provide a favorable healing microenvironment. A warm, moist environment is recognized to encourage fast and effective healing, particularly when dealing with chronic wounds (Sibbald et al., 2003; Bergstrom et al., 2005; Lee et al., 2009). The global market currently offers different types of wound dressings, made of natural or synthetic polymers, as well as their combinations. Applied in different forms (films, foams, hydrocolloids and hydrogels), these materials may contain drugs, growth factors, peptides, and other bioactive substances that accelerate healing (Bergstrom et al., 2005). The actual requirements of an "ideal dressing" are quite demanding: it must provide a moist environment, thermal insulation and effective oxygen transfer; ensure liquid drainage and epithelial migration; absorb wound exudates; provide an antimicrobial barrier; it must be easy to apply and painless to remove; finally, it should be biocompatible without inducing allergic reactions (Watson and Hodgkin, 2005; Fonder et al., 2008). Therefore, the selection of an appropriate dressing is determined by the particularity of every individual occurrence, since none of the currently existing materials are able to fulfill all of these requirements (Simões et al., 2018). Among different dressing materials, hydrogels are currently highlighted for the treatment of burns and chronic wounds. These naturally occurring or chemically cross-linked three-dimensional (3-D) networks of polymer chains or macromolecules are filled with liquid and provide a supportive environment for tissue regeneration. These materials follow the contours of the wound surface and ensure oxygen and water permeation, while protecting the surface from bacterial invasion (Quinn et al., 1985; Caló and Khutoryanskiy, 2015). One naturally derived hydrogel with wide potential for dressings production is bacterial nanocellulose (BNC). BNC is produced by some bacteria belonging to the genera *Acetobacter, Rhizobium, Agrobacterium, Aerobacter, Achromobacter, Azotobacter, Salmonella, Escherichia,* and *Sarcina* (Shoda and Sugano, 2005). BNC production for the specific purpose of wound dressing dates back to the early 1980s (Ring et al., 1986; Farah, 1990). Its use as a wound healing material is governed by its peculiar features: it has a high tensile strength, conformability and water holding capacity, a pronounced permeability to gases and liquids, and a great compatibility with living tissues (Czaja et al., 2006). BNC can also undergo tailor-made modifications to achieve all the requirements essential to function as a wound dressing material. Its high porosity and specific surface area allow the potential for introduction and release of antimicrobial agents and medicines (Siró and Plackett, 2010; Shah et al., 2013). The inclusion of other compounds that can accelerate healing, the preparation of BNC-based composites and the chemical reactivity of the

polymer chain could all contribute to the development of novel dressing materials with improved characteristics for treatment of any type of wound (Haimer et al., 2010; Klemm et al., 2011; Hu et al., 2014).

Vitamin D$_3$ (Vit D$_3$, cholecalciferol), is a water insoluble molecule associated to the bone physiology, where its receptors are mostly expressed. Its main functions comprise the increment of calcium absorption in the intestinal tract and the promotion of normal bone formation and mineralization (Goltzman, 2018). Vitamin D can act locally and regulate, for example, the epidermal keratinocytes through the modification of some growth factors or cytokines, therefore influencing wound healing (Burkiewicz et al., 2012). Vit D$_3$ is involved in the regulation of hCAP18 expression which is processed into LL37, an antimicrobial peptide belonging to the cathelicidin family. In addition to antimicrobial activity this peptide presents a multifunctional bioactivity, responsible for e.g. wound healing and tissue regeneration (Kittaka et al., 2013; Cheredd et al., 2014; Bandurska et al., 2015). Vit D$_3$ also directly upregulates the hCAP18 transcription in many kinds of cells, like keratinocytes, monocytes and neutrophils. In an *in vivo* acute skin inflammation model, topical treatment with Vit D$_3$ improved the regulation of LL37 expression (Gombart et al., 2007; Heilborn et al., 2010; Lee et al., 2012; Harder et al., 2013;). At skin level, binding of this vitamin to its cells' receptors increases cathelicidin expression, the importance of which in wound healing, namely associated to its angiogenic activity, was already addressed (Ramos et al., 2011; Gombart, 2011; Burkiewicz et al., 2012; Reinholz et al., 2012).

Despite the attractiveness of Vit D$_3$ for wound treatment, it is poorly soluble in aqueous solutions and sensitive to oxidation. To overcome these limitations, we propose using a hyaluronic acid nanogel (HA) as a drug delivery system, providing the possibility of controlled release, improved solubility and bioavailability.

HA is the most abundant natural polymer in human body and has a high hydrophilicity. It has main structural and hydration actions, but it also acts in metabolic regulation, cell migration and adhesion. Low molecular weight HA is pro-inflammatory, immuno-stimulatory and angiogenic, whereas high molecular HA is anti-angiogenic and non-immunogenic (Schanté et al., 2011; Pedrosa and Gama., 2014). Recently, we developed a self-assembling hyaluronic acid nanogels by grafting an expensive hydrophobic molecule (11-amino-1-undecanethiol) to HA (Pedrosa et al., 2014). The obtained amphiphilic conjugates self-assembled in aqueous environments and allowed the entrapment of bioactive molecules (namely water-insoluble) in their hydrophobic core.

This work aimed at the development of a new delivery patch using BNC membranes as a support for the controlled release of Vit D_3 to wounds. To overcome its high lipophilicity, Vit D_3 was entrapped in a new hyaluronic acid-based amphiphilic nanogel, established by conjugating a hydrophobic molecule – hexadecylamine (an inexpensive molecule and more hydrophobic than 11-amino-1-undecanethiol previously used) – to the HA chain (HA-Hexa). In aqueous environments HA-Hexa self-assembles into nanosized structures with a hydrophilic shell and a hydrophobic core, able to incorporate lipophilic molecules, like Vit D_3. We characterized this nanogel, loaded and non-loaded with Vit D_3, in terms of size, cytotoxicity, loading efficiency using different Vit D_3 concentrations and time-stability at different temperatures. Moreover, the potential of BNC membranes as a Vit D_3 -releasing system was assessed through *in vitro* diffusion and permeation studies.

5.2 MATERIAL AND METHODS

5.2.1 Hyaluronic Acid Nanogel

5.2.1.1 Nanogel production

The production of hyaluronic acid nanogel was done similarly to Pedrosa et al., 2014, in two reaction steps. First, sodium hyaluronate (Mw 4.7 - 7.46x10^3 Da, Lifecore Biomedical, USA) was modified to solubilize it in DMSO, by exchanging the sodium ion of sodium hyaluronate with the lipophilic tetrabutylammonium cation (Sigma-Aldrich). For this, 1 g of AG 50W cationic resin (Bio-Rad USA) and 3.5 g of tetrabutylammonium fluoride trihydrate (TBA+-F) were dissolved in 12.5 mL of ultrapure water (Milli-Q®), at room temperature and under mild stirring during 1 h, allowing the cationic resin to become impregnated with TBA+ ions. After this time, the solution was filtered under vacuum using a cellulose acetate membrane filter with 0.45 μm pore size and further washed with ultrapure water. Afterwards the washed AG 50W cationic resin was transferred to a 1 % (m/v) solution of sodium hyaluronate, final volume 25 mL. Ion exchange proceeded for 2 h, at room temperature and under slow agitation (Figure 1 A) (Schanté et al., 2011; Pedrosa et al., 2014). The resin was then removed by centrifugation at 3000×g for 2 min (Eppendorf Centrifuge 5430R) and the supernatant was collected, frozen at -80 °C and freeze-dried for 8 days (Scanvac Coolsafe). The resulting material, hyaluronic acid-tetrabutylammonium (HA-TBA), was stored in a desiccator, at room temperature, until use. Ion exchange was confirmed with ^{1}H nuclear magnetic resonance (^{1}H-NMR) (section 5.2.1.2).

In the second reaction step, conjugation of a hydrophobic molecule, hexadecylamine (Hexa) (Aldrich Chemistry) to the HA chain, yielding an amphiphilic material able to self-assemble into a nanogel in

aqueous environments. HA-TBA was conjugated with the hydrophobic Hexa through amide bond formation using the 1-ethyl-3-(3-dimethylaminopropyl) carbodiimide/N-hydroxysuccinimide (EDC/NHS) chemistry (Grabarek and Gergely, 1990). In this regard, 1 % (m/v) of HA-TBA (350 mg, 5.65×10^{-4} mol) was solubilized in DMSO and 136 mg (5.65×10^{-4} mol) of EDC (Acros Organics) and 68 mg (5.65×10^{-4} mol) of NHS (Fluka Analytical) were added. Hexadecylamine was then grafted to the HA chain. Briefly, 20 mg of Hexa (corresponding to 15 % of the number of HA disaccharide monomeric units used - 8.5×10^{-5} mol) was added to the previous solution, which was stirred for 24 h at room temperature to allow amide bond formation between HA and Hexa (Figure 1 B). Then, the solution was dialysed (MWCO = 1000 Da) against a 150 mM sodium chloride solution (NaCl), for 3 days, to exchange TBA^+ ions for sodium ions, and then with distilled water for 2 more days, to further remove excess NaCl (Figure 1 B).

The resulting hyaluronic acid-hexadecylamine conjugate – henceforth designated by HA-Hexa (Figure 1 B) – was frozen at -80 °C, freeze-dried for 5 days (Scanvac Coolsafe) and analysed regarding the degree of substitution (DS) of hexadecylamine in the HA chain, using ^{1}H-NMR spectroscopy (section 5.2.1.2).
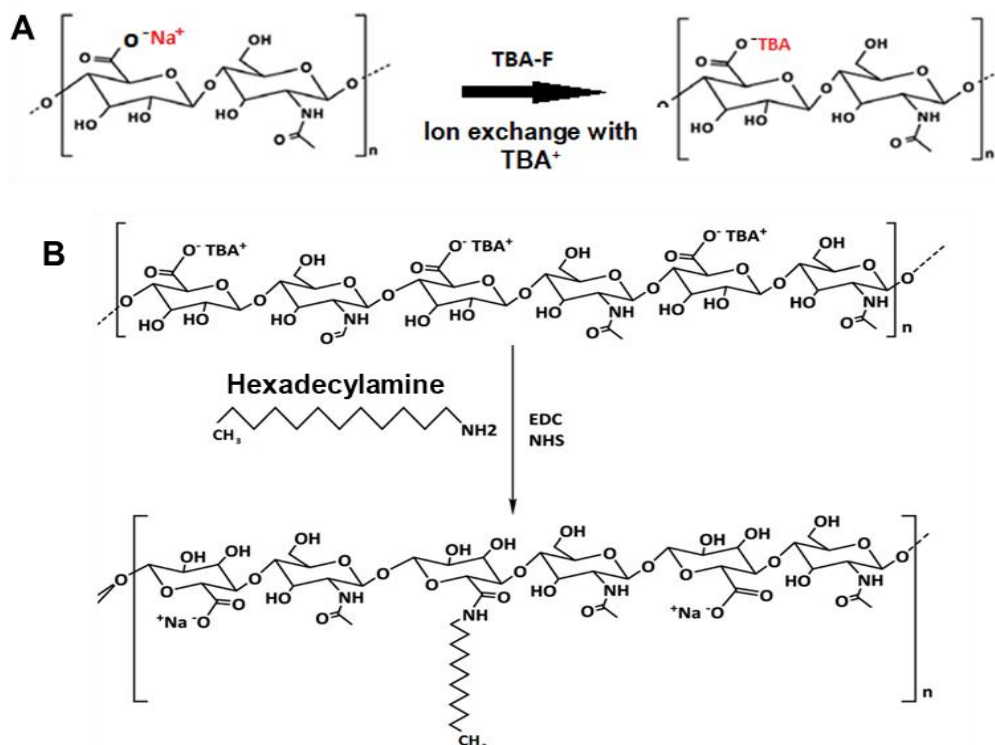
Figure 1 - Schematic representation of the ion exchange step which renders HA soluble in DMSO. **A)** Sodium ions (Na^+) interacting with the carboxylic groups of HA were exchanged with the lipophilic tetrabutylammonium (TBA^+). **B)** Representative illustration of the synthesis of the amphiphilic HA-Hexa nanogels. Hydrophobization of HA-TBA through amide formation with hexadecylamine in the presence of EDC and NHS, resulting in amphiphilic conjugates. Subsequent dialysis against NaCl removes TBA^+ ions and dialysis against distilled water removes excess Na^+, completing the synthesis of the amphiphilic conjugate. (Adapted from: Pedrosa et al., 2014).

5.2.1.2 ¹H NMR spectroscopy analysis and determination degree of substitution (DS)

Conjugation steps were confirmed by ¹H NMR spectroscopy. The HA-TBA or HA-Hexa (7 mg/mL) were dissolved in 100 atom % D of deuterium oxide (Acros) and the ¹H NMR spectra obtained using a Varian Unity Plus 300 spectrometer, operating at 299.94 MHz (25 °C).

From the ¹H NMR spectrum, the degree of substitution (DS) which corresponds to the number of hexadecylamine molecules per 100 disaccharide units of HA, was calculated based on equation 1:

$$DS = \frac{11 \times (\delta\ 0.8 \rightarrow 1.1)}{3 \times (\delta\ 3.3 \rightarrow 4.6)} \times 100$$

(Eq. 1)

whereby DS is calculated taking in account the intensity of the peak from the methyl group of grafted hexadecylamine.

5.2.1.3 HA-Hexa Nanogel preparation

HA-Hexa solutions with a concentration of 0.5, 1 or 1.5 mg/mL were dissolved in phosphate buffered saline solution – PBS (137 mM NaCl, 2.7 mM KCl, 10 mM Na_2HPO_4 and 1.8 mM KH_2PO_4 with pH 7.4) - and used in all subsequent assays. These solutions were obtained after dissolution for 24 h, mixing at low speed on a turning wheel, at room temperature. After this, the nanogel was filtered with a polyethersulfone (PES) membrane 0.22 µm pore size and further characterized.

5.2.1.4 HA-Hexa nanogel characterization

The nanogel was analysed by Dynamic Light Scattering (DLS), using a Zetasizer Nano ZS (Malvern Instruments, UK), with a detector angle of 173°, at 25°C. Results were expressed in terms of volume and intensity distributions, zeta potential, hydrodynamic diameter (size) and polydispersity index (PdI).

5.2.1.5 Cytotoxicity tests

Tests of *in vitro* cytotoxicity of HA-Hexa nanogel were performed according the International Standard ISO 10993-5:2009(E) through assessment of metabolic activity (MTT reduction assay).

- Cell Culture

L929 mouse fibroblasts were cultured in Dulbecco's Modified Eagle Medium (DMEM, Biochrom GmbH, Germany) supplemented with 10 % of bovine calf serum (Biochrom AG, Germany) and 1 % of a penicillin/streptomycin solution (Biochrom, Germany) in a humidified incubator (37 °C, 5 % CO$_2$). Subcultures were performed by trypsinization once cells reached 70-80% confluency.

- MTT assay

For MTT assay, L929 cells were seeded at a density of $1x10^4$ cells per well in 96 well-plates, Cells were incubated for 24 h, at 37 °C, 5 % CO$_2$, for cell adhesion before adding the nanogel solutions. Basal metabolic activity was determined after 3 h of incubation, which was the time required for cell adhesion.

HA-Hexa was tested at 0.5, 1, 1.5 and 2 mg/mL. All these nanogel HA-Hexa solutions were dissolved in DMEM without supplements. Antibiotic and serum were added to the nanogel solutions immediately before adding the solutions to the cells. After cell adhesion (24 h), the medium was removed and 200 µL of samples for each tested condition were added to the respective plates. Cells were incubated at 37 °C and 5 % CO$_2$ for 24 h. Cells exposed to 10 % DMSO were considered as a positive control.

MTT (3-(4,5-dimethylthiazol-2-yl)-2,5-diphenyltetrazoliumbromid, Sigma-Aldrich, USA) was dissolved in DMEM without supplements or phenol red at a final concentration of 1 mg/mL and sterilized using a 0.22 µm PES membrane. Following 24 h incubation with the nanogel solutions, the cell culture medium was replaced by 50 µL of the MTT solution. Cells were further incubated for 2 h at 37 °C and 5 % CO$_2$. The solution was then removed and the formazan crystals dissolved in 100 µL of isopropanol under mild shaking.

Absorbance was analysed in a Synergy HT (Bio-Tek) microplate reader at 570 nm and 650 nm (reference wavelength), and the metabolic activities were determined according to equation 2, where OD corresponds to the mean value (out of three independent assays (n=3)) of the measured optical density in each sample after subtracting the blank (MTT solution in DMEM without phenol red).

$$\text{Metabolic activity (\%)} = \frac{\text{OD}_{570-650}\,(\text{sample})}{\text{OD}_{570-650}\,(\text{control})} \times 100$$

(Eq. 2)

Results were expressed as percentage of metabolic activity relatively to the values obtained at 3 h and considering the metabolic activity of non-treated cells as 100 %.

5.2.2 Vitamin D$_3$ formulation

5.2.2.1 Vitamin D$_3$ loading in hyaluronic acid nanogel — HA-Vit D$_3$

A stock solution (25 mg/mL) of Vit D$_3$ (Acros Organics, New Jersey, USA) was firstly prepared in absolute ethanol. Vit D$_3$ was then added to of HA-Hexa nanogel dispersions with concentrations of 0.5, 1 and 1.5 mg/mL, in a total volume of 2 mL. The final Vit D$_3$ concentrations attained in the samples were 50, 100, 200 and 500 μM, which correspond to 19.2; 38.0; 76.9 and 192.3 μg/mL, respectively. The ethanol content was less than 1 % (v/v) in all conditions. A positive and negative control with the same final volume and 38.0 μg/mL of vitamin were made with ethanol and PBS, respectively.

The obtained solutions were left agitated in a rotating wheel for 16 h, at room temperature to allow vitamin loading. All working solutions containing Vit D$_3$ were protected from light. Samples obtained after 16 h of encapsulation were then centrifuged at 4000×g for 10 min (Eppendorf Centrifuge 5430 R) and the supernatant containing the loaded Vit D$_3$ was collected. Since Vit D$_3$ is insoluble in PBS, its presence in the pellets was quantified after dissolving them in absolute ethanol. The total drug concentration, corresponding to solubilized (in the nanogel) and insoluble fractions, was also quantified before centrifugation. Insoluble fractions were dissolved in absolute ethanol (8 times concentrate).

5.2.2.2 Vitamin D$_3$ loading quantification/characterization and encapsulation efficiency (EE)

To determine the amount of Vit D$_3$ loaded in the HA-Hexa nanogel, UV-Vis spectrophotometry was used (Luo et al., 2012; Almouazen., 2013; Mohammadi et al., 2014; Ramalho et al., 2015;). Optimal wavelength for Vit D$_3$ (alone or loaded into HA-Hexa nanogel) detection and quantification was identified by scanning wavelength spectrum between 190 to 380 nm, in 1 nm intervals. The 266 nm was the optimal wavelength to detected Vit D$_3$ (alone or loaded into HA-Hexa nanogel). This scan was also performed for the PBS and ethanol controls. Vit D$_3$ concentration was determined by interpolation from a linear calibration curve (Absorbance= 0.0474*[Vit D$_3$] + 0.5062; r^2= 0.9964) for different standard concentrations of Vit D$_3$ dissolved in ethanol in the range of concentrations 2- 64 μg/mL, obtained at 266 nm. All samples were analysed in the UV-Vis using a Jasco V-560 spectrophotometer. The effect of different loaded amounts of Vit D$_3$ on the HA-Hexa nanogel's particle size and PdI was performed using Dynamic Light Scattering.

The encapsulation efficiency (EE) of Vit D$_3$ was indirectly determined from equation 3:

$$EE\ (\%) = \frac{\text{Amount of Vit D}_3 \text{ in supernatant}}{\text{Amount of total Vit D}_3 \text{ in control (ethanol)}} \times 100$$

(Eq. 3)

5.2.2.3 Stability of the HA-Hexa nanogel loaded with vitamin D₃

Samples with 1 mg/mL HA-Hexa were selected to encapsulate 192.3 µg/mL of Vit D₃. The supernatant obtained with encapsulated HA-Vit D₃ was collected and analysed by UV-Vis (266 nm) and DLS. The colloidal suspensions of HA-Vit D₃ were stored at 4 and 36 ±1 °C and analysed at different time points, (0.5, 8, 10, 24, 48, 72, 96, 168 and 720 h), to assess its stability. This study was performed using separate tubes with 1 mL of supernatant HA-Vit D₃ for each time point (n=3).

5.2.3 Bacterial nanocellulose as a drug delivery system

5.2.3.1 Bacterial nanocellulose preparation

Commercial BNC was obtained from Vietnam *HTK Food., Ltd*. The BNC membranes were purified as follows: BNC sheets with 1-1.5 cm of thickness were first washed exhaustively with distilled water. Then, BNC membranes were placed in a 0.1 M NaOH solution, at room temperature. This solution was renewed every 24 h for three days; afterwards, the alkali bath was substituted by distilled water washes until the pH value became that of the distilled water. Finally, BNC membranes were sterilized by autoclaving at 121 °C for 20 minutes and 1 bar. BNC membranes were compressed between two metallic plates until 90 - 95 % of the water was removed, thus obtaining membranes with a uniform thickness of 1 mm, that corresponding at 6±1.9 % solids. Then, the compressed BNC sheets were sliced in circles with 2 cm of diameter. The final wet compressed BNC was designated wBNC.

5.2.3.2 Swelling assays

The water absorption ability of wBNC membranes was measured. For these tests, each 2 cm discs obtained as described above were weighted (W_{t0}) and then immersed in 6-well plates containing 10 mL of PBS and kept under shaking (bioSan Orbital Shaker PSU-10i, 80 rpm) at 4 °C until a constant weight was attained. The wBNC disks were weighted at several time points (W_t) (0.5, 1, 1.5, 2, 4, 6, 8, 16 and 24 h). The excess of surface water was gently removed with a tissue paper before weighting the samples. The degree of swelling of the disks at each time point was defined by the following equation:

$$\text{Swelling degree (\%)} = \frac{W_t - W_{t0}}{W_t} \times 100$$

(Eq. 4)

The tests were carried out using four independent membranes (n=4) per time point.

5.2.3.3 Preparation of BNC membranes impregnated with HA-Vit D₃ nanogel (wBNC-HA-Vit D₃)

To prepare the wBNC-HA-Vit D₃ dressings, the BNC disks prepared as described in section 5.2.3.1, were immersed in 1 mL of HA-Vit D₃ nanogel solution. The HA-Vit D₃ nanogel solution its samples with 1 mg/mL HA-Hexa loading with 192.3 µg/mL of Vit D₃. The impregnation was performed for 14-16 h, at 4 °C in the dark. The disks were turned over during the impregnation time to allow the complete absorption of the HA-Vit D₃ nanogel solution.

5.2.3.4 *In vitro* release studies

- Submerged membrane

The wBNC-HA-Vit D₃ disks prepared as described in section 5.2.3.1 and 5.2.3.3 were immersed in a glass vessel containing 5 mL of PBS. The assays were carried out at 36 ±1 °C and 50 rpm (Heidolph Unimax 1010 and Heidolph Inkubator 1000). At each time point (0.25, 0.5, 1, 2, 4, 6, 8, 10, 24, 48, 72 and 96 h), the BNC membranes were removed and immediately placed in a 5 mL plastic tube, frozen at -80 °C and freeze-dried (Scanvac Coolsafe). Afterwards, the Vit D₃ concentration remaining in the BNC membrane at each time point was estimated following extraction, as described in section 5.2.4.

Nine membranes were processed for each interval of time. The assay and lyophilization procedures were performed always keeping the membranes in the dark.

- *Franz* cell assays

Permeation assays were conducted on a *Franz* diffusion cells with a receptor volume of ˜ 40 mL and a diffusion area of 3.14 cm² using PBS as the continuously stirred receptor medium. The temperature in the receptor chamber was set at 36 ± 1°C. The wBNC-HA-Vit D₃ membrane prepared as described in section 5.2.3.1 and 5.2.3.3 was placed on the donor chamber. The diffusion experiments were performed under occluded conditions by sealing the donor chamber and sampling port with aluminium foil. At each time point (0.25, 0.5, 1, 2, 4, 6, 8, 10, 24, 48, 72 and 96 h), the BNC membrane was removed and

immediately placed in a 5 mL plastic tube, frozen at -80 °C and freeze-dried (Scanvac Coolsafe). Afterwards, the Vit D$_3$ concentration remaining in the BNC membrane at each time point was estimated following extraction, as described in section 5.2.4. Eight membranes were processed for each interval of time. The assay and lyophilization procedures were performed always keeping the membranes protected to the light.

5.2.4 Extraction of vitamin D$_3$ from BNC membranes

The Vit D$_3$ in the lyophilized membranes was extracted using pure ethanol as solvent. Briefly, the same volume of solution HA-Vit D$_3$ used to impregnate each BNC disk (section 5.2.3.3) was added and the membranes were incubated for 6 h at room temperature under rotation on a turning wheel. During this time, every 2 h the tubes were cooled in ice, to minimize ethanol evaporation, and the BNC membranes were compressed to expel the entrapped Vit D$_3$. After extraction quantitative analysis UV-Vis using a Jasco V-560 spectrophotometer of remaining Vit D$_3$ on BNC membranes was performed.

5.2.5 Statistical analysis

The statistical analysis was done with the GraphPad Prism software for windows version 5.01. Normality of the samples distribution was firstly assessed using Kolmogorov-Smirnov and Shapiro-Wilk normality tests, and considering the acceptability of skewness and kurtosis values. For assays the one-way ANOVA followed by Bonferroni's and Dunnett´s multiple comparison test and two-way ANOVA was used.

5.3 RESULTS AND DISCUSSION
5.3.1 Production and characterization of the HA-Hexa Nanogel
5.3.1.1 Production of HA-Hexa conjugate

The hyaluronic acid analysis by ^{1}H-NMR spectroscopy revealed its characteristic spectra, with chemical shifts in the region δ=3.3→ 4.6, featuring the peaks assigned to 11 protons of HA at δ =4.51 (G1), δ =4.61 (N1), δ =3.40 (G2), δ =3.92 (N2), δ =3.63 (G3), δ = 3.74–3.85 (N3, N6, G4, G5), δ =3.51–3.62 ppm (N4, N5) (box 1) (Bodnár et al., 2009) (Figure 2 A). Following modification with TBA[+], new peaks assigned to tert-butyl amine were detected in the region δ=1→ 2 (Figure 2 B). Figure 2 C shows the ^{1}H NMR spectra of HA-Hexa nanogel, showing the grafting of a hydrophobic chain of hexadecylamine (CH$_3$(CH$_2$)$_{15}$NH$_2$) in addition to the HA peaks (box 1). The proton peak assigned to 3 protons from the methyl (-CH$_3$) group of hexadecylamine was observed at δ =0.8-1 ppm (box 2), as previously reported

(Dantas-Santos et al., 2012). The absence of signal around 1 ppm also indicates that TBA⁺ ions were fully

exchanged by Na⁺ ions during dialysis, as described elsewhere (Oudshoorn et al., 2007).
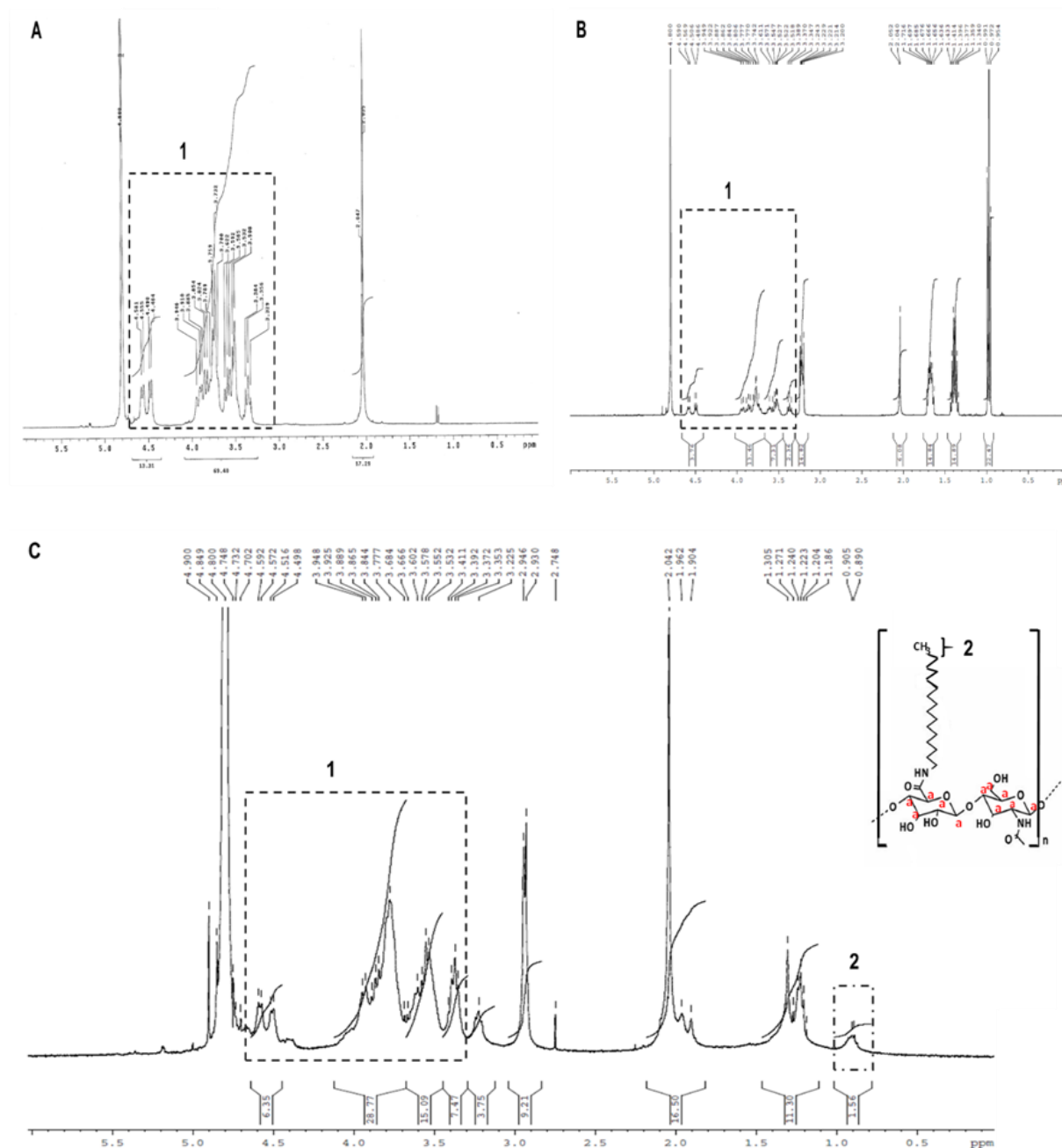
Figure 2 - ¹H-NMR spectrum of: **A)** native hyaluronic acid (HA); **B)** HA modified with TBA⁺ ions; **C)** HA-Hexa nanogel and the respective scheme of the conjugate**.** "1" represents the hyaluronic acid peaks and "2" corresponds to the hexadecylamine graft used for the degree of substitution calculation.

Different HA-Hexa batches were produced with a mean degree of substitution of 10.3 ±1.1 %. A

substitution reaction yield of around 68.9 ±7.0 % was estimated considering the theoretical DS of 15 %.

The reaction proved to be reproducible, all batches presenting similar DS and substitution reaction yields.

5.3.1.2 HA-Hexa conjugation and characterization

The binding of hexadecylamine to the hyaluronic acid creates an amphiphilic molecule with the ability of self-assembling into nanostructures, in aqueous environments. Figure 3 presents the results of the DLS analysis of the colloidal nanogel. DLS provides the particle size distribution by intensity according to the particle scattering intensity, which is greatly influenced by large particles or aggregates. The size distribution by volume is a conversion of the intensity distribution, enhancing the small population and resulting in a size distribution, being considered more realistic. For colloidal suspensions with high polydispersity, the Z-average is considered a good indication of the average size of the population (Takahashi et al., 2008; Goldburg, 2014; Stetefeld et al., 2016).
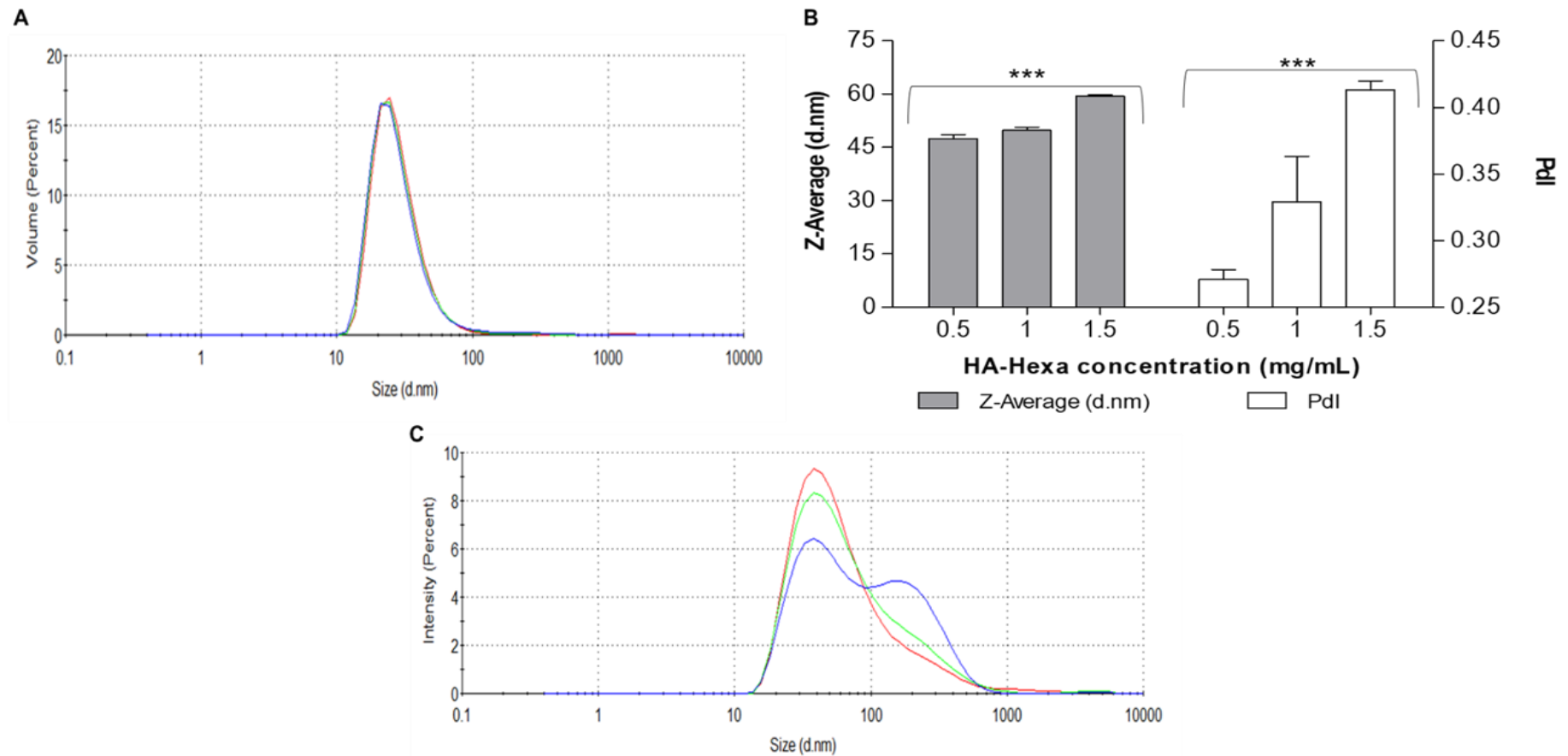
Figure 3 - Dynamic Light Scattering analysis of the HA-Hexa nanogel. **A)** Size distribution by volume of the different HA-Hexa nanogel concentrations. (red curve)- 0.5 mg/mL; (green curve)- 1 mg/mL and (blue curve)- 1.5 mg/mL; **B)** Mean Z-average and PdI of different HA-Hexa nanogel concentrations. Bars show the mean ± standard deviation and the obtained significant differences. ***$p < 0.001$, after one-way ANOVA followed by Bonferroni's multiple comparison test between different HA-Hexa concentrations. **C)** Size distribution by intensity of the different HA-nanogel concentrations. Results were analyzed by DLS and show the mean size of 7 repeated measurements of the same sample.

The results in Figure 3 A show that HA-Hexa nanogel dispersed in PBS at concentrations of 0.5, 1 and 1.5 mg/mL present an unimodal volume distribution and the Z-average presented significantly different value: 47.46 ±1.14 nm, 49.87 ±0.87 and 59.38 ±0.49 nm, respectively (Figure 3 B). The wider range of particle sizes is associated with a higher PdI, a lower PdI being generally indicative of the HA nanogel stability, with reduced aggregation and higher uniformity (Masarudin et al., 2015). Results in Figure 3 B show that the PdI significantly increased with HA-Hexa concentration. For concentrations of 0.5 and 1 mg/mL the PdI values obtained (between 0.1-0.4) evidence low heterogeneity (moderate polydisperse), while for the higher concentration tested a PdI above 0.4 indicates a broader size distribution (Nobbmann, 2014), as confirmed by the intensity size distribution, Figure 3 C. A colloidal particles presented a negative zeta potential, as expected due to the presence of ionized carboxylate groups, with values of -20.1 ± 2.6 mV, -27.8 ± 0.9 mV and -28.8 ± 1.1 mV, for increasing concentrations.

Nanocarriers smaller than 200 nm, bearingan hydrophilic and negative charged surface are valuable as drug delivery systems, since they may avoid the recognition by the phagocytic systems and enhanced the circulation time within the body (Tabata et al., 1988; Chacko et al., 2012; Jin et al., 2012). Particles with negative charge are more resistant and stable to clearance mechanisms (compared to neutral or positively-charged particles). They also avoid undesired protein binding that may trigger foreign body reaction and phagocytosis (Oh et al., 2010; Li et al., 2010).

5.3.1.3 Cytotoxicity evaluation

Results in Figure 4 showed that the HA-Hexa nanogel formulation did not affect the cell viability at concentrations of 0.5 and 1 mg/mL, since no differences were observed with regards to the control (p>0.05). However, using 2 mg/mL further reduced the cell metabolic activity to 49 ±7.8 %. Silva et al. 2016 and Pedrosa et al. 2016 evaluated the metabolic activity of RAW 264.7 macrophages and 3T3 fibroblasts, respectively, in the presence of a HA-AT nanogel. Although different cell lines were used in the different works, a general similar trend is observed, a small decrease in metabolic activity being observed for the higher concentrations of nanogel.

A drug/material is considered cytotoxic when it reduces the cell metabolic activity to less than 70 % (ISO 10993-5, 2009). Thus, HA-Hexa nanogel may be considered safe up to concentrations of 1.5 mg/mL.
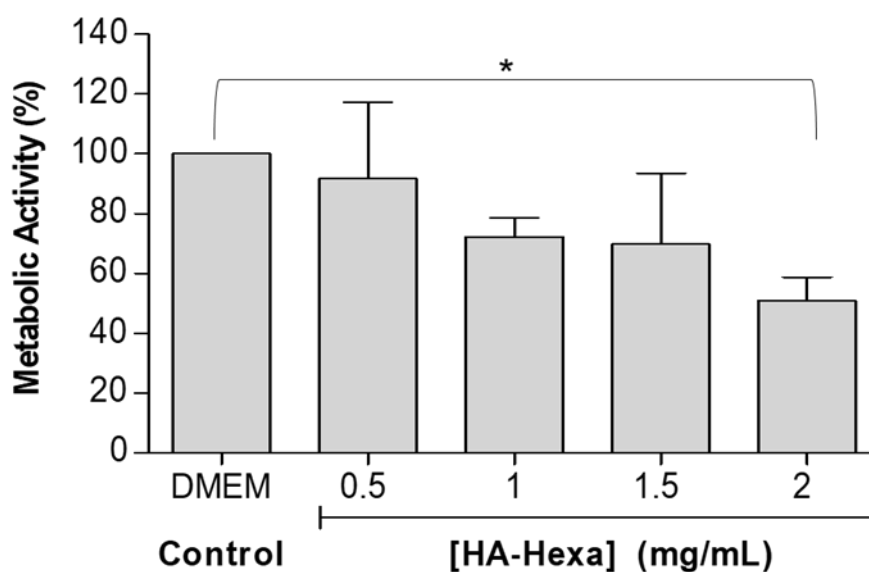
Figure 4 - Evaluation of the effects of HA-Hexa nanogels on the metabolic viability of L929 cells. Cell viability is expressed in % relative to a control of cells incubated only with culture media (DMEM). Data is represented as mean ± standard deviation (n=3) and the obtained significant differences. *$p < 0.05$, when compared the 2 mg/mL HA-Hexa with the control using one-way ANOVA followed by Bonferroni's multiple comparison. There were no significant differences between nanogel concentrations.

5.3.2 Vitamin D$_3$ encapsulation

5.3.2.1 Characterization of Vitamin D$_3$ loading into the HA-Hexa nanogels

Following HA-Hexa nanogel synthesis, the Vit D$_3$ loading ability was assessed. Vit D$_3$ was mixed with HA-Hexa nanogel in PBS and the amount solubilized was quantified by UV-Vis. Results in Figure 5 A confirm that PBS (PBS line) and ethanol (Ethanol line) did not interfer with the quantification of Vit D$_3$, given the lack of absorption in the range of the spectra used for that purpose (190 to 380 nm). Vit D$_3$ solubilized in ethanol (Control Ethanol-VitD3 line) featuring a strong absorption at 266 nm, but not in PBS, as expected (Control PBS-VitD3 line) (Figure 5 A).

The Vit D$_3$ loading in HA-Hexa nanogel was also analysed by UV-Vis absorbance. Figure 5 B shows that the characteristic absorption of Vit D$_3$ at 266 nm is detected in the nanogel suspension, confirming the encapsulation of the hydrophobic drug (HA-VitD3_Total line). Moreover, after centrifugation to remove any non-encapsulated vitamin, a similar absorption spectrum was obtained, confirming the successful complete loading of the drug (HA-Vit D$_3$_Loaded line and HA-Vit D$_3$_Total line, Figure 5 B). Also, it was possible to observe that the HA-Hexa nanogel does not interfere with Vit D$_3$ quantification (HA-Hexa line) (Figure 5 B).
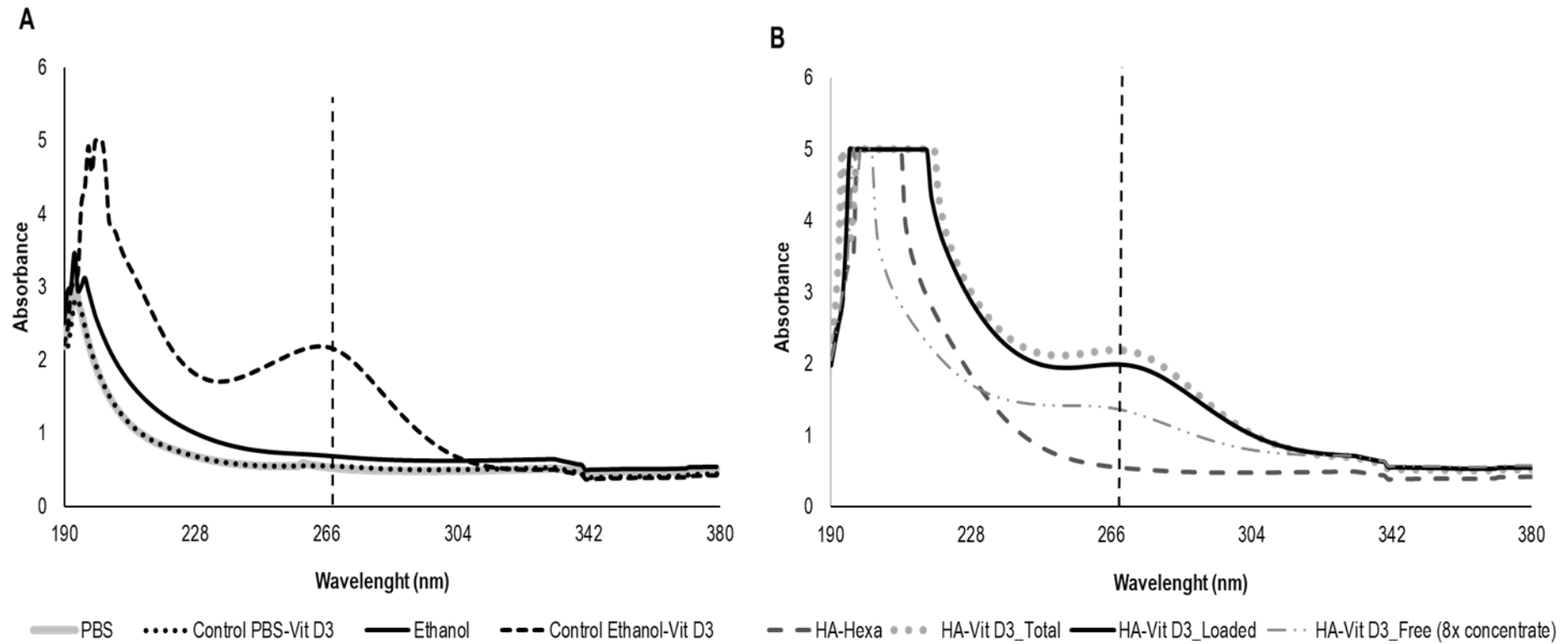
Figure 5 - A) UV-Vis absorbance spectrum in different solvents, blanks (━━ ethanol line and ─── PBS line), positive control (ethanol with 38 µg/mL of Vit D₃, ─── line) and negative control (PBS with 38 µg/mL of Vit D₃, ••••• line). **B)** UV-Vis absorbance spectrum of vitamin D₃ at a 38 µg/mL concentration in the presence of 1 mg/mL HA-Hexa nanogel (••• line, represents the total of Vit D₃ solubilized, the ━━ and ─·· lines represents the amount of Vit D₃ loaded in HA nanogel and the amount of Vit D₃ insoluble, respectively and these fractions were obtained after centrifugation) and HA-Hexa nanogel as control (─ ─ line).

The encapsulation efficiency (EE) was assessed by quantifying the Vit D_3 loaded into HA-Hexa nanogel by UV-Vis spectrophotometry. The insoluble (free) Vit D_3 was quantified after centrifugation and solubilization in ethanol (Figure 6).
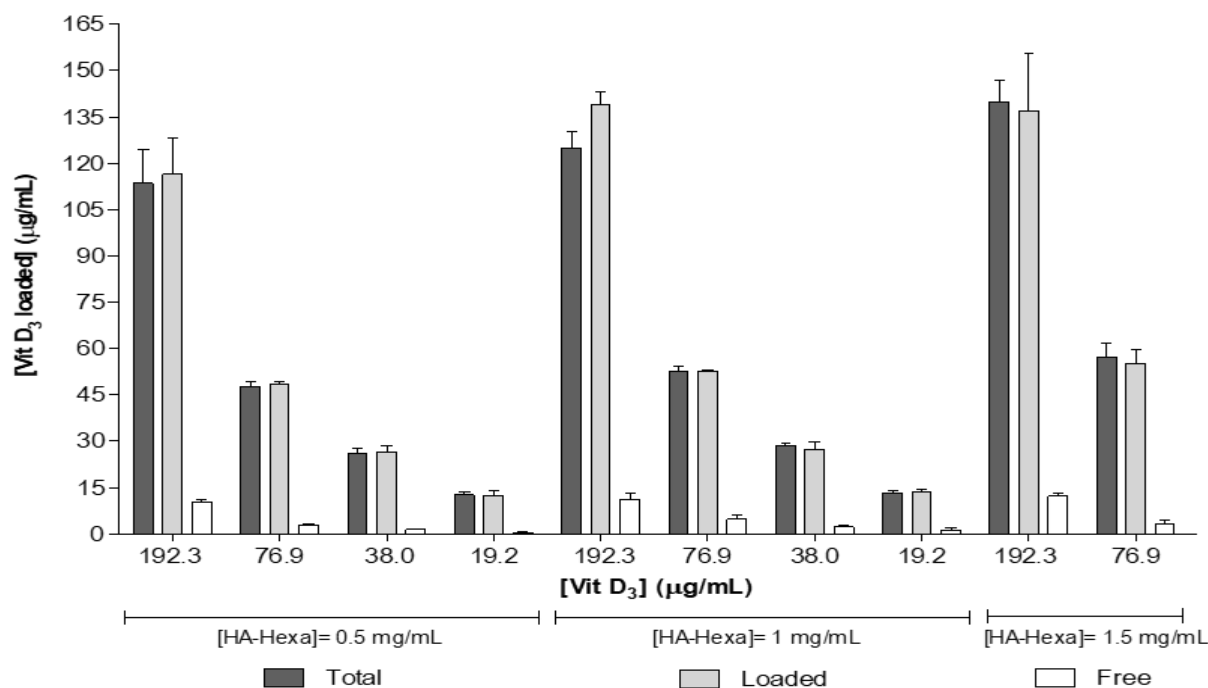
Figure 6 - Vit D_3 loading obtained using different concentrations of HA-Hexa nanogel and Vit D_3. The values represent the mean ± standard error of three independent assays (n = 3).

Vit D_3 encapsulation efficiency (EE) studies suggested that in every condition Vit D_3 was present mainly dispersed in the supernatant (Figure 6), i.e., it was successfully entrapped into the HA-Hexa nanogel. Indeed, no significant differences ($p > 0.05$) were observed between the total (vitamin solubilized in the nanogel + insoluble fraction) and loaded (in the nanogel). A small amount of free drug was detected in the pellet obtained by centrifugation, which corresponds to non-loaded material. All of the HA-Hexa dispersions showed high encapsulation efficiency, between 60-94 % (Table 1). As expected, the EE increased with the reduction of Vit D_3 concentration and the increase of the nanogel concentration (Table 1).

Size of the drug-loaded particles was also analysed by DLS and compared to non-loaded HA-Hexa (Table 1). The size of nanogels generally increased with the amount of entrapped Vit D_3 (significant differences were observed, Table 1). The mean size of the nanogel increased from around 40 nm up to around 200 nm (Table 1), as more vitamin was loaded. We further observed that a similar particle size was obtained using different concentrations of HA-Hexa and the same concentration of Vit D_3 ($p > 0.05$) (Table 1). Interestingly, the polydispersity index decreased for increasing Vit D_3 load, indicating a decrease

in the heterogeneity of the population (Table 1), a unimodal distribution being obtained for the higher loadings (supplementary material, Figure S1).

Table 1 - Vit D_3 encapsulation efficiency (EE) yield of the HA-Hexa nanogel and evaluation of the effect of different loaded of Vit D_3 at different HA-Hexa nanogel concentrations on particles size and PdI (by DLS analysis). Analysis before and after drug loading with drug loaded concentration in the supernatant.

HA-Hexa (mg/mL)	Vit D_3 (µg/mL)	EE (%)	Z-Average (d.nm)	PdI
0.5	0	—	47.5 ±1.14***	0.271 ±0.008
	19.2	87.4 ±10.54	117.0 ±1.27***	0.239 ±0.012
	38	85.2 ±6.55	150.9 ±2.09***	0.154 ±0.014
	76.9	74.06 ±1.28	187.5 ±1.49***	0.110 ±0.017
	192.3	61.2 ±6.12*	216.9 ±1.06***	0.148 ±0.071
1	0	—	49.9 ±0.87***	0.329 ±0.034
	19.2	94.6 ±6.82	106.3 ±0.97***	0.269 ±0.009
	38	88.09 ±7.78	140.2 ±1.20***	0.199 ±0.012
	76.9	80.8 ±0.45	187.7 ±1.21***	0.129 ±0.012
	192.3	71.4 ±2.27	209.0 ±0.69***	0.091 ±0.006
1.5	0	—	59.38 ±0.49***	0.413 ±0.006
	76.9	85.0 ±7.32	177.6 ±2.43***	0.225 ±0.020
	192.3	72.0 ±9.69	220.4 ±1.09***	0.146 ±0.019

*** $p<0.001$, compared Z-Average between all Vit D_3 concentration for each nanogel concentration using one-way ANOVA followed by Bonferroni's multiple comparison.

* $p<0.05$, compared EE between 0.5 mg/mL and 1, 1.5 mg/mL of HA-Hexa at the same Vit D_3 concentration using one-way ANOVA followed by Bonferroni's multiple comparison.

5.3.2.2 Stability of HA-Hexa nanogel loaded with vitamin D_3

The stability of the nanoformulation is important to preserve the solubility of Vit D_3 under different conditions, namely during impregnation in the BNC membranes. Considering the results of EE (Figure 6 and Table 1), size distribution (Table 1) and cytotoxicity, the formulation with 1 mg/mL of HA-Hexa nanogel loaded with 192.3 µg/mL of Vit D_3 was chosen for further assays. Figure 7 present the results of the stability tests performed.
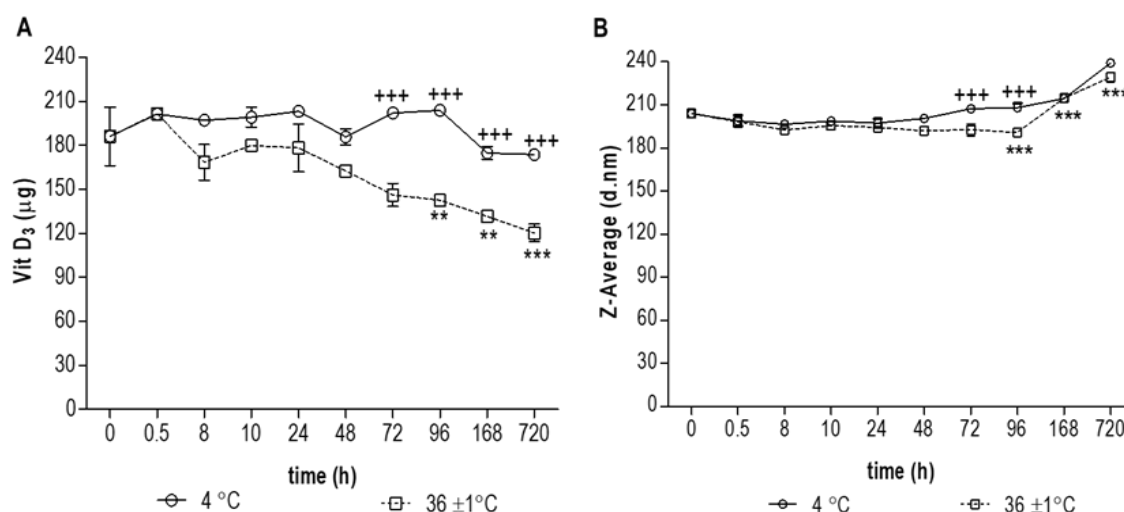
Figure 7 - Stability evaluation of 1 mg/mL of HA-Hexa nanogel loaded with 192.3 µg/mL of Vit D$_3$ at 4 and 36 ±1 °C. **A)** Quantification of soluble Vit D$_3$ over time, at 4 and 36 ±1°C. **B)** Size analysis by DLS at 4 and 36 ±1 °C. The values represent the mean ± standard error of three independent tubes for each time point (n = 3) with the obtained significant differences. **$p<0.01$, ***$p<0.001$ compared each time-point with initial time-point to 36 ±1 °C using one-way ANOVA followed by Dunnett's Multiple Comparison Test. $^{+++}p<0.05$ compared each time-point between each temperature using two-way ANOVA followed by Bonferroni post test.

The results show that the nanoformulations HA-Vit D$_3$ stored at 36 ±1 °C are stable over a period of 72 h as the mass of Vit D$_3$ entrapped remained practically constant. After this period of time, the mass stability of entrapped Vit D$_3$ started to decrease, significant differences in the soluble amount being noticed (Figure 7 A). However, at 4 °C the nanoformulations remained stable (no statistical differences were observed, $p>0.05$). Similar findings were attained regarding mean size distribution (Figure 7 B). At longer time points, the size of the nanoformulations increased slightly (but significantly), possibly due to aggregation (Figure 7 B). The polydispersity index remained very low, displaying average values of 0.103 ±0.032 and 0.093 ±0.0098 at 4 and 36 ±1 °C, respectively. This indicates that the distribution of nanoparticles remained unimodal (supplementary material, Figure S2). Additionally, the analysis of different batches demonstrated the good reproducibility of the nanogel preparations. This is an interesting result for studies that required a prolonged use/application of HA and HA-Vit D$_3$ (for example topical applications during *in vivo* assays).

5.3.3 Bacterial nanocellulose as a drug delivery system

5.3.3.1 Swelling assays

Swelling assays were performed using compressed BNC membranes (wBNC membranes) to determine the timeframe required for the highest achievable volume of liquid absorption by BNC membranes. According to previous work by Kwak et al., 2015, the swelling process was expected to be fast. Indeed, the absorption data (Figure 8) demonstrates a quick process, as the samples were almost fully swollen after being immersed in PBS for 0.5 h. However, the membranes were left equilibrating for approximately 14-16 h as to ensure the penetration of HA-Vit D₃ micelles inside the tridimensional matrix of BNC membranes. After this period, each wBNC membrane reabsorbed a maximum of around 0.8-1 mL/g hydrated BNC, corresponding to a water absorption ability of wBNC membrane of about 70 %. The good swelling ability of BNC may also help in the absorption of the wound exudates and maintain a moisturized environment.
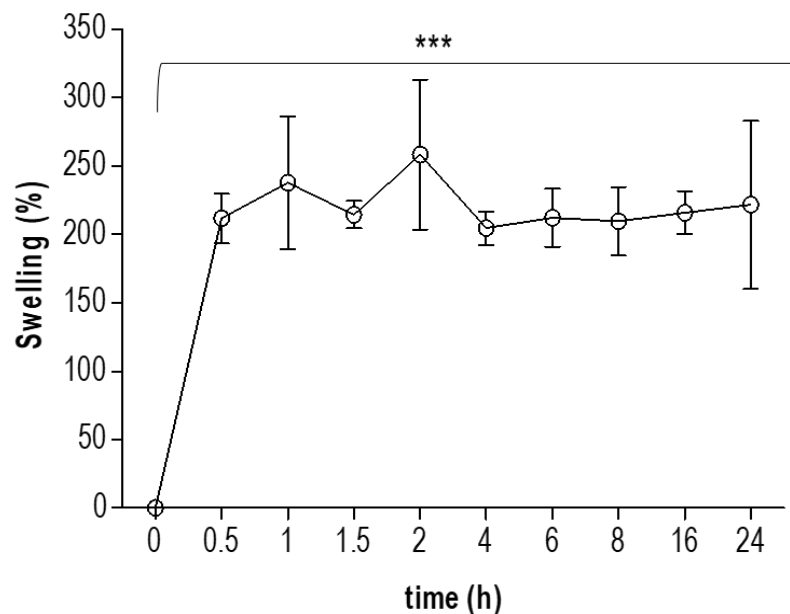
Figure 8 - Swelling ratio of wet BNC membranes with 1 cm of initial thickness and compress to 1 mm (wBNC) with 6±1.9 % solids at 4 °C. The results are shown as the mean values ± standard deviation of four independent cellulose disks for each time-point (n=4). One-way ANOVA followed by Bonferroni post-test analysis showed significant differences (*** $p<0.001$) when compared each time-point with initial time (0 h). However, no differences were observed ($p>0.05$) between each time point from 0.5 h of immersion.

5.3.3.2 *In vitro* release studies – submerged BNC membrane and *Franz* cell assays

Release assays were performed to investigate whether BNC-nanogel formulations have a suitable performance as a Vit D_3 drug delivery system and to assess the kinetics and extent of the release process. For wound treatment it is important that the release starts swiftly and proceeds at a constant rate over a suitable period (from several hours up to few days) (Horrocks, 2006; Wilhelms et al., 2007).

Figure 9 A and B demonstrated a gradual release across the porous BNC membranes over time. The cumulative release of HA-VitD$_3$ revealed an initial burst (around 44 %) within the first 8 h reaching a plateau and equilibrium conditions after 48 h, resulting in a total release of Vit D_3 of around 70 %. BNC membrane has a pore size of around 1 μm, after cryo-SEM analysis (graphical abstract); hence it is not expected to hinder the encapsulation/release of the nanogel with 200 nm. The release started immediately after placing the membrane in contact with the receptor liquid in the *Franz* cell. The quick and sustained release profile between 8 h and 48 h is a promising result, as it may trigger a prompt therapeutic response in *in situ* conditions, leading to a decrease in treatment time and possibly reduce patch changes during treatment. Although the release was not complete, *in vivo*, hyaluronic acid will be naturally degraded by enzymatic (hyaluronidase, β-*D*-glucuronidase or β-N-acetyl-hexosaminidase) or non-enzymatic processes (degradation by oxidants) leading to full vitamin release and its solubilization in body fluid (Schanté et al., 2011, Fallacara et al., 2018). Proteins with the ability to bind HA are called hyaladherins and include, for example, proteoglycans and HA receptors (like CD44). A huge portion of HA degradation continues intracellularly, after HA binds to the CD44^{+} receptor cells. While HA binding to proteoglycans creates complexes that act as structural components of blood vessels, skin, brain or cartilage, HA receptors like CD44 act in cell proliferation and differentiation, cell-cell and cell-matrix adhesion and angiogenesis (Fallacara et al., 2018). So, it is quite reasonable to expect that the HA that reaches the wounded skin (loaded with the Vit D_3) may itself further contribute to reduce the healing time.
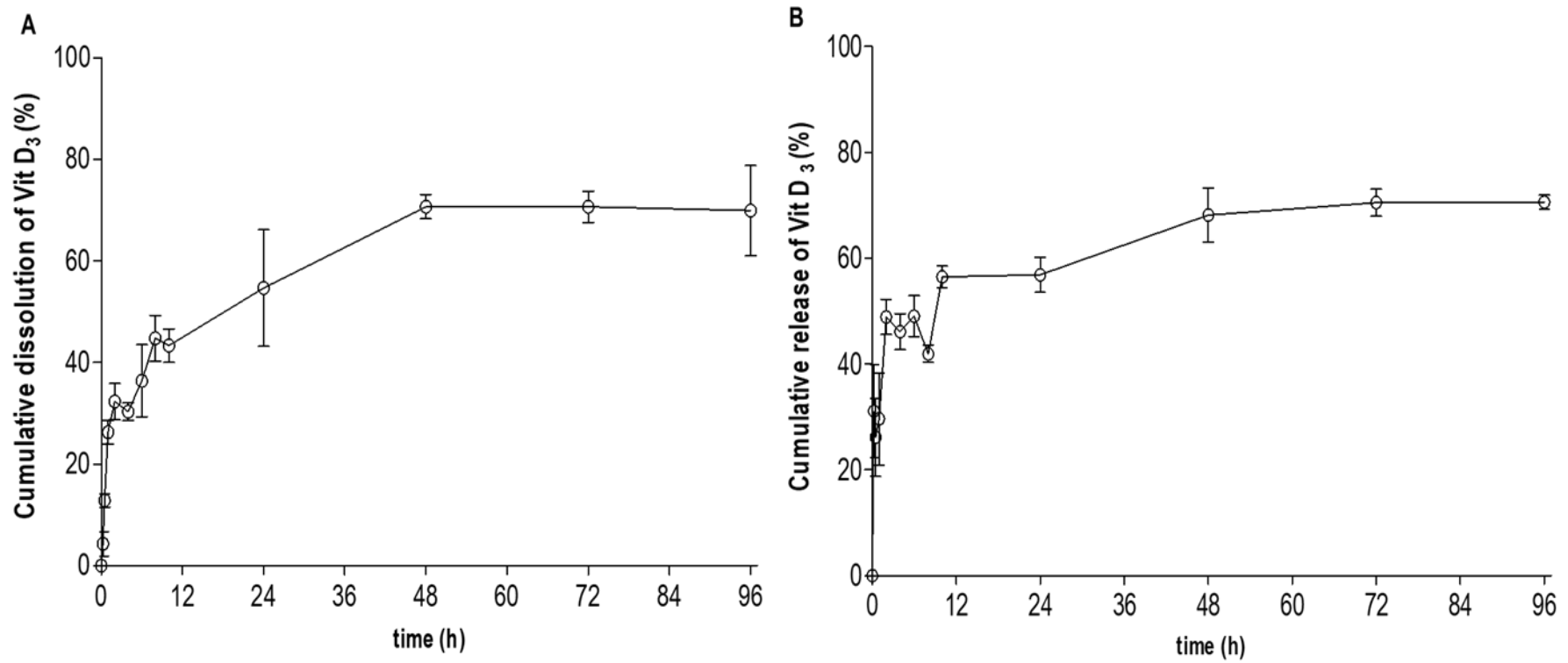
Figure 9 - Vit D₃ release from wBNC membranes in a buffer solution PBS at 36 ±1 °C, in submerged (**A** – glass vessel) and permeation assays (**B -** *Franz* cell), respectively. The results are shown as the mean values ± standard deviation, n= 9 and n= 8 to A and B studies, respectively.

5.4 CONCLUSIONS

Chronic and burn wounds are a global public health concern. Neither of these kinds of wounds follow the normal healing process, which increase the health care costs, hospitalization times and susceptibility to other diseases.

We developed an innovative BNC-based dressing loaded with Vit D_3 that will expectedly act as a safe and efficient drug delivery system, with potential to maintain the wound moist and absorb the exudates. The use of Vit D_3 is highly advantageous as compared to other molecules currently being employed in wound treatments, as it is not cytotoxic at low concentrations, it is easy to obtain in large amounts and at reduced production costs and it is able to promote the endogenous synthesis of other molecules (e.g. LL37) with reported wound healing properties.

Vitamin D_3 was successfully loaded into a hyaluronic acid nanogel grafted with hexadecylamine and presenting a high encapsulation efficiency. The solution HA-Vit D_3 have high stability at 4 and 36 °C. Furthermore, no Vit D_3 was released from HA-Hexa nanogel in aqueous buffer solution. Additionally, HA-VitD$_3$ was gradually released from the BNC membrane.

Nevertheless, despite the promising results obtained, demonstration of our system's efficacy *in vivo* is still required to further confirm its potential application as a wound healing dressing.

5.5 APPENDIX A. SUPPLEMENTARY DATA
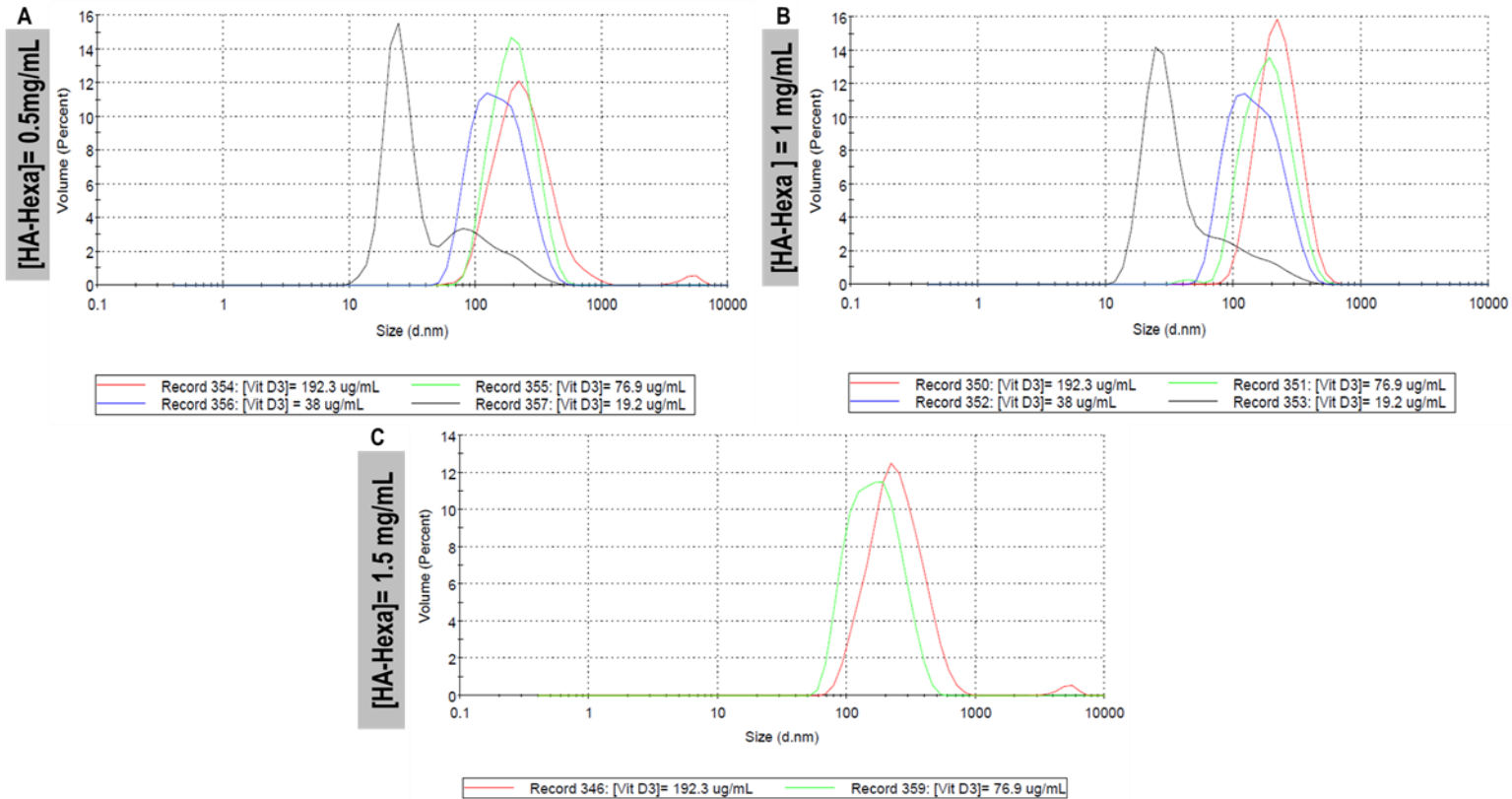
Supplementary material, Figure S1 - Mean Z-average distribution by volume of different HA-Hexa nanogel concentrations loading **A)** 0.5, **B)** 1 and **C)** 1.5 mg/mL with different vitamin D₃ concentrations.
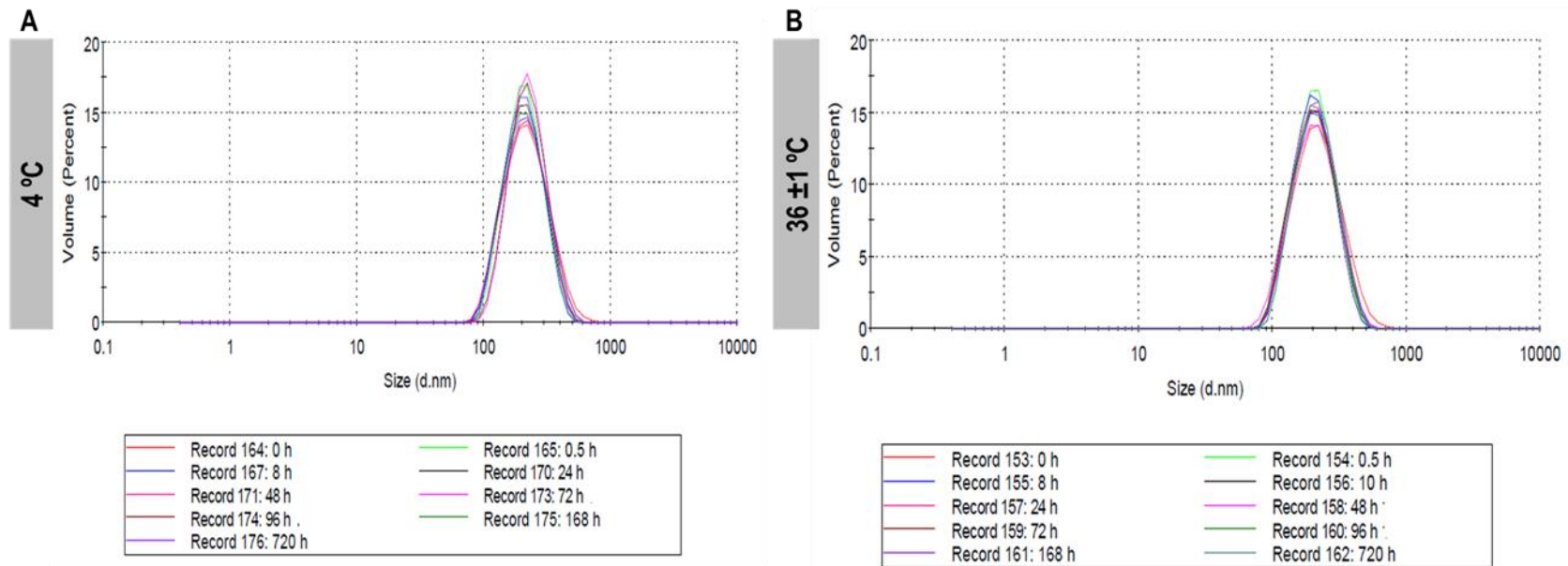
Supplementary material, Figure S2 - Mean Z-average distribution by volume of HA- Vit D_3 nanogel solution (1 mg/mL HA-Hexa and 192.3 µg/mL) along the time at **A)** 4 and **B)** 36 ±1°C.

5.6 REFERENCES

Almouazen, E., Bourgeois, S., Jordheim, L. P., Fessi, H., Brianon, S. 2013. Nano-encapsulation of vitamin D_3 active metabolites for application in chemotherapy: Formulation study and *in vitro* evaluation. Pharmaceutical Research. 30: 1137–1146.

Bandurska, K., Berdowska, A., Barczyńska-Felusiak, R., Krupa, P. 2015. Unique features of human cathelicidin LL-37. Biofactors. 41(5): 289-300

Bergstrom, N., Horn, S. D., Smout, R. J., Bender, S. A., Ferguson, M.L., Taler, G., et al., 2005. The national pressure ulcer long-term care study: outcomes of pressure ulcer treatments in long-term care. Journal of American Geriatrics Society. 53: 1721–1729.

Bodnár, M., Daróczi, L., Batta, G., Bakó, J., Hartmann, J. F., and Borbély, J. 2009. Preparation and characterization of cross-linked hyaluronan nanoparticles. Colloid and Polymer Science, 287(8): 991-1000.

Burkiewicz, C. J. C. C., Guadagnin, F. A., Skare, T. L., do Nascimento, M. M., Servin, S. C. N ., de Souza, G. D. 2012. Vitamin D and skin repair: a prospective, double-blind and placebo controlled study in the healing of leg ulcers. Revista do Colégio Brasileiro de Cirurgiões. 39: 401–7.

Caló, E. and Khutoryanskiy, V. V. 2015. Biomedical applications of hydrogels: A review of patents and commercial products. European Polymer Journal. 65: 252–267.

Chacko, R.T., Ventura, J., Zhuang, J., Thayumanavan, S. 2012. Polymer nanogels: A versatile nanoscopic drug delivery platform. Advanced Drug Delivery Reviews. 64: 836–851.

Cheredd, K. K., Her, C.-H., Comune, M., Moia, C., Lopes, A., Porporato, P. E., Vanacker, J., Lam, M. C., Steinstraesser, L., Sonveaux, P., Zhu, H., Ferreira, I. S., Vandermeulen, G., Préat, V. 2014. PLGA nanoparticles loaded with host defense peptide LL37 promote wound healing. Journal of Controlled Release. 194: 138-147

Czaja, W., Krystynowicz, A., Bielecki, S., Brown Jr., R.M. 2006. Microbial cellulose—the natural power to heal wounds. Biomaterials. 27: 145–151.

Dantas-Santos, N., Almeida-Lima, J., Vidal, A. A. J., Gomes, D. L., Oliveira, R. M., Santos Pedrosa, S., et al. 2012. Antiproliferative Activity of Fucan Nanogel. Mar Drugs, 10(9): 2002-2022.

Fallacara, A., Baldini, E., Manfredini, S., Vertuani, S. 2018. Hyaluronic Acid in the Third Millennium. Polymers. 10: 701.

Farah, L. F. X., 1990 Mar 27. Process for the preparation of cellulose film, cellulose film produced thereby, artificial skin graft and its use. United States patent US 4912049.

Fonder, M. A., Lazarus, G. S., Cowan, D. A., Aronson-Cook, B., Kohli, A. R., Mamelak, A. J. 2008. Treating the chronic wound: a practical approach to the care of nonhealing wounds and wound care dressings. Journal of American Academy of Dermatology. 58: 185–206.

Goldburg, W.I., 1999. Dynamic light scattering. American Journal of Physics. 8:1152–1160.

Goltzman, D. 2018. Functions of vitamin D in bone. Histochemistry and Cell Biology. 149: 305–312.

Gombart, A. F. 2011. The vitamin D-antimicrobial peptide pathway and its role in protection against infection. Future Microbiology. 4: 1151–1165.

Gombart, A. F., O'Kelly, J., Saito, T., Koeffler, H. P. 2007. Regulation of the CAMP gene by 1,25(OH)2D3 in various tissues. The Journal of Steroid Biochemestry and Moecular Biology. 103: 552–557.

Haimer, E., Wendland, M., Schlufter, K., Frankenfeld, K., Miethe, P., Potthast, A., et al., 2010. Loading of bacterial cellulose aerogels with bioactive compounds by antisolvent precipitation with supercritical carbon dioxide. Macromolecular Symposia. 294: 64–74.

Harder, J., Schroder, J. M., Glaser, R. 2013. The skin surface as antimicrobial barrier: Present concepts and future outlooks. Experimental Dermatology. 22: 1–5.

Heilborn, J. D., Weber, G., Grönberg, A., Dieterich, C., Ståhle, M. 2010. Topical treatment with the vitamin D analogue calcipotriol enhances the upregulation of the antimicrobial protein hCAP18/LL-37 during wounding in human skin *in vivo*. Experimental Dermatology. 19: 332–338.

Horrocks, A. 2006. Protosan wound irrigation and gel: management of chronic wounds. British Journal of Nursing. 15: 1222–1228.

Hu, W., Chen, S., Yang, J., Li, Z., Wang, H. 2014. Functionalized bacterial cellulose derivatives and nanocomposites. Carbohydrate Polymers. 101: 1043–1060.

International Standard ISO 10993-5. Biological Evaluation of Medical Devices. Part 5 - Tests for *in vitro* cytotoxicity. 3 Ed. 2009.

Jin, Y. J., Termsarasab, U., Ko, S.H., et al. 2012. Hyaluronic acid derivative-based self-assembled nanoparticles for the treatment of melanoma. Pharmaceutical Research. 29: 3443–3454.

Kittakaa, M., Shibaa, H., Kajiyaa, M., Fujitaa, T., Iwataa, T., Rathvisal, K., Ouharaa, K., Takedaa, K., Fujitaa, T., Komatsuzawa, H., Hidemi, K. 2013. The antimicrobial peptide LL37 promotes bone regeneration in a rat calvarial bone defect. Peptides. 46: 136-142

Klemm, D., Kramer, F., Moritz, S., Lindström, T., Ankerfors, M., Gray, D., et al., 2011. Nanocelluloses: a new family of nature-based materials. Angewandte Chemie International Edition. 50: 5438–5466.

Kwak, M. H., Kim, J. E., Go, J., et al. 2015. Bacterial cellulose membrane produced by Acetobacter sp. A10 for burn wound dressing applications. Carbohydrate Polymers. 122: 387–398.

Lee, J.C., Kandula, S., Sherber, N.S., 2009. Beyond wet-to-dry: a rational approach to treating chronic wounds. Eplasty. 9-14.

Lee, W. J., Cha, H. W., Sohn, M. Y., Lee, S. J., Kim, D. W. 2012. Vitamin D increases expression of cathelicidin in cultured sebocytes. Archives of Dermatolological Research. 304: 627–632.

Li, F., Bae, B.C., Na, K. 2010. Acetylated hyaluronic acid/photosensitizer conjugate for the preparation of nanogels with controllable phototoxicity: Synthesis, characterization, autophotoquenching properties, and *in vitro* phototoxicity against hela cells. Bioconjugate Chemistry. 21: 1312–1320.

Luo, Y.,Teng, Z. Wang, Q. 2012. Development of zein nanoparticles coated with carboxymethyl chitosan for encapsulation and controlled release of vitamin D_3. Journal of Agricultural and Food Chemistry. 60: 836–843.

Masarudin, M. J., Cutts, S. M., Evison, B. J., Phillips, D. R., and Pigram, P. J. 2015. Factors determining the stability, size distribution, and cellular accumulation of small, monodisperse chitosan nanoparticles as candidate vectors for anticancer drug delivery: application to the passive encapsulation of [14C]-doxorubicin. Nanotechnology Science and Applications. 8: 67-80.

Mohammadi, M., Ghanbarzadeh, B., Hamishehkar, H. 2014. Formulation of nanoliposomal vitamin D$_3$ for potential application in beverage fortification. Advanced Pharmaceutical Bulletin. 4: 569–75.

Nobbmann, U. 2014. Dispersity or Polydispdersity is a key parameter for GPC SEC.

Oh, E.J., Park, K., Kim, K. S., et al. 2010. Target specific and long-acting delivery of protein, peptide, and nucleotide therapeutics using hyaluronic acid derivatives. Journal of Controlled Release. 141: 2–12.

Oudshoorn, M. H. M., Rissmann, R., Bouwstra, J. A., and Hennink, W. E. 2007. Synthesis of methacrylated hyaluronic acid with tailored degree of substitution. Polymer. 48(7): 1915-1920.

Pedrosa, S. and Gama, M. 2014. Hyaluronic acid and its application in nanomedicine. Carbohydrates Applications in Medicine. 55-89 ISBN: 978-81-308-0523-8 Editor: M. H. Gil.

Pedrosa, S. S., Gonçalves, C., David, L., Gama, M. 2014. A Novel Crosslinked Hyaluronic Acid Nanogel for Drug Delivery. Macromolecular Bioscience. 1556–1568.

Pedrosa, S. S., Pereira, P., Correia, A., Moreira, S., Rocha, H., Gama, F. M. 2016. Biocompatibility of a Self-Assembled Crosslinkable Hyaluronic Acid Nanogel. Macromolecular Bioscience. 16(11): 1610-1620.

Quinn, K. J., Courtney, J. M., Evans, J. H., Gaylor, J. D. S., Reid, W.H. 1985. Principles of burn dressings. Biomaterials. 6: 369–377.

Ramalho, M. J., Loureiro, J. A., Gomes, B., Frasco, M. F., Coelho, M. N., Carmo Pereira, M. 2015. PLGA nanoparticles as a platform for vitamin D-based cancer therapy. Beilstein Journal of Nanotechnology. 6: 1306–1318.

Ramos, R., Silva, J. P., Rodrigues, A. C. et al. 2011. Wound healing activity of the human antimicrobial peptide LL37. Peptides. 32:1469–1476.

Reinholz, M., Ruzicka, T., Schauber, J. 2012. Cathelicidin LL-37: An Antimicrobial Peptide with a Role in Inflammatory Skin Disease. Annals of Dermatology. 24:126–135.

Ring, D.F., Nashed, W., Dow, T., 1986 May 13. Liquid loaded pad for medical applications. United States patent US 4588400 A.

Schanté, C. E., Zuber, G., Herlin, C., Vandamme, T. F. 2011. Chemical modifications of hyaluronic acid for the synthesis of derivatives for a broad range of biomedical applications. Carbohydrate Polymers. 85: 469–489.

Shah, N., Ul-Islam, M., Khattak, W.A., Park, J.K. 2013. Overview of bacterial cellulose composites: a multipurpose advanced material. Carbohydrate Polymers. 98: 1585–1598.

Shoda, M. and Sugano, Y., 2005. Recent advances in bacterial cellulose production. Biotechnolology Bioprocess Engineering 10: 1–8.

Sibbald, G. R., Orsted, H., Schultz, G. S., Coutts, P., Keast, D. 2003. Preparing the wound bed: Focus on infection and inflammation. Ostomy Wound Manage. 49: 24–51.

Silva, J. P., Gonçalves, C., Costa, C., et al. 2016. Delivery of LLKKK18 loaded into self-assembling hyaluronic acid nanogel for Tuberculosis treatment. Journal of Controlled Release; 235: 112–124.

Simões, D., Miguel, S. P., Ribeiro, M. P., Coutinho, P., Mendonça, A. G., Correia, I. J. 2018. Recent advances on antimicrobial wound dressing: A review. European Journal of Pharmaceutics and Biopharmaceutics. 127: 130–141.

Siró, I. and Plackett, D. 2010. Microfibrillated cellulose and new nanocomposite materials: a review. Cellulose. 17: 459–494.

Stetefeld, J., McKenna, S. A., Patel, T. R. 2016. Dynamic light scattering: a practical guide and applications in biomedical sciences. Biophysical Reviews. 8: 409–427.

Tabata, Y. and Ikada, Y. 1988. Effect of the size and surface-charge of polymer microspheres on their phagocytosis by macrophage. Biomaterials. 9: 356–362.

Takahashi, K., Kato, H., Saito, T., Matsuyama, S., Kinugasa, S. 2008. Precise measurement of the size of nanoparticles by dynamic light scattering with uncertainty analysis. Part Part Syst Charact. 8:31–38.

Watson, N. F. S. and Hodgkin, W. 2005. Wound dressings. Surgery. 23: 52–55.

Wilhelms, T., Schulze, D., Alupeil, C., I, Rohrer, C., Abel, M., Wiegand, C., Hipler, U.C. 2007. Release of polyhexamethylene biguanide hydrochloride (PHMB) from a hydroballanced cellulose wound dressing with PHMB. 17th Conference of the European Wound Management Association Glasgow.

6 THE EFFECT OF HA-LLKKK18 AND HA-VITAMIN D₃ FORMULATIONS IN WOUND REPAIR
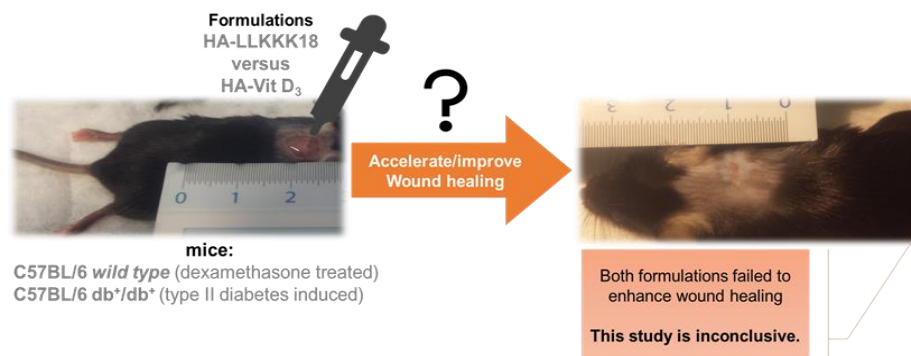
Impaired wound healing and its medical complications remain one of the most prevalent and economically burdensome healthcare issues in the world. In particular, the development of chronic wounds is one of the most serious and debilitating complications of diabetes. In recent years, there have been efforts to develop new advanced methodologies to heal chronic wounds. Unfortunately, in many cases, the therapeutic efficacy is low, the therapies are expensive and require application in a clinical facility, and the dressings have no antimicrobial activity. Therefore, development of new therapeutics is absolutely necessary and important to satisfy these unmet clinical needs. Antimicrobial peptides (AMPs) synthesized in the skin provide a barrier to infection and some of them are very important for the regeneration of skin. LL37 is the most important AMP in skin, acts as a first line of defense against bacteria, virus and fungi, playing an important role in immunomodulation, angiogenesis and wound healing. An analogue of LL37, LLKKK18, also demonstrated a similar wound healing activity. The vitamin D_3 (Vit D_3) pathway of LL37 induction was identified as the major regulator of cathelicidin expression. Consequently, Vit D_3 entered the spotlight as an immune modulator with impact on both innate and adaptative immunity. Therapies targeting Vit D_3 signalling may provide new approaches for infection, inflammatory skin diseases and wound healing by affecting both innate and adaptative immune functions. The use of Vit D_3, if successful, could overcome several of the limitations associated to AMPs: cost, stability, regulatory issues.

This work presents an exploratory investigation on the potential topical application the HA-LLKKK18 and HA-Vit D_3 formulations as active agents in wound repair using excision and chronic wound models was performed. Wound healing experiments were performed in dexamethasone -treated mice C57BL/6 *wild type* (to impair heling) and db⁺/db⁺ C57BL/6 mice (type II diabetes induced). In this study the topical application of both formulations failed to enhance wound healing. Since LLKKK18 has been consistently demonstrated to contribute to a faster regeneration of wounds, this study is inconclusive.

6.1 INTRODUCTION

Wound healing is a biological process which involves hemostasis, inflammation, cell migration and proliferation, and tissue maturation. Diabetic individuals, for example, have impaired healing and it is well known that the healing treatments of diabetic (chronic) wounds are not satisfactory. In this type of lesions, angiogenesis seems to be the most compromised phase, as a result of VEGF synthesis impairment (Bitto et al., 2008).

Current wound therapeutics consist of dressings comprising a bioactive agent. Most commonly used bioactive agents are often associated with high production costs, incomplete healing and/or tissue toxicity (Broussard and Powers, 2013). For example, many therapeutic agents, including growth factors (e.g. EGF, TGF-beta) and hormones, have been tested in wound treatment, but their high production costs deter their wider application (Hrynyk et al., 2012). Antimicrobial agents like silver sulfadiazine, iodine or medical grade honey have also been incorporated into dressings to preserve wounds safe from infections. However, some studies have shown that treatment with these agents alone does not achieve complete healing and in some cases, toxicity problems occur (Broussard and Powers, 2013). Antimicrobial peptides (AMPs), which are commonly small, cationic and amphipathic peptides, arise as suitable candidates for wound therapeutics. LL37, the only known human cathelicidin (family of AMPs) is overexpressed in several cell types (e.g. monocytes, neutrophils, mast cells and B cells, natural killer cells, but also epithelial cells, macrophages, keratinocytes). Besides its antimicrobial activity, LL37 is important for mast cells/leukocytes chemotaxis, angiogenesis and to promote wound healing (Koczulla et al., 2003). Indeed, LL37 overexpression has been shown in the epidermis and within the wound itself after injury (Dorschner et al., 2001). Moreover, AMPs can be easily and cost-effectively produced through recombinant technology, as previously shown in our lab (Ramos et al., 2010). LL37 was reported to accelerate the dexamethasone-impaired healing of excisional wounds in C57BL/6 mice (Ramos et al., 2011). LL37 is very sensitive to proteolytic degradation, which decreases its half-life and demands the use of higher concentrations, which may be potentially cytotoxic (Korting et al., 2012; Afacan et al., 2012). Recently, new AMPs have been synthesized aiming to improve the properties of natural AMPs. Their activities depend on structural and physicochemical parameters, such as cationicity, hydrophobicity and amphipathicity. By tuning these parameters, the intensity of its activities can be manipulated (Nagaoka et al., 2002). For example, analogues of LL37, like LLKKK18, have been designed to improve the antimicrobial activity. This peptide is a shorter and truncated variant

of LL37, with 14 and 5 amino acid residues less at N- and C-terminal, respectively. Further substitution of negative (aspartic acid) and uncharged residues (glutamine and asparagine) by three positively-charged lysine (K) residues results in a more hydrophobic and more cationic peptide (+8) (Silva et al., 2015). These modifications make the LLKKK18 analogue a stronger antimicrobial agent, while maintaining a high chemoattractant activity (Ciornei et al., 2005; Silva et al., 2015). The wound healing activity of LLKKK18 peptide has not been so extensively characterized as for LL37 (Koczulla et al., 2003; Ramos et al., 2011; Steinstraesser et al., 2014). Silva et al. 2015 demonstrated the ability of LLKKK18 to accelerate the regeneration of rat burn wounds after *in vivo* administration of the peptide conjugated with dextrin and further embedded in a Carbopol hydrogel. The peptide was shown not only to decrease the healing time, but also to promote a faster resolution of the inflammatory stage, besides stimulating angiogenesis and collagen deposition (Silva et al., 2015). These results thus suggested that LLKKK18 could be a promising alternative as a wound healing agent.

By gathering several relevant bioactivities (antimicrobial and regenerative) LL37 (and LLKKK18) are promising medicines for wound healing. Despite the reported major advances concerning the therapeutic use of LL37 and LL1KKK8 for wound therapeutics (Ramos et al., 2011; Silva et al.,2015), a few limitations still remain, especially concerning their production costs (therapeutic doses are too low to consider large scale production). A therapeutic approach based on the induction of the peptides expression (Ong et al., 2002; Carretero et al., 2008), thus assumes itself as a promising alternative strategy. Vitamin D₃ (Vit D₃), is a widely available lipophilic vitamin, non-expensive, easy-to-use, has a wide therapeutic window and is well tolerated by the organism. It plays an important role in wound healing as an inducer of LL37 expression. For example, Vit D₃ can influence keratinocyte differentiation and is therefore used in the treatment of several skin disorders including psoriasis (Burkiewicz et al., 2012; Ramezanli et al., 2017), representing a great option for wound treatment instead the direct use of AMPs.

The use of drug delivery systems could be another promising option for the application of a regulated dose with improved pharmacokinetics (Harris and Chess., 2003). A self-assembled hyaluronic acid (HA) nanogel developed in our lab may efficiently encapsulate hydrophobic molecules and proteins/peptides, especially those cationically-charged. These HA nanogels are expected to facilitate LLKKK18 and Vit D₃ cell targeting and internalization, while allowing its sustained release, thus enhancing the bioactive agent effect. In normal physiological conditions, macrophages do not internalize HA. However, Sladek and collaborators, 2009, showed that

macrophages express the CD44 receptor in the beginning of an inflammatory response. Since activated macrophages express CD44 and can internalize HA (Underhill et al., 1993), these nanogels seem to be a promising option to deliver drugs to infected macrophages. Of note, HA modulation of cell migration and inflammation has been reported to enhance wound repair (Chen and Abatangelo., 1999). Still, a proper carrier may help administer and sustainably release the peptide and Vit D$_3$.

In this work we incorporated the bioactive agents LLKKK18 and Vit D$_3$ in the HA-Hexa nanogels for topical administration. Exploratory *in vivo* trials were performed using dexamethasone-impaired wound healing C57BL/6 *wild type* and db$_+$/db$_+$ C57BL/6 mice (type II diabetes induced) in excision and chronic wound models.

6.2 METHODS

6.2.1 Production of self-assembling hyaluronic acid-based nanogels - HA-Hexa nanogels

Production and characterization of self-assembling HA-Hexa nanogels were performed as described in chapter 5, section 5.2.1.1 to 5.2.1.4.

6.2.2 Encapsulation into HA-Hexa nanogels

6.2.2.1 LLKKK18 encapsulation (HA-LLKKK18)

Peptide encapsulation was performed by gently mixing 100 μM LLKKK18 (Schafer-N, Denmark), which corresponds to 220 μg/mL, with 1 mg/mL HA nanogels in Phosphate Buffered Saline (PBS) in a rotating wheel, for 24 h at room temperature. Unloaded peptide was removed by transferring the solution into Amicon® Ultra-centrifugal filter units (Millipore) with a molecular weight cut-off of 100 kDa and centrifugation for 2 min at 2000 rpm. The original volume in the concentrated solution containing the peptide-loaded nanogels was then restored. The amount of free and loaded LLKKK18 was quantified by the quantitative Micro BCA™ Protein Assay Kit (Thermo Scientific™) and the encapsulation efficiency was expressed as the percentage of loaded peptide relatively to the total (loaded + free) peptide. The peptide-nanogel solution was sterilized through filtration using a 0.22 μm polyethersulphone (PES) syringe filter.

6.2.2.2 Vitamin D$_3$ loading (HA-Vit D$_3$)

A stock solution (25 mg/mL) of Vit D$_3$ (Acros Organics, New Jersey, USA) was prepared in absolute ethanol and used to prepare the PBS dispersions with the nanogel. Vit D$_3$ was added in sterile conditions to dispersions of 1 mg/mL HA-Hexa nanogel previously dissolved in Phosphate Buffered Saline (PBS) under mild rotation in a wheel, for 24 h at room temperature, and then sterilized through filtration using a 0.22 µm polyethersulphone (PES) syringe filter. The final Vit D$_3$ concentration attained in the sample was 500 µM, which corresponded to 192.3 µg/mL. The ethanol content was less than 1 % (v/v) in all conditions.

The obtained solutions were left rotating in a turning wheel for 16 h, at room temperature, to allow vitamin loading. All working solutions containing Vit D$_3$ were protected from light. Samples obtained after 16 h of encapsulation were then centrifuged at 4000×g for 10 min (Eppendorf Centrifuge 5430 R) and the supernatant containing the loaded Vit D$_3$ was collected in sterile conditions for further utilization. The total drug concentration, corresponding to soluble (in the nanogel) and insoluble fractions previously dissolved in a small volume of absolute ethanol, was also quantified before centrifugation.

6.2.3 Characterization of the nanogels

HA-Vit D$_3$ was characterized as described in chapter 5 section 5.2.1.4. HA-LLKKK18 was analysed by Dynamic Light Scattering (DLS), using a Zetasizer Nano ZS (Malvern Instruments, UK), with a detector angle of 173°, at 25 °C. Results were expressed in terms of volume and intensity distributions, zeta potential, hydrodynamic diameter (size) and polydispersity index (PdI).

6.2.4 Wound healing assay

- **Animals**

This work was carried out at *Biotério da Faculdade de Medicina da Universidade do Porto*. All animal testing procedures were performed in conformity with the European norms for animal welfare (European Directive 2010/63/EU) and with the approval of veterinary authorities of Portugal (Direção Geral de Alimentação e Veterinária) (Portaria 1005/92) and ORBEA in accordance with European Communities Council Directive 86/609/EEC. Humane endpoints were followed in accordance to the OECD Guidance Document on the Recognition, Assessment and Use

of Clinical Signs as Humane Endpoints for Experimental Animals Used in Safety Evaluation. Adequate measures were taken to minimize pain and discomfort, considering humane endpoints for animal suffering and distress.

- *In vivo* trials

Twenty-eight C57BL/6 *wild type* (dexamethasone treated) and twenty eight C57BL/6 *db⁻/db⁻* (type II diabetes induced) mice (purchased at Charles River, Wilmington, MA) with 6–8 weeks old were used in this study. After general anesthesia with 3 % Isoflurane, hair on the dorsal side of the animals was shaved and the skin was cleaned with 70 % (v/v) alcohol. Two full thickness wounds extending through the panniculus carnosus were made on the dorsum on each side of midline, using an 8 mm biopsy punch. Following the surgical procedure, the animals were individually housed. Four groups (n=7) were treated with different formulations: #G1- HA-Hexa; #G2- HA-LLKKK18; # G3- HA-Vit D₃ and #G4- Control- PBS solution. The different formulations were applied topically twice a day (80 µl). The applied doses of each formulation are presented in Table 1. Wounds were left open and not covered by any type of dressing. To delay healing (which would otherwise be very fast), C57BL/6 *wild type* mice were treated at each 48 h with dexamethasone (0.25 mg/kg of body weight of Vetacort, intramuscularly). Mice were examined daily for wound-healing progression; at each 48 h photographs of the wounds were taken using a digital camera, until total closure of wounds. Wound size was then determined until re-epithelialization was achieved. After total closure of wounds in all groups, the animals were euthanized, and wound tissue was collected for histological analysis.

Table 1 - Doses of each formulation in 80 µL of solution.

Formulation	Dose (80 µL, twice a day)
#G1- HA-Hexa	80 µg HA-Hexa
#G2- HA-LLKKK18	80 µg HA-Hexa + 18 µg LLKKK18
#G3- HA-Vit D₃	80 µg HA-Hexa + 11 µg Vit D₃
#G4-Control- PBS	80 µL PBS

- **Tissue histology**

Histological analysis was performed on wound tissues collected at specific time points after the wound was created. Skin wound tissue specimens were fixed in 10 % neutral-buffered formalin solution and paraffin embedded. Histological analyzes were performed in 3 µm tissue sections. Sections were stained with Hematoxylin and Eosin (H&E). Connective tissue was analyzed by staining wound sections with a modified Masson's Trichrome stain (ScyTek Laboratories, Logan, UT), according to the manufacturer's protocol. Sections were, mounted on a microscopy slide and visualized in a Leica iCC 50 w microscope with a Nikon digital camera. The slides were further visualized by a pathologist, and different wound healing-related parameters (angiogenesis, inflammation, epidermis and collagen deposition) were assessed. These parameters are listed in Table 2, along with the semi-quantitative scale used. The mean value was used for statistical comparison.

Table 2 - Histological parameters to determining healing level.

Staining	Histological parameter	Scale
H&E	**Angiogenesis** (presence of blood vessels)	1- low 2- moderate 3- intense
	Inflammation (presence of inflammatory cells like, fibroblasts, neutrophils, lymphocytes monocites and macrophages)	
	Epidermis	normal hyperplasic ulcerated
Masson's Trichrome stain	**Collagen deposition** (collagen stained blue/green, keratin appeared red, cytoplasm stained pink and cell nuclei were black)	1- low 2- moderate 3- intense

6.2.5 Statistical analysis

The statistical analysis was performed using the GraphPad Prism software for windows version 5.01. Normality of the samples distribution was firstly assessed using Kolmogorov-Smirnov and Shapiro-Wilk normality tests, and considering the acceptability of skewness and kurtosis values. Potential significant differences between treatments were assessed with the two-way ANOVA followed by a Bonferroni's post-hoc test.

6.3 RESULTS AND DISCUSSION

6.3.1 LLKKK18 encapsulation and Nanogel characterization

Nanogel loading with 100 µM LLKKK18 allowed an encapsulation efficiency (EE) of approximately 70 %, it was accordingly with the results obtained before by the group (Silva et al., 2016). The cationicity and hydrophobicity of the peptide may act as a driving force leading to its encapsulation within the hydrophobic core of the negatively charged nanogel. Taking that into consideration, nanogel formulations for *in vivo* trials were prepared with 30 % excess peptide (143 µM), to obtain the desired final concentrations (around 100 µM of LLKKK18, corresponding to the mass of presented in Table 1). LLKKK18-loaded HA-Hexa nanogels were characterized by DLS for the Z-average (mean diameter) and polydispersity index (PdI). Encapsulation of LLKKK18 into the HA-Hexa nanogel resulted in self-assembling particles with an average size of approximately 77 ±5.5 nm (Figure 1 A). Size (intensity) distribution shows that peptide-loaded nanogels are constituted by two populations (Figure 1 B). However, the size distribution by volume shows the prevalence of particles of smaller size, with around 30 nm (Figure 1 A). The PdI values obtained were above 0.4, which is an indicative of a broad size distribution and therefore a high dispersity (Nobbmann, 2014).

The nanogel's Zeta potential was also characterized, since this plays an important role in the dispersity and stability of colloidal dispersions (Delgado et al., 2007). Results in Figure 1 C show that the superficial charge of the empty nanogel was of -27.8 ± 0.9 mV, due to the negatively charged HA backbone (carboxylic groups). When loaded with the cationic peptide LLKKK18 (+8), the nanogel superficial charge increased to -3.25 ± 0.2 mV which suggests an interaction of LLKKK18 with the surface of the nanogel neutralizing of the hyaluronic acid negative charge (Mohanty et al., 2013). Charge neutralization may decrease the nanogels cytotoxicity characteristic of charged – especially anionic - nanoparticles (Schaeublin, et al., 2011; Tomita, et al., 2011).
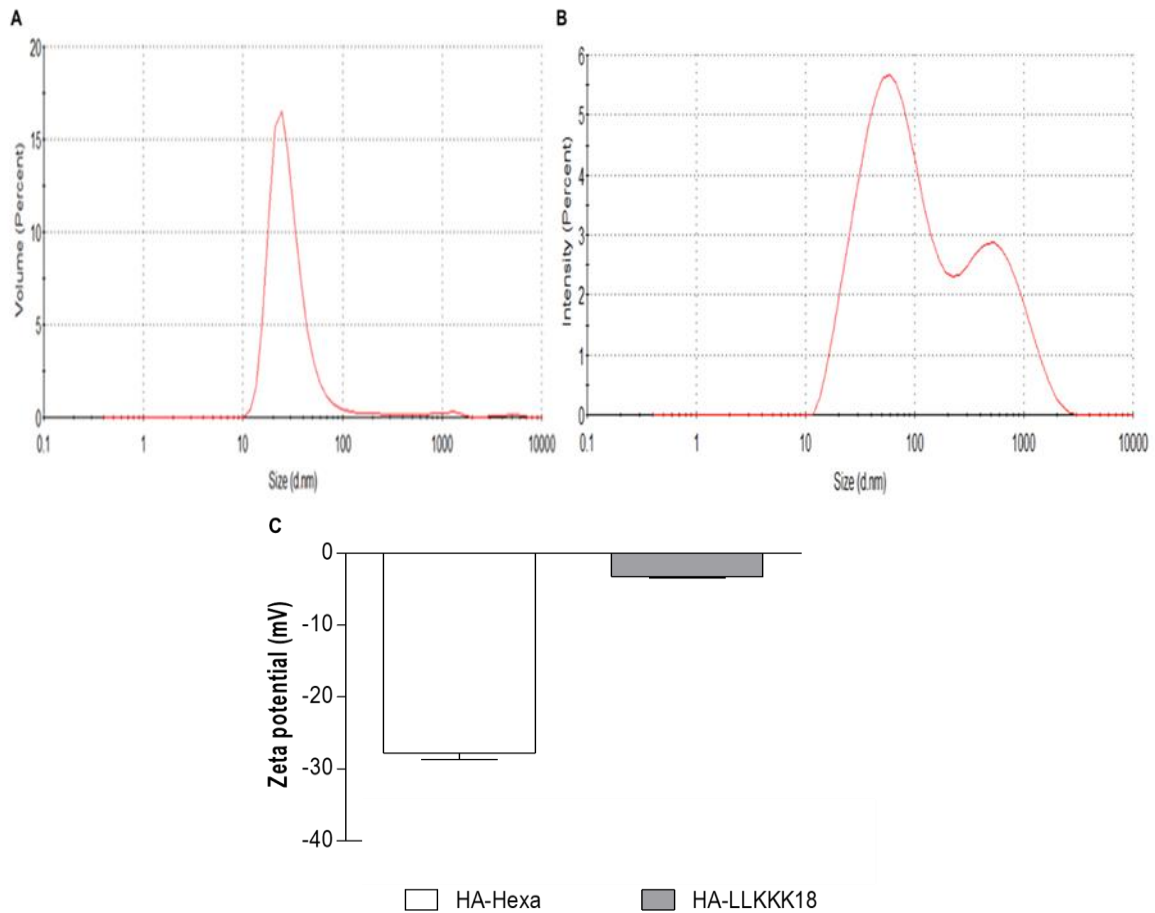
Figure 1 - Size distribution by volume **A)** and intensity **B)** of the LLKKK18-loaded HA-Hexa nanogel. **C)** The effect of LLKKK18 encapsulation on zeta potential. Results show the mean size of 5 repeated measurements of the same sample.

6.3.2 Wound healing assays – *in vivo* trials

The biological effects of the formulations HA-LLKKK18 and HA- Vit D$_3$ nanogels in wound repair were further assessed in a set of exploratory assays performed in dexamethasone -treated C57BL/6 *wild type* and C57BL/6 db$^+$/db$^+$ mice (type II diabetes induced) full thickness excisional and chronic wound models. Delayed wound healing is a major complication of diabetes and is caused by increased apoptosis, delayed cellular infiltration, reduced angiogenesis, decreased formation and organization of collagen fibres and reduced expression of several growth factors and receptors, contributing, at least in part, for reduced rate of healing (Asai et al., 2012). Diabetic mice, in particular, are considered a good model for chronic wound.

Wound areas were monitored over the time, up to total closure of wound. At day 2, all animals showed an increase of wound size, which we assign to the animal´s ability to reach and scratch the wounds. However, no significant differences were observed (p>0.05).

In the case of dexamethasone -treated C57BL/6 *wild type* mice at day 7, HA- Vit D$_3$ nanogel - showed an acceleration of wound healing as compared to the other groups: wound closure of 47 % as compared to 14 % (HA-Hexa), 9 % (HA-LLKKK18) and 20 % (PBS). The faster wound closure in this group was observed during the remaining period of the assay (Figure 2 A and Figure S1 A), suggesting that Vit D$_3$ may have some healing activity. The results also suggest that the HA-Hexa nanogel did not negatively affect wound healing rate. On the other hand, in the animals treated with HA-LLKKK18, contrary to what was expected, and previous works reported Ramos et al., 2011 and Silva et al., 2015, the wound closure did not accelerate as compared with the control.

In the case of the C57BL/6 db$^+$/db$^+$ mice, no significant differences in the rate of wound closure were observed between all groups tested (p>0.05) (Figure 2 B and Figure S1 B). As expected, the time required for wound healing was longer in diabetic animals, since diabetes compromises the immune system in a way that hampers the healing process (Järbrink et al., 2016). No adverse effects on body weight, general health, or behavior of the mice were observed after all groups treated.
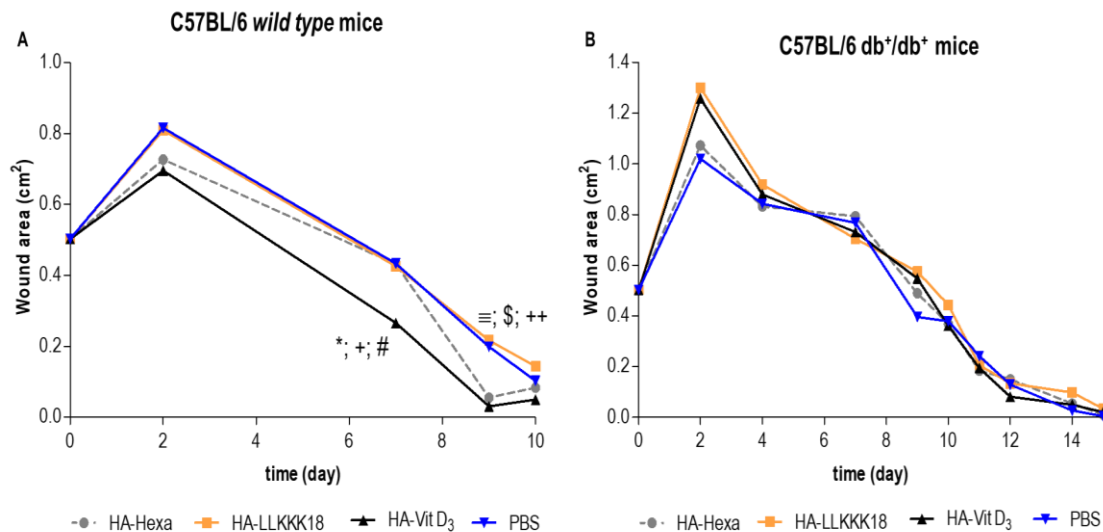

Figure 2 - *In vivo* wound closure in different experimental groups. **A)** dexamethasone treated C57BL/6 *wild type* mice and **B)** C57BL/6 db$^+$/db$^+$ mice. Wound closure in wounds treated with vehicle PBS, HA-Hexa nanogel (80 µg per application), HA-LLKKK18 nanogel peptide (18 µg per application), HA- Vit D$_3$ (11 µg per application). Wound areas were quantified, and the results are average ± SD (n=7). In graphs A, $p <$ 0.05, $^+p < 0.05$, $^\#p < 0.05$ indicates statistical significance between treatment groups HA-Hexa and HA-Vit D$_3$; HA-LLKKK18 and HA-Vit D$_3$; HA-Vit D$_3$ and PBS at day seven, respectively. $^\equiv p < 0.05$, $^\$p < 0.05$ indicates statistical significance between treatment groups HA-Hexa and HA-LLKKK18; HA-Vit D$_3$ and PBS at day nine, respectively. $^{++}p < 0.01$, indicates statistical significance between treatment groups HA-LLKKK18 and HA-Vit D$_3$ at day nine. Statistical analysis was performed using two-way ANOVA followed by Bonferroni's multiple comparison.

The effect of different formulations on wound healing was assessed by histological examination of epithelial gap closure. Skin sections were stained with hematoxylin and eosin (H&E) for general observation of skin layers. Relevant factors in wound healing process were analyzed, such as formation of blood vessels (angiogenesis), degree of inflammation and epidermis aspects. The formation of new blood vessels is a prerequisite for tissue repair and wound healing (Carmeliet, 2000). Fibroblasts participate in the whole process of wound healing and influence the formation of collagen. Collagen deposition is an important factor that affects wound reconstruction, likely avoiding scar formation (Xue and Jackson, 2015).

The results obtained after H&E and Masson's Trichrome staining (collagen deposition) observations for dexamethasone -treated C57BL/6 *wild type* and C57BL/6 db⁺/db⁺ mice demonstrated that different wound groups did not experience noticeable changes ($p > 0.05$) (Figure 3 A and 4, Table S1). Although formulation HA-Vit D₃ in dexamethasone -treated C57BL/6 *wild type* animals presented a faster wound closure, this did not translate into significant differences in tissue morphology. Considering all these results did not indicate differences between the formulations tested at the end of healing time for dexamethasone -treated C57BL/6 *wild type* animals (10 days) the score of healing indicates a moderate healing level and the epidermis presented closure (normal or hyperplasia) for group treated with Vit D₃ and for other groups the epidermis remained ulcerated (Figure 3 and Table S1). In the case of diabetic animals (chronic wounds) after 15 days the wounds presented low collagen deposition and low to moderate inflammation, moderate angiogenesis; the epidermis remained ulcerated for formulation HA-LLKKK18 and normal (closed) for the other three groups (Figure 4, Table S1).

Thus, although this study does not reveal consistent benefits associated to the use of the AMP and Vit D₃, we believe these results are inconclusive since the effect of LL37 and LLKKK18 is already well documented in excision wounds. We thus assign the lack of positive results to the operational conditions used. The difficulty in controlling the movement of animals after the sample application certainly resulted in partial loss of the applied sample. Thus, the amount of medicine applied was likely well below the expected. Given the results obtained, no further characterization was performed.

A

C57BL/6 *wild type* mice
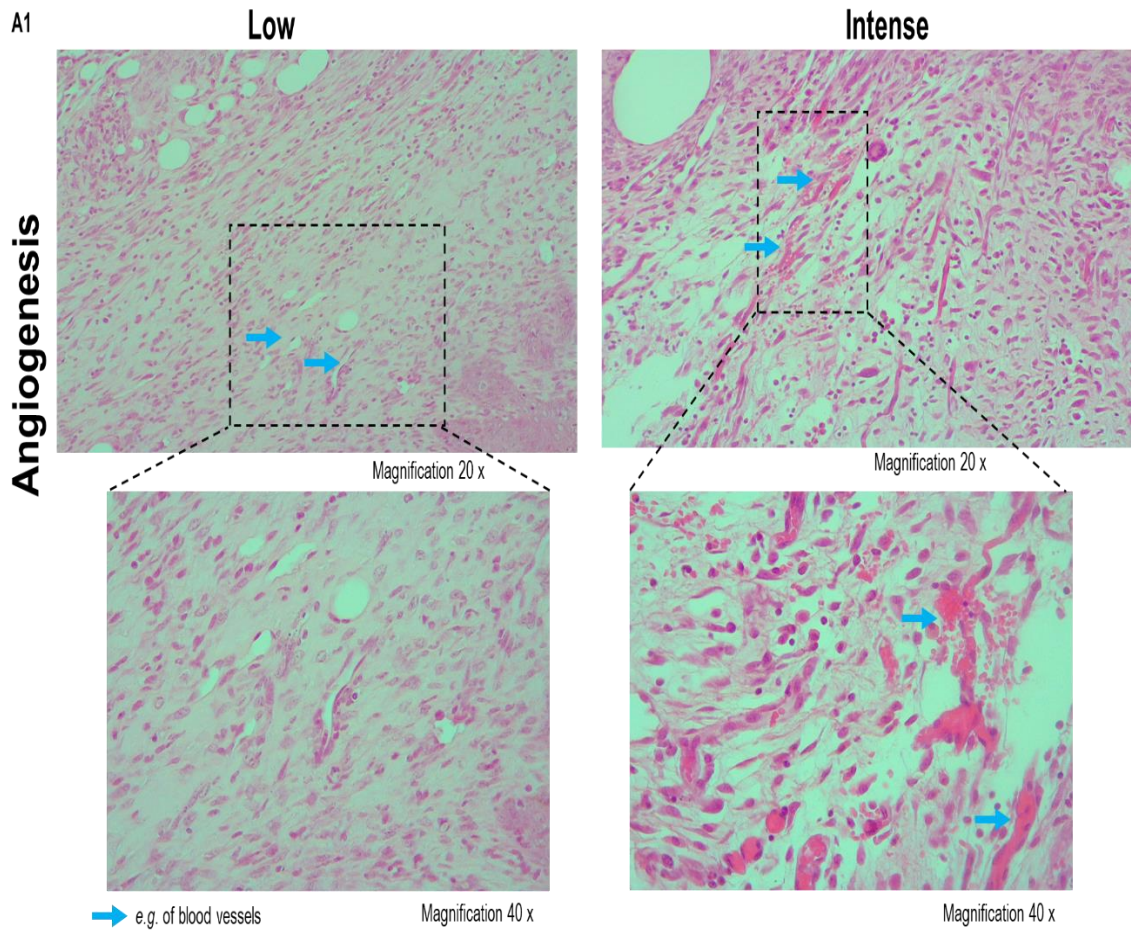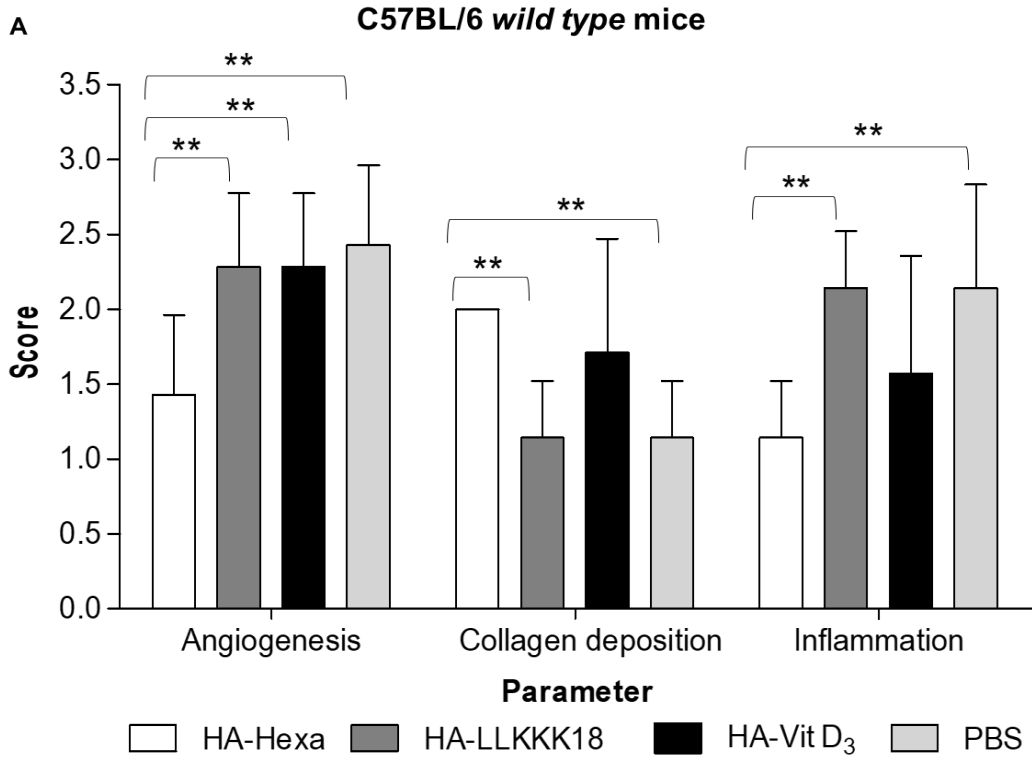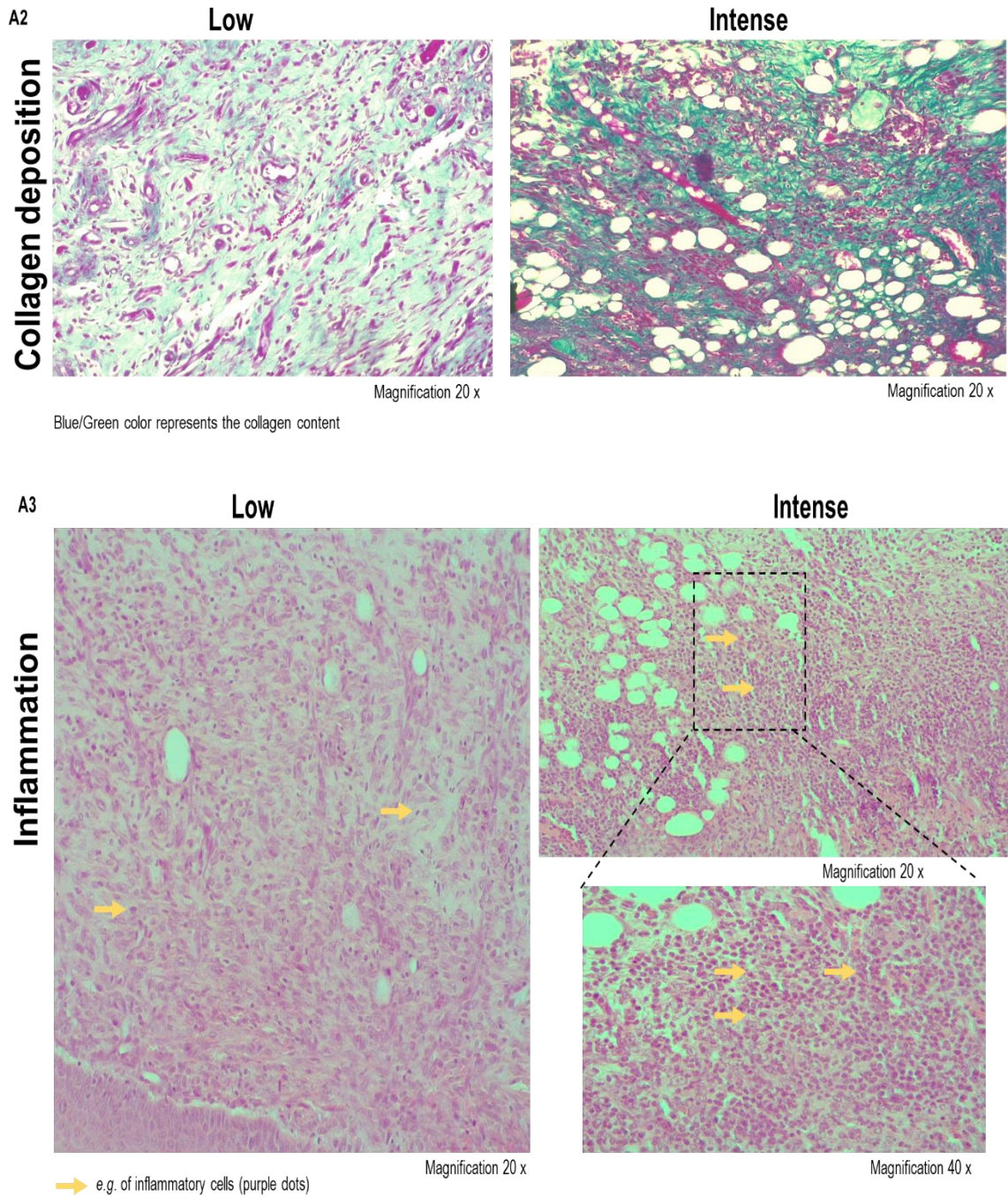
Figure 3 - Quantitative evaluation of histological changes/structures during skin wound healing in **A)** dexamethasone -treted C57BL/6 *wild type* mice. Values are presented as mean ± standard deviation (n=7). [++]$p < 0.01$, indicates statistical significance between treatment groups. Statistical analysis was performed using two-way ANOVA followed by Bonferroni's multiple comparison. **A1) A2) and A3)** Represents an example of the histological differences between the significant groups of wound cross-sections for angiogenesis, collagen deposition and inflammation, respectively.
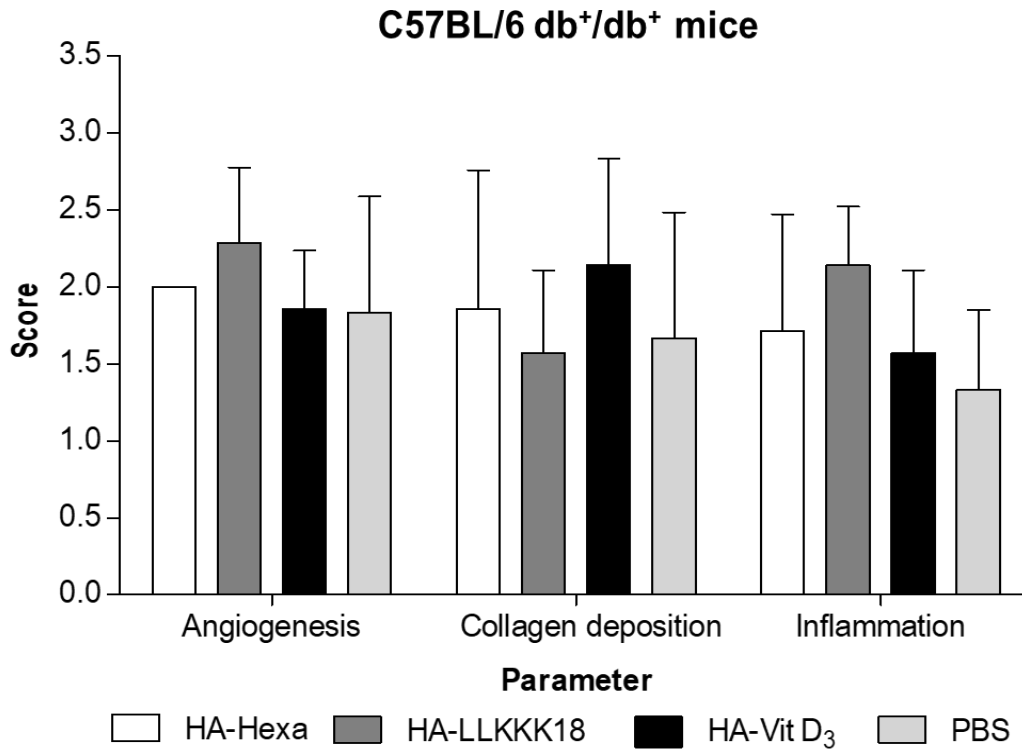
Figure 4 - Quantitative evaluation of histological changes/structures during skin wound healing in C57BL/6 db$^+$/db$^+$ mice.

6.4 CONCLUSIONS

In conclusion, the HA-Hexa nanogel also allowed the incorporation and delivery of diverse bioactive agents, including short half-life agents like the antimicrobial peptide LLKKK18. However, the testing formulations containing the agents LLKKK18 and Vit D$_3$ did not promote improving the wound healing.

6.5 APPENDIX A. SUPPLEMENTARY DATA
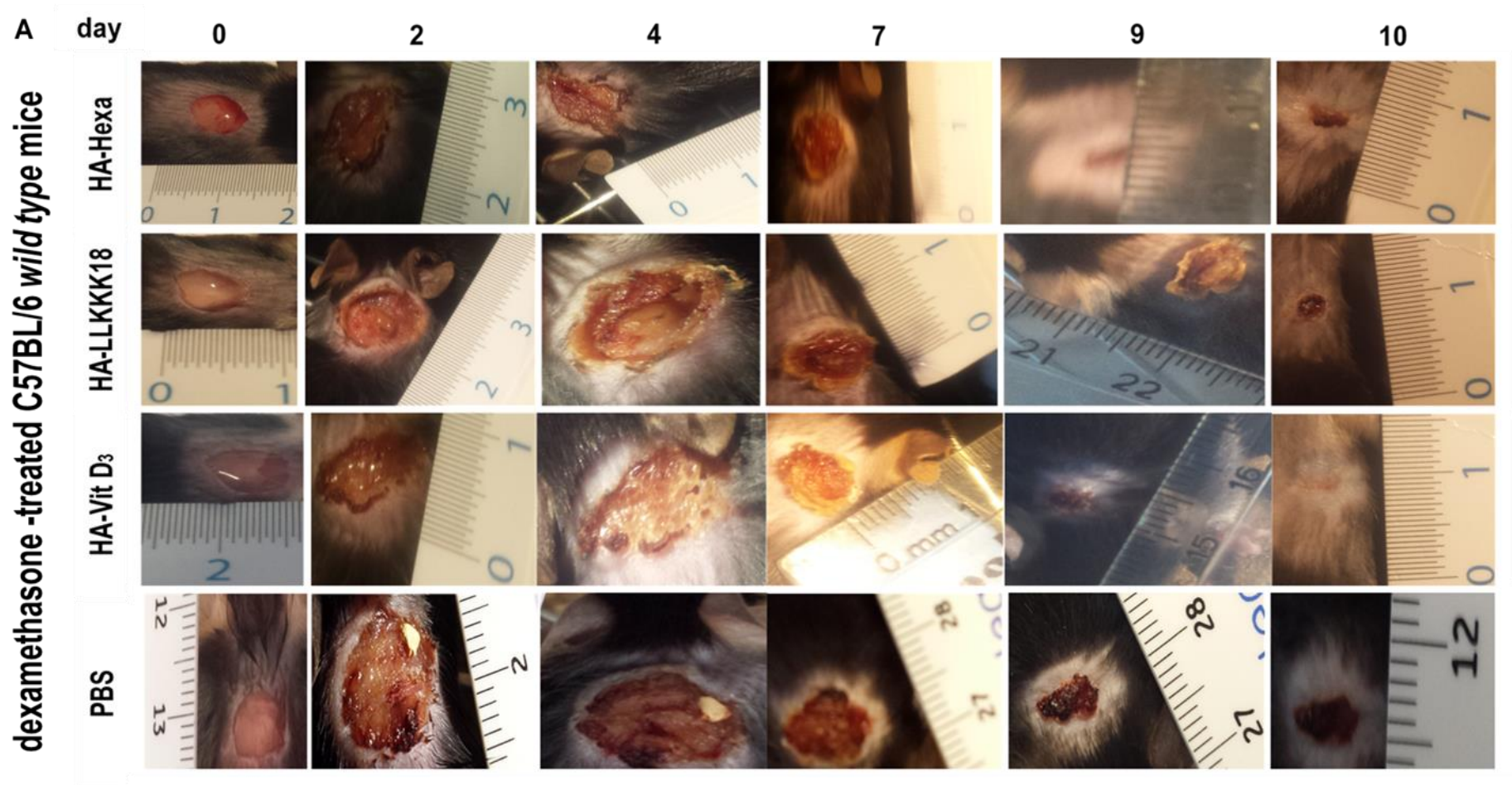
Supplementary material, Figure S1- A) *In vivo* wound area closure for dexamethasone-treated C57BL/6 wild type mice, respectively. Optical images of full-thickness wounds during the healing time for the different experimental groups.
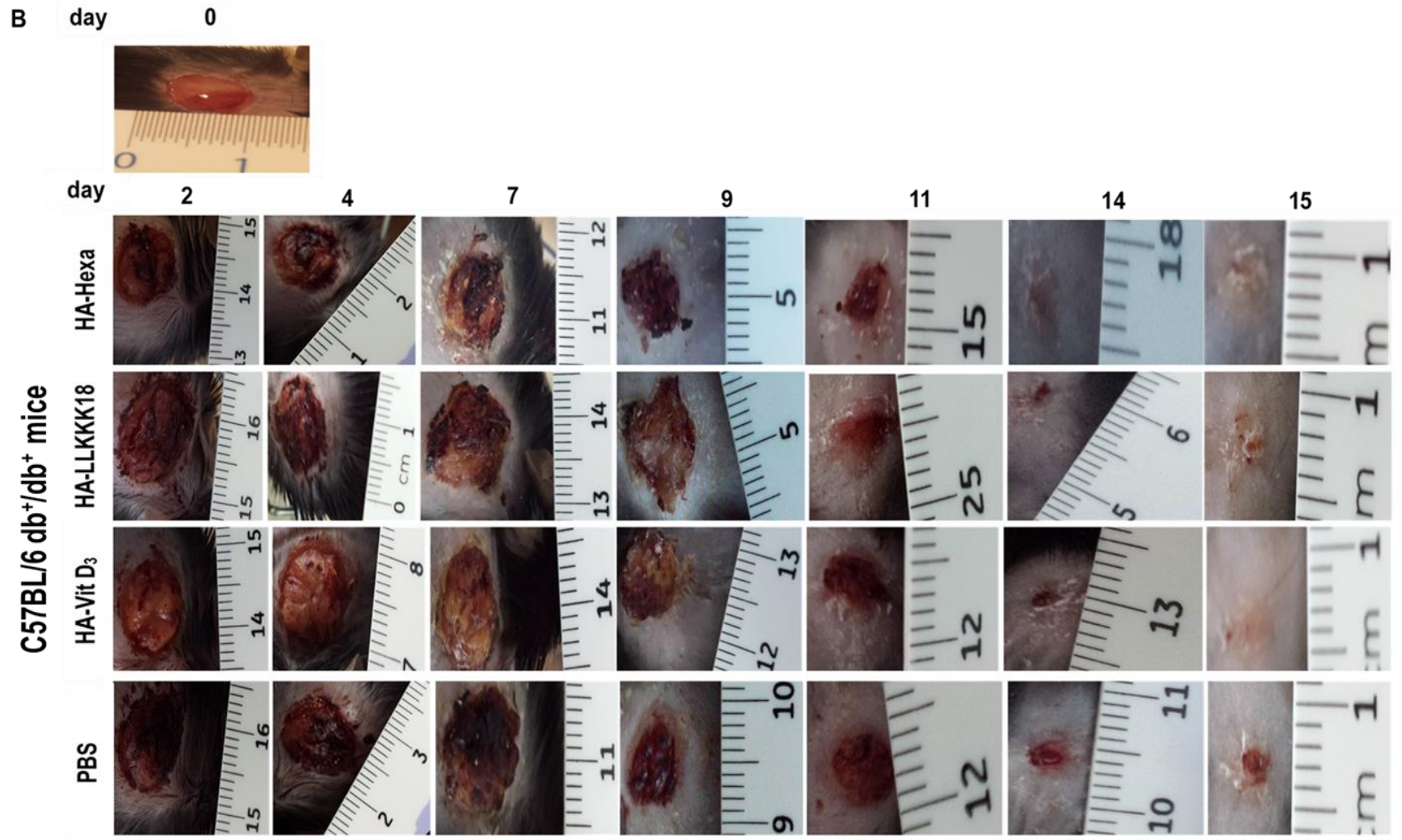
Supplementary material, Figure S1- B) *In vivo* wound area closure for C57BL/6 db⁺/db⁺ mice, respectively. Optical images of full-thickness wounds during the healing time for the different experimental group.

Table S 1 - Histopathological findings observed.

Parameter	Level	dexamethasone-treated C57BL/6 *wild type* mice (%)				C57BL/6 db⁺/db⁺ mice (%)			
		HA-Hexa	HA-LLKKK18	HA-Vit D₃	PBS	HA-Hexa	HA-LLKKK18	HA-Vit D₃	PBS
Angiogenesis	1- low	57.1	0	0	0	0	0	14.3	33.3
	2- moderate	42.9	71.4	71.4	57.1	100	71.4	85.7	50
	3- intense	0	28.6	28.6	42.9	0	28.6	0	16.7
Collagen deposition	1- low	0	85.7	14.3	85.7	42.9	42.9	14.3	50
	2- moderate	100	14.3	42.9	14.3	28.6	57.1	57.1	33.3
	3- intense	0	0	14.3	0	28.6	0	28.6	16.7
Inflammation	1- low	71.4	0	57.1	14.3	42.9	0	42.9	66.7
	2- moderate	28.6	85.7	28.6	57.1	42.9	85.7	57.1	33.3
	3- intense	0	14.3	14.3	28.6	14.3	14.3	0	0
Epidermis	normal	28.6	14.3	28.6	14.3	57.1	28.6	57.1	50
	hyperplasic	14.3	14.3	28.6	28.6	0	0	0	16.7
	ulcerated	57.1	71.4	42.9	57.1	42.9	71.4	42.9	33.3
	open	0	0	0	0	0	0	0	0

6.6 APPENDIX B. ANINAL-WELFARE BODY OPINION

U.PORTO
FMUP FACULDADE DE MEDICINA
UNIVERSIDADE DO PORTO

ANIMAL-WELFARE BODY OPINION

After meeting the animal welfare body (ORBEA) of the Faculty of Medicine of Porto, we inform that we have nothing to oppose the project presented entitled *"Avaliação de parâmetros da biocompatibilidade de biomateriais e sua utilização em regeneração de feridas"*, in which Professor Raquel Ângela Silva Soares Lino is PI, after clarifying the doubts raised its analysis.

Thus, the animal welfare is assured, supports the appropriateness of the methodology adopted, the adequacy of the number of animals, the implementation of measures to ensure pharmacological sedation, analgesia and anesthesia of the animals, as well as its euthanasia at the end of the study.

Porto, 29 April 2016

President,

_____
(Professor Doutor Manuel Nuno Alçada)

6.7 REFERENCES

Afacan, N. J., Yeung, A. T., Pena, O. M., and Hancock, R. E. 2012. Therapeutic potential of host defense peptides in antibiotic-resistant infections. Current Pharmaceutical Design. 18(6): 807-819.

Asai, J., Takenaka, H., Hirakawa., Sakabe, J.-I., Hagura, A., Kishimoto, S., Maruyama, K., et al., 2012. Topical Simvastatin accelerates wound healing in diabetes by enhancing angiogenesis and lymphangiogenesis. The American journal of Pathology. 181(6): 2217-2224.

Bitto, A., Minutoli, L., Altavilla, D., Polito, F., Fiumara, T., Marini, H, et al. 2008. Simvastatin enhances VEGF production and ameliorates impaired wound healing in experimental diabetes. Pharmacological Research. 57: 159-169.

Broussard, K. C and Powers, J. G. 2013. Wound Dressings: Selecting the Most Appropriate Type. American Journal of Clinical Dermatology 14:449-459.

Burkiewicz, C. J. C. C., Guadagnin, F. A., Skare, T. L., do Nascimento, M. M., Servin, S. C. N., de Souza, G. D. 2012. Vitamin D and skin repair: a prospective, double-blind and placebo controlled study in the healing of leg ulcers. Revista do Colégio Brasileiro de Cirurgiões. 39: 401–7.

Carmeliet, P., 2000. Mechanisms of angiogenesis. Nature Medicine. 6: 389-395.

Carretero, M., Escámez, M. J., García, M., Duarte, B., Holguín, A., Retamosa, L., et al. 2008. *In vitro* and *in vivo* wound healing-promoting activities of human cathelicidin LL-37. Journal of Investigative Dermatology. 128: 223–236.

Chen, W. Y. and Abatangelo, G. 1999. Functions of hyaluronan in wound repair. Wound Repair and Regeneration. 7: 79-89.

Ciornei, C. D., Sigurdardóttir, T., Schmidtchen, A., Bodelsson, M. 2005. Antimicrobial and chemoattractant activity, lipopolysaccharide neutralization, cytotoxicity, and inhibition by serum of analogs of human cathelicidin LL-37. Antimicrobial Agents Chemotherapy. 49: 2845–2850.

Delgado, A. V., Gonzalez-Caballero, F., Hunter, R. J., Koopal, L. K., and Lyklema, J. 2007. Measurement and interpretation of electrokinetic phenomena. Journal of Colloid Interface Science. 309(2): 194-224.

Dorschner, R. A., Pestonjamasp, V. K., Tamakuwala, S., Ohtake, T., Rudisill, J., Nizet, V., Gallo, R. L. 2001. Cutaneous injury induces the release of cathelicidin antimicrobial peptides active against group A *Streptococcus*. The Journal of Investigation in Dermatology 117: 91-97.

Harris, J. M. and Chess, R. B. 2003. Effect of pegylation on pharmaceuticals. Nature reviews. Drug discovery. 2:214-221.

Hrynyk, M., Martins-Green, M., Barron, A. E., Neufeld, R. J. 2012. Alginate-PEG Sponge Architecture and Role in the Design of Insulin Release Dressings. Biomacromolecules. 13:1478-1485.

Järbrink, K., Ni, G., Sönnergren, H., Schmidtchen, A., Pang, C., Bajpai, R., Car, J. 2016. Prevalence and incidence of chronic wounds and related complications: a protocol for a systematic review. Systematic reviews. 8(1): 152-158.

Koczulla, R., von Degenfeld, G., Kupatt, C., Krotz, F., Zahler, S., Gloe, T., Bals, R. 2003. An angiogenic role for the human peptide antibiotic LL-37/hCAP-18. The Journal of Clinical Investigation. 111: 1665-1672.

Korting, H.C., Schöllmann, C. Stauss-Grabo, M. Schäfer-Korting M. 2012. Antimicrobial Peptides and Skin: A Paradigm of Translational Medicine. Skin Pharmacology and Physiology. 25: 323–334.

Mohanty, S., Jena, P., Mehta, R., Pati, R., Banerjee, B., Patil, S., Sonawane, A. 2013. Cationic antimicrobial peptides and biogenic silver nanoparticles kill mycobacteria without eliciting DNA damage and cytotoxicity in mouse macrophages, Antimicrobial Agents Chemotherapy. 57: 3688–3698.

Nagaoka, I., Hirota, S., Niyonsaba, F., Hirata, M., Adachi, Y., Tamura, H., et al. 2002. Augmentation of the lipopolysaccharide-neutralizing activities of human cathelicidin CAP18/LL-37-derived antimicrobial peptides by replacement with hydrophobic and cationic amino acid residues. Clinical and Diagnostic Laboratory Immunology. 9(5): 972-982.

Nobbmann, U. 2014. Dispersity or Polydispdersity is a key parameter for GPC SEC. Retrieved 14/11, 2017, from http://www.materials-talks.com/blog/2014/10/23/polydispersity-what-does-it-mean-for-dls-and-chromatography/.

Ong, P.Y., Ohtake, T., Brandt, C., et al. 2002. Endogenous Antimicrobial Peptides and Skin Infections in Atopic Dermatitis. The New England Journal of Medicine. 347: 1151–1160.

Ramezanli, T., Kilfoyle, B. E. Zhang, Z., Michniak-Kohn, B. B. 2017. Polymeric nanospheres for topical delivery of vitamin D3. International Journal of Pharmaceutics. 516: 196-203.

Ramos, R., Domingues, L., Gama M. 2010. Escherichia coli expression and purification of LL37 fused to a family III carbohydrate-binding module from Clostridium thermocellum. Protein Expression and Purification. 71:1-7.

Ramos, R., Silva, J. P., Rodrigues, A. C., Costa, R., Guardão, L., Schmitt, F., Gama, M. 2011. Wound healing activity of the human antimicrobial peptide LL37. Peptides. 32: 1469-1476.

Schaeublin, N.M., Braydich-Stolle, L.K., Schrand, A.M., Miller, J.M., Hutchison, J., Schlager, J.J., Hussain, S.M., 2011. Surface charge of gold nanoparticles mediates mechanism of toxicity, Nanoscale. 3: 410–420.

Silva, J. P., Dhall, S., Garcia, M., et al. 2015. Improved burn wound healing by the antimicrobial peptide LLKKK18 released from conjugates with dextrin embedded in a carbopol gel. Acta Biomaterials. 26:249–262.

Silva, J. P., Gonçalves, C., Costa, C., Sousa, J., Silva-Gomes, R., Castro, A. G., et al. 2016. Delivery of LLKKK18 loaded into self-assembling hyaluronic acid nanogel for tuberculosis treatment. Journal of Controlled Release. 235: 112–124.

Sladek, Z and Rysanek, D. 2009. Expression of macrophage CD44 receptor in the course of experimental inflammatory response of bovine mammary gland induced by lipopolysaccharide and muramyl dipeptide, Research in Veterinary Science. 86: 235–240.

Steinstraesser, L, Lam, M. C., Jacobsen, F., Porporato, P. E., Chereddy, K. K., Becerikli, M., et al. 2014. Skin electroporation of a plasmid encoding hCAP-18/LL-37 host defense peptide promotes wound healing. Molecular Therapie. 22:734-742.

Tomita, Y., Rikimaru-Kaneko, A., Hashiguchi, K., Shirotake, S. 2011. Effect of anionic and cationic n-butylcyanoacrylate nanoparticles on NO and cytokine production in RAW264.7 cells. Immunopharmacology and Immunotoxicology. 33:730–73.

Underhill, C.B., Nguyen, H.A., Shizari, M., Culty, M. 1993. CD44 positive macrophages take up hyaluronan during lung development. Development Biology. 155: 324–336.

Xue, M. and Jackson, C. J. 2015. Extracellular Matrix Reorganization During Wound Healing and Its Impact on Abnormal Scarring. Advances in Wound Care. 4(3): 119–136.

7 GENERAL CONCLUSIONS AND FINAL REMARKS

This chapter presents the overall conclusion and the main outcomes of this thesis. Also, suggestions for future work given, taking in account the results obtained.

7.1 GENERAL CONCLUSIONS

The large-scale production of BNC is still expensive. Increasing the production scale while reducing the production cost remains a challenge. Besides the choice of bacterial strain, several other factors can affect the BNC production. In this work, some aspects of the static culture of the *K. xylinus* BPR 2001 (ATCC 700178) strain were optimized. Low cost by-products of the food industry, molasses and corn steep liquor, were used as the source carbon and nitrogen, respectively. An experimental design based on the response surface methodology - central composite design – was used to optimize the culture medium formulation. The results achieved indicates that it is possible to produce high BNC yield, in static conditions, using a simple formulation, inexpensive and widely available nutrient sources. It was also found that the BNC dry mass production increases with the surface area of the cultivation vessel, and with the depth of the culture medium and fermentation time. Thus, as long as depletion of nutrients does not occur, the fermentation proceeds and the membrane grows overtime, eventually completely filling the vessel. The pre-inoculum preparation was also optimized. It was observed that there is not a straightforward relation between the initial cell density and BNC yield produced under static culture. Furthermore, the initial inoculum volume required may be much lower than the usually recommended (5-10 % (v/v)), a relevant finding when the large-scale production is envisaged. Indeed, using volumes as low as 0.1-0.5 % (v/v) yields similar BNC productivities. Altogether, these results may contribute to conceive a viable large-scale production in static conditions.

Bacterial nanocellulose has been studied as a drug delivery system of bioactive agents for wound care. In this work, we assessed a strategy to impregnate the BNC membrane with a poorly water-soluble molecule, Vit D_3. For that purpose, a self-assembled hyaluronic acid nanogel (HA-Hexa) was used to solubilize Vit D_3 and then successfully loaded into the BNC membrane. The loaded system- HA-Vit D_3- was embedded into BNC, conceived as a transdermal delivery system. The release of Vit D_3 was monitored over time using a *Franz* cell device. Around 70 % of the initial Vit D_3 available was released from BNC membranes in the first 48 h. This work demonstrates an approach towards the use of an highly hydrophilic material as a controlled delivery system for hydrophobic pharmaceuticals. Given the excellent properties of BNC as a wound dressing, the potential to incorporate poorly water-soluble drugs is quite relevant.

Exploratory trials attempting to ascertain whether the AMP cathelicidin can improve the healing of wounds in a diabetic mice were not successful. However, the peptide did not improve also the regeneration of wounds in wild type animals, which is contradictory with substantial evidence in the

literature. Thus, this needs to be re-assessed, in order to determine whether **i)** cathelicidin may improve the healing of diabetic wounds; **ii)** whether BNC membranes loaded with HA-Vit D_3 may be useful dressing for wound healing, since Vit D_3 stimulates the endogenous expression of cathelicidin.

7.2 SUGGESTIONS FOR FUTURE WORK

The present work brings new insights on the BNC static production, contributing to the optimization of some relevant aspects of the process. This work also widens the scope of BNC as a controlled drug delivery system. Here, some aspects for further development are identified:

- Further optimization of the culture medium formulation attempting to improve the productivity of BNC;

- Assessment of the costs associated to the waste-water management. This aspect is normally overlooked when considering alternative design of the culture medium for BNC production. Indeed, not only the cost of the substrates must be taken in account, but also the processing of the generated waste-waters;

- Balancing pros and cons of using low cost substrates (but heavily loaded with contaminant organic matter) versus synthetic medium (more expensive but cleaner and easier to wash out after production of the BNC membrane);

- Clarification of the reason why the exponential phase is so very short in the stirred bioreactor, cells rapidly loosing viability although nutrients are still available;

- Evaluate whether conclusions reached for the strain BPR 2001 can be generalized for other strains;

- Further assessment of the potential of incorporation of hydrophobic drugs in BNC membranes, using micellar systems (medical grade block polymers) for the straightforward assembling of the polymer-drug and facile incorporation into the BNC membrane;

- The diffusion of vitamin D_3 using BNC- HA-Vit D_3 membranes across the skin should be performed using as skin model, human skin wound or human full-thickness skin equivalents (*e.g.* EpidermFT);

- Reassessment of the potential of cathelicidin and BNC membranes for the regeneration of diabetic and hard to treat wounds.